



THE UNIVERSITY
of ADELAIDE

**Holistic Investigation of Robotically-Assisted 3D Printed
Cob Walls: From Fabrication to Environmental Impacts**

By

Mohamed GOMAA

Thesis submitted in fulfillment of the requirements for the degree of

Doctor of Philosophy

The University of Adelaide

Faculty of Engineering, Computer and Mathematical Sciences

School of Architecture and Built Environment

Copyright © April 2021

Table of Contents

Table of Contents.....	iii
Abstract.....	vii
Statement of originality.....	x
Acknowledgements.....	xi
Summary of abbreviations.....	xii
List of figures (Excluding figures in papers).....	xiii
Chapter 1 Introduction.....	1
1.1 Research background.....	1
1.2 Research scope.....	5
1.3 Research aims and objectives.....	5
1.4 Research impacts.....	7
1.5 Research methods.....	8
1.6 Thesis outline.....	9
Chapter 2 Literature Review.....	12
2.1 Introduction.....	12
2.2 Digital fabrication in architecture.....	12
2.2.1 Implementing additive manufacturing in construction.....	14

2.2.2	Sustainability of additive manufacturing	16
2.3	Cob construction	19
2.3.1	Vernacular architecture.....	19
2.3.2	Traditional cob construction	22
2.3.3	3D Printed earth construction	25
2.4	Building performance.....	26
2.4.1	Structural performance	29
2.4.2	Thermal and energy performance	32
2.4.3	Life Cycle Assessment.....	34
2.5	Identifying research gaps	38
Chapter 3	Research Methodology	40
3.1	Exploration of the geometrical and physical properties.....	41
3.2	Exploration of the structural properties.....	42
3.3	Exploration of the thermal properties	43
3.4	Assessment of the environmental impacts	45
Chapter 4	Exploration of Geometry and Physical Characteristics	47
4.1	Introduction	47
4.2	List of manuscripts.....	47
4.3	Development of a 3D Printing System for Earth-based Materials: Case Study of Cob.....	50

Chapter 5	Exploration of the Structural Performance of 3DP Cob	102
5.1	Introduction	102
5.2	List of manuscripts	102
5.3	Feasibility of 3DP cob walls under compression loads in low-rise construction.....	105
Chapter 6	Exploration of the Thermal properties of 3DP cob.....	149
6.1	Introduction	149
6.2	List of manuscripts	149
6.3	Thermal performance exploration of 3D printed cob	153
Chapter 7	Exploration of the Environmental Implications of 3DP Cob (LCA)	172
7.1	Introduction	172
7.2	List of manuscripts	172
7.3	Environmental Assessment of large-Scale 3D Printing in Construction: A Comparative Study between Cob and Concrete	176
Chapter 8	Discussion and Closing Remarks	218
8.1	Introduction	218
8.2	The Geometry and Physical Characteristics	218
8.3	The Structural Performance	221
8.4	The Thermal properties	223

8.5 The Environmental Implications.....	226
Chapter 9 Conclusions.....	229
References (Excluding references in papers).....	232
Appendix I: Manuscript- Development of a 3D printing system for earth-based construction: case study of cob.	240
Appendix II: Manuscript- Feasibility of 3DP cob walls under compression loads in low-rise construction.....	272
Appendix III: Manuscript- Thermal performance exploration of 3D printed cob.	302
Appendix IV: Environmental assessment of large-scale 3D printing in construction: a comparative study between cob and concrete.	310

Abstract

The rapid increase in the adoption rate of large-scale 3D printing into the construction industry has revealed a number of potential applications. This rapid implementation has also led to a higher degree of construction process optimisations and increased ability of mass customisation. Most existing applications of 3D printing technologies in construction are, however, heavily dependent on concrete and other cement-based materials, resulting in a pursuit to explore other building materials with lower environmental impact and higher adaptability to natural contexts. This pursuit has led to re-approaching earth materials and architecture to be applied in modern constructions.

For centuries, earth architecture has offered potential solutions for several problems associated with buildings, such as high CO₂ emissions, high embodied energy of the construction process, and depletion of natural resources. Yet this method of construction is possibly on the edge of extinction as its slow and very labour-intensive process requires highly skilled craftsmen. Thanks to digital construction methods and technologies, earth materials can now become a key to promoting a new range of sustainable construction solutions that are adaptable to a local context. ‘Cob’ stands as one of many types of earth construction methods that has been utilised all over the world. Its mix consists of subsoil (earth), water, and fibrous material (typically straw), and its construction can comprise a variety of geometries and design goals without the need for formwork or any mechanical compaction method.

The main aim of this research is to leverage the qualities of conventional cob construction as a groundwork for digital innovation through robotic-supported 3D printing (3DP) techniques. This aim has been approached through a comprehensive feasibility assessment of 3DP cob walls. The feasibility study included four main lines of exploration. First is the material fabrication and design process. In this line, the research systematically explored the relationship between the revised cob recipes and the geometrical and design characteristics offered by the new 3DP system. The findings of this exploration provide a new understanding about the opportunities and challenges of the current 3DP cob process, which becomes the basis to develop a novel 3DP system for earth-based materials.

The second line examined the structural feasibility of using 3DP cob walls used in low-rise residential buildings. This investigation involved monotonic axial compression tests, in addition to a numerical modelling via Finite Element Analysis (FEA). The results proved the ability of 3DP cob load-bearing walls to support a two-storey residential house and meet building regulations. The test also established an optimised design chart, describing the relationship between building design and the loadbearing capacity of 3DP cob buildings.

The third line of exploration involved investigating the thermal conductivity of 3DP cob walls. The assessment has revealed a lower thermal conductivity of 3D printed cob (as low as 0.32 W/mK) compared to its manually constructed cob counterparts, which means using 3DP cob for the building walls would potentially reduce heating and cooling energy use in the building.

The fourth exploration focused on assessing the environmental impacts of 3DP cob walls using a Life Cycle Assessment (LCA) method, from cradle to site. The results showed a superior environmental performance of 3DP cob over the concrete-based construction methods while providing the same structural functionality in a one-story house. The results also indicate that the use of renewable energy resources can further boost the environmental potentials of 3DP cob for future construction.

In summary, this research brings 3DP cob construction closer to full-scale applications. On a broader scale, the study contributes to the disciplines of architectural design and construction by providing a framework capable of bridging the knowledge gap between vernacular modes of architecture and contemporary digital practice. Moreover, this technology is not exclusive for new buildings as it can potentially be a useful strategy for conservation and repairing existing cob buildings. This is expected to benefit architects, designers and researchers currently looking into indigenous crafts as a source of material and design knowledge for a revisited digital-based architecture.

Statement of originality

I, Mohamed Gomaa, certify that this work contains no material which has been accepted for the award of any other degree or diploma in my name in any university or other tertiary institution and, to the best of my knowledge and belief, contains no material previously published or written by another person, except where due reference has been made in the text.

I certify that no part of this work will, in the future, be used in a submission in my name for any other degree or diploma in any university or other tertiary institution without the prior approval of the University of Adelaide and where applicable, any partner institution responsible for the joint award of this degree.

I acknowledge that copyright of published works contained within this thesis resides with the copyright holder(s) of those works.

I also give permission for the digital version of my thesis to be made available on the web, via the University's digital research repository, the Library Search and also through web search engines, unless permission has been granted by the University to restrict access for a period of time.

I acknowledge the support I have received for my research through the provision of the Adelaide Scholarship international.

Signed...

Acknowledgements

My PhD has been a long journey that has come to an end now. During that journey, I have met people who made my experience richer, helped me stand up every time I fell and lit a candle every time it got dark. For those people I am forever grateful and thankful.

My first and foremost gratitude goes to my principle supervisor Professor Veronica Soebarto from the University of Adelaide. You have been a great mentor, a good friend, and also a caring family. I will always remember your support during the hard times of the pandemic.

I also would like to thank Professor Michael Griffith, my supervisor from the University of Adelaide, and Professor Wassim Jabi my supervisor from Cardiff University for their invaluable guidance. I am especially thankful to Professor Wassim Jabi for the opportunity of joining his project in Cardiff. I have learnt a lot from you on many levels, in both my academic career and my personal life.

I would like to extend my appreciation to Dr Ehsan Sharifi from the University of Adelaide. Our short discussions in the early times of my PhD were always insightful and they helped shaping my PhD the way it is now. My gratitude also goes to the amazing friends and colleagues I have met in both Australia and UK, especially my friends from Kathleen Lumley College in Adelaide.

My sincerest thankfulness goes to my beloved family in Egypt. Your support gave me the power to overcome all the challenges and achieve the best of my abilities.

Finally, I would like to express my appreciation to the University of Adelaide for providing the scholarship to support my PhD study. I also appreciate the funding I received through the Engineering and Physical Sciences Research Council (EPSRC) in the UK to support my research at Cardiff University.

Summary of abbreviations

3DP	Three-dimensional printing/ printed.
3DCP	Three-dimensional Concrete Printing
AM	Additive manufacturing
CAD	Computer Aided Design
CAM	Computer Aided Manufacturing
CNC	Computer Numerically Controlled
DB	DesignBuilder software
DF	Digital Fabrication
FEA	Finite Element Analysis
GH	Grasshopper tool
IAAC	The Institute for Advanced Architecture of Catalonia
LCA	Life Cycle Assessment
LCI	Life Cycle Inventory
LCIA	Life Cycle Impact Assessment
LSD	Limit State Design
KSA	Kingdome of Saudi Arabia
UAE	United Arab Emirates

List of figures (Excluding figures in papers)

Figure 1. 3DP building in Dubai by Apis-cor (Left) (Apis-cor 2019), and 3DP house in Saudi Arabia by CyBe (Right) (CyBe 2019).....	2
Figure 2. 3DP earth house by WASP 3D (3D-WASP 2020).	4
Figure 3. Different types of 3D digital fabrication techniques: 1) Additive (3D-WASP 2020); 2) Subtractive; 3) Formative (Kalo 2020); 4) Assembly (Kohler 2006).	13
Figure 4. 3DP building in Dubai by Apis-cor (Apis-cor 2019)(Left) and 3DP house in Saudi Arabia by CyBe (CyBe 2019) (Right).....	15
Figure 5 The Embodied carbon in different masonry materials (Morton et al. 2005)	22
Figure 6. Cob building in Totnes, UK (Veliz Reyes et al. 2018) (left); and Keppel Gate cob house in Devon, UK by Kevin McCabe (McCabe 2020).....	23
Figure 7. Earth house prototype by WASP in Italy (left), and the 3D printing system of earth (Right)(3D-WASP 2020).	25
Figure 8. The construction Life cycle (nordic.saint-gobain, 2017)	35
Figure 9. The main four phases of LCA study	36
Figure 10. diagram of the 3D printing system. 1) The KUKA kr60 HA robotic arm, 2) the material extruder as mounted on the robot (left) and as stationary (right)....	41
Figure 11. The compression testing set up: the specimens design (right) and Dartec compression testing machine (left).	43
Figure 12: Alternate printed patterns considered in this study.	43
Figure 13. Heat flow meter Netzsch HFM 446	44

Figure 14. The used 3DP cob specimens for the thermal conductivity testing. From left to right: 1) Solid wall; 2) Double-layered with single gap wall; 3) Triple-layered with dual gaps.44

Figure 15. Prototypes of the functional units in the LCA study.....46

Figure 16. Problems with drying and shrinkage of the fresh cob mixtures.219

Figure 17. Modelling an idealised 3DP cob house in Designbuilder for operational energy simulation.....226

Chapter 1 Introduction

1.1 Research background

The past two decades have witnessed a dramatic increase in the uptake of digital fabrication technologies in the construction industry. 3D printing (3DP) technology in particular has been under intense investigation, in an eager attempt to adopt it using an upscaled version (Feng et al. 2015). In their studies, Kazemian et al. (2017) and Zareiyan and Khoshnevis (2017) demonstrated that a well-developed automated construction process, like 3D construction printing (3DCP), offers various benefits to the industry, such as freedom of design, higher degree of customization, and accelerated productivity. Leveraging 3DP technologies in construction has been the most explored technique of digital fabrication, with concentrated focus on cement-based materials (Le et al. 2012; Perrot, Rangeard, and Pierre 2016; Veliz Reyes et al. 2018).

Nowadays, several institutions and companies around the world have been racing to provide prototypes of full-scale 3DP buildings (Alhumayani et al. 2020). In the past two years, the largest 3DP buildings in the world have been constructed in the Middle East region, particularly in the United Arab Emirates (UAE) and Saud Arabia (KSA). Both countries are pushing their technological boundaries to adopt 3DP technique in a broad scale. UAE has contracted a Russian company Apis-core to construct several 3DP concrete buildings for the government (Apis-cor 2019), while KSA contracted a Dutch company CyBe to construct 1.5 million houses using 3D concrete printing before 2030 (CyBe 2019) (Figure 1).



Figure 1. 3DP building in Dubai by Apis-cor (Left) (Apis-cor 2019), and 3DP house in Saudi Arabia by CyBe (Right) (CyBe 2019).

This relentless pursuit after technological advancement in the construction industry is expected to cause a massive expansion in the building construction sector, resulting in rising concerns over the probable associated environmental implications. Even without this technological advancement, the construction sector is already responsible for almost 40% of the energy consumption and greenhouse gas emissions worldwide (Agustí-Juan and Habert 2017). Furthermore, 50% of the world's processed raw materials are used for construction (Weißenberger, Jensch, and Lang 2014), while five to eight % of global CO₂ emissions are generated from cement production (Kajaste and Hurme 2016). Increasing adverse impacts from the building industry on the environment and climate has been a global concern over the past few decades, making it difficult to achieve zero carbon buildings (Gupta, Barnfield, and Hipwood 2014).

Fortunately, the implementation of digital technology in construction offers great potential to minimise environmental impacts from buildings. Agustí-Juan et al. (2017) and Shrubsole et al. (2019) suggest that research on implementing 3D printing into large-scale construction processes can provide numerous applications for the

architecture and construction industry. This pursuit of a highly automated construction process, combined with the need for low environmental impacts of buildings, has resulted in reapproaching earth materials in modern building construction.

In a modern context, earth construction such as cob offer potential solutions for several problems associated with buildings, such as the high CO₂ emissions, high embodied energy of the construction process, and depletion of natural resources, all of which are usually associated with the use of concrete (Benardos et al. 2014; Chandel et al. 2016). Cob is a type of earth construction, traditionally made of soil, water and straw. Cob buildings are known for their high thermal mass, leading to good passive thermal design when using thick external walls of 45 cm or thicker (Hamard et al. 2016; Ben-Alon et al. 2019). Cob is also significantly cheaper compared to standardised building materials (Quagliarini et al. 2010).

Unfortunately, cob construction is possibly on the edge of extinction. Earth architecture, in general, is slow and labour-intensive construction processes, while earth materials remain one of the least studied methods of construction (Gargiulo and Bergamasco 2006; Liu et al. 2010; Chandel, Sharma, and Marwah 2016; Hamard et al. 2016). Digital construction of earth materials could be key to promoting the reuse of earth construction in a modern context. Liu et al. (2010) and Chandel et al. (2016) have stated that it is important to develop more flexible modern construction systems that integrate features of vernacular architecture and sustainable construction techniques. In addition, Agustí-Juan et al. (2017) and Veliz Reyes et al. (2018) have demonstrated that sustainability potentials can be

achieved through the integration of digital fabrication techniques into earth-based materials in construction.

Agustí-Juan and Habert (2017) have highlighted the essential need for more research into the environmental benefits of additive manufacturing in construction while the technology still relatively experimental. In this respect, the feasibility of 3DP earth-based materials have been under investigation over the past few years by institutions such as the Institute for Advanced Architecture of Catalonia (IAAC) and Cardiff University (Veliz Reyes et al. 2019). WASP is an Italian company that has taken this investigation further and managed to produce prototypes of 3D printed earth-based houses (3D-WASP 2020) (Figure 2).



Figure 2. 3DP earth house by WASP 3D (3D-WASP 2020).

Despite these recent studies, there is a lack of definitive information on the construction workflow of 3DP cob buildings. The current experiments and applications of 3D printing of earthen materials are still in their early stages and remain fragmented (Brans, 2013; Wu et al., 2016). Moreover, the conducted investigations on the engineering properties (i.e. workability, extrudability, rheology), as well as the performance aspects (i.e. thermal, structural, and

environmental performance) of 3DP cob are very little. This lack of information or evidence would create reluctance in approving the technique in the modern construction industry by practitioners and the regulating authorities.

1.2 Research scope

Realising the promise that can be delivered by 3DP technologies to the building construction sector and understanding the various benefits of earth construction, this research focuses on exploring the potentials of a new digital-based earth construction technique, merging 3DP technologies with cob. The explorations have been conducted in the form of a feasibility study, where several material/ building performance aspects of the material underwent investigations to test the technique's viability for the modern construction industry. There are a number of performance aspects to be considered in such a study (as will be discussed in section 2.4); however, since 3DP cob technique is proposed as a sustainable construction technique, there are certain performance aspects that must be prioritised under the umbrella of sustainability. Hence, the research focuses on the fundamental performance aspects that explore material workability (i.e. material mechanical properties and structural performance) and the environmental performance aspects (i.e. thermal properties and environmental impacts).

1.3 Research aims and objectives

This research aims to develop new digital-driven knowledge on the use of cob within the 3D printing and robotic fabrication workflow for the buildings industry. This new

knowledge will be based on a comprehensive analysis of 3D printed cob structures for real-scale construction.

Four objectives have been set to achieve the main aim of the research. Each objective combines several sub-objectives, as follow:

- I. Objective 1:** To explore the geometrical potentials and possible limitations in the process of designing and fabricating 3D printed cob structures.
 - Objective 1.1: To investigate cob mixture's workability and extrudability within the 3D printing system.
 - Objective 1.2: To investigate the correlations between the material physical characteristics and the different techniques of material extrusion systems.

- II. Objective 2:** To investigate the structural capabilities of 3DP cob walls.
 - Objective 2.1: To define the basic mechanical properties of 3DP cob.
 - Objective 2.2: To evaluate the impact of wall section design on the load-bearing functionality of 3DP cob walls.
 - Objective 2.3: To develop a structural design framework for low-rise 3DP cob buildings.

- III. Objective 3:** To investigate the thermal performance of 3DP cob walls.
 - Objective 3.1: To define the thermal conductivity of 3DP cob walls and compare it to conventional cob walls.
 - Objective 3.2: To investigate the influence of wall section design of 3DP cob walls on the thermal conductivity.

IV. Objective 4: To investigate the environmental impacts of 3DP cob walls used in low-rise constructions.

- Objective 4.1: To compare the environmental impacts of 3DP cob walls to that of conventional cob walls using Life Cycle Assessment (LCA).
- Objective 4.2: To compare the environmental impacts of 3DP cob walls to that of 3DP concrete walls, and conventional reinforced concrete walls.

1.4 Research impacts

The outcome of this research is expected to bring 3D printed cob construction closer to full-scale applications. On a broader scale, the study contributes to the disciplines of architectural design and construction by providing a framework that will bridge the knowledge gap between earth construction and contemporary digital practice. The research is expected to provide practical guidelines for utilising 3DP cob technique in construction, which will enable stakeholders to make an informed decision on the selection of 3DP cob as a substitute to other 3DP techniques such as 3DP concrete. The research outcomes are therefore expected to provide the following key contributions:

- Providing fundamental understanding of the rheological behaviour and workability aspects of a revised cob mixture under a developed 3DP system.
- Establishing a structural design framework for 3DP cob buildings, which allows optimisation of 3DP wall designs based on the structural performance and material efficiency.

- Identifying the basic thermal performance characteristics of 3DP cob as a material, which allows optimisation of 3DP wall designs based on their thermal efficiency.
- Providing fundamental understanding of the associated environmental implications of 3DP cob construction, and how it compares to other conventional and 3DP techniques.

1.5 Research methods

This research has been conducted using a quantitative approach for data collection and production through physical experimentation and numerical simulations. The research has four lines of investigations, each corresponding to a fundamental performance aspect of 3DP cob as indicated in the research scope (1.2). Those four investigations are as follow:

- 1) Exploration of the geometrical and physical properties: this has been conducted through laboratory testing of the 3DP cob composite within the 3DP tools and systems.
- 2) Exploration of the structural performance: this has been conducted through laboratory testing of the 3DP cob samples under compression loads. The collected data are then used for numerical structural modelling using limit-state design (LSD) framework.
- 3) Exploration of the thermal properties: this has been conducted through laboratory testing of the 3DP cob samples using heat flow meters to determine the thermal conductivity of 3DP cob. The collected data can

facilitate the process of estimating the operational energy performance of 3DP cob houses using numerical simulation tools.

- 4) Exploration of the environmental impacts: this has been conducted by applying Life Cycle Assessment (LCA) as a method for estimating the associated environmental impacts with 3DP cob walls.

1.6 Thesis outline

This thesis is structured as a “thesis by publications”, which means, according to The University of Adelaide’s Graduate Centre (2020), it “*includes journal publications that have been published and / or accepted and / or submitted for publication, and / or unpublished and unsubmitted work prepared in manuscript-style*”. This thesis includes four manuscripts, two of which are published (Chapters 6 and 7), one is fully accepted (Chapter 4) and the last one is accepted with revisions (Chapter 5). Those four manuscripts all together form chapters 4 to 7, in correspondence with the four main investigations as stated in the research objectives section.

All the chapters in the thesis are presented as follows:

Chapter 1 provides a brief background to the thesis, which exhibits the research significance and key contributions to the field. The chapter then describes the aims and the objectives of the research, followed by defining the thesis outline.

Chapter 2 presents a comprehensive review of the recent literature in the fields of 3D printing technologies in construction and cob construction, with a particular focus on the aspects of feasibility assessment.

Chapter 3 outlines a brief methodology for the conducted investigations in the study. The study employed both experimental and numerical methods of investigations. Note that the details of the methods for each investigation are explained in each corresponding chapter.

Chapter 4 explores the basic correlations between the robotic 3D Printing system and the characteristics of cob as construction material. These explorations establish a fundamental understanding about the 3D printed material behaviour and how it affects the whole design and fabrication process under a robotic 3DP framework. This chapter presents an accepted paper for publishing:

Gomaa, M., Jabi, W., Veliz Reyes, A., Soebarto, V. 2020. Development of Large-scale Extrusion System for 3D Printing of Cob Walls. *The Journal of Automation in Construction*. (Accepted manuscript in October 2020).

Chapter 5 presents the experimental and modelling work to investigate the structural capacity of 3DP cob walls to act as load-bearing walls in low-rise buildings. The experimentation defines the basic mechanical properties of 3DP cob walls and provides a structural design framework and guideline for 3DP cob. This chapter presents an accepted paper for publishing:

Gomaa, M., Vaculik, J., Soebarto, V. & Griffith, M 2020. Feasibility of 3DP cob walls under compression loads in low-rise construction. *Journal of Construction and Building Materials*. (Accepted with minor revisions in November 2020).

Chapter 6 presents experimental work to investigate the thermal properties of 3DP cob. The thermal conductivity of various designs of 3DP cob walls was examined

and compared to other conventional cob samples. This chapter presents a published work:

Gomaa, M., Carfrae, J., Goodhew, Jabi, W., Veliz, A., 2019. Thermal performance exploration of 3D printed cob. *Architectural Science Review*, pp. 1–8. doi: 10.1080/00038628.2019.1606776.

Chapter 7 presents the final feasibility assessment of 3DP cob through a Life cycle assessment (LCA) using the cradle-to-site approach. The assessment establishes a comparison of the environmental impacts between 3DP cob construction and other 3D printing and conventional construction methods. This chapter presents a collaboration between two studies on 3DP cob and 3DP concrete respectively, resulting in a published paper:

Alhumayani, H., **Gomaa**, M., Soebarto, V., and Jabi, W. 2020. “Environmental Assessment of Large-Scale 3D Printing in Construction: A Comparative Study between Cob and Concrete.” *Journal of Cleaner Production*, June. <https://doi.org/10.1016/j.jclepro.2020.122463>

Chapter 8 discusses all the findings and concludes the final outcomes of the research. The major limitations of the research are also noted, along with recommendations for future studies.

Chapter 2 Literature Review

2.1 Introduction

This chapter reviews relevant literature in order to highlight existing gaps in knowledge about 3D printing technology in building construction, particularly of earth construction, from issues relating to fabrication to issues relating to assessing its environmental impacts. Four major fields of research will be reviewed as follows: (1) digital fabrication in construction, (2) sustainability potentials of 3D printing technology, (3) vernacular architecture and cob construction, and (4) building performance assessments. The sequence of the literature review is designed to establish a logical understanding on the emerging need to explore the feasibility of implementing 3DP cob construction in a modern context.

2.2 Digital fabrication in architecture

The never-ending quest of the construction industry for more complex forms and faster process has made traditional construction methods obsolete. The implementation of Computer Aided Manufacturing (CAM) and Computer Numerically Controlled (CNC) fabrication processes in the building industry have empowered designers with digitally driven solutions to achieve the desired complexity in their geometries (Soto et al. 2018). The term CNC, also commonly known as digital fabrication, includes two main categories: 2D fabrication and 3D fabrication. The 2D fabrication technique is basically the CNC cutting technologies, such as laser or water-jet nozzles, where the motion of the cutting head involves only two axes. The 3D fabrication techniques include four subcategories of fabrication:

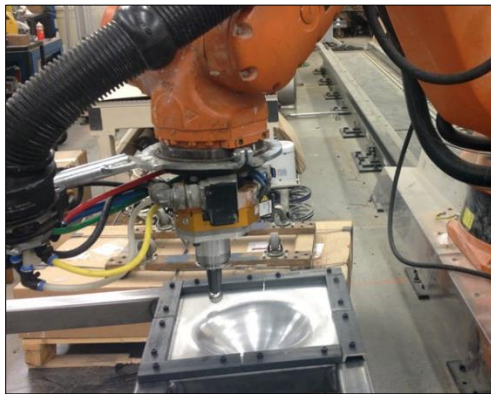
subtractive, additive, formative and assembly (Figure 3). The Additive Fabrication / Manufacturing (AF/AM) is defined as the method of creating geometries by materials in a layer-by-layer fashion (Kolarevic 2001). A study by Hague et al. (2003) has classified the approaches to digital fabrication in two categories, reductive (milling, cutting, and eroding) and additive fabrication (3D printing and assembly).



(1)



(2)



(3)



(4)

Figure 3. Different types of 3D digital fabrication techniques: 1) Additive (3D-WASP 2020); 2) Subtractive; 3) Formative (Kalo 2020); 4) Assembly (Kohler 2006).

Additive manufacturing techniques, and 3D printing techniques specifically, are currently receiving a growing interest within many industries worldwide (Wu, Wang, and Wang 2016; Hague, Campbell, and Dickens 2003). There has been a dramatic increase in recent years in the amount of research on implementing 3D printing into

large-scale processes, which has revealed many potential applications for architecture and the construction industry (Wu, Wang, and Wang 2016; Agustí-Juan and Habert 2017).

2.2.1 Implementing additive manufacturing in construction

The perception of the modern construction industry has changed as the industry has been actively participating in Additive Manufacturing (AM) and 3D printing (Rayna and Striukova 2016; Wu, Wang, and Wang 2016). In recent years, there have been multiple attempts in the construction industry to use 3D printing technologies, which has led to a substantial enhancement of large-scale 3-D printing techniques for building components (Ishak, Fisher, and Larochelle 2016; Wu, Wang, and Wang 2016; Baumers et al. 2016). According to Hamard et al. (2016), the recent engagement between industrial robotic arms and existing AM technologies has boosted the capabilities of the 3D printing process and offered significant solutions to the current limitations in conventional gantry-style 3D printers. In addition, Lim et al. (2016) has pointed out that using 3D robotic printing methods can increase printing quality (finishing), shorten printing time, and enhance surface strengths. Several universities and companies around the world such as the Swiss Federal Institute of Technology (ETH), the Institute for advanced architecture of Catalonia (IAAC), WASP© (Italy), Api-Cor© (Russia), CyBe© (Netherlands), and Winsun© (China) are aggressively upscaling the 3D printing process to produce full-scale construction (Hager, Golonka, and Putanowicz 2016; Geneidy, Ismaeel, and Abbas 2019). In 2019, both Apis-Cor and CyBe managed to build two of the largest 3D printed concrete buildings in the world (Figure 4). Just in 2020, CyBe©, which

specialises in developing large-scale concrete 3DP systems for on-site construction, has been contracted by eight institutions around the world to supply concrete 3DP systems.



Figure 4. 3DP building in Dubai by Apis-cor (Apis-cor 2019)(Left) and 3DP house in Saudi Arabia by CyBe (CyBe 2019) (Right).

Despite the demonstrated benefits of AM and 3DP in the construction industry, there are a few shortcomings in the technology that still require further research and technological developments. Craveiro et al. (2019) highlights that 3DP technology still requires intense development of current construction materials to adapt to the 3DP process. In addition, these revised materials will require new codes and standards of practice. Further research should also investigate the basic material characteristics such as physical, mechanical, thermal, and structural properties. On the other hand, Baumers et al. (2016), Wu, Wang, and Wang (2016) and Craveiro et al. (2019) have demonstrated that current 3DP technologies have limitations in producing certain construction components on large scale in terms of shape and topology, where fabricating large non-supported horizontal structures (i.e. ceilings and roofs) in addition to vertical voids/ openings (i.e. windows and doors) are still a great challenge to the technology.

Further challenges to 3DP were pointed out by Ngo et al. (2018) in his study, where he demonstrated that the design to fabrication process still suffers from a level of divergent, as the 3D printed models can exhibit some defects as compared to the numerical models, which happen particularly in curved surfaces. In addition, the nature of the layer-by-layer printing process causes an anisotropic behaviour in the mechanical properties of the material, which means that the microstructure of the material inside each layer is different as compared to that at the contact surfaces between layers. Another challenge is the corrugated appearance of the surface finishing due the nature of additive manufacturing, where in buildings flat-finished surfaces are often preferred due to its better functionality (Geneidy et al. 2019).

2.2.2 Sustainability of additive manufacturing

Sustainability, as a holistic concept, incorporates three main aspects: environment, society, and economy. The construction industry has a significant influence in all three aspects of sustainability (Ding 2008; Zabihi, Habib, and Mirsaedie 2012). The rapid emergence of AM in contemporary construction is causing an urge to investigate the influence of AM on sustainability (Ford and Despeisse 2016).

Ford and Despeisse (2016) and Agustí-Juan and Habert (2017) have demonstrated in their studies that the adoption of AM in modern industries has three significant sustainability benefits. Firstly, it offers an improved efficiency of resources implementation during production and use phase, with an estimated 25-60% in material reduction and 30 % time saving as compared to traditional manufacturing techniques. Secondly, it potentially extends product life as processes such as repair and refurbishment become easier from a technical perspective. Third, it reconfigures

value chains, as AM provides shorter and simpler and more localised production and supply chains. According to Soto et al. (2018), leveraging AM in construction leads to shorter workflow, with great design adjustability in late stage of the process for less cost as compared to conventional construction. However, this improved cost efficiency is subject to complexity level of construction. Both Agustí-Juan et al. (2017) and Soto et al. (2018) demonstrated in their studies that conventional construction outperforms AM in terms of cost, and even environmental efficiency, when building simpler geometries.

Looking into the aspect of environmental sustainability (which is the focus of this research), most current research and application of 3D printing technology in construction are heavily concentrated on using concrete and cement-based materials (Siddika et al. 2019; Geneidy, Ismaeel, and Abbas 2019; Ngo et al. 2018; Shakor et al. 2019). This raises concerns over the sustainability of using concrete and cement in 3D printing (Kajaste and Hurme 2016) because cement production is well known for its high CO₂ emissions, with a 4 % contribution to fossil fuel emissions and 8 % to global CO₂ emission per year (Andrew 2019). Agustí-Juan et al. (2017) supports this by stating that the use of concrete and cement in 3D printing may result in buildings with high embodied energy and environmental impact. All this contributes to the negative influence of the building and construction industry, as it accounts for 40% of the CO₂ emissions and 36% of global fine energy use according to IEA and UNEP in (2018).

The pursuit of a highly automated construction process combined with the need for building material with low environmental impacts has encouraged re-approaching

earth materials in modern construction. Hamard et al. (2016) and Chandel, Sharma, and Marwah (2016) stated that the integration of vernacular architecture into modern construction can enhance the environmental performance of buildings due to the improved energy efficiency. Dili, Naseer, and Zacharia Varghese (2010) discussed the passive features of vernacular architecture and demonstrated that it leads to a comfortable indoor environment without the input of air conditioning equipment. As a result, this improves the operational energy in buildings since it reduces the energy demand for heating and cooling. Praseeda, Mani, and Reddy (2014) revisited and corrected the previous statement by demonstrating in his study that the operational energy efficiency of vernacular buildings is strongly influenced by the project location and the climate conditions.

Furthermore, improving the thermal performance of cob walls usually requires larger thicknesses of walls due to its large thermal mass, which then increases the embodied energy as it involves consuming more raw material (Hamard et al. 2016; Chandel, Sharma, and Marwah 2016). Generally, on the aspect of embodied energy, modern construction materials such as concrete tend to have higher embodied energy as compared to this of vernacular materials (Shukla, Tiwari, and Sodha 2009). Yet, this statement is subject to the sourcing location of the raw material, where transportation strongly contributes to the total embodied energy of materials. In a recent a study by Alhumayani et al. (2020), a cob building was shown to have 80% less embodied energy as compared to a conventional concrete structure for the same construction location.

Despite all the claimed benefits that AM promises to offer to sustainability, the three aspects of sustainability are still considered in need of further exploration. To date, investigations into the sustainability of AM have been either focused on the environmental aspect (Baumers et al. 2016; Agustí-Juan and Habert 2017; Alhumayani et al. 2020) or more recently on the economic aspects (Soto et al. 2018; De Schutter et al. 2018), both applied on limited scales. In addition, research on assessing the social implications of implementing AM in construction is still lacking (Soto et al. 2018; Kothman and Faber 2016; Ford and Despeisse 2016).

2.3 Cob construction

Moving from the subject of AM, this section discusses and reviews the topic of vernacular architecture in which cob architecture sits, which is essential to provide some basic understanding before reviewing the application of entwining AM and cob construction.

2.3.1 Vernacular architecture

Vernacular architecture is an architectural style based on three main pillars; local materials, local needs, and skills of local builders. The perception of vernacular architecture has been evolving to reflect different environmental, technological and cultural contexts (Niroumand, Barceló Álvarez, and Saaly 2016). Vernacular architecture offers potential solutions for several problems associated with buildings, such as high CO₂ emissions, high embodied energy of construction process, and the depletion of natural resources (Benardos et al., 2014; Chandel, Sharma, and Marwah 2016). However, in a modern context, the environmental performance of vernacular

buildings and techniques must still be assessed, most likely under the umbrella of a life cycle analysis (LCA) (Häfliger et al. 2017; Agustí-Juan and Habert 2017). It is critical to consider the associated impacts of sourcing both the raw material and the skilled labour, where remote sourcing greatly influences the overall environmental performance of a vernacular construction due to transportation of the materials. Transportation is considered one of the major contributors to the environmental impacts of construction processes (Alhumayani et al. 2020).

Earthen materials constructions, used in some vernacular buildings, have received a renewed interest in the past few years because, in fact, they provide potential solutions for the current environmental issues associated with conventional concrete construction. Raw-earth materials are environmentally friendly and highly bio-sustainable due to requiring limited amount of energy to produce and construct (Martín, Mazarrón, and Cañas 2010). However, the energy efficiency of the construction process of earth materials is also location-dependent, where transportation of raw materials plays a critical role in determining the embodied energy of the construction process (Arrigoni et al. 2017; Alhumayani et al. 2020). On the other hand, historical earth buildings do not necessarily provide the same thermal efficiency as compared to some modern brickwork or light-weight concrete block walls (Quagliarini et al. 2010; Martín, Mazarrón, and Cañas 2010). For instance, a traditional 600 mm cob wall has a U -value of $0.65 \text{ W/m}^2\text{K}$, which is nearly double the acceptable value ($0.35 \text{ W/m}^2\text{K}$) for external walls by modern standards (Butler 2012), while for rammed earth walls a typical 300-400 mm walls have U -values vary between 1.55 to $1.89 \text{ W/m}^2\text{K}$ (Hall and Allinson 2009).

The explanation of why earth walls had a historic reputation of being thermally efficient in both winter and summer lies in their large thermal mass, which causes a slow temperature cycling from the outdoor environment to the indoor. Thermal mass is a time dependent thermal behaviour, where the U-value on the other hand, is relevant to the steady-state case (Goodhew and Griffiths 2005; Reardon, Caitlin, and Geoff 2013). Yet, interestingly, Fox et al. (2019) in his study proposed newly designed mixtures for earth-based walls that have lowered U-values, varying between 0.34 to 0.14 W/m²K, which meet modern building regulation requirements.

Several authors such as Liu et al. (2010) and Chandel, Sharma, and Marwah (2016) have highlighted another importance of the energy efficient characteristics in earth constructions. Most earth constructions have very low embodied energy as compared to other conventional materials in construction such as concrete and masonry (Hamard et al. 2016). Morton et al. (2005) highlighted in his comprehensive investigation on the CO₂ emissions of earth masonry in modern wall construction that earth bricks had much lower level of embodied energy compared to other modern masonry materials (Figure 5). These findings mean that a house made of earth walls with an area of 92 m² can achieve a reduction of 14 tons of CO₂ emissions compared to aerated concrete blocks. Moreover, according to Pacheco-Torgal and Jalali (2012), an estimated reduction of 100 thousands tons of CO₂ emissions every year could be achieved just by replacing 5% of concrete block masonries by earth masonry (the case of UK).

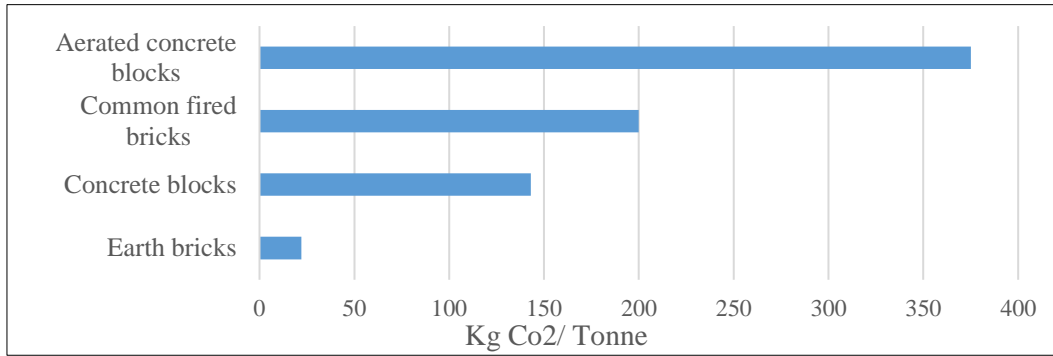


Figure 5 The Embodied carbon in different masonry materials (Morton et al. 2005)

2.3.2 Traditional cob construction

Cob stands as one of many methods of vernacular earth construction (Figure 6). Cob is a natural building material that consists of subsoil (earth), water, fibre material (typically straw), and sometimes lime. Sand and clay could be also added if required (Robert, 2009; Hamard et al. 2016). Cob is inexpensive and fireproof, while being durable and resistant to weathering (Keefe 2005). Cob surpasses other earthen materials techniques such as adobe and rammed earth as it provides higher freedom of design and ease of construction. The basic difference between Cob and other techniques is that Cob constructions are built while the mixture is wet, giving more freedom to form organic shapes and curved geometries. Cob also gives the ability to modify by cutting out or adding on easily at any time, even after being dry (matching perfectly with the 3D printing techniques, as will be discussed later). Adobe walls, on the contrary, are built as dried blocks that have to be dried first in the sun (Evans et al., 2002).



Figure 6. Cob building in Totnes, UK (Veliz Reyes et al. 2018) (left); and Keppel Gate cob house in Devon, UK by Kevin McCabe (McCabe 2020)

Another study by Hamard et al. (2016) shows different classifications of the earthen materials construction process. The most appropriate classification is the one based on the distinction between wet and dry compaction methods of producing the mixtures and constructing the geometries. The wet process describes the use of earthen materials at a plastic state, where the mechanical strength of the structure is created through the drying shrinkage densification, like Cob and Adobe constructions. The dry process, on the other hand, describes the use of earth mixtures after reaching the optimum water content and mechanical strength compaction densification (Compressed Earth Block and rammed earth) before being placed into the construction (Hamard et al. 2016).

Cob bricks can be used to build a single-story wall while it is still wet. However, it is recommended that to build with wet cob, and maintain good mechanical performance, the construction process should be proceeded as a layer by layer technique (like 3D Printing). Each layer (lifts) should not exceed 0.5-0.7 m height before proceeding with the next layer, meaning there will be waiting time for each

lift to dry. The continuity between the dried and wet layer of cob wall is guaranteed due to the high friction coefficient between different surfaces (Quagliarini et al. 2010).

The structural system for cob construction in multi-story buildings usually comprises timber framing for floors and roofs. The roofs are sloped with eaves for rain protection. The walls traditionally have a thickness of 60 cm (600 mm) on average, while the thicknesses of the walls vary according to the expected loads and the number of stories (Quagliarini et al. 2010; Weismann and Bryce 2006). Cob wall thickness increases proportionally with the number of stories or the height of the building, where also the wall can taper to be thicker at the bottom and thinner at the top. For example, a two story cob house will have a wall thickness of 60 cm at the bottom (Earth Devon 2008), and it can reach up to 150 cm thick at the bottom for a three-story cob house (Hamard et al. 2016). The determination of the required thickness also takes in consideration the concentration of loads in the wall, such as sections under the bearings of floor beams or between two large openings, where the thickness must be larger to withstand the higher loads (Earth Devon 2008).

The mechanical properties of cob depend on several factors: subsoil properties, water content, the use of fibres, and the quality of craftsmanship. In a cob construction, the load-bearing capacity of cob walls (usually represented as the compressive strength) is considered a fundamental mechanical property (Quagliarini et al. 2010; Pullen and Scholz 2011). Cob walls are designed with large wall thickness to increase the compressive strength in cob construction. However, when compared to concrete or other types of masonry, cob construction has a dramatically lower compressive

strength (Earth Devon 2008). Cob compressive strength can reach a maximum of 1.4 MPa (Miccoli, Müller, and Fontana 2014), while the minimum compressive strength of concrete with the same dimension is 17 MPa and can reach up to 70 MPa (NRMCA 2020).

2.3.3 3D Printed earth construction

Several prototypes of digitally manufactured earth have emerged in recent years to explore the potentials of reviving earth material in the modern construction context. The Italian company WASP (3D-WASP 2020) has been working actively on developing 3DP printers of clay and earth materials for several years. In 2018, WASP presented the first 3DP earth house using their new 3D printer Crane WASP© (Figure 7). The house was entirely printed onsite using locally available material and took 10 days to print all its 30 square meters of walls. The earth composite combined subsoil, water, rice straw, rice husk, and lime. Rice straw was also used to fill the inner voids in the walls for added insulation. However, the house design did not utilise the printed cob walls as load-bearing walls, where it used timber frames to support the roof loads.



Figure 7. Earth house prototype by WASP in Italy (left), and the 3D printing system of earth (Right)(3D-WASP 2020).

In 2018, Perrot et al. (2018a) conducted a study which is considered the first published attempt to explore the structural performance aspect of 3DP earth material. The material composite was made from a mix of earth material and alginate seaweed biopolymer (as a substitute for straw). The study demonstrated the ability for 3DP cob to act as load bearing construction member. Yet, the study also suggested that 3DP of earth material still requires further exploration for different mixtures, and also pointed out the importance of improving the 3DP printing tools.

To date, most of the research on 3DP in construction is focused on using cement and clay-based materials, which consequently led to an accelerated development of the 3D printing tools and systems for these specific materials (Geneidy, Ismaeel, and Abbas 2019; Shakor et al. 2019). This continuous development in the 3DP systems has improved the quality and productivity of 3DP concrete construction over the years. Yet, as this was not the case for earth-based materials, the 3DP systems for cob still suffers major challenges and limitations that must be overcome before 3DP cob is introduced as a viable construction method (Francis 2018; Veliz Reyes et al. 2018).

2.4 Building performance

To understand how 3D printed cob construction performs, it is important to address the issue of building performance. The concept of building performance has been used for many years in academia and the building industry. Its importance comes from the role it plays in designing new buildings, as well as refurbishing the existing ones, when it comes to making decisions to improve the efficiency of the built environment. Several international standards have been created to address and

describe the standards of building performance such as ISO 9836:2017, ISO 52000:2017 and ISO 15392:2019. Nowadays, there are many disciplines that are concerned with building performance aspects and its analysis methods (de Wilde 2018). In addition, modern construction industry has been strongly focused on performance and efficiency, driven by the need to make processes, products and human activities better. The Oxford English Dictionary (2010) defines performance as “the action or process of performing a task or function”.

Buildings are complex systems that reflect different types of functions. Building performance can be approached from either a technical or an aesthetic perspective (de Wilde 2018). In both approaches, a building must be designed to exhibit high efficiency between its range of functions. All functions must work together to provide the following benefits:

1. Ensure safety of occupants through an adequate structural system.
2. Protect inhabitants from environmental condition and provide comfort.
3. Deliver good investment and economical returns.

The technical performance approach relates to aspects where the building responds to external innervation, such as structural loading and weather conditions. According to de Wilde (2018) a building must perform a range of functions; building performance, then, measures how well the building carries out those functions. de Wilde (2018) defines building performance as:

“Building performance relates to either a building as an object, or to building as construction process. There are three main views of the concept: an engineering, process and aesthetic perspective. The engineering view is

concerned with how well a building performs its tasks and functions. The process view is concerned with how well the construction process delivers buildings. The aesthetic view is concerned with the success of buildings as a form for presentation or appreciation.”

From an architectural point of view, building performance covers a wide domain of technical aspects such as structural and thermal performance (Kolarevic and Malkawi 2005; Bakens, Foliente, and Jasuja 2005). Moreover, the rising fears of the ever-diminishing resources such as material, energy and money have brought several other technical aspects of performance to the light, such as energy efficiency, environmental impacts, and productivity, which together form key aspects later of life cycle assessment of the building (Hitchcock 2002).

Both Preiser and Vischer (2005) and Becker (2008) in their studies stated a list of priorities for building performance aspects which includes health, safety, security, comfort, function, efficiency, durability, sustainability and aesthetic. Performance aspects can be represented as categories. Hartkopf, Loftness, and Mill (1986) demonstrated those categories of performance aspects as follows:

- 1) Building integrity: such as structural loads, moisture, temperature, fire, natural disasters.
- 2) Thermal performance: such as air temperature, humidity and air speed.
- 3) Indoor air quality: such as fresh air and pollutants.
- 4) Spatial performance: such as the layout of spaces, services and amenities, occupants' convenience.

- 5) Acoustical performance: such as sound source, sound path, and sound receivers.
- 6) Visual performance: such as lighting, contrast and brightness.

According to Deru and Torcellini (2005), it is critical to consider that each building has its own specific reason for being, which must correspond with selected performance aspects for analysis. Hence, selecting performance aspects must start with a clear vision of the envisaged goals and objectives of the performance analysis. In addition, the performance requirements are not necessarily associated with the whole building. It can only relate to parts of the building such as a building component or a specific system (CIB Working Commission 1982). Kolarevic and Malkawi (2005) supported this by stating that the review of building performance requirements must be within a context of a specific interest.

This research mainly focuses on the workability and sustainability of 3DP cob within a modern context. Hence, the selected performance aspects must correspond to the study specific interest. This research is an early feasibility stage of a new construction technique, where technicality of the material performance itself is essential to establish design foundations. This means that performance aspects such as structural performance and thermal/energy performance play a more critical role at this stage than the other performance aspects in the previously mentioned list by Hartkopf, Loftness, and Mill (1986).

2.4.1 Structural performance

For centuries, humans have designed numerous types of constructions to facilitate their life and meet their needs. From the beginning, it has become clear that dealing

with the statics and mechanics of material is essential, which led to the emergence of the early principles of structural analysis and design. This was not exclusive to the building industry, but was applied to a wide variety of systems such as the automotive and aerospace industries (Rajan 2001). The past 150 years has witnessed revolutionary developments in the field of structural engineering, and over the years, these developments have led to tremendous enhancements in the use of construction materials and in analysing their performance. As the construction methods improve, so do the analysis techniques. The need for an early imitation of the imagined structures on paper has grown. By the 1950s, the advent of modern computers made it possible to analyse more complex structural systems accurately and efficiently (Rajan 2001). The term finite element analysis emerged as a good example of utilising computational power, which was followed by the evolution of several other numerical techniques that enabled solving and optimising structural problems.

The primary role of structural analysis is to calculate the actions and responses that happen to a structure while being exposed to a set of external environmental forces such as mechanical loads, imposed deformations, and settlements of supports. According to Khalfallah (2018), there is a number of important common features of structural performance during the design phase, which are as follows:

- 1) Internal forces: axial force, shear force, bending moment and torsion moment.
- 2) Reaction from structure support.
- 3) Deflections due to external loads.

Building structures must be designed to withstand the multiple types of loads applied to them. Further to the previous three classifications, the loads on a structure can be alternatively classified into five families (Khalfallah 2018):

- 1) Mechanical loads: usually represents the permanent loads applied to the structure (i.e. structure system own weight, deadloads).
- 2) Thermal loads: described as the impact of temperature variations on the structural elements.
- 3) Environmental loads: represents loads from the external environment conditions such as wind and snow.
- 4) Seismic or dynamic loads: usually represent the force at the base of a construction due to the transmission of seismic waves from the ground to the construction.

A structural and/or civil engineer must carefully evaluate all of the actions that potentially impact the studied structure. While the classical methods of calculating and analysing structural performance has limitations, the evolution of computer-based techniques has led to a huge development in the analysis methods. In general, the purpose of both the classical and computer-based structural analysis is to ensure that the structural design meets the criteria of resistance and economy simultaneously (Khalfallah 2018).

2.4.2 Thermal and energy performance

Buildings are considered large consumers of energy worldwide, with a rapidly growing demand for energy to make it functional and comfortable for occupants. Most of the energy consumption in the building is associated with achieving thermal comfort (Balaji, Mani, and Venkatarama Reddy 2013). Thus, the need for energy saving design and strategies in buildings that can also ensure comfort have been gaining an increased attention over the past decades. The building envelope consists of a configuration of building materials, and the thermal properties of these building materials have a critical role in achieving comfort and energy efficient design (Balaji, Mani, and Venkatarama Reddy 2013).

The thermal properties of a material are the properties that describe the material's behaviour when it is subject to heat transfer. Thermal properties come under the broader topic of the physical properties of materials. According to Clarke, Yaneske, and Pinney (1990), the fundamental thermo-physical properties of a certain material are:

- 1) Thermal conductivity (W/mK).
- 2) Specific heat capacity (J/kgK).
- 3) Density (kg/m³).

Thermal conductivity refers to the intrinsic ability of a material to transfer or conduct heat. It is one of the three methods of heat transfer, besides convection and radiation (de Wilde 2018). Specific heat, on the other hand, is the amount of heat per unit mass of a material required to raise the temperature by one degree Celsius. Defining the thermal conductivity, specific heat and density of a material is an essential step to

estimate the thermal performance of the building and how it will influence the thermal comfort of the occupants or the energy use of the building (CIBSE 2015; Balaji, Mani, and Venkatarama Reddy 2013; Gomaa et al. 2019).

Nowadays, the common method of estimating thermal comfort and energy consumption in buildings depends on analysing the thermal performance of the building via experimentation or modelling tools (de Wilde 2018). These modelling tools utilise the basic thermal properties of materials to measure all the possible heat exchanges between the building envelope and its surroundings. This then helps estimate the energy demand of the building through calculating the expected cooling and heating loads (Becker 2008). Thermal modelling software depends on sophisticated algorithms that use the thermo-physical properties of materials, as well as the local weather data, to calculate the expected building's thermal performance. This consequently enables assessing the potentials of energy efficiency and thermal comfort in buildings (Becker 2008).

The early understanding of the building material's impact on thermal performance is essential to determine energy efficient materials and strategies from the early stages of the building design (Joseph, Jose, and Habeeb 2015). In addition, it is also used in existing buildings as a tool for energy efficient retrofitting, or in other cases for the energy rating processes of buildings (Soebarto & Williamson, 2001; Freney 2014). Analysing the thermal performance requires knowledge of the heat flow processes through various building elements such as walls, roof, door, windows, etc.

A building consumes two types of energy during its entire life cycle; embodied energy and operational energy. The embodied energy refers to the consumed energy

during the extraction of materials, production, construction and maintenance phases, as well as demolition and disposal at the end of building life. The operational energy, on the other hand, refers to the consumed energy during the use of the building, such as the energy demands for heating, cooling and electricity (Iddon and Firth 2013; Hollberg and Ruth 2016; Ortiz, Castells, and Sonnemann 2009). Strict building regulations that aim to reduce the operational energy in buildings have been actively implemented by many governments around the world during the past few years. These implemented measures have caused a shift in the ratio of embodied energy to operational energy through the building life cycle (Hollberg and Ruth 2016).

2.4.3 Life Cycle Assessment

The environmental implications of the construction industry have come into focus during the past few years. The term Life Cycle Assessment (LCA) has been used extensively since the 1990s as tool for decision makers, basically to assess the resources, the energy flows, and the environmental performance associated with the life cycle of certain product (Ekvall and Finnveden 2001; Nilsson and Eckerberg, 2007; Finnveden et al. 2009). According to Cabeza et al. (2014) and Finnveden et al. (2009), the life cycle has four main phases; (1) raw materials extraction. 2) Manufacturing (includes transportation). (3) The use/ operation phase. (4) The end-of-life phase, which includes the disposal and/or recycling (Figure 8).



Figure 8. The construction Life cycle (nordic.saint-gobain, 2017)

The International Organisation for Standardisation (ISO) has been publishing a range of standards to guide LCA studies such as ISO 14040, ISO 14041 and ISO 14044, which describes many aspects of LCA practices. Generally, LCA study consists of four main phases (Figure 9):

- 1) **Goal and Scope Definition:** This phase explains the reason to conduct the study, while it defines the desired application, the system boundaries, the chosen functional unit and intended audiences (Finkbeiner et al. 2006; Cabeza et al. 2014). The functional unit has two types; “Whole building” and “Building materials component combination” (Kotaji et al. 2003). Within the building materials component combination type, the functional unit is defined as an appropriate numerical measure of the functions that the goods (or service) provide (Finnveden et al. 2009; Cabeza et al. 2014).

- 2) Life Cycle Inventory (LCI): This is the phase where all the materials/resources and energy that flow within the life cycle stages are counted and quantified as inputs, then all the associated emissions to air, water and soil per each input are calculated as outputs, all in relation to the functional unit.
- 3) Life Cycle Impact Assessment (LCIA): This phase aims to evaluate the significance of the possible environmental impact “indicators” (such as global warming, ozone depletion, land use, water use) during the LCI stage.
- 4) Interpretation: This final phase aims to evaluate all the data from the LCI and LCIA phases in order to discuss the assumptions and limitations, state conclusions and draw recommendations (Finkbeiner et al. 2006; Finnveden et al. 2009; Ekvall and Finnveden 2001).

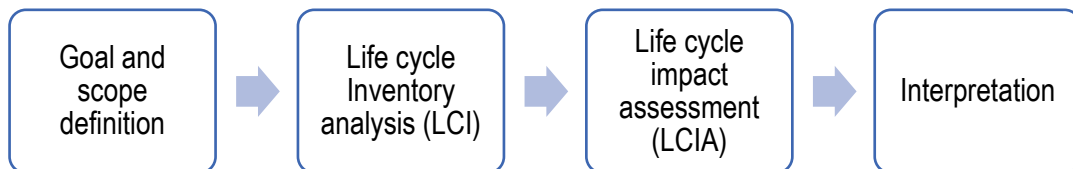


Figure 9. The main four phases of LCA study

Most of the current LCA studies on buildings focus on the external envelope, specifically external walls as it forms the majority of building envelopes and have greater effect on the building operational energy (Ingrao et al. 2016). A study by Agustí-Juan and Habert (2017) has conducted an LCA comparison between digitally fabricated and conventional building elements; wall, floor and ceiling. The digital fabrication wall and ceiling were constructed using in-situ robot arm (assembly technique), while the conventional elements were built using conventional methods and had the same size. The study’s main conclusion showed that the use of digital fabrication technologies can save raw materials as compared to the conventional

methods, which consequently reduces the environmental impact. The study also highlighted that extra functions (e.g. structural, environmental functions) in the digitally fabricated construction has high potentials to reduce the overall environmental impacts, as these added functions increase the total value. However, these added functions may require more materials, which will be disadvantageous from an environmental point of view.

Another study was conducted by Agustí-Juan et al. (2017) that compared a 3D printed concrete wall to a conventional concrete wall. The evaluation mainly concentrated on the impact of complexity level of the wall geometry. The study performed an LCA analysis from cradle-to-gate stages which included data from materials extraction and production, digital technologies production, and robotic 3DP operation. The results of the study showed that significant environmental benefits are achieved by using digital fabrication for structures with a high level of complexity. However, it is highly recommended to conduct further research on improving the environmental benefits with a lower level of complexity so that it would compete more effectively with the conventional methods.

Evaluating and optimising the environmental performance of the building sector has become essential. Consequently, LCA has become a widely used methodology in the construction industry over the past 20 years to evaluate the impacts of materials, construction elements, and buildings during their life cycle (Hoxha et al. 2014; Ortiz, Castells, and Sonnemann 2009). It is highly recommended to implement LCA studies during the early stages of architectural design, as a way to build an informed estimation of the associated environmental impacts to the project. Recently, several

studies have been conducted on investigating the environmental performance of building and construction materials through LCA. These studies aim to empower the decision makers with the essential information for the selection of materials and technical solutions according to its associated environmental impacts (Singh et al. 2011; Cabeza et al. 2014; Ingrao et al. 2016).

2.5 Identifying research gaps

The review of the literature has highlighted the importance of developing 3D printing systems that integrate the sustainability features of vernacular architecture and innovative digital construction techniques. Despite the dramatic adoption rate of concrete 3D printing in construction in the recent years, the development of earth materials 3D printing in construction still suffers a considerable gap, with several major applicability challenges to encounter. The research gaps can be summarised as follows:

- 1) The current experiments on 3DP cob are still in their early stages and remain fragmented. The known examples of 3DP cob structures are constructed mainly as showcases of the technology capabilities, while the actual performance aspects (i.e. thermal, structural) are poorly investigated, with no published information on the systematic testing for these aspects.
- 2) There is also lack of definitive information on the material processing and workability within a 3DP system framework, and the correlations between material properties and the 3DP tools, which together should provide critical information for enhancing the applicability and productivity of 3DP cob technique in modern construction.

- 3) There is a lack of definitive information on the mechanical properties of 3DP cob buildings, which consequently would create reluctance in adopting the technique in modern construction. To date, only one published study has been conducted to investigate the engineering properties of 3DP cob. Yet, there are no published works that establish design guidelines or a code of practice for 3DP cob.
- 4) The potential benefits of 3DP cob for operational energy saving in buildings have not yet been explored. These benefits could be expressed as the thermal efficiency of 3DP cob represented by its thermal conductivity. This aspect reflects the required energy for cooling or heating in a 3DP house, which will facilitate the comparison with other types of construction materials, leading to an informed decision making on how and when to use 3DP cob in construction.
- 5) In general, there is an essential need for more research into the environmental benefits of additive manufacturing in construction while the technology is still relatively experimental. Hence, Life Cycle Assessment (LCA) studies have become a must, as a mean to build an informed estimation of the environmental impacts. This directly applies to 3DP cob, where there are no studies on its environmental impacts.

This work aims to address all of the previous research gaps through the described methodologies in the following chapter.

Chapter 3 Research Methodology

In order to achieve the objectives of this research, several research methods were leveraged to acquire the missing knowledge in the literature. This research adopts a quantitative approach that depends on experimentation and numerical simulations for data collection and production. The research consists of four lines of investigation, covering the chapters from 4 to 7. Each line/ chapter utilises specific methodologies that fit its objectives. The detailed methodology for each line of investigation will be explained thoroughly in each corresponding chapter.

In general, all the four investigations in this research utilise the same cob mixture and 3D Printing tools, which were used for the prototyping of the tests' specimens. The formulation process of cob mixtures follows the recommended recipes by Weismann and Bryce (2006) and Hamard et al. (2016). The traditional recipe for a cob mix consists of 78% subsoil, 20% water and 2% fibre (straw) by weight.. The subsoil properties itself is recommended as 15–25% clay (wet) to 75–85% aggregate/sand. The subsoil and the straw for this research are both sourced from Cardiff in UK. This recipe will be tested and refined to match the requirements of the 3DP system.

A 3D printing system usually consists of two devices: the motion controller and the material extruder) (*Figure 10*). This research uses a 6-axes KUKA KR60 HA robotic arm as the motion controller, programmed by Rhinoceros via Grasshopper package and KUKA PRC® for robotic control. As for the material extrusion, the study utilises electromechanical ram extruders in different mounting styles as shown in *Figure 10*

(left and right). The arrangement of the selected methods for each chapter is summarised in the below sections.

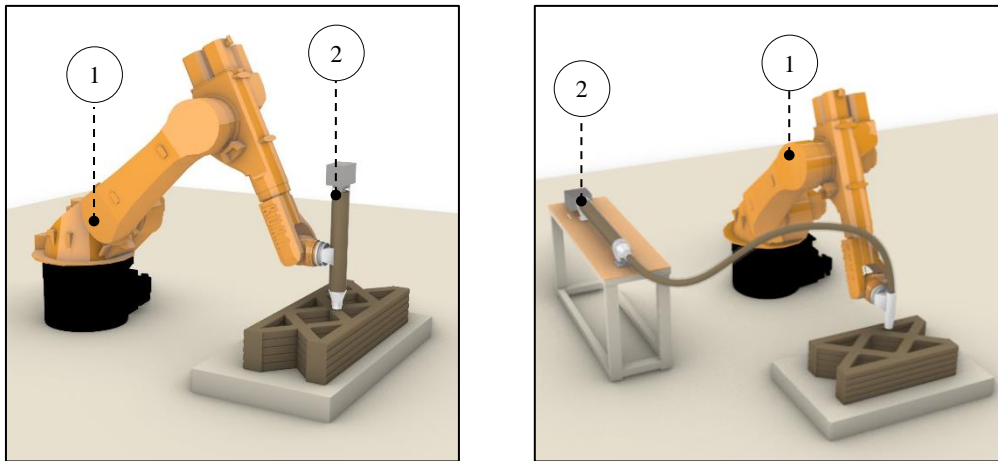


Figure 10. diagram of the 3D printing system. 1) The KUKA kr60 HA robotic arm, 2) the material extruder as mounted on the robot (left) and as stationary (right).

3.1 Exploration of the geometrical and physical properties

This investigation starts by experimenting with the correlations between the material mixture and the 3DP system. This is approached through the following methods:

- 1) *Testing of extrusion systems*: where different pneumatic and electromechanical extrusion systems are tested to determine the most suitable system for cob extrusion.
- 2) *Testing of the material mix workability*: this involves a systematic testing of correlations between 3D printing workability parameters such as: 1) Extrusion rate; 2) Robotic arm motion speed; 3) Nozzle size; 5) Layer height; and 6) printing path width.
- 3) *Prototyping of geometries*: this involves exploration of various geometries to examine the capabilities and challenges of the 3D printing system.

3.2 Exploration of the structural properties

This phase involves both experimental testing and numerical simulations and optimisation to obtain the compressive characteristics of 3DP cob walls. The testing in this investigation has three phases:

- 1) Conducting a standard compression test using a Dartec universal testing machine, following the standardised procedure in EN 772-1 (CEN 2011). The investigation uses three 3DP cob specimens shaped as cylinders of 400 mm tall and 200 mm in diameter (Figure 11)
- 2) Applying a numerical structural modelling using limit-state design (LSD) framework. The structural analysis will consider only design actions from gravity loads, while it will exclude possible loads from the wind or earthquake. The analysis involved three prototypes of 3DP cob walls (Figure 12). Those prototypes' designs are chosen to represent three of the most common wall sections in the current 3D printing in the construction industry. They also align with the chosen wall designs in other analyses in this research (i.e. the thermal conductivity testing, the environmental impact assessment).
- 3) Modelling and optimising an idealised low-rise building to examine the feasibility of using 3DP cob walls as loadbearing structural elements. The building is tested as one- and two-storey small houses. The study leverages two optimisation tools: MATLAB® and Galapagos, which is an evolutionary optimiser in the Rhino-Grasshopper® package by McNeel.

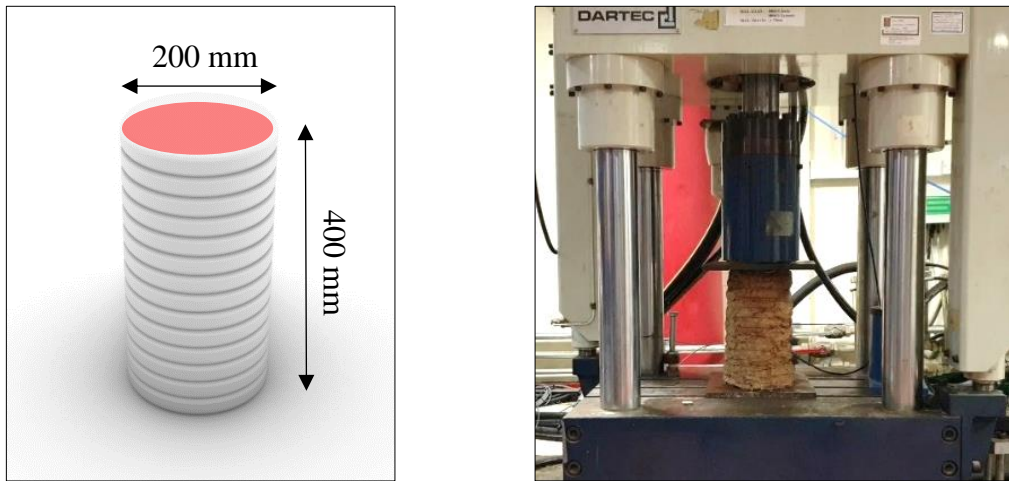


Figure 11. The compression testing set up: the specimens design (right) and Dartec compression testing machine (left).

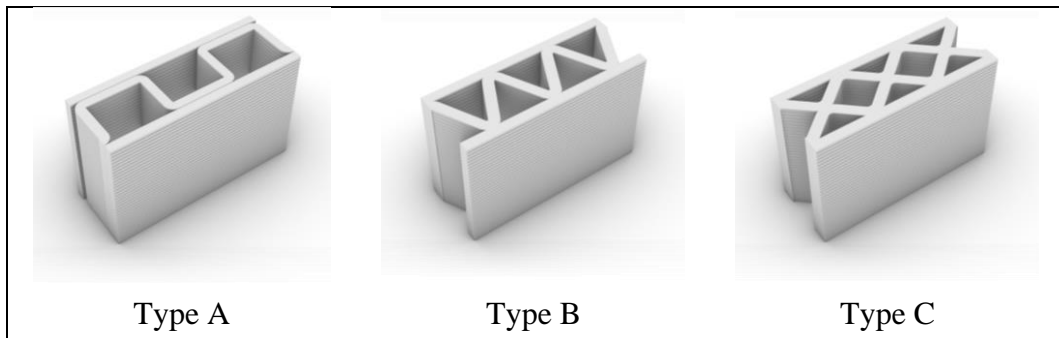


Figure 12: Alternate printed patterns considered in this study.

3.3 Exploration of the thermal properties

This phase involves experimental testing of the thermal conductivity of the 3DP cob. The test uses a heat flow meter Netzsch HFM 446 for thermal conductivity analysis (Figure 13). Four scaled specimens are used to represent four envisaged prototypes of 3DP cob walls. Each prototype is expected to have different thermal performance, which reflect the possible wall designs at full construction scale. Those prototypes are as follows (Figure 14):

- 1) Solid wall design.

- 2) Double-layered wall with a single air pocket.
- 3) Triple-layered wall with dual air pockets.
- 4) Double-layered wall with a single air pocket filled with straw.

The resulting thermal conductivity from the 3DP cob specimens will then be compared to several manually built cob specimens provided through the Cobbauge project at the University of Plymouth.



Figure 13. Heat flow meter Netzsch HFM 446

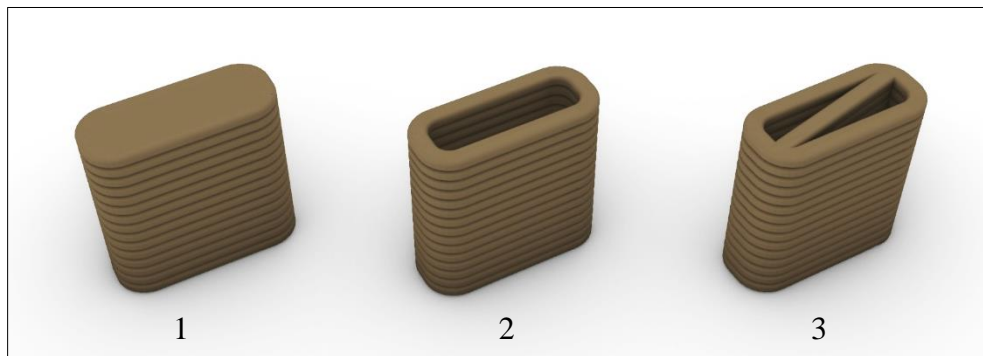


Figure 14. The used 3DP cob specimens for the thermal conductivity testing. From left to right: 1) Solid wall; 2) Double-layered with single gap wall; 3) Triple-layered with dual gaps.

3.4 Assessment of the environmental impacts

This investigation utilised the Life Cycle Assessment (LCA) as a method for estimating the associated environmental impacts with 3DP cob walls. Guided by ISO 14040, ISO 14041 and ISO 14044, the LCA study involved the following four phases:

- 1) Goal and scope: this LCA study aimed to investigate the environmental impacts of 3DP cob through a multi-objective comparison. Two materials (i.e. cob and concrete) within two construction techniques (i.e. 3D printing and conventional) were compared: 3DP cob wall, 3DP concrete wall, conventional cob wall and conventional concrete blockworks wall (which included reinforced concrete column and beam). The chosen functional unit was a 1.0 m² load-bearing external wall. Wall thicknesses varied in each type based on the followed construction recommendation. The chosen scope of the study was cradle to site since 3DP cob technology is relatively new and the information on the end of life stage (i.e. recycling and waste) are limited.
- 2) Life Cycle Inventory (LCI): The study used the SimaPro 9.0.0.35 software with the Ecoinvent v3.1 database (Acero, Rodríguez, and Citroth 2014). The chosen processes for the LCA of the constructed walls were raw material extraction, transport, material manufacturing, and the energy required for construction.
- 3) Life Cycle Impact Assessment (LCIA): The ReCiPe Midpoint (H) v1.03 method for impact assessment was used as it provides a wide range of environmental categories (Huijbregts et al., 2017; Agustí-Juan et al., 2017). This study focused

on the seven most relevant impact categories, as advised by PEFCR Guidance:
1) global warming; 2) stratospheric ozone depletion; 3) fine particulate matter formation; 4) marine eutrophication; 5) land use; 6) mineral resource scarcity; and 7) water use (AWARE).

- 4) Interpretation: This final phase involved evaluating all the data from the LCIA comparisons in order to discuss the assumptions and limitations and state initial conclusions. This was followed by a sensitivity analysis to further understand the impacts and draw recommendations for improvement.

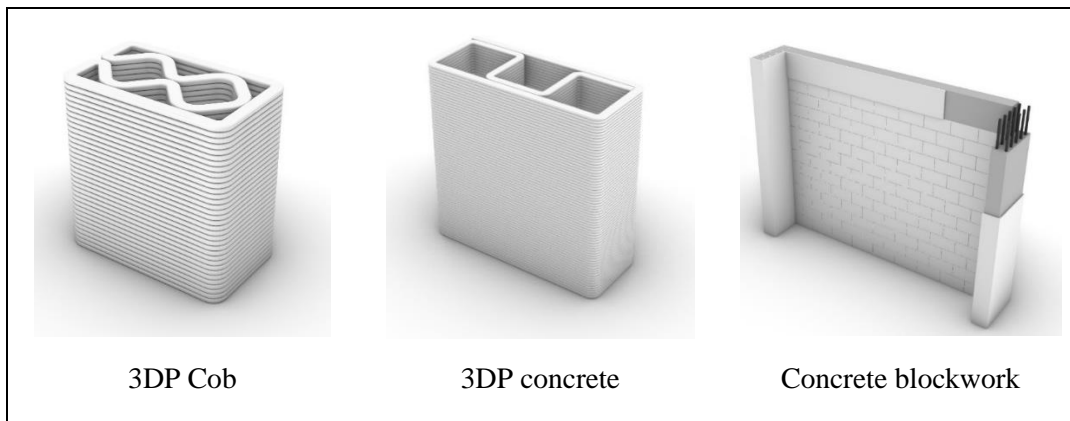


Figure 15. Prototypes of the functional units in the LCA study.

The following four chapters will present details of the research undertaken to address all the research questions.

Chapter 4 Exploration of Geometry and Physical Characteristics

4.1 Introduction

The transitional process from vernacular modes of architecture to a digital approach of construction requires establishing a revised understanding of the material behaviour under the new digital workflow. Hence, this chapter presents a comprehensive investigations of the basic relationships between the robotic 3DP system and the rheological properties of cob. The investigations started by revisiting the traditional cob recipe and testing its workability within the 3DP system. The process of material testing involved examining several extrusion systems. The chapter then addresses an exploration of the new geometric and design possibilities that 3DP cob system offers. The findings are expected to establish a fundamental understanding of the workability potentials and limitation of 3D printed cob.

4.2 List of manuscripts

This part of the research has been produced as a journal article, published in the Journal of Automation in Construction:

Gomaa, M., Jabi, W., Veliz Reyes, A., Soebarto, V. 2020. 3D Printing system for earth-based construction: Case study of Cob walls. *Automation in Construction*. Vol124, 2021, <https://doi.org/10.1016/j.autcon.2021.103577>.

The paper is presented here in a reformatted version for consistency of the presentation of this thesis. The accepted manuscript can be found in Appendix I.

Statement of Authorship

Title of Paper	3D Printing system for earth-based construction: Case study of Cob walls
Publication Status	<input checked="" type="checkbox"/> Published <input type="checkbox"/> Accepted for Publication <input type="checkbox"/> Submitted for Publication <input type="checkbox"/> Unpublished and Unsubmitted work written in manuscript style
Publication Details	Gomaa, M., Jabi, W., Veliz Reyes, A., Soebarto, V. 2020. 3D Printing system for earth-based construction: Case study of Cob walls. <i>Automation in Construction</i> . Vol124, 2021, https://doi.org/10.1016/j.autcon.2021.103577

Principal Author

Name of Principal Author (Candidate)	Mohamed Gomaa		
Contribution to the Paper	Physical prototyping (70% of elements), Conceptualization, Methodology, Data curation, Formal analysis, Investigation, Resources, Software, Validation, Visualization, Writing, review & editing, and acting as corresponding author.		
Overall percentage (%)	85 %		
Certification:	This paper reports on original research I conducted during the period of my Higher Degree by Research candidature and is not subject to any obligations or contractual agreements with a third party that would constrain its inclusion in this thesis. I am the primary author of this paper.		
Signature		Date	11/11/2020

Co-Author Contributions

By signing the Statement of Authorship, each author certifies that:

- the candidate's stated contribution to the publication is accurate (as detailed above);
- permission is granted for the candidate to include the publication in the thesis; and
- the sum of all co-author contributions is equal to 100% less the candidate's stated contribution.

Name of Co-Author	Wassim Jabi		
Contribution to the Paper	Conceptualization, Methodology, Review & editing, Resources, Supervising		
Signature		Date	3/12/2020

Name of Co-Author	Alejandro Veliz Reyes		
Contribution to the Paper	Conceptualization, Review & editing, Resources		
Signature		Date	23.11.2020

Name of Co-Author	Veronica Soebarto		
Contribution to the Paper	Reviewing & editing, Supervising		
Signature	Professor Veronica Soebarto	<small>Digitally signed by Professor Veronica Soebarto DN: cn=Professor Veronica Soebarto, o=The University of Adelaide, ou=School of Architecture and Built Environment, email=veronica.soebarto@adelaide.edu.au, c=AU Date: 2020.11.27 10:02:13 +10'30'</small>	Date 27/11/2020

Development of a 3D Printing System for Earth-based construction: Case Study of Cob Construction

Abstract

This paper describes a comprehensive investigation of a robotic 3D printing system using *Cob* which is an earth-based traditional building material. 3D printed earthen construction materials embody a transition from a vernacular approach to a digital research and development process. The paper describes the methodology of producing revised cob recipes to suit the purpose of 3D printing. The exploration involved the development of a novel 3D printing system based on experimentations with several extrusion methods. The paper then addresses a systematic exploration of the relationship between the developed 3DP system and Cob, and the new geometric and design opportunities it offers. The findings are expected to bring 3D printed cob construction closer to full-scale applications. On a broader scale the study contributes to the disciplines of architectural design and construction by providing a framework capable of bridging the knowledge gap between vernacular modes of building production and contemporary digital practice.

Keywords

3D printing; Additive manufacturing; Robotic construction; Digital fabrication; Extrusion systems; Cob; Earth-based material.

1. Introduction

An increasing amount of research on implementing 3D printing (3DP) systems for large-scale formats has exposed multiple potential applications for architecture and the construction industry (Tay et al. 2017; Wu, Wang, and Wang 2016). Concurrent research highlights the advantages of 3D printing in construction to achieve a higher degree of process optimisations (e.g. financial, construction time, staffing resource), the emergence of new digital processes associated to Building Information Modelling and potential for mass customisation, and environmental benefits towards the life cycle of 3D printed objects and building elements (Wu, Wang, and Wang 2016). Additionally, research such as the review paper by Tay et al. (2017) outlines environmental benefits of 3DP in construction as a result of a reduced use of formwork (Kothman and Faber 2016).

Cob stands as one of many types of earth construction methods and it had been utilised historically all over the world. Its mix consists of subsoil (earth), water, and fibrous material (typically straw). However, similarly to related construction methods, cob buildings embody both a material mix, as well as its associated construction method. Cob walls are typically built using hand-made material deposition on top a plinth, then corrected (e.g. correction of vertical planes) with material added or removed before or after drying (Hamard et al. 2016). As a result building elements can comprise a variety of geometries, yet the builder is required to constantly negotiate the execution with the material properties (e.g. water content, drying speed) necessary to achieve the intended design goals without the need for formwork or any mechanical compaction method (Figure 1). As a result:

- Cob provides a high degree of design freedom and adaptability throughout the construction process, where the builder negotiates with the material (and its properties) as the building process proceeds (Veliz Reyes et al. 2019), challenging the normalised view of robotic 3D printing as a linear process from design to production.
- Cob can be reutilised throughout the construction process, providing the opportunity for testing and prototyping design solutions (Kennedy, Smith, and Wanek 2015), reducing the amount of waste material and enabling low-cost project corrections and modifications on-site.
- Recent research demonstrates that cob complies with modern regulations such as UK building performance standards (Steven Goodhew and Griffiths 2005).
- When compared to other massing construction materials and methods (e.g. concrete), cob has lower CO₂ emissions, low embodied energy (Benardos, Athanasiadis, and Katsoulakos 2014) and requires a lower degree of depletion of natural resources (Steven Goodhew and Griffiths 2005).

These criteria suggest that 3D printed cob requires further investigation as a potential pathway toward more sustainable 3DP practices, with a lesser environmental impact when compared to concrete 3D printing (Alhumayani et al. 2020). An early study conducted on small material samples (Gomaa et al. 2019) provides evidence that 3D printed cob elements have competitive thermal performance standards when compared to other materials such as concrete, brickwork, and conventional cob construction.



Figure 1. Exposed cob construction in Totnes, UK.

Hamard et al. (2016) and Agustí-Juan et al. (2017b) highlight that the integration of digital fabrication techniques with vernacular modes of architectural production can reveal sustainability potentials for construction applications as compared to other cement-based 3D printing methods. This, mainly due to existing forms of cob knowledge production (e.g. vernacular construction techniques), emerges from long-lasting local environmental, material, social and skills contexts of construction practice. This research recognises the potential of developing building technologies associated with vernacular knowledge and building practices, generating a research and development process highly grounded on responsible innovation by leveraging local industries and technologies, utilising local materials and workforce (Garrett 2014). Moreover, the study challenges normalised models of design-to-fabrication research by incorporating local, vernacular and material knowledge as a methodological consideration and engagement process throughout the study. This negotiation between disparate frameworks of material practice (detailed in Veliz Reyes et al, 2019), established both in R&D research and in vernacular construction,

not only results in emergent material opportunities within a standard design-engineering professional delivery framework but also enables novel methodological approaches to architectural tectonics, local materials and skillsets, digital discourses and building technologies.

A substantial share of recent research on 3DP for construction addresses 3D printing of cement and mortar-like materials. As a result, there has been a huge development in 3D printing systems for cement-based materials in recent years (Geneidy, Ismaeel, and Abbas 2019; Shakor et al. 2019). Different types of extrusion systems are currently used for 3D printing; varying from pneumatic pumps and electromechanical ram extruders. In spite of these developments, 3D printing of earth-based materials, such as cob, still presents several challenges to the market-available 3D printing systems such as material granularity, material properties and mix ratios, or the use of local organic fibres, which must be addressed through extensive experimental research before delivering a feasible construction method (Veliz Reyes et al. 2018). These requirements highlight the opportunities of vernacular knowledge as a source of digital innovation, as it has already tested, iterated and perfected mix ratios and earthen architecture production typologies around the world.

Following early studies of cob 3DP technology (e.g. Veliz Reyes et al, 2018) the sensitivity of the printing process to the material mix is currently a major limiting factor in the development of construction-scale 3D printing. The hardening property of the material mix creates a critical constraint on the speed of the 3D printing process (Perrot, Rangeard, and Courteille 2018; T. T. Le et al. 2012). The interrelation between hardening time and printing velocity must be monitored carefully, as each printed layer must be hard enough to support the weight of the

successive layers. At the same time, the material mix must sustain a certain rheological behaviour that enables it to be extruded smoothly through the 3DP printing system (Perrot, Rangeard, and Pierre 2016; Veliz Reyes et al. 2018). Moreover, effective design of material delivery systems may offset some irregularities that may be unavoidable in a commercial application, particularly considering the effect of specific geological, environmental or geographic conditions on the quality of 3DP cob mix.

Panda and Tan (2018) demonstrated in their study the importance of establishing a clear understanding of the rheological behaviour of highly viscous 3D printed materials such as concrete. One of the major issues with 3D printing of such materials is to balance between the fluidity level and sufficient viscosity simultaneously in a way to ensure smooth flow of material through the extrusion system without clogging while maintaining the extruded material shape during the printing process. In concrete 3D printing, the developed mixtures must be thixotropic in nature, which means it should have high yield stress and low viscosity (Panda, Unluer, and Tan 2018). Other studies by Lipscomb and Denn (1984), (Le et al. (2015) and Choi, Kim, and Kim (2014) also highlighted the critical influence of mixture components, such as particle size, gradation, surface area and paste/aggregate volume on the flow property of the material as they govern the yield stress and viscosity. In his study, Perrot et al. (2016) proposed a theoretical framework for the structural built-up of 3DP of cement-based materials. His proposal showed the correlation between vertical stress acting on the first deposited layer with the critical stress related to plastic deformation that is linked to the material yield stress.

In earth construction, the rheology of the material is the key to control the quality of the structures. Historically, adjusting the consistency of cob mixtures depended greatly on the on the local know-how, simply through controlling the water to soil ratios, or by adding other ingredients such as fibres or lime (Perrot, Rangeard, and Lecompte 2018). As the construction industry shows a growing interest in earth materials via 3D printing, the need to develop simple and rapid testing for estimating earth material workability and rheological properties has increased (Bruno et al. 2017; Khelifi et al. 2013). According to Perrot, Rangeard, and Lecompte (2018), field-oriented tests can be leveraged to estimate material parameters such as the yield stress, which will provide important information to describe the rheological behaviour of the earth material. Weismann and Bryce (2006) demonstrated in their book “Building with cob: a step-by-step guide” detailed the methods for simple field tests of subsoil and cob characteristics. The recommended testing procedures were established on historical methods for building with cob, all aiming to provide clear understanding of the subsoil workability and rheology properties.

This research leverages the qualities of cob construction to utilise it as a groundwork for digital innovation through robotic 3D printing of building elements. This line of research has maintained the craft quality of cob as a source of innovative knowledge, often developed outside the boundaries of professional and academic frameworks - a “vernacular” understanding of the material usually communicated through making and practice instead of standard academic communication pathways (Niroumand, Barceló Álvarez, and Saaly 2016). This evolutionary approach of vernacular architecture as a driver for novel environmental, technological and cultural discourses is exploited in this study through an iterative design research method, which has developed a material mix for cob 3D printing applications, an innovative

extrusion system for cob 3D printing applications, and a series of tests attempting to outline emerging large-scale design opportunities resulting from this technology.

2. Methods and Material

2.1. The material

In cob construction, printing material properties must be considered and formulated carefully according to both its wet and hardened states. Wet properties are those related to the material in its fresh, or 'green' state, i.e. the state that the material is in from initial mixing to the point at which it is deployed on site, before drying or hardening (Perrot et al. 2018a). According to Le et al., (2012), three basic criteria must be met to ensure a successful 3D printing process; extrudability, buildability, and workability with time. This means that the material must flow efficiently through the system without excessive force and be deposited in layers with minimal deformations. At the same time it must be able to support the loads of subsequent layers before hardening and reaching some degree of structural integrity. The transition from printing to hardening must occur within a time frame considering the material hardening rate while meeting the overall construction requirements such as tolerances for deformation. A similar process is conducted during hand constructed cob, as the builder must skillfully negotiate water contents, structural integrity and building design throughout the construction process.

In the context of this study, mix ratios have been reached through an iterative process of testing and material characterisation. Weismann and Bryce (2006) and Hamard et al. (2016) recommended that the composition of a cob mixture (averages) to be 78% subsoil, 20% water and 2% fibre (straw) by weight. The recommendation for the

subsoil formula itself is 15-25 % clay to 75-85 % aggregate/sand. This mix, however, requires adaptation for 3D printing applications that maximises its fluidity, while maintaining printability properties (e.g. layer definition) and structural cohesion (e.g. layer height). This study used subsoil sourced from a farmland near Cardiff, UK, for the cob specimens. Subsoil specimens were examined according to the recommended testing methods in the literature (Steve Goodhew, Grindley, and Probeif 1995; Weismann and Bryce 2006): shake test, brick test, sausage test, ball drop test. These tests utilized simple deposition tests in order to acknowledge typically utilized on-site tests as well as to eventually simplify the material characterization process should this method be used in different contexts with little or no access to material testing facilities (Figure 2).

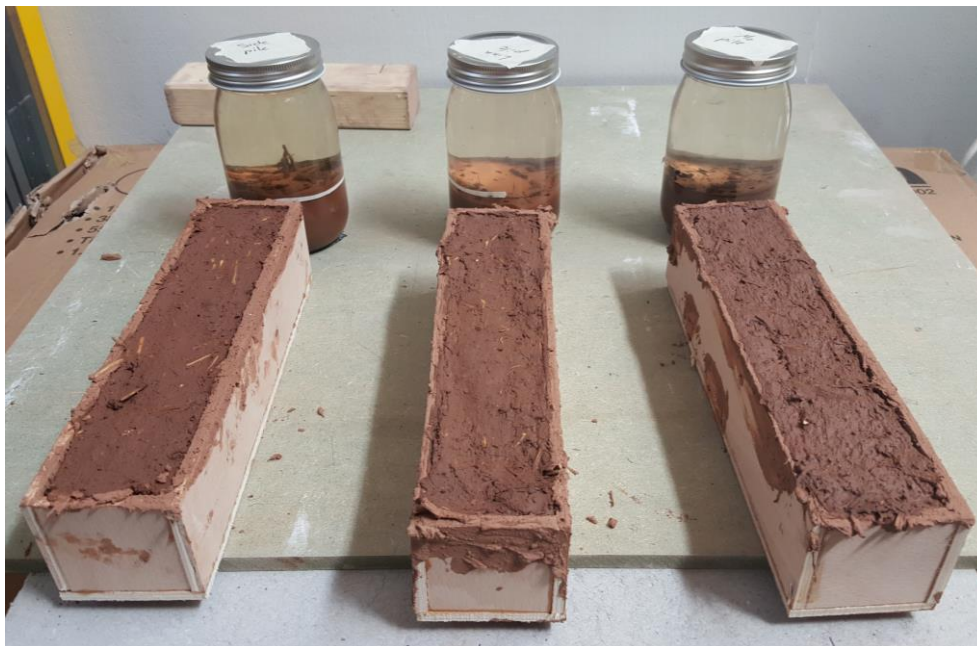


Figure 2. The shake test and the brick tests to the three subsoil samples from Cardiff.

However, as cob is traditionally mixed in a nearly dry state, the recommended compositions above do not necessarily fit the purpose of 3DP applications where a

less viscous rheology is required. Lower water content in the mix leads to higher friction between the material and extrusion cycle parts, creating massive pressure on the extrusion mechanisms, resulting in increasing wear rate of the parts and reduce the long-term efficiency and printing quality. Gooma et al. (2019) conducted a number of systematic tests to reach suitably modified proportions of cob mixtures for 3D printing purposes. The testing process included systematic alteration of several factors. Water contents of 22, 24, 26, and 28% were tested. The study concluded that the water content in the 3D printed cob mixture should be increased to an average of 25% while straw remains at 2%, resulting in a subsoil percentage of 73% (by weight).

It was anticipated that the increase in the water content will alter the rheology of the cob mix during and after the extrusion process. Therefore, it was important to examine the behaviour of the cob mix under the extrusion force. This examination seeks a systematic understanding of the variation in the printed path size in relation to the extrusion rate through the nozzle and motion speed on one side, and nozzle size and layer height on the other. Extrusion rate is usually used to express the volume of material passing through a given cross sectional nozzle area per unit time (mm^3/sec). Linear extrusion rate, on the other hand, represents the passing length of the material over unit time (mm/sec) (Khan Academy 2015; Zareiyan and Khoshnevis 2017). The study at first examined the synchronization process between linear extrusion rate and motion speed. Linear extrusion is chosen so that changes in the cross sections of different nozzles will not alter the outcome. Yet, the study focused on understanding the vital relation between the layer height and nozzle size, and their impact on the printed outcome. Understanding this relation is essential

during the process of transforming the designed geometry into accurate contours and path lines for the 3D printing framework. The correct, and accurate, estimation of the 3D printed size of path lines and the geometry in total increases the quality of the outcome.

A series of tests were conducted to define this relationship mathematically. The tests set the nozzle diameter and the motion speed as constants at 45 mm and 80 mm/sec respectively, with a synchronised linear extrusion rate at 105 % of the nozzle motion speed (approximately 85 mm/sec). The printed file consisted of five path lines. Each line had a different layer height, starting from 15 mm and ending at 35 mm with 5 mm intervals. Each printed line was then measured and assigned to its respective height. This test was repeated three times to observe any possible variation to the outcome and increase credibility of estimations.

2.2. The equipment

A complete 3D Printing (3DP) system consists of two separate devices: a motion controller and a material delivery system. The two must be designed in coordination to realise the final 3D printed outcome: the weight of the extrusion system can affect the motion controller, or the accuracy of the motion controller can affect the tolerance and deformation of the final printed element. The study used a 6-axes KUKA KR60 HA robotic arm as the motion controller. The computer software package for robotic control was Rhinoceros via Grasshopper and KUKA PRC®. The material delivery system is the part of the printer setup which stores, transports, and deposits the print medium. The design of the material delivery system is vital to successful printing, as the material must be layered with enough accuracy, at a consistent and synchronized extrusion rate with the robot motion. Not meeting these

needs can easily jeopardise the resulting print quality, which could significantly affect the shape and the structural integrity of a printed element. The material delivery tool (i.e. the extrusion system) replicated commercial clay extruders that exist in the market, which usually use both pneumatic and electromechanical techniques. The study then developed a new bespoke extrusion system which will be detailed later in the paper.

2.3. Extrusion system

Two types of material extrusion methods were tested in this research; 1) Screw-pump, and 2) Ram extrusion. The screw pump is a method that utilises an auger screw in order to transport and compress the material to a specific point, which in the case of 3D printing is the nozzle. Upon rotation, the screw acts as a type of rotational positive displacement pump, transporting material in the axial direction of the screw (Figure 3). Auger extrusion systems may be vertically or horizontally oriented. The screw sits within a material hopper, which is filled with material to be extruded. The rotating screw then pulls the material through the system. This method is used by the WASP Company in their Delta 3MT and 12MT printers, which they used to experiment with 3D printing of earth-based materials (Figure 4) (3D-WASP 2020).

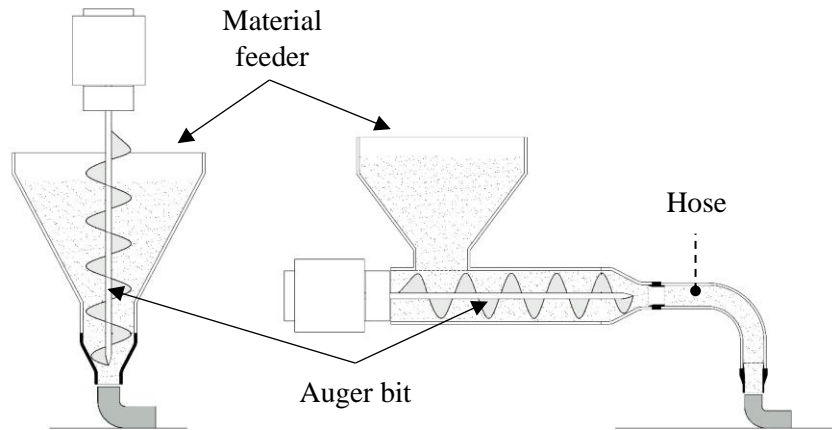


Figure 3. The two types of the screw pump: vertical screw (left) and horizontal screw (right)



Figure 4. Figure Screw pump extruder by WASP

In ram extruders, a linear force is applied on a piston inside a cylinder ram filled with the material. The generated pressure then forces the material through the nozzle once a threshold of pressure is reached. These systems are also commercially known as linear actuators. The exerted force in linear actuators is generated by two methods (Figure 5);

1) Pneumatic, using air/gas, by increasing the pressure on one side of a pneumatic cylinder, leading to linear motion and an applied force on the plunger of the extrusion device.

2) Electromechanical, using lead screw or screw-jack, which translates circular motion from a motor into the linear motion and force exertion required to extrude the material.

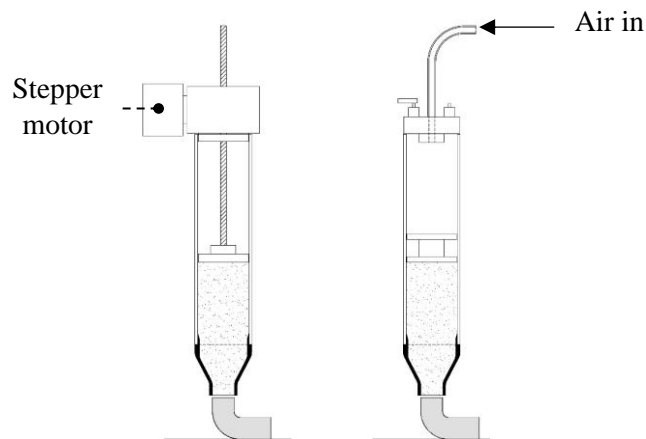


Figure 5. Scheme of the Pneumatic (right) and electromechanical (left) ram extruders.

2.4. Prototyping and Geometry

The prototyping process included two stages; the first stage is the calibration of the 3D printing settings, and the second stage is geometry prototyping. The calibration of settings is an important step to enhance the relationship between the robotic arm and the extrusion system. The calibration process was designed as a set of 3D printed path lines with variable layer heights and speeds. An understanding of the material behaviour is pursued through observing the relationship between the layer height, extrusion rate and nozzle dimension. The applied changes in the layer heights varied

from 15 to 35 mm. These heights are chosen to represent a range of ratios in relation to the nozzle size, which has a diameter of 45 mm.

The second stage of prototyping focused on the geometry potentials and limitations. The main aim of this step is to examine several geometrical challenges that encounter the robotically assisted 3D printing of cob such as the inclined surfaces, arch based shapes and maximum height per printing period. The maximum height per printing period reflects the achieved geometry height before pausing the printing process until the printed geometry gain structural strength through the transformation process from wet to dry state (3D WASP 2016). Additionally, it must be acknowledged that cob can be reutilised after printing, either through the modification of a printed object (while still wet) or through trimming excess cob from already set built elements. As a result, the geometric and prototyping processes of cob 3D printing comprise an iterative quality which facilitates testing.

3. Results and Discussion

3.1. Extrusion System

3.1.1. Bespoke Screw pump

Inspired by the vertical screw extrusion system in the commercial Delta12MT WASP® (Figure 4), the research team developed a screw pump based on an auger bit device. The initial concept was to create a more robot-friendly extruder, where the material feed point was stationary, and the extruded material was delivered to the robot arm end-effector point through a hose. This design concept aimed to provide a higher freedom of movement for the robot, besides an improved practicality of material feeding technique as compared to the available cob and clay extrusion

system in the market, which requires regular human interference with the extruder for material feeding while on the move.

The used device for this testing was a repurposed auger conveyor, originally designed to transport sand. Alterations were made in order to make it suitable for cob extrusion (Figure 6). The initial testing of the device showed remarkable improvement in terms of extrusion rate, consistency and scale of the printed outcome. It was able to achieve a maximum extrusion rate of 80 mm/sec with a 50mm nozzle diameter. However, this system revealed several major shortcomings that required further stage of developments:

- The extruder jammed consistently due to the build-up of straw and rough aggregate at two points in the system; one at the interface between the auger tip and the nozzle and another at the interface between the hopper (feed point) and the auger.
- It still required constant human interaction to feed the material through the hopper.
- The whole mechanism was heavy and relatively large, which compromised the freedom of movement of the robot, and consequently limiting the complexity level of the geometry designs.
- The attempt of making the screw device stationary and install a hose at the screw end (as shown in Figure 3- right) was unsuccessful. Installation of the hose increased both the load and the material travel distance beyond the auger direct contact surface. The increase in hose length has an inverse proportional

relation with the extrusion rate, accompanied by noticeable material retraction at the feeding point.



Figure 6. The prototype of the bespoke screw pump.

3.1.2. Pneumatic

The experimentation of this extrusion type was inspired by most of the industrial clay and concrete extruders, which are based on exerting linear force by using pneumatic pumps. The study used a pneumatic linear ram extruder, in which the pressure was manually controlled. The ram cylinder had a maximum capacity of 4000 ml and the used nozzle size was 30 mm Figure 7. The system was compact enough to be mounted easily on the robot arm and enable remote control of system at the same time. Despite the acquired strength from this extruder, the use of pneumatic system for a dense material like cob revealed a series of challenges in terms of controlling the extrusion rate, quality and consistency of extrusion. Furthermore, it required consistent human interaction throughout the print process to adjust the extrusion rate, fix faults and prevent collapses.

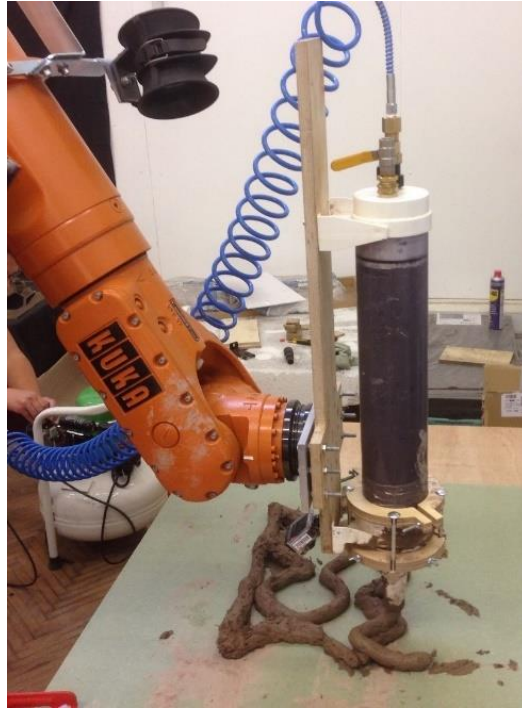


Figure 7. The pneumatic linear ram extruder

3.1.3. Electromechanical

In order to overcome the drawbacks of the pneumatic system, the study switched again to the use of the electromechanical extrusion method in its third phase. This phase used a commercial small size screw-jack extruder provided by 3D potter ® (Figure 8). The benefit of a screw-jack is that it includes a gearbox, providing extra torque at a lower speed. The new system provided a better control over the extrusion rate and consistency due to the use of a stepper electric motor, which resulted in a higher print quality. However, this extruder by 3D potter is designed to execute small-medium size prototypes of clay-based materials, as the standard maximum nozzle size was 16 mm. The system had to be modified by attaching a larger 25mm bespoke nozzle to be more suitable for cob extrusion. Despite the dramatic increase in the printing quality, the new system suffered from a slow printing speed limited to 5 mm/sec due to the increased nozzle size. This rate of 3D printing had restricted

the progress of the experimentation, while it also restricted the scale of the printed outcome which may represent actual wall in a building. Furthermore, the capacity of the material container was too small (3000ml) for a large print to be made without refilling, and the process of refilling the device was slow as it required almost a partial disassembly of the whole extruder (Veliz Reyes et al. 2018).

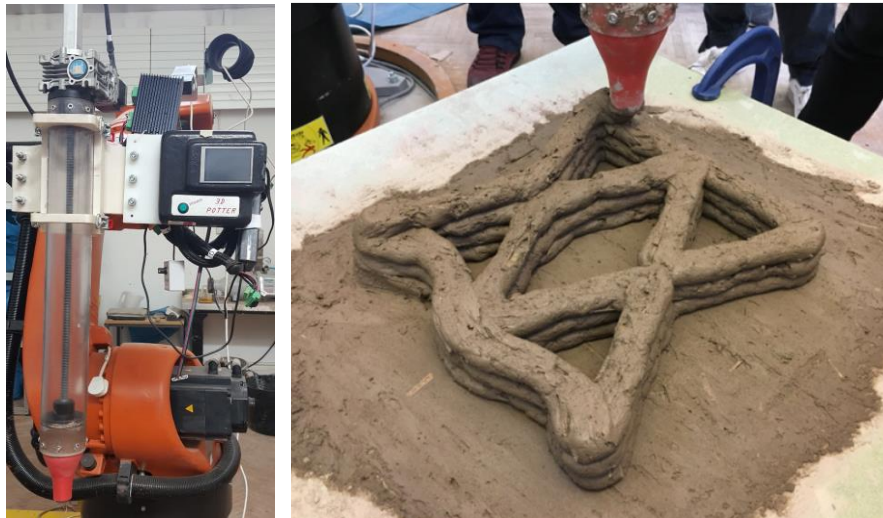


Figure 8. The electromechanical linear ram extruder and its 3D printed outcome.

3.1.4. Bespoke electromechanical dual ram extruder

All the previous experimentations of different extrusion methods have led to the development of a completely new extrusion method that can accelerate the creation of prototypes, leading to an increased productivity and greater research potentials. The previous three experimentations have exposed five critical challenges that face robotically assisted 3D printing of cob:

- 1) Continuity of printing process.
- 2) Maximum extrusion rate.
- 3) Consistency and quality of outcome.
- 4) The freedom of movement.

5) Reduction of human interaction (remote control).

Each tested extrusion system exhibited a number of advantages and limitations. Table 1 summarises the efficiency level of each tested extrusion system based on the five previous criteria. The efficiency levels are expressed as Low, Medium and High, where low refers to limitations and high refers to advantages.

Table 1. Efficiency level of the tested criteria of each extrusion systems

	Continuity	Extrusion rate	Consistency	Movement Freedom	Human interaction
Screw pump	Medium	High	Medium	Low	Low
Pneumatic	Low	Medium	Low	Medium	Medium
E-mechanical	Low	Low	High	Medium	Medium

These criteria are crucial challenges to improve the workability and productivity of 3D printed cob research and practice. The successful encounter of these issues will open the window for more sophisticated explorations on both the 3DP cob mix properties and the geometry design aspects. Out of all the previous three introduced extruding systems, the electromechanical linear ram has shown promising potentials in overcoming the five challenges. However, it suffered mainly from the slow extrusion speed and the lengthy process of material reloading. Therefore, it has become important to build a new -off the shelf- extrusion system, inspired by the core concept of electromechanical screw jacks and capable of tackling the limitations of the previous systems.

The design process of the new system went through different iterations of trials and failures before reaching the final design. The initial concept started with the aim of building a simple upscaled version of the existing electromechanical screw jacks,

shifting it from a single 2000ml cartridge to a single 8000ml, while adding a quick release system to accelerate the refill process. However, while this partially solved the issue of material quantity, it did not solve the continuity issue as the system still required to be on hold while the cartridges were being replaced. To solve this problem, an auxiliary cartridge was added in order to cover the hold time for the main cartridge to be replaced, but with the two cartridges working sequentially. The concept was inspired by small scale PLA and ceramic dual extruder by Leu et al. (2011) and 3D-WASP (2020). The first trials were proofs of concept, where preliminary prototypes of the system were made in 1:4 scale using 3D printed plastic parts. These trials used the standard 2000ml cartridges from the existing 3D potter electromechanical screw jack (Figure 9). The dual joint tested two different angles (45° and 22.5°) to ensure a smooth merge of the material between the two channels. The lower angle (22.5°) showed a smoother merge, hence it was selected to be applied in the full-scale prototype.

The full-scale prototype initially used 3D printed plastic joints and fixtures. The whole system was then fixed on a mobile plywood platform (Figure 10). The first set of tests of the prototype showed success in terms of proving the workability of dual extrusion concept, yet it revealed two critical flaws which affected the extrusion process. The plastic parts were receiving a huge amount of pressure externally from the screw jacks and internally from the material flow, which eventually led to a quick wear and destruction of the parts at the mounting points (Figure 11-left). In addition, the accumulating pressure along the axis between the screw jack mounting point and the dual joint mounting point made the plywood platform buckle from the middle. This buckling forced the cartridge to bend, leading to a material leakage then

eventually a massive crack in the plastic cartridge (Figure 11-right and Figure 12). Therefore, to avoid these flows in the final prototype, it was obvious that the system components must be fabricated from stronger materials such as aluminium, whereas the platform must be reinforced with a metal structure to prevent bending. The extrusion system can then be mobile by mounting the whole platform on a mobile table.

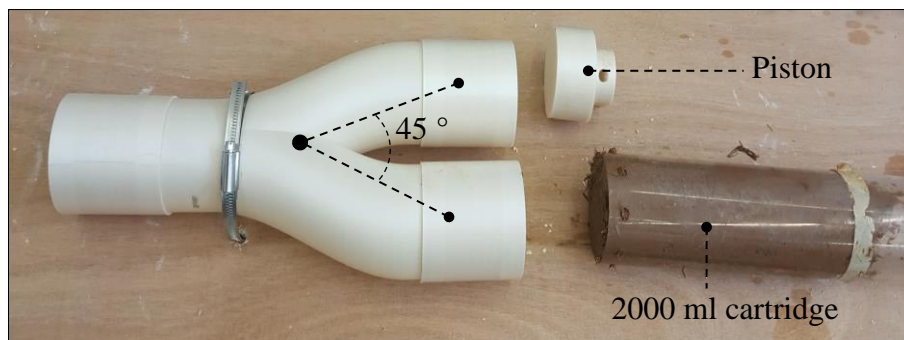


Figure 9. Initial proof of concept of the system in 1:4 scale using the 45 degrees dual joint.

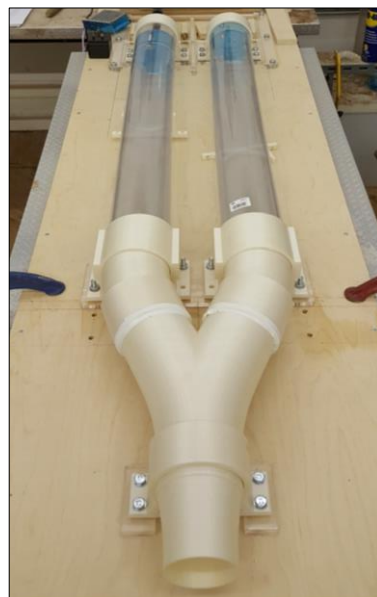


Figure 10. The initial full-scale prototype using 3DP PLA joints and fixtures on a plywood platform.

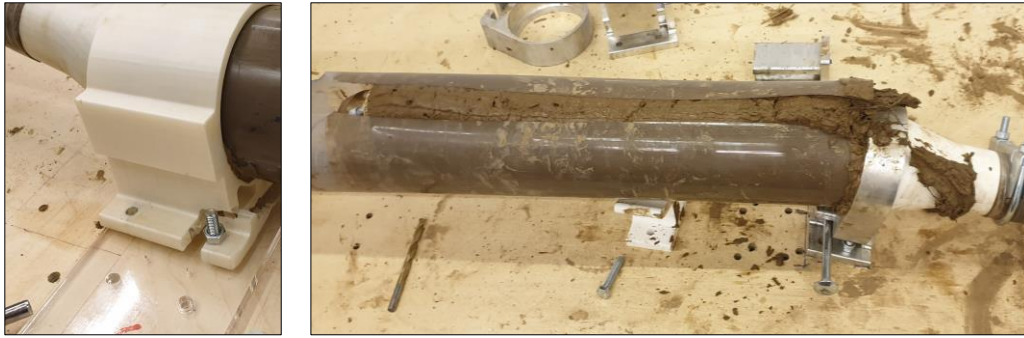


Figure 11. Destruction of the 3DP PLA joints due to pressures caused by the cob mix (left) and the destruction of the cartridge due to pressures caused by the bending plywood platform (right).



Figure 12. Buckling of the plywood platform due to accumulated pressures on nutting points

The final system prototype introduces a bespoke extrusion system with a unique dual-cartridge design (Figure 13, Figure 14). Each cartridge has a capacity of 8000 ml (total of 16000ml both) and powered by a heavy-duty electric screw jack. The screw jacks are supplied by ZIMM® with 25 kN nominal capacity, leveraging a 1000 mm stroke and capable of delivering 80 mm/sec operating travel speed. The screw jacks are powered by two 3-phase motors, 0.75kW each. The motors combine electromagnetic braking system that ensures immediate stop to the stroke, which minimizes the dynamic response. These specs were specially requested based on

calculations of the expected loads in the system, considering factors such as the material weight inside the system and the desired extrusion rate. As budget was limited, some adjustment to the system design were applied to simplify the manufactured parts and reduce the cost without affecting the targeted efficiency. Figure 13 shows a scheme of the bespoke dual extruder different components.

Material cartridges and screw jacks are connected together by bespoke aluminium parts, which are designed to provide smooth and fast reloading process. The most distinctive aluminium part is the Y-shaped joint that merges the material dual flow from both cartridges into a single flow then feed it to a hose. The used hose is 3-meter-long, made from PVC with a steel-wire reinforcement. The complete system is mounted on a mobile platform, allowing transitions around the robotic arm.

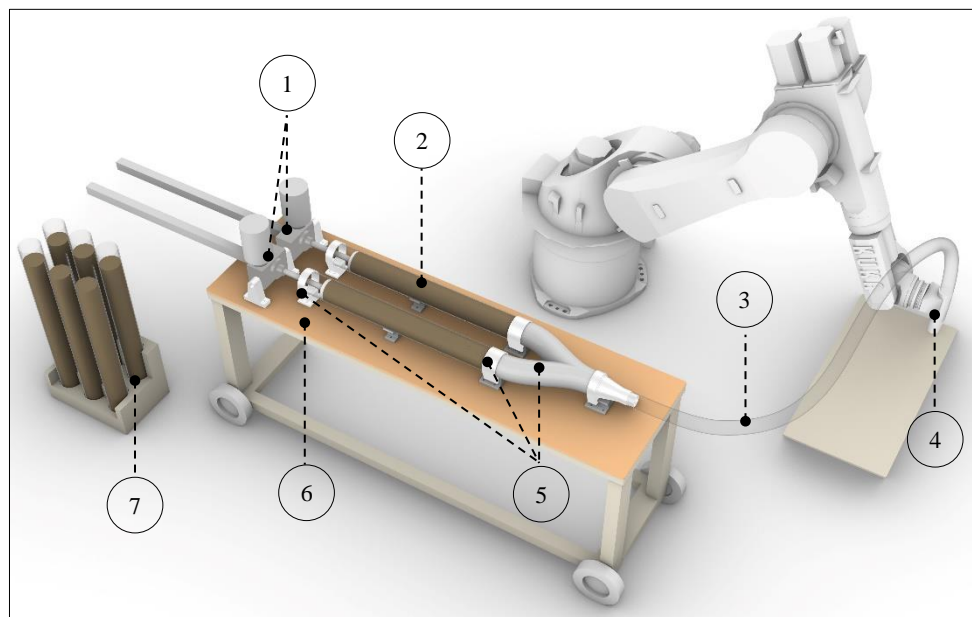


Figure 13. Scheme of the new bespoke dual extruder components: 1) Screw jack, 2) Cob Cartridge, 3) Steel-wired PVC hose, 4) Nozzle, 5) Aluminum parts, 6) Mobile platform, 7) Cartridges Rack.

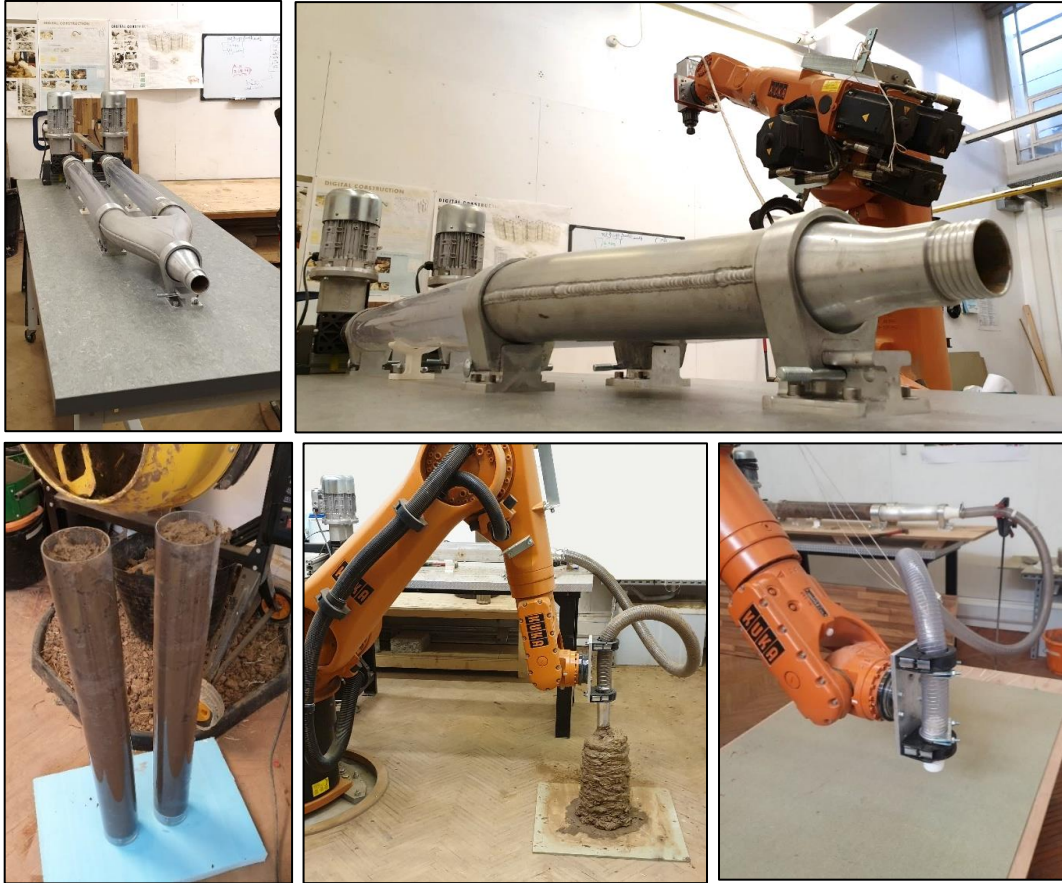


Figure 14. The components of the bespoke dual extruder.

The new system was tested extensively through sequence of calibrations and prototyping process, which took place as part of an experiential studio on 3D printing of cob at the Welsh School of Architecture in Cardiff University. The system proved to be successful in overcoming the five previous challenges as follows:

1- Continuity of printing process:

The new system adopts a sequential process of extrusion based on dual lines of cartridges. This process can be described in 6 steps as shown in Figure 15:

Step 1: The process preparation starts by loading two filled cob cartridges on the platform. Each cartridge, with its attached screw jack, form a line of extrusion.

Few other cartridges are filled with the required amount of cob for the whole print and kept in a rack, ready to be loaded on the system later.

Step 2: The printing process starts by pumping cob through one cartridge at a time using one screw jack (line 1), simultaneously with initiating the robotic arm motion to exert the required design.

Step 3: As the operating screw jack on line 1 reaches its stroke end, it stops and immediately triggers the second screw jack to start pumping cob through the second cartridge on line 2 while the first screw jack is retracting. After the complete retraction of the first screw jack, the empty cartridge is removed and a full cartridge is reloaded.

Step 4: By the time the first cartridge is reloaded, the operating cartridge will be reaching its end of stroke, which then releases the stopping brakes and triggers the first screw jack to start pumping cob through the first cartridge while the second screw jack is retracting.

Step 5: After the complete retraction of the second screw jack, the empty cartridge is removed and a full cartridge is reloaded on line 2.

Step 6: The process then repeats sequentially until the end of the required 3D printed outcome.

It is recommended to estimate the whole required amount of material before the printing process, then preparing either the exact number of cartridges (for small tasks) or just a few extra cartridges and store them in a rack. This will create a buffer margin between the process of refilling and reloading, which will ensure continuity

of the process and constant flow of cob throughout the whole process, with no need to interfere, stop or slow it down. The special design of the aluminium parts also enhances the continuity of the process as they combine rails with latching mechanism, offering smooth reloading of cartridges on the platform.

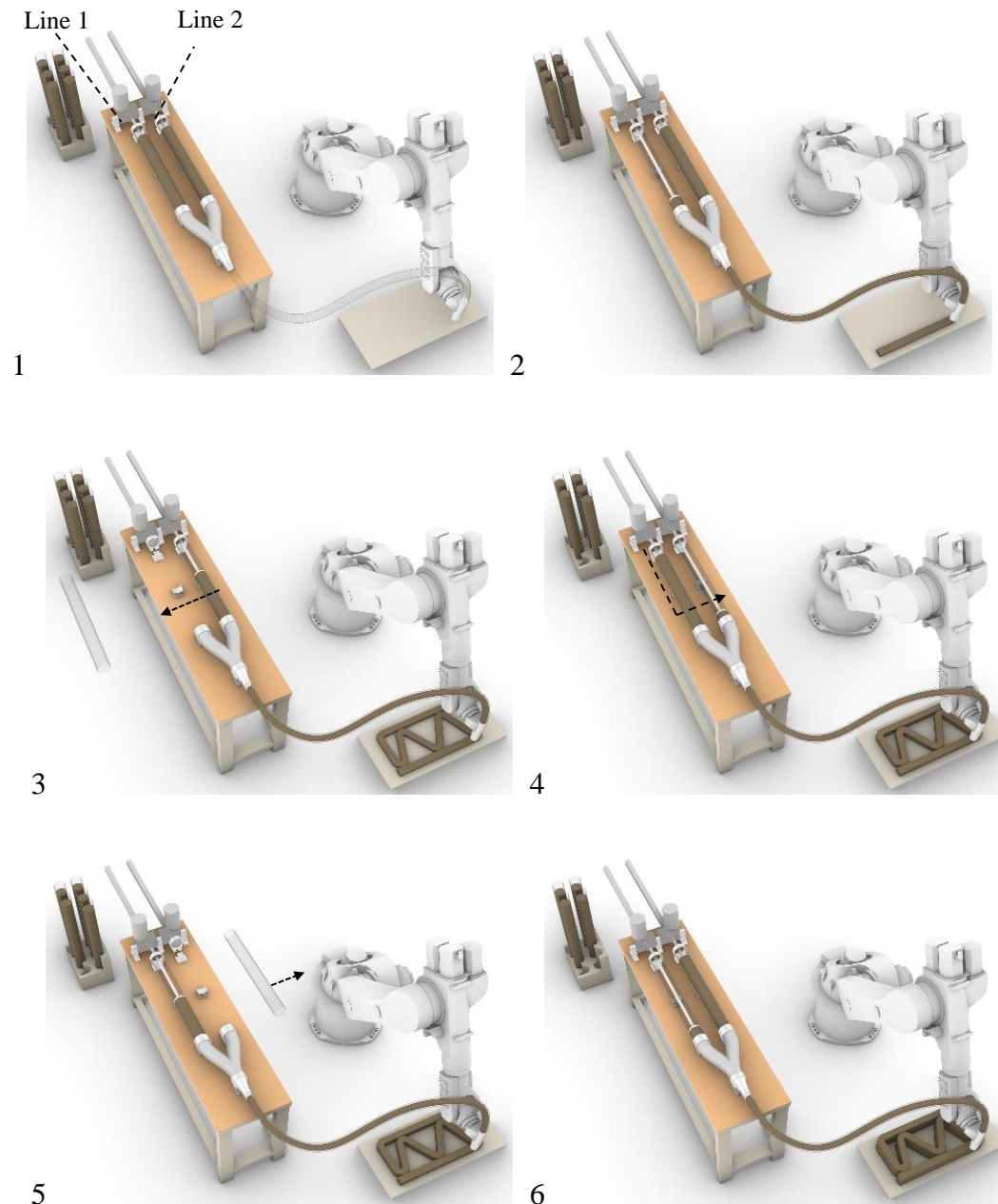


Figure 15. The six steps of the extrusion process in the bespoke dual extruder.

2- Maximum extrusion rate:

The upgraded screw jacks can deliver up to 80mm/sec operating travel speed. Using this travel speed with a 45mm diameter nozzle elevates the extrusion rate of cob on the nozzle to 120mm/sec, which is nearly 20 times faster than the previous small linear ram extruder with 30 mm nozzle. However, based on calibration tests, it was found that 50 to 80mm/sec extrusion rate is sufficient for most of the geometry testing in this project. Moderate speeds offer a relaxed reloading process and gives time to extruded layer of cob to strengthen slightly before receiving the subsequent layers.

3- Consistency and quality of outcome:

The new screw jack by ZIMM leverages a 25KN ball screw gearbox and 3-phase motor controlled by variant frequency driver (VFD). This enables a steady operational torque and an accurate control over travel speed, which provides a consistent flow of cob. This consistent flow dramatically improves the quality of the printed outcome as compared to the previous extruders.

4- The freedom of movement

The new system uses a hose to link between the main body of the extruder on the platform and the nozzle point. This minimises the mounted mass/ load on the robot's end-effector, as now it only carries the nozzle joint with the hose instead of carrying the whole extruder as in the previous pneumatic and small electromechanical linear ram extruders. Minimising the contact size between extruder and robot enables more degrees of freedom for the robot to move, resulting on broader complexity levels in the geometry design if needed. Moreover, the platform itself is mobile and can be

easily moved around the robot if required to compensate the possible limitation in the hose length.

5- Reduction of human interaction (remote control)

The new system is designed to separate between the material feeding point on the platform and the extrusion point on the robot's end-effector. This separation enables the reloading of the cartridges without the need to interrupt (stopping or slowing down) the robot movement. The cartridges system and the simple latching mechanism of aluminium parts also minimise the time required for reloading and reduce human interaction time consequently.

3.1.5. Remarks on the dual extrusion system

Besides the five previous advantages, the simple, yet innovative, design of the new extrusion system made it replicable and also affordable to build as compared to the available commercial options. Moreover, the design enables the system to operate either as a single or dual extruder with different nozzle sizes. This facilitates the 3D printing process for small and medium size prototypes without the need to operate the full system. In addition, the new system has potential for successful implementation into full autonomous large-scale 3D printing process. The study suggests leveraging two on-site 3D printing concepts for that purpose; first one is inspired by mobile crane 3DP system by Contour Crafting (2020) Figure 16-left, where the robotic arm and the extrusion system can be combined in the crane system. The second is inspired by the mobile robotic vehicles which is presented in a study by Zhang et al. (2018) Figure 16- right. A revised design for mobile robot vehicle

that can combine both the extruder and the collaborative robotic station is suggested as in Figure 17.

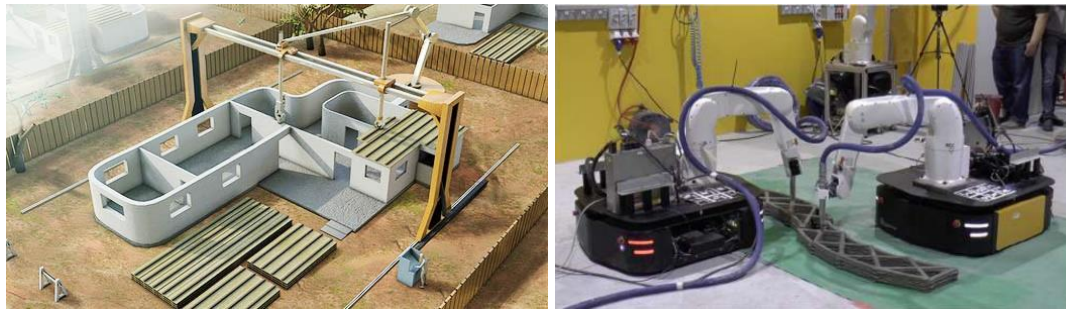


Figure 16. Mobile crane system for 3DP by Contour crafting (left), mobile robotic vehicles by Zhang et al (2018) (Right)

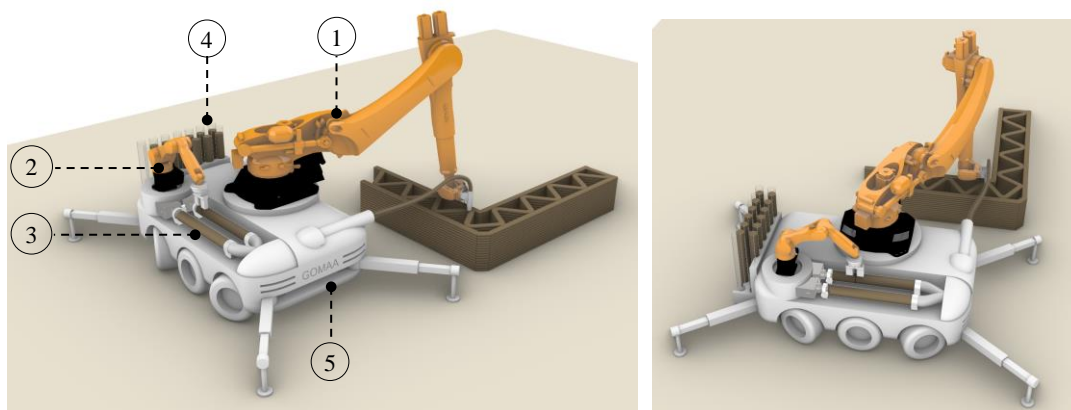


Figure 17. Design of mobile robot vehicle combining both the cob extruder and the collaborative robotic station. 1) Primary robot for printing. 2) Secondary robot for cartridges reloading. 3) Cob extruder. 4) Cartridges rack. 5) Autonomous robotic vehicle.

It is however important to state that the system is an initial prototype that also requires some enhancements and future upgrades. The current design still depends on human interaction to initiate and terminate the 3D printing process, in addition to preparing the cob mixtures, refilling and reloading the cartridges on the platform. It

also very important to follow good practice while filling the cartridges to avoid air pockets and inconsistency, which causes high dynamic response. Also, the current material capacity is limited to 12.0 kg/cartridge, which forces large number of refills to print a real scale wall. For example, 1×1×0.5 m cob wall would require nearly 45 cartridges. Another current limitation is associated with the hose length. Increasing the hose length over 3 meters was found to be harder to mount on the robot and creates higher resistance towards moving and bending. Longer hose is also harder to be cleaned from cob leftovers after each printing process. Therefore, several planned upgrades will involve:

- Connecting the VFDs (controllers) of the screw jacks directly to the Robot controller unit, where the extruder will be operated simultaneously with the robot using the same code file.
- Increasing the material capacity of the system through upgrading the screw jack power and the cartridges volume. Moreover, the current dual-piston design could be redesigned to combine four pistons, capable of accommodating four cartridges at a time.
- The introduction of a collaborative robotic process, where a smaller robot arm will be part of the extruder platform to execute the cartridge reloading task. The required amount of material will be calculated ahead of the process, then translated into a number of cartridges. Another machine will be dedicated for mixing and refilling the empty cartridges while the prefilled cartridges are being used in the extruder.
- Implementing a shutter mechanism over the main dual AI connections can add extra layer of controllability as it will prevent any possible backflow of

material during the cartridge reloading process. The current system design, however, does not suffer from material backflow due to the acute angle (45 degrees) of the dual Al piece and the relatively high viscous nature of the cob mix.

3.2. Material mix properties

The increased water content to 25 % in the new 3DP cob composite, instead of 20% for conventional cob composite, has shown satisfactory extrusion in terms of consistency and quality of extrusion. It was naturally anticipated that the increase in fluidity has proportional relation to the rheology of the cob mix during and after the extrusion process. First set of tests explored the synchronization process between extrusion rate and robot motion speed. It was clear from the start that the extrusion rate must be synchronised with the motion speed of the robotic arm on a 1:1 rate at least. Slower rate of extrusion will result in an intermittent printed outcome as can be seen in Figure 18-left. On the contrary, increasing the extrusion rate in relation to the robot motion speed (using a constant layer height) will result in a more consistent print and wider path lines. In Figure 18-right, the path lines A and B reflect a ratio of 1.15:1, while path lines C and D reflect a ratio of 1.05:1. The increased ratio of extrusion rate to motion speed results in wider path lines under a constant layer height. Table 2 below describe the relationship between extrusion rate and robot arm motion speed.

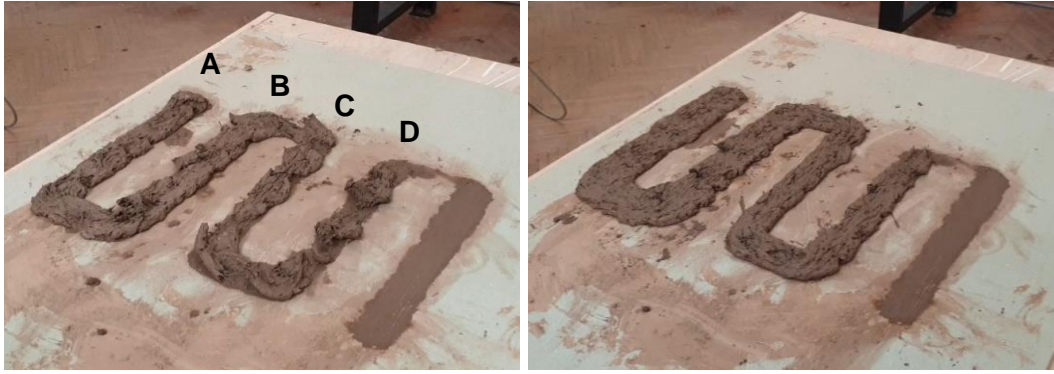


Figure 18. Explorations of the synchronization process between extrusion rate and robot motion speed (left & right)

Table 2. Relationship between extrusion rate and robot arm motion speed

Path line code	A-B	C-D	Unit
Nozzle diameter (D)	45	45	mm
Layer height (h)	15	15	mm
Extrusion rate	92	85	mm/sec
Robot motion speed	80	80	mm/sec
Path width (w)	88	70	mm
Extrusion rate to motion speed ratio	115	105	%

The study concluded after several trials that 3D printing with a liner extrusion rate of 105-110% of the robot motion speed (1.1:1) considered favourable due to the nature of the cob mix, where there are chances of having inconsistent sections of materials inside the cartridges that cause slight interruptions in the extrusion rate from time to time. It is possible to overcome this issue by installing an extrusion rate sensor at the nozzle end that can give live feedback to the variant frequency driver (VFD) of the actuator to make the proper adjustments to power. Worth mentioning that the study also observed that the slightly higher extrusion rate has a “ramming

effect” on the printed outcome, where the printed path lines become denser and gain more structural strength with each new printed layer.

The second set of tests on the relationship between the layer height, nozzle size and path line width has improved the understanding of their influence on the 3D printed outcome and printing process in general. As can be seen in Figure 19, each printed path line (A to E) is designed to reflect the relation between a specific layer height and its respective path width, where the extrusion rate to robot motion speed ratio is set to 110% as advised previously, and the nozzle size is fixed at 45mm. The layer heights started with 15 mm at path line A, then the heights were increased discretely with 5 mm increment per each path line, ending with 35 mm layer height at path line E. Each increase in the layer height exhibited a decrease in the path line width. These relationships between the change in layer heights and path line width has been recorded and described as the expansion factor in Table 3. This test eventually resulted in a model that can estimate the path line width in accordance to the layer height and the nozzle size (Figure 20).

The linear relationship presented in Figure 20 can be described using the following equation:

$$\textit{Estimated path line width (mm)} = \textit{Nozzle size (mm)} \times \textit{Expansion factor}$$

where the expansion factor can be obtained from the chart. To explain further; for example; under a synchronised motion speed and linear extrusion rate, with a 45mm in diameter extrusion nozzle and 25mm layer height (layer height is 56 % of the nozzle size) and an expansion factor of 1.6, :

$$\textit{Estimated path line width (mm)} = 45 \times 1.6 = 70 \textit{ mm}$$

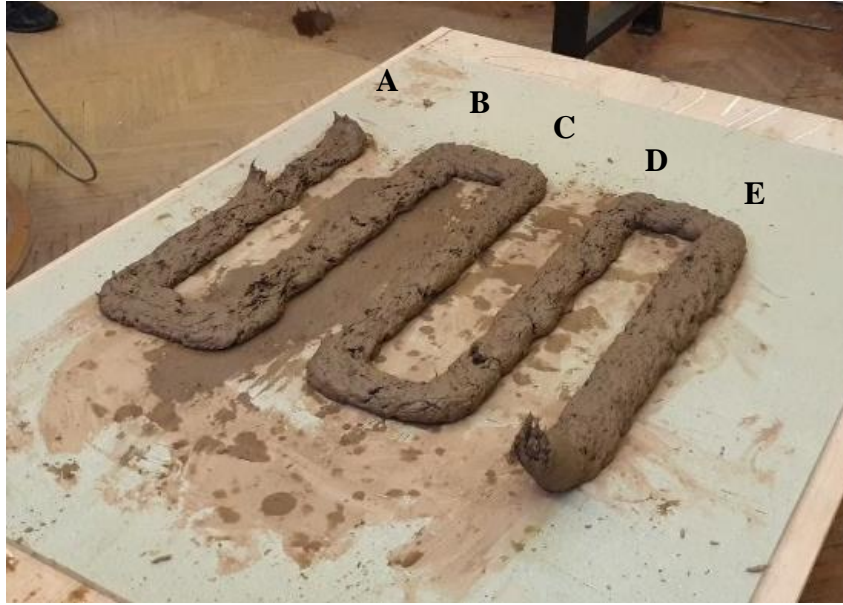







Figure 19. Exploring the relationship between layer height and nozzle size

Table 3. Description of the testing on the relationship between layer height, nozzle size and path line width.

Path line code	A	B	C	D	E	Unit
Scheme of path line cross section						--
Nozzle diameter (D)	45	45	45	45	45	mm
Layer height (h)	15	20	25	30	35	mm
Path width (w)	88	79	70	62	52	mm
Layer height to nozzle D ratio	33	44	56	67	78	%
Path width multiplication factor	1.9	1.7	1.56	1.3	1.16	--

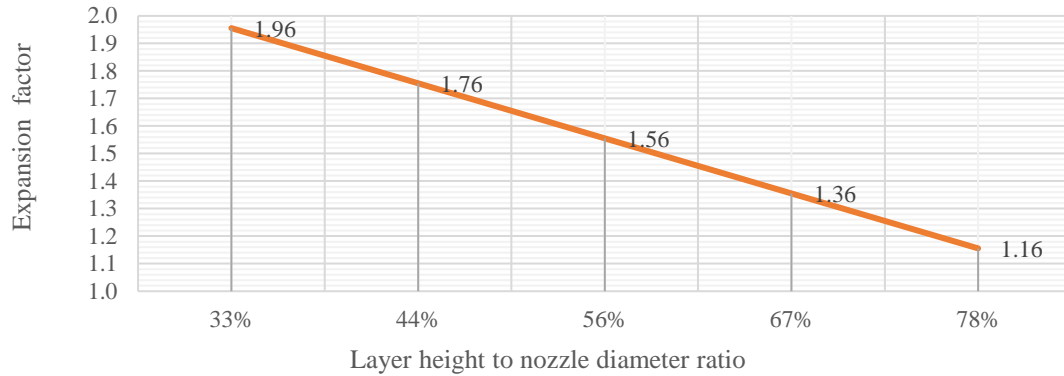


Figure 20. Path line width estimation chart

The early estimation of path line's printed width has enabled the study team to implement a code in the Grasshopper definition as part of the 3D model files to estimate the printed outcome to provide informed decisions for geometry planning. For example, when planning to print a cob wall that has a thickness of 500 mm, using a layer height of 25 mm would require a distance of 430 mm between the two path lines creating the inner and outer sides of the wall. Increasing the layer height to 30mm (while using the added definition in the 3D models) will then automatically update the distance between the wall path lines to 448 mm.

In addition to the previous changes in path line width due the extrusion process and the forced height by the nozzle, 3D printed cob encounters another cause of lateral deformation due to the accumulative loads of each added layer. As the 3D printing process continues, more printed layers accumulate on top of each other to create the desired height of the geometry. This increase in loads leads to further slight lateral and longitudinal deformation as compared to the original virtual model, where it is mostly seen in the bottom layers (Figure 21, left & right). It was observed during all experiments that the level of deformation depends primarily on the water content in the cob mix, as lower water content minimises the deformation to a negligible level

(Figure 21- left), which was an early prototype with 22% water content. The higher water content of 24-25% leads to a noticeable deformation as in Figure 21- the prototype to the right, where the gradual increase in layer heights is slightly noticeable from the bottom to the top layers. The recorded overall deformation was approximately 2% in the longitudinal direction of the total height of the model (around 1 cm for each 50 cm of height). Further exploration for the deformation aspects will be tested and presented in future work.



Figure 21. Prototypes showing the longitudinal deformation due to accumulative weight of layers (lower water content to left, higher water content to the right).

3.3. Geometry exploration

An exploration of various geometries was conducted to examine the capabilities of the 3D printing system. The study experimented with three types of geometries. The criteria of geometry selection were established on exploring the geometrical challenges that face the robotic 3D printing of a simple cob wall with an opening. Figure 22 suggests a traditional cob wall with arch-shaped opening to represent possible challenges while 3D printing cob walls, without using form work to create the openings. The challenges were found to be as follow:

- A. Lift height (Max. height of continuous 3D printing)
- B. Inclined 3-axis 3D printing (horizontal corbelling)
- C. Inclined 6-axis 3D printing (radial corbelling)

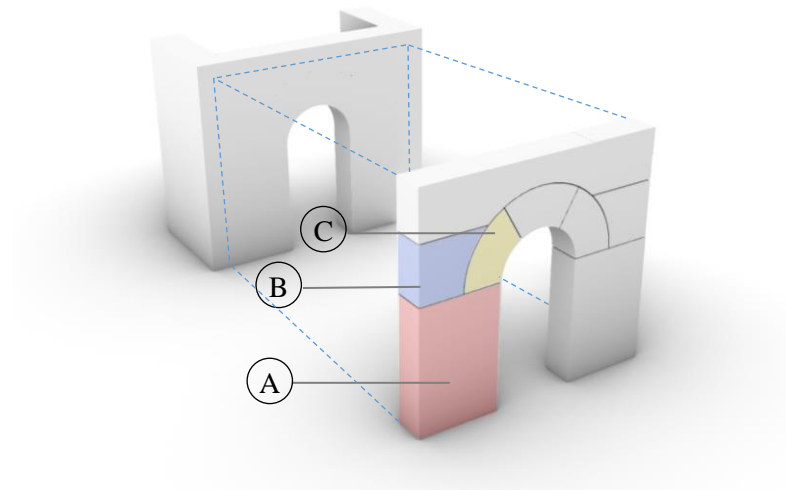


Figure 22. Geometry challenges in a regular cob wall with an opening. 1) Lift height- 3 axis 3D printing; 2) Inclined 3-axis printing (corbelling); 3) Inclined 6-axis 3D printing.

3.3.1. Lift height.

Cob walls are conventionally built of successive monolithic layers of earth called lifts. Each lift must be dry enough to a degree that enables it to bear the loads from the subsequent lifts. Lift height has an average of 60 cm. (Hamard et al. 2016; Weismann and Bryce 2006; Snell and Callahan 2005). Hence, the first geometry exploration aimed to examine the maximum height per lift (Figure 23). The geometry footprint was designed to have a rectangular footprint of 60x40 cm, with a serpentine printing path line that creates the inner pattern of the wall. A serpentine path line was selected for two reasons; first is to improve the structural performance of the wall

(Emmitt and Gorse 2005); second is to extend the printing time per each path line as this should give more time for each layer to start drying and gain rigidity before receiving the successive layers.

This test showed that the maximum stable height of the lift was 58 cm, very similar to the traditional cob method. Exceeding this height increasingly jeopardised the stability of the geometry and it starts showing toppling signs. This finding is also supported by the prototypes by WASP (3D WASP 2016). This finding highlighted the importance of pausing or reducing the 3D printing speed to give a chance to the freshly printed layers to settle properly and gain more structural strength throughout the drying process.



Figure 23. Testing the maximum height per printing period.

3.3.2. Inclined 3-axis 3D printing (horizontal corbelling)

The Second geometry exploration aimed to examine inclined 3-axis 3D printing, where the corbelling happens in the horizontal XY plane only. The study examined two main approaches, straight and gradual inclination (Figure 24, left-right). Based on several trials, it was found that cob can sustain up to 40 degrees of straight

inclination with 1:1.25 slope as shown in Figure 24-left. This was possible to achieve without using inner patterns but with slow printing speed of 30 mm/sec. Based on several trials, it was observed that high inclinations (more than 40 degrees) are less stable and require denser design for inner patterns. On the other hand, using gradual inclination required the addition of inner patterns to the geometry, but it showed a possibility to achieve nearly 90 degrees of inclination as shown in Figure 24- left. However, the increase of the inner pattern, in addition to the serpentine path line, caused a dramatic consumption of material per unit volume.

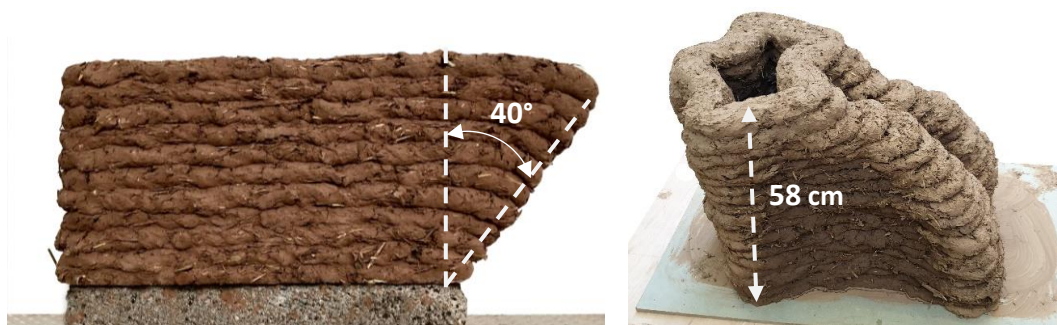


Figure 24. Examining the inclined 3-axis 3D printing; straight inclination (left) and gradual inclination (right)

3.3.3. Inclined 6-axis 3D printing (radial corbelling)

The third exploration aimed to exercise a more complex style of movement that involved all the six axes of the robotic arm. Such added complexity can be leveraged to construct arch-based shapes, like catenary vaults and arches Figure 22-C. The test was able to achieve 45 degrees of radial inclination in a one continuous print (Figure 25). It was possible to continue achieving higher degree of inclination, however, the geometry started to show instability due to its relatively small footprint (40 x 40 cm). It is worth mentioning that 75 degrees of inclination were successfully achieved in a

previous study under this project using the small scale nozzle and less water content (Veliz Reyes et al. 2018). During the printing process of the arch prototype, the study observed that the 3D printed cob can gain structural strength from the ramming process, which is created by the extrusion forces and robotic arm compression. Also, similar to the previous two tests, it was necessary to add an inner pattern to geometry to increase the structural rigidity and the printing time per layer.



Figure 25. Testing complex movement through 3D printing arch-based geometry.

3.3.4. Remarks on geometry testing

Generally, the previous prototypes generated a record that has become useful to the planning of the future work on 3DP cob. Table 4 shows the different characteristics for each 3DP geometry. In addition, the testing process have revealed other factors which influence the geometry formation and its achieved quality. These factors are as follow:

- The overall footprint of the printed geometry: As longer foot prints, such as the external walls of a small house for instance, means more time is spent in each layer, which consequently enables the fresh 3D printed layers of cob to gain further strength as they dry. The footprint of the geometries (e.g. Walls),

can be also increased by designing denser inner patterns inside the walls, which increase the stability of the printed structure, and also improve the thermal performance (Gomaa et al. 2019).

- Layer height to path line ratio: As discussed earlier in section 3.2, lower layer height creates wider path line. The increased footprint of path line offers greater stability to the geometry. However, reducing the layer height means additional material is consumed due to the increased number of required layers to reach the desired total height of the geometry. This also will increase the overall printing time.
- The relation between printing velocity and hardening time: where this study did not test systematically the competition between printing velocity and material hardening, the study observed that shorter printing paths per layer jeopardise the ability of each printed layer to harden sufficiently in order to sustain the loads of the successive layers. For instance, in geometry 2, the small squared footprint created shorter printing path per layer, which consequently required slower printing velocity, while in geometry 1, the larger rectangular footprint enabled higher printing velocity. However, this issue can be compensated by reducing the printing velocity or design the printing process to follow longer paths. This explains why the extrusion rates as per Table 4 were all maintained at 6.7 kg/ min while testing the current geometries despite the ability of system to reach a flow rate of up to 11 kg/min. Worth mentioning that replacing the empty cartridge manually takes nearly 30 seconds, which is less than the time needed to extrude the other full

cartridge This means that the extrusion does not stop at any moment during the total printing process.

Table 4. The different characteristics for each 3DP geometry in the three tests.

	Test 1	Test 2	Test 3	Unit
Printing speed	50	50	50	mm/sec
Volume of printed cob	0.11	0.1	0.08	m ³
Weight of printed cob	198	182	132	kg
Number of used cartridges	16	15	11	
Total printing time	30	27	20	min
Extrusion rate	6.7	6.7	6.7	Kg/min

4. Conclusion

This paper explored the feasibility of combining a low cost and sustainable material (Cob) with an innovative robotic 3D printing process that features pre-filled cartridges within an innovative dual-extrusion system. The research project's aim is to shift the focus away from complete automation and towards a human-robot collaborative system. Its ethos and origin, as evidenced in previous publications by the authors, is based on a model of research grounded in vernacular knowledge, local skillsets, and materials. It aims to support local development through digital R&D and employability through integrating a declining workforce (traditional cob construction) with an emerging technological sector (robotics).

Counter to conventional wisdom, this paper evidenced that cob can be printed with complex geometries using more than three axes. Unlike traditional cob construction, the conducted studies found that 3D printed cob walls do not have to be solid which

will lead to reduced material use and higher insulation values (due to the air cavities inside the geometry) without losing their structural stability. The dual extruder system, invented and built by the authors, allows for continuous printing without the need to lift the material above the current print layer. Cob can be pre-prepared and sealed ahead of time in modular tubes to be inserted at the time of printing. This enables a two-stage process where the material preparation phase can happen independently of the printing phase. Producing modular tubes independently can lead to a small to medium-scale, decentralized manufacturing business where local entrepreneurs provide the supply material in a standard format for 3D printing. This model is not dissimilar to the process of providing and recycling pre-filled propane gas tanks or desktop printer cartridges. Furthermore, we envisage an automatic feeder added to the system where tubes are automatically and alternately loaded and unloaded – ready to deliver material for 3D printing and where empty tubes can be collected and re-filled. A simple computation of printing speed, volume, and daily schedule can inform the size of buffer needed for pre-filled tubes and the required rate of exchange and delivery.

The development of a cob dual-extrusion system involved building a series of prototypes through a standard innovation delivery process, from basic ideation and research, up to proof of concept and prototyping stages. Although further development is required before achieving a commercial cob extrusion system, the impact of this technology comprises not only the introduction of a new extrusion system into the building industry, but more generally addresses the need to acknowledge and further investigate the potential of vernacular knowledge and buildings to facilitate further research and development. As a result, this technology is not only applicable to new buildings but can potentially be a useful resource for

cob building repairs (e.g. crack filling, construction of pre-dried cob blocks), as well as providing some degree of adaptation and customisation for cob building design.

5. Acknowledgements

We would like to acknowledge Jack Francis and Dr Peter Theobald for their valuable collaboration and support (Cardiff University). We also extend our gratitude to Aikaterini Chatzivasileiadi and Anas Lila (Cardiff University) for their invaluable help. Special thanks also must be made to EMAR Engineering Services in Egypt for their technical support.

6. Funding sources

This work was supported financially by the Engineering and Physical Sciences Research Council (EPSRC) and The University of Nottingham under the Network Plus: Industrial Systems in the Digital Age, Grant number: EP/P001246/1.

This work is also partially supported financially by the University of Adelaide through the Research Abroad Scholarship scheme.

7. References

- 3D-WASP. 2020. “3D Printers | WASP | Leading Company in the 3d Printing Industry.” 2020. <https://www.3dwasp.com/en/>. [accessed 31-08-2020]
- 3D WASP. 2016. “The Clay and Straw Wall by The 3 M| Stampanti 3D | WASP.” 2016. <https://www.3dwasp.com/en/il-muro-di-terra-e-paglia-alle-soglie-dei-3-metri/>. [accessed 31-08-2020]
- Agustí-Juan, Isolda, Florian Müller, Norman Hack, Timothy Wangler, and Guillaume Habert. 2017. “Potential Benefits of Digital Fabrication for Complex

- Structures: Environmental Assessment of a Robotically Fabricated Concrete Wall.” *Journal of Cleaner Production* 154: 330–40.
<https://doi.org/10.1016/j.jclepro.2017.04.002>.
- Alhumayani, Hashem, Mohamed Gomaa, Veronica Soebarto, and Wassim Jabi. 2020. “Environmental Assessment of Large-Scale 3D Printing in Construction: A Comparative Study between Cob and Concrete.” *Journal of Cleaner Production* 270 (June): 122463. <https://doi.org/10.1016/j.jclepro.2020.122463>.
- Benardos, A., I. Athanasiadis, and N. Katsoulakos. 2014. “Modern Earth Sheltered Constructions: A Paradigm of Green Engineering.” *Tunnelling and Underground Space Technology* 41 (1): 46–52.
<https://doi.org/10.1016/j.tust.2013.11.008>.
- Bruno, Agostino Walter, Domenico Gallipoli, Céline Perlot, and Joao Mendes. 2017. “Mechanical Behaviour of Hypercompacted Earth for Building Construction.” *Materials and Structures/Materiaux et Constructions* 50 (2).
<https://doi.org/10.1617/s11527-017-1027-5>.
- Choi, Myoung Sung, Young Jin Kim, and Jin Keun Kim. 2014. “Prediction of Concrete Pumping Using Various Rheological Models.” *International Journal of Concrete Structures and Materials* 8 (4): 269–78.
<https://doi.org/10.1007/s40069-014-0084-1>.
- ContourCrafting. 2020. “Building Construction - CC-Corp.” 2020.
<https://contourcrafting.com/building-construction/>. [accessed 08-02-2020]
- Emmitt, Stephen, and Christopher A. Gorse. 2005. *Barry’s Introduction to Construction Management. Introduction to Construction Management*. Cornwall: Blackwell Publishing Ltd. <https://doi.org/10.4324/9781315755229>.
- Francis, Jack Stuart. 2018. “Re-Designing an Extrusion System for Accelerated

- Testing of 3D-Printing Earth- Based Construction Materials.” Cardiff University.
- Garrett, Banning. 2014. “3D Printing: New Economic Paradigms and Strategic Shifts.” *Global Policy* 5 (1): 70–75. <https://doi.org/10.1111/1758-5899.12119>.
- Geneidy, Omar, Walaa S.E. Ismaeel, and Ayman Abbas. 2019. “A Critical Review for Applying Three-Dimensional Concrete Wall Printing Technology in Egypt.” *Architectural Science Review* 0 (0): 1–15. <https://doi.org/10.1080/00038628.2019.1596066>.
- Gomaa, Mohamed, Jim Carfrae, Steve Goodhew, Wassim Jabi, and Alejandro Veliz Reytez. 2019. “Thermal Performance Exploration of 3D Printed Cob.” *Architectural Science Review*, April, 1–8. <https://doi.org/10.1080/00038628.2019.1606776>.
- Goodhew, Steve, P.C. Grindley, and S.D. Probeif. 1995. “Composition, Effective Thermal Conductivity And Specific Heat Of Cob Earth-Walling.” *WIT Transactions on The Built Environment* 16 (January). <https://doi.org/10.2495/STR950231>.
- Goodhew, Steven, and Richard Griffiths. 2005. “Sustainable Earth Walls to Meet the Building Regulations.” *Energy and Buildings*. Elsevier. <https://doi.org/10.1016/j.enbuild.2004.08.005>.
- Hamard, Erwan, Bogdan Cazacliu, Andry Razakamanantsoa, and Jean Claude Morel. 2016. “Cob, a Vernacular Earth Construction Process in the Context of Modern Sustainable Building.” *Building and Environment* 106: 103–19. <https://doi.org/10.1016/j.buildenv.2016.06.009>.
- Kennedy, Joseph F., Michael G. Smith, and Catherine Wanek. 2015. *The Art of Natural Building*. Edited by C Wanek, M Smith, and JF Kennedy. Vancouver,

Canada: New Society Publishers. ISBN: 0865714339

- Khan Academy. 2015. "What Is Volume Flow Rate? (Article) | Fluids | Khan Academy." 2015. <https://www.khanacademy.org/science/physics/fluids/fluid-dynamics/a/what-is-volume-flow-rate>. [accessed 01-09-2020]
- Khelifi, H., A. Perrot, T. Lecompte, and G. Ausias. 2013. "Design of Clay/Cement Mixtures for Extruded Building Products." *Materials and Structures/Materiaux et Constructions* 46 (6): 999–1010. <https://doi.org/10.1617/s11527-012-9949-4>.
- Kothman, Ivo, and Niels Faber. 2016. "How 3D Printing Technology Changes the Rules of the Game Insights from the Construction Sector." *Journal of Manufacturing Technology Management* 27 (7): 932–43. <https://doi.org/10.1108/JMTM-01-2016-0010>.
- Le, H. D., E. H. Kadri, S. Aggoun, J. Vierendeels, P. Troch, and G. De Schutter. 2015. "Effect of Lubrication Layer on Velocity Profile of Concrete in a Pumping Pipe." *Materials and Structures/Materiaux et Constructions* 48 (12): 3991–4003. <https://doi.org/10.1617/s11527-014-0458-5>.
- Le, T. T., S. A. Austin, S. Lim, R. A. Buswell, R. Law, A. G.F. Gibb, and T. Thorpe. 2012. "Hardened Properties of High-Performance Printing Concrete." *Cement and Concrete Research* 42 (3): 558–66. <https://doi.org/10.1016/j.cemconres.2011.12.003>.
- Leu, Ming C., Lie Tang, Brad Deuser, Robert G. Landers, Gregory E. Hilmas, Shi Zhang, and Jeremy Watts. 2011. "Freeze-Form Extrusion Fabrication of Composite Structures." *22nd Annual International Solid Freeform Fabrication Symposium - An Additive Manufacturing Conference, SFF 2011*, no. June 2015: 111–24.
- Lipscomb, G. G., and M. M. Denn. 1984. "Flow of Bingham Fluids in Complex

- Geometries.” *Journal of Non-Newtonian Fluid Mechanics* 14 (C): 337–46.
[https://doi.org/10.1016/0377-0257\(84\)80052-X](https://doi.org/10.1016/0377-0257(84)80052-X).
- Niroumand, Hamed, Juan Antonio Barceló Álvarez, and Maryam Saaly. 2016. “Investigation of Earth Building and Earth Architecture According to Interest and Involvement Levels in Various Countries.” *Renewable and Sustainable Energy Reviews* 57: 1390–97. <https://doi.org/10.1016/j.rser.2015.12.183>.
- Panda, Biranchi, and Ming Jen Tan. 2018. “Experimental Study on Mix Proportion and Fresh Properties of Fly Ash Based Geopolymer for 3D Concrete Printing.” *Ceramics International* 44 (9): 10258–65.
<https://doi.org/10.1016/j.ceramint.2018.03.031>.
- Panda, Biranchi, Cise Unluer, and Ming Jen Tan. 2018. “Investigation of the Rheology and Strength of Geopolymer Mixtures for Extrusion-Based 3D Printing.” *Cement and Concrete Composites* 94 (November 2017): 307–14.
<https://doi.org/10.1016/j.cemconcomp.2018.10.002>.
- Perrot, A., D. Rangeard, and E. Courteille. 2018. “3D Printing of Earth-Based Materials: Processing Aspects.” *Construction and Building Materials* 172: 670–76. <https://doi.org/10.1016/j.conbuildmat.2018.04.017>.
- Perrot, A., D. Rangeard, and T. Lecompte. 2018. “Field-Oriented Tests to Evaluate the Workability of Cob and Adobe.” *Materials and Structures/Materiaux et Constructions* 51 (2): 1–10. <https://doi.org/10.1617/s11527-018-1181-4>.
- Perrot, A, D Rangeard, and A Pierre. 2016. “Structural Built-up of Cement-Based Materials Used for 3D- Printing Extrusion Techniques.” *Materials and Structures*, 1213–20. <https://doi.org/10.1617/s11527-015-0571-0>.
- Shakor, Pshtiwan, Shami Nejadi, Gavin Paul, and Sardar Malek. 2019. “Review of Emerging Additive Manufacturing Technologies in 3d Printing of Cementitious

- Materials in the Construction Industry.” *Frontiers in Built Environment* 4 (January). <https://doi.org/10.3389/fbuil.2018.00085>.
- Snell, Clarke., and Tim Callahan. 2005. *Building Green : A Complete How-to Guide to Alternative Building Methods : Earth Plaster, Straw Bale, Cordwood, Cob, Living Roofs*. Lark Books. ISBN: 9781579905323
- Tay, Yi Wei Daniel, Biranchi Panda, Suvash Chandra Paul, Nisar Ahamed Noor Mohamed, Ming Jen Tan, and Kah Fai Leong. 2017. “3D Printing Trends in Building and Construction Industry: A Review.” *Virtual and Physical Prototyping* 12 (3): 261–76. <https://doi.org/10.1080/17452759.2017.1326724>.
- Veliz Reyes, Alejandro, Mohamed Gomaa, Aikaterini Chatzivasileiadi, and Wassim Jabi. 2018. “Computing Craft: Early Stage Development Of a Robotically-Supported 3D Printing System for Cob Structures.” In *ECAADe-Computing for Better Tomorrow*, 1:791–800. Lodz: cuminCad. <https://pearl.plymouth.ac.uk/handle/10026.1/12769>
- Veliz Reyes, Alejandro, Wassim Jabi, Mohamed Gomaa, Aikaterini Chatzivasileiadi, Lina Ahmad, and Nicholas Mario Wardhana. 2019. “Negotiated Matter: A Robotic Exploration of Craft-Driven Innovation.” *Architectural Science Review* 0 (0): 1–11. <https://doi.org/10.1080/00038628.2019.1651688>.
- Weismann, Adam, and Katy Bryce. 2006. *Building with Cob: A Step-by-Step Guide*. Devon: Green Books Ltd. ISBN: 1903998727
- Wu, Peng, Jun Wang, and Xiangyu Wang. 2016. “A Critical Review of the Use of 3-D Printing in the Construction Industry.” *Automation in Construction* 68: 21–31. <https://doi.org/10.1016/j.autcon.2016.04.005>.
- Zareiyan, Babak, and Behrokh Khoshnevis. 2017. “Interlayer Adhesion and

Strength of Structures in Contour Crafting - Effects of Aggregate Size, Extrusion Rate, and Layer Thickness.” *Automation in Construction* 81 (June): 112–21. <https://doi.org/10.1016/j.autcon.2017.06.013>.

Zhang, Xu, Mingyang Li, Jian Hui Lim, Yiwei Weng, Yi Wei Daniel Tay, Hung Pham, and Quang Cuong Pham. 2018. “Large-Scale 3D Printing by a Team of Mobile Robots.” *Automation in Construction* 95 (August): 98–106. <https://doi.org/10.1016/j.autcon.2018.08.004>.

Chapter 5 Exploration of the Structural Performance of 3DP Cob

5.1 Introduction

This chapter presents an investigation of the structural feasibility of 3D printed (3DP) cob to be used in low-rise buildings. This was conducted through both experimental testing and numerical simulations and optimisation to obtain the mechanical characteristics of 3DP cob walls. The obtained values have been utilized in modelling an idealised low-rise cob building, as the work ultimately aims to generate structural design guidelines for low-rise 3DP cob buildings. These guidelines are expected to enable designers to optimise the 3DP cob walls construction according to the structural performance and material efficiency.

5.2 List of manuscripts

This part of the research has been produced as a journal article, accepted in the *Journal of Construction and Building Materials*:

Gomaa, M., Vaculik, J., Soebarto, V. & Griffith, M 2020. Feasibility of 3DP cob walls under compression loads in low-rise construction. *Journal of Construction and Building Materials*. (Accepted with minor revisions in November 2020).

The paper is presented here in a reformatted version for consistency of the presentation of this thesis. The accepted manuscript can be found in Appendix II.

Statement of Authorship

Title of Paper	Feasibility of 3DP cob walls under compression loads in low-rise construction
Publication Status	<input type="checkbox"/> Published <input type="checkbox"/> Accepted for Publication <input checked="" type="checkbox"/> Submitted for Publication <input type="checkbox"/> Unpublished and Unsubmitted work written in manuscript style
Publication Details	Mohamed Gomaa, Jaroslav Vaculik, Veronica Soebarto, Michael Griffith, Wassim Jabi (2020). Feasibility of 3DP cob walls under compression loads in low-rise construction. <i>Construction and Building Materials</i> .

Principal Author

Name of Principal Author (Candidate)	Mohamed Gomaa			
Contribution to the Paper	Physical prototyping, Conceptualization, Methodology, Data curation, Formal analysis, Investigation, Resources, Software, Validation, Visualization, Writing - original draft, Writing - review & editing, Project administration, Funding acquisition			
Overall percentage (%)				
Certification:	This paper reports on original research I conducted during the period of my Higher Degree by Research candidature and is not subject to any obligations or contractual agreements with a third party that would constrain its inclusion in this thesis. I am the primary author of this paper.			
Signature	<table border="1" style="width: 100%;"> <tr> <td style="width: 60%;"></td> <td style="width: 20%;">Date</td> <td style="width: 20%;">11/11/2020</td> </tr> </table>		Date	11/11/2020
	Date	11/11/2020		

Co-Author Contributions

By signing the Statement of Authorship, each author certifies that:

- i. the candidate's stated contribution to the publication is accurate (as detailed above);
- ii. permission is granted for the candidate to include the publication in the thesis; and
- iii. the sum of all co-author contributions is equal to 100% less the candidate's stated contribution.

Name of Co-Author	Jaroslav Vaculik			
Contribution to the Paper	Methodology, Data curation, Formal analysis, Investigation, Software, Validation, Visualization, Writing - review & editing, acting as corresponding author.			
Signature	<table border="1" style="width: 100%;"> <tr> <td style="width: 60%;"></td> <td style="width: 20%;">Date</td> <td style="width: 20%;">14/11/2020</td> </tr> </table>		Date	14/11/2020
	Date	14/11/2020		

Name of Co-Author	Veronica Soebarto			
Contribution to the Paper	Review & editing, Supervision			
Signature	<table border="1" style="width: 100%;"> <tr> <td style="width: 60%;"></td> <td style="width: 20%;">Date</td> <td style="width: 20%;">2/12/2012</td> </tr> </table>		Date	2/12/2012
	Date	2/12/2012		

Professor
Veronica
Soebarto

Digitally signed by Professor
Veronica Soebarto
DN: cn=Professor Veronica
Soebarto, o=The University of
Adelaide, ou=School of
Architecture and Built Environment,
email=veronica.soebarto@adelaide.
edu.au, c=AU
Date: 2020.12.02 19:34:23 +10'30'

Name of Co-Author	Michael Griffith		
Contribution to the Paper	Review & editing, Supervision		
Signature		Date	30/11/2020

Name of Co-Author	Wassim Jabi		
Contribution to the Paper	Review & editing, Supervision		
Signature		Date	3/12/2020

Feasibility of 3DP cob walls under compression loads in low-rise construction

Abstract

The rapid adoption of 3D printing (3DP) technologies in construction, combined by an increased willingness to reduce the environmental impact of building industry, has facilitated reapproaching earth materials for modern building industry. The feasibility of 3DP earth-based materials has been under investigation in recent years, with a particular focus on cob due to its favourable characteristics toward the 3DP process. Yet, there is a lack of definitive information on the construction of 3DP cob. Hence this paper investigates the structural feasibility of 3D-printed (3DP) cob walls in low-rise buildings. The investigation involved experimental compression tests on 3DP cob samples to obtain key mechanical properties including the compressive strength and modulus of elasticity. These properties were then used as inputs for structural analyses with respect to three alternate types of 3DP cob wall patterns to evaluate their load-carrying capacity based on a limit state design framework. Results from the analyses were implemented in modelling an idealised low-rise cob building covering a range of floor spans and wall heights. The analytical study found that 3D-printed walls have the potential to sustain gravity loads typical of residential construction. Further, since the 3DP material was shown to have similar mechanical performance to conventional (non-3DP) cob on the material scale, the 3D printing process provides the opportunity to produce wall sections that are structurally more efficient than the solid section used in conventional cob construction. This results in lower material consumption, making 3DP cob attractive from the point of view of resource efficiency. An important outcome of the study is the demonstration of a model design technique for low-rise 3DP cob buildings that could be implemented

as part of a broader optimisation procedure to satisfy structural and architectural design objectives.

Keywords:

Additive manufacturing; 3D printing; Cob; Compression test; Limit state design; Structural performance optimisation.

1 Introduction

Digital fabrication technologies, especially 3D printing (3DP), have been witnessing an increasing uptake in many areas of industry (Feng et al. 2015). The construction industry has been adopting a scaled-up version of 3DP over the past two decades. The increased demand for 3DP technologies in construction industry has also encouraged researchers to develop novel ideas toward the full automation of the construction process. Several studies have proven that a well-developed digital-based process of construction offers various benefits such as larger design freedom, accelerated productivity, higher degree of customisation, and improved safety of construction personnel (Kazemian et al. 2017; Zareiyan and Khoshnevis 2017).

Among the developed techniques of digital fabrication in construction, 3DP has been the most studied, and has seen a particular focus on cement-based materials (Khoshnevis 2004; Le et al. 2012; Perrot, Rangeard, and Pierre 2016; Wang et al. 2020). This has led in recent years to a rapid spread of 3DP building prototypes around the world, as 3DP technology has been increasingly embraced by the construction industry (Alhumayani et al. 2020). Among the most notable examples are two concrete buildings constructed in 2019: One is the world's largest 3DP building, constructed by Apis-Cor in Dubai, United Arab Emirates having two storeys, a plan area of 640 m² and height of 9.5 m. The second is a 80 m² prototype

house built by CyBe as part of their contract with the Saudi Arabia Ministry of Housing with an ambitious goal to build 1.5 million houses using 3D concrete printing (CyBe 2019) (Figure 1).



Figure 1: 3DP concrete building in Dubai by Apis-Cor (Left) and 3DP house in Saudi Arabia by CyBe (Right).

The accelerating rate of global present-day construction is well known to produce adverse environmental impacts. Fortunately, the implementation of digital technology in construction offers great potential for sustainability (Shrubsole et al. 2019). For instance, according to Ford and Despeisse (2016), additive manufacturing (e.g. 3D printing) in construction has several sustainability benefits such as improving efficiency of resources, extending product life, and upgrading the value and supply chains.

The increased motivation to harness the sustainability benefits of 3DP technology in construction has also recently renewed the interest in earthen construction materials after many decades of neglect [11],[14]. Significantly, a recent study by Hamard et al. (Hamard et al. 2016) has revealed that considerable sustainability benefits can be realised through the integration of digital fabrication techniques with earth-based materials, which have low embodied energy, are highly recyclable, and generate limited waste. Furthermore, these materials typically have high material density and thus high thermal mass, which can lead to favourable thermal comfort performance

particularly in areas where there is a large difference in daytime and night-time temperatures (Hamard et al. 2016; Morton et al. 2005; Ben-Alon et al. 2019). As a further benefit, earth-based materials are significantly cheaper per unit volume compared to conventional building materials such as concrete or steel (Quagliarini et al. 2010), and can under many circumstances result in more economical small-scale structures.

Earthen construction has three famous forms: cob, adobe, and rammed earth. Cob, which is the focus of this study, is a traditional building material comprising a mixture of subsoil, water and straw (or other fibres). It differs from adobe and rammed earth by using a wet-based construction technique that offers freedom of design while not requiring formwork. It also exhibits excellent maintenance characteristics through the ability to apply add-ons or create cuts-out, even after the cob is dry (Akinkurolere et al. 2006; Fordice and Ben-Alon 2017; Kianfar and Toufigh 2016). This makes cob particularly attractive for 3D printing.

In recent years, the performance of cob manufactured digitally using 3D-printing has been the focus of emergent research at several institutions such as IAAC, Cardiff University and Plymouth University (Veliz Reyes et al. 2019). A proof of concept of the idea has also been successfully demonstrated by the 3D-printer manufacturer WASP3D by constructing two prototypes of cob houses (3D-WASP 2020) (Figure 2). And while the focus of the studies to date has been to examine feasibility with regard to aspects such as geometry and fabrication process (Gomaa et al. 2021), thermal performance (Gomaa et al. 2019), and life cycle assessment (LCA) (Alhumayani et al. 2020), examination of structural performance not yet been carried out in any significant detail. As a consequence, the pursuit of fully implementing 3D

cob in modern construction remains hindered by a lack of engineering guidance for structural design. Overcoming this hurdle requires establishing a reliable body of experimental test data on the mechanical (structural engineering) properties of 3DP cob, as well the development of appropriate structural design and modelling tools that can be used by engineering practitioners.



Figure 2: 3DP cob house fabricated by WASP3D.

While numerous studies have focused on the mechanical properties of 3DP concrete (Feng et al. 2015)(Wang et al. 2020), to the knowledge of the authors only a single study to date has investigated the mechanical properties of any 3DP cob-like material (Perrot, Rangeard, and Courteille 2018). This study, by Perrot et al., tested material made from a mix of earth material and alginate seaweed biopolymer (as a substitute for straw which is traditionally used), and demonstrated compressive strength similar to that of conventional (non-3DP) cob. Besides this study, however, there is no existing research into the mechanical properties of traditional (straw-fibre) cob passed through the 3DP process. Moreover, there are, to the authors' knowledge, no existing studies involving the translation of these fundamental properties toward engineering design of 3DP cob on neither the wall nor building scale.

To address these gaps, this study aims to provide insight into the expected structural load-bearing capability 3DP cob walls. This is approached through two steps: The first conducts an experimental compression test on 3DP cob samples to obtain the

basic mechanical properties including compressive strength, Young's modulus, and Poisson's ratio. The second step evaluates the wall section geometries (dimensions) necessary to perform a load-bearing function in typical residential construction for alternate 3DP patterns through a first-principles analysis approach. This is combined with an optimisation process to examine the relationship between structural efficiency and several design variables such as variable room size, floor heights, number of storeys, and wall section properties. The outcomes are expected to empower architects and engineers with a model approach for the structural design and construction process of 3DP cob. The paper also acts as an essential part of larger overarching research by the authors on the feasibility of 3DP cob in modern construction.

2 Structural performance of cob as a building material

Cob buildings are well-known for their durability and resistance to weathering (Keefe 2005). However, the lack of a binding agent (e.g. cement) makes the compressive strength of cob (typically < 2 MPa) much weaker compared to concrete (typically > 20 MPa) and even other traditional materials such as rammed earth (typically 5–20 MPa). This combined with the fact that cob buildings were historically built without reinforcement means that building heights are typically restricted to low-rise (i.e. between one to three storeys), with most being 2-storey (Quagliarini et al. 2010). Some very rare but notable examples of high-rise are found however, such as the world heritage-listed towers in Yemen which have up to 9 storeys (Damluji 2008)(Smith 2020). Cob's low compressive strength compared to other traditional materials is generally compensated-for by large wall thickness (Earth Devon 2008; Weismann and Bryce 2006). Multi-storey cob houses typically

incorporate light-weight floor and roof systems in the form of timber framing. Floors usually comprise joists with wooden decking, while roofs include timber rafters plus purlins and have a typically sloped profile with extended eaves to protect walls from rain. Walls in multi-storey houses are typically around 600 mm thick, and for efficiency they are typically made thinner at upper storeys relative to the ground floor (Quagliarini et al. 2010; Weismann and Bryce 2006).

Mechanical properties of cob are dependent on a number of factors: subsoil composition including clay content, straw and water content, degree of compaction, and the general quality of the workmanship (Miccoli, Müller, and Fontana 2014), (Earth Devon 2008), (Wright 2019). Studies into the influence of the mix composition have demonstrated compressive strength to be generally enhanced by increased straw content (due to acting as local tensile reinforcement) and reduced by higher moisture content (Akinkulore et al. 2006; Saxton 1995). Table 1 provides a generalised overview of test studies to date, summarising the range of reported compressive strength (f_c) and Young's modulus of elasticity (E). It is important to note that the cob mixtures in these studies vary in terms of their composition, with the intention of the table being to demonstrate the broad range of property values rather than parametric trends. Compressive strength can be considered to be the fundamental engineering property of interest for earthen-material structures, as it controls the load-bearing capacity of walls under gravity loads (Quagliarini et al. 2010; Pullen and Scholz 2011). As indicated by Table 1, compressive strength usually falls between 0.4–1.35 MPa, although values less than 0.1 MPa and as high as 5 MPa have been reported. Notably, low values of strength (< 0.4 MPa) are usually for mixtures with high moisture content ($> 15\%$) (Quagliarini et al. 2010), (Saxton 1995). Among the studies in Table 1, the range of scatter in compressive strength

(where reported) varies between 2–21%. Stochastic variability has implications toward the lower-bound characteristic value that can be adopted in limit state design as discussed later.

The modulus of elasticity varies drastically among the published studies. Most reported values fall within the range 4–200 MPa, but outlying values as little as 0.33 MPa and as high as 850 MPa have been reported. As will be shown later (Section 4) the elastic modulus has particular importance toward the load-bearing capacity of 3DP cob walls due to the potential for local buckling of the printed sections. Data on Poisson's ratio is limited to two studies (Miccoli, Müller, and Fontana 2014) and (Quagliarini and Maracchini 2018), who reported mean values of 0.15 and 0.12 respectively. Additionally, cob exhibits considerably higher material ductility than rammed earth and adobe (Miccoli, Müller, and Fontana 2014; Quagliarini and Maracchini 2018), as characterised by the ability to maintain stress resistance into the post-peak phase of stress-strain response. Miccoli et al. (Miccoli, Müller, and Fontana 2014) demonstrated this to be the case under both compressive and shear loading. The observed ductility of cob can be attributed to the influence of fibres, with fibres in cob being typically longer than those in adobe. This favourable behaviour implies that cob may be able to outperform the alternate earthen materials under deformation-controlled loading such as earthquake. While this warrants further investigation, it is outside the scope of the current paper.

Table 1: Compressive strength (f_c), elastic modulus (E), and Poisson's ratio (ν) for non-3DP cob. Values presented as a range a–b cover different cob mixtures, if applicable. Percentages in brackets denote the intra-batch CoV if specified. Unless noted otherwise, the mixtures have moisture content (mc) < 15%.

Source	f_c (MPa)	E (MPa)	ν
Houben and Guillaud (1994)	0.10	–	–
Saxton (1995)	0.35–1.75 (mc<15%) 0–0.2 (mc>15%)	–	–
Ziegert (2003)	0.45–1.40	170–335	–
Coventry (2004)	0.48–1.24 (3%–10%)	0.33–1.25	–
Akinkurolere et al. (2006)	0.6–2.2	–	–
Weismann and Bryce (2006)	0.77	–	–
Quagliarini et al. (2010)	0.24–0.40 (mc>15%)	4.0–40 *	–
Pullen and Scholz (2011)	0.45–0.89 (22%)	11–69	–
Keefe (2005)	0.6–1.4	–	–
Minke (2012)	0.5–5.0	60–850	–
Miccoli et al. (2014)	1.59 (2%)	651 (68%)	0.15 (4%)
Rizza and Bottger (2015)	0.60 (13%)	71.5	–
Brunello et al. (2018)	0.71–0.87 (8%–15%)	–	–
Quagliarini and Maracchini (2018)	1.12 (5%)	16.9 (4%)	0.12 (66%)
Vinceslas et al. (2018)	0.50–0.76	110–350	–
Wright (2019)	1.22–1.53 ** (18%–21%) 0.77–2.45 ***	–	–
Jiménez Rios and O'Dwyer (2020)	0.70 (12%)	143 (23%)	–

Notes:

* E determined from reported stress-strain curves

** Specimens with varied straw content

*** Specimens with varied soil clay content.

The only study, to the authors' knowledge, that has undertaken material testing on any 3D-printed earthen material is a recent study by Perrot et al. (Perrot, Rangeard,

and Courteille 2018), which used a cob-like material incorporating alginate seaweed biopolymer as a substitute for straw. The produced material achieved a compressive strength between 1.2–1.8 MPa, demonstrating that 3DP earth material has the potential to achieve compressive strength toward the higher end of that for conventional non-3DP cob (Table 1).

3 Compression tests on 3D-printed cob cylinders

This section reports laboratory tests performed on 3DP-cob cylinders to quantify fundamental mechanical properties necessary for design. Among the side objectives of these tests was also to ensure that the 3D printing process did not produce any unexpected strength reduction compared to conventional non-3DP cob (Table 1). Such a reduction could be conceivable due to the altered form of the material as a result of being stacked in layers rather than being a homogeneous mass. Due to the lack of a structural testing standard specific to earthen materials, the study adopted general principles for the testing of quasi-brittle materials, as recommended by (Fabbri, Morel, and Gallipoli 2018).

3.1 Test Specimens

3.1.1 Material mix preparation

In the 3D-printing process, the material must flow efficiently through the system, be deposited as layers and harden properly to reach a structural integrity threshold within an acceptable time frame that meets the construction requirements (Le et al. 2012). The properties of the input material must therefore be formulated carefully considering both their wet (pre-hardening) and hardened states. According to Weismann and Bryce (Weismann and Bryce 2006) and Hamard et al. (Hamard et al.

2016), traditional cob mixture typically comprises 78% subsoil, 20% water and 2% fibre (straw) by weight. This however produces a nearly dry mixture with low flowability, making it unsuitable for 3D printing. To overcome this, the adopted mixture followed an alternate, 3DP-suitable mix developed by the authors in a precursor study (Gomaa et al. 2019). In the adopted mix, the water content was increased to an average of 25%, subsoil was reduced to 73%, and straw was maintained at 2% (by weight). The mixture used locally-sourced wheat straw chopped into lengths between 30 and 50 mm, as longer straw lengths were found to be unsuitable causing blockage inside the extrusion system. The composition of the subsoil (sourced from Cardiff, UK) was examined using methods recommended by (Goodhew, Grindley, and Probeif 1995; Weismann and Bryce 2006) and found to contain 19–20% clay and 80–81% aggregate/sand. This is in good agreement with subsoil composition recommended in the literature (Weismann and Bryce 2006) (Hamard et al. 2016) (15–25% clay to 75–85 % aggregate/sand).

It is worth mentioning that, despite the increased moisture content in the 3DP cob mixture prior to the printing process, the final printed cob (forming the geometry) tends to have a lower moisture content. This phenomenon was observed during the extrusion process, where the cob mixture loses some of its moisture while being compressed inside the extrusion system. The moisture is released in the form of leakage around the cob cartridges connections. The moisture loss estimated by 3%, leaving the actual printed cob structure with 22% moisture content. This favourable reduction in moisture content improves the structural stability of the printed layers and reduce shrinkage. Shrinkage is an important aspect in cob construction, however, it was outside the scope of this study, especially as the observed shrinkage in the

used specimens was very small (2% approximately), and there were no signs of cracks in the specimens during the drying period.

3.1.2 3D-printing of the test specimens

The test specimens in this study were printed using a 6-axis KUKA KR60 HA robotic arm (Figure 3). The software package for robotic control was Rhinoceros via Grasshopper and KUKA PRC®. An electromechanical dual ram extruder, developed by the authors in a previous study (Gomaa et al. 2021), was used for the material delivery. The test specimens comprised 400 mm-tall cob cylinders with an average diameter of 200 mm (Figure 4). Each cylinder was contoured as 14 successive layers, with an average height of 28.6 mm per layer. The nozzle had a 45 mm diameter. The robotic arm moved in a circular pattern, with an average motion speed of 35 mm/sec.

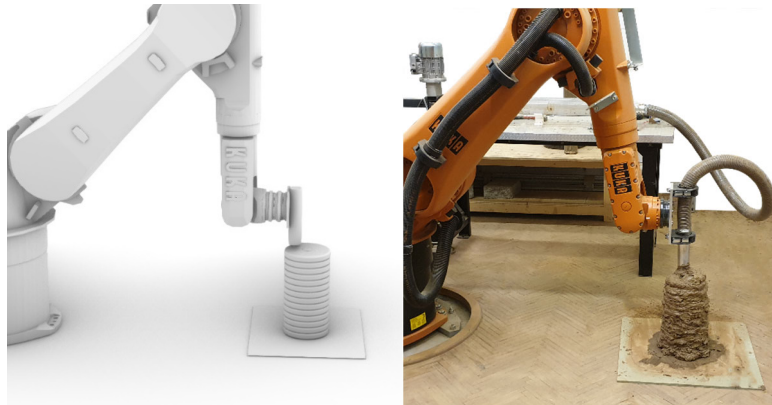


Figure 3: Robotic 3D printing of the cob specimens: virtual model on Rhino (left) and the real output (right).

3.2 Test arrangement and method

The wet test specimens were left to dry after 3D printing for 29 days prior to testing date. The specimens were subjected to uniform axial load in a universal testing machine (Figure 4). Prior to the test, the loading platens of the machine were coated with grease to minimise frictional confinement. The rate of applied load was approximately 0.077 MPa/min, with each test taking about 10 minutes to perform.

The test apparatus monitored the applied load and axial (longitudinal) displacement between the two platens using a built-in linear variable differential transformer (LVDT). Due to the impracticality of applying strain gauges to the irregular surface of the specimens, horizontal deformation (necessary to evaluate the Poisson's ratio) was quantified in post-processing using digital image correlation using high-resolution video footage captured during the test. A total of three samples were tested, with examples of the failed specimens shown in Figure 5.



Figure 4: Compression test setup (left) and the cylindrical specimen (right).



Figure 5: Typical examples of specimens after compressive failure.

3.3 Results

The observed stress-strain behaviour is shown in Figure 6. Each specimen exhibits quasi-brittle response with an approximately linear rising branch, followed by a reduction in slope up to the peak, and continued softening in the post-peak zone. The plotted stress was calculated as $\sigma = P/A$, where P is the applied force and A is the average cross-sectional area of the specimen (31,400 mm²). Axial strain was computed as $\epsilon_{\text{axial}} = \Delta/L$, where Δ is the displacement measured platen-to-platen, and L is the length of the specimen (400 mm).

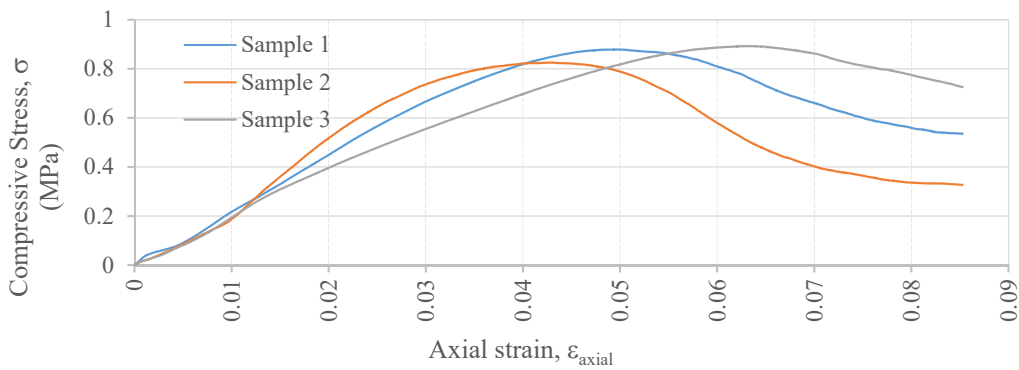


Figure 6: Stress-strain behaviour of compression test specimens.

The properties derived from the test, including the compressive strength, elastic modulus, and Poisson's ratio, are summarised in Table 2. The average unconfined compressive strength (f_c) of the specimens is 0.87 MPa. This compares favourably to the strength of non-3DP cob reported in the literature (Table 1) with most reported values falling within 0.4–1.35 MPa. On this basis there does not appear to be any obvious reduction in strength introduced by the 3DP process. Despite a limited number of samples, the variability is low (CoV = 4%). It should be noted that the reported compressive strength corresponds directly to the peak stress reached during the test. To account for the size-effect in quasi-brittle materials as well as

confinement resulting from the compression apparatus platens, test standards typically apply a correction factor to the measured peak stress to obtain a size-invariant unconfined compressive strength. For instance if these results were to be interpreted according to the test standard for masonry units (EN 772-1, (CEN 2011)) a correction factor of 1.25 would apply on the basis of the test specimen dimensions. However, for conservatism in the subsequent analysis in Section 4 this factor is taken as 1.

The elastic modulus (E) was evaluated as the slope of the σ - ε curve along the initial rising branch before the onset of nonlinearity. The mean E of the tested specimens is 22.9 MPa (CoV = 10%). This falls into the lower end of values determined for non-3DP cob (Table 1) (median \approx 60 MPa). As demonstrated later (Section 4), the elastic modulus is influential on wall load-bearing strength as it controls the local buckling capacity of the printed cross section, providing impetus for future investigations into 3DP-suitable cob mix design to focus on increasing the material stiffness. Poisson's ratio (ν) was calculated as the ratio of lateral to longitudinal strain over the initial elastic portion of response, producing a mean value of 0.22. This is consistent with the range of scatter reported by (Miccoli, Müller, and Fontana 2014) and (Quagliarini and Maracchini 2018) for non-3DP cob (Table 1).

Table 2: Results of compression test including unconfined compressive strength (f_c), elastic modulus (E), and Poisson's ratio (ν).

Sample	f_c (MPa)	E (MPa)	ν
1	0.88	22.7	0.16
2	0.83	25.3	0.28
3	0.89	20.6	0.21
Mean value	0.87	22.9	0.22
CoV	4%	10%	28%

4 Evaluation of the feasibility of loadbearing 3DP cob walls

This section examines the feasibility of using 3DP cob walls as loadbearing in low-rise residential buildings. The design actions considered here are from gravity loads only, excluding possible loads from the wind or earthquake which can be highly region-specific.

4.1 Method of structural analysis

While there are some expected similarities between the general behaviour expected for 3DP cob walls and walls constructed using unreinforced masonry or concrete, the design codes for these more established materials are not necessarily translatable to 3DP cob. Therefore, the wall's load-carrying capacity is evaluated using first principles while adhering to the concepts of limit state design. This includes using characteristic values of material stress capacity (rather than mean values), and applying factors to upscale design loads and downgrade the design capacity.

4.1.1 Limit state design

Capacity adequacy checks were performed according to a limit state design framework. With reference to the compressive strength, the design check can be expressed using the generalised form

$$N_c^* < \phi N_c \quad (1)$$

In Eq. (1), N_c^* is the design compressive force acting on the wall, determined as γS , with S being the unfactored working load and γ being the load factor (greater than 1). In turn, ϕN_c is the design compressive capacity of the wall, determined as the basic capacity N_c multiplied by the capacity reduction factor ϕ (less than 1). To account for the fact that the material stress capacities exhibit stochastic variability,

capacity N_c is calculated using the characteristic compressive strength, f_c' , defined as the lower-5th-percentile value.

4.1.2 Selection of wall sections

Three different types of printed patterns were considered as part of this feasibility study; these are referred to as A, B and C, as shown in Figure 7. These three designs align carefully with the wall sections in two previous studies that investigated the thermal performance and life cycle analysis (LCA) of 3D-printed cob by Gomaa et al. (Gomaa et al. 2019) and Alhumayani et al. (Alhumayani et al. 2020) respectively. The criteria for choosing these wall sections are based on meeting variable design requirements such as adequate thermal insulation, efficient use of material and structural integrity. A generic vertical cross section of a wall is shown in Figure 8. Because the 3D printing process in the current study dispenses the cob material in circular cross sections while being flattened down into wider layers, the resulting vertical shells do not have a constant thickness (Figure 8). Rather the shell thickness ranges between an inner value, t_{in} , and outer value, t_{out} , as shown. Both t_{in} and t_{out} could be estimated for a specific geometry according to a number of parameters in the 3D-printing process setup, such as the layer height, nozzle size and the extrusion rate (Gomaa et al. 2021). On the basis of typical printed patterns, $t_{out} - t_{in}$ is taken as 20 mm, and the average thickness (t) is defined as $t = (t_{in} + t_{out})/2$. For each section type, the nominal wall depth (d) is defined as the distance between the centrelines of the two external 'face' shells; and a denotes the dimension between the internal 'web' shells (Figure 8). In all of the subsequent analyses, a was taken equal to d .

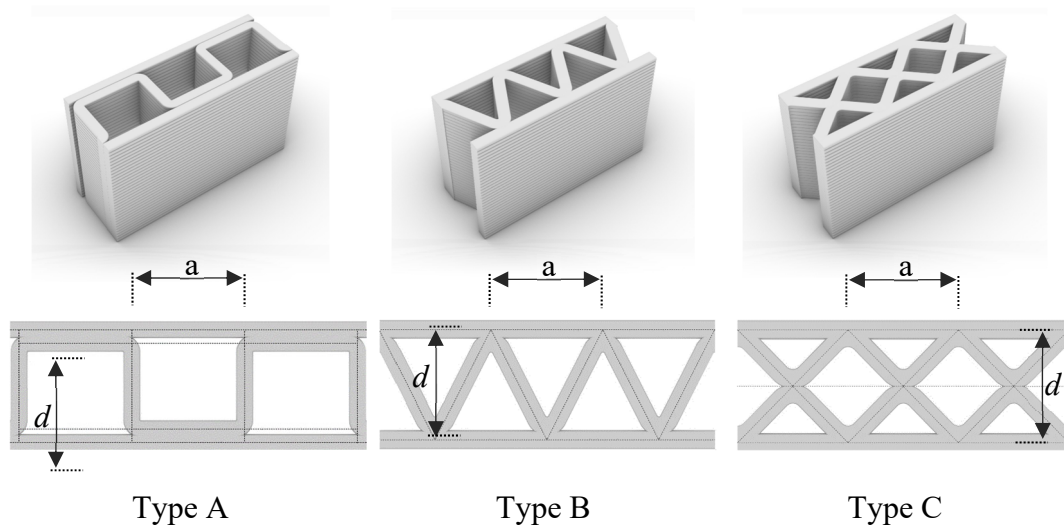


Figure 7: Alternate printed patterns considered in this study.

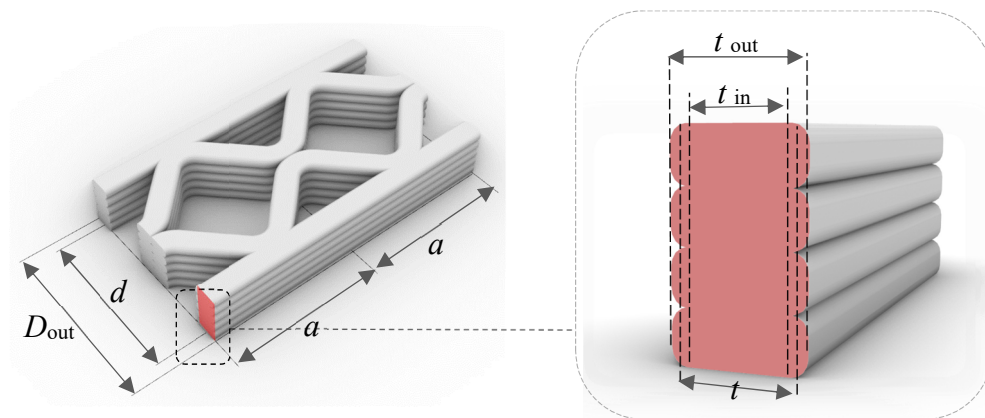


Figure 8: Definition of geometric properties along a generic cross section. d (wall thickness), a (distance between the pattern cycles).

Evaluation of the wall's compressive capacity requires the wall's area (A) and out-of-plane moment of inertia (I). These were calculated for each type of section by conservatively taking the shell thickness as t_{in} . For comparative purposes, the sectional properties of the three pattern types are provided in Table 3.

Table 3: Section properties for the alternate printed patterns. Each considers a reference section with $t_{in} = 50\text{mm}$ and $d = 500\text{mm}$. Properties accented by a bar (\bar{X}) denote the value per unit length run of the wall.

Wall Type	t_{in} (mm)	t (mm)	d (mm)	\bar{A} (mm ² /m)	\bar{I} (mm ⁴ /m)	$\bar{P}_{\text{buck,loc}}$ (kN/m)
A	50	60	500	200,000	9.32×10^9	145
B	50	60	500	212,000	8.60×10^9	137
C	50	60	500	241,000	9.23×10^9	181

4.1.3 Wall compressive strength

The compressive strength of a generic (3DP or no-3DP) cob wall requires consideration of its member capacity under combined axial load and eccentricity moment with the potential for global buckling combined with material failure. A 3DP wall however differs from a solid wall in that the section capacity can be governed by local buckling of the shell structure. Thus, the compressive stress capacity of the section was evaluated as

$$\sigma_{c,\text{max}} = \min(\sigma_{\text{mat}}, \sigma_{\text{buck,loc}}) \quad (2)$$

i.e. the lesser of the stress to cause material crushing (σ_{mat}) and local buckling ($\sigma_{\text{buck,loc}}$).

The material crushing limit in Eq. (2) was taken as the characteristic (lower-5th-percentile) compressive strength ($\sigma_{\text{mat}} = f_c'$). The characteristic strength was estimated to be 0.62 MPa, based on the assumption that it follows a lognormal distribution with mean = 0.87 MPa (Table 1) and CoV = 20%. The capacity of each of the three section types to withstand local buckling was determined using the finite element analysis package ABAQUS. The model analysed for each type of printed

section was built using shell elements and comprised a full-sized wall subjected to a uniform compressive force at its top and bottom boundaries. Since the study did not experiment physically a full-size 3DP cob walls, the FEA assumed that the joints between the web and the outer flanges of the walls are well-bonded. However, this assumption may not reflect the actual testing conditions of 3DP walls and it requires future verifications of results. The length and height of each wall were taken as 2 m. These dimensions were chosen using trial and error by satisfying the conditions of being sufficiently large not to influence the computed local buckling stress, but not excessive to cause global buckling.

A visual examination of the resulting buckling mode shape was undertaken to confirm that it indeed corresponded to local buckling of the shell structure. A typical local buckling shape is shown in Figure 9 and is characterised by the face- and web-shells deforming perpendicular to their local planes in an alternating pattern, while maintaining the original angle at shell junctions. The corresponding load capacities are summarised in the last column of Table 3 as the load per unit length of the wall ($\bar{P}_{\text{buck,loc}}$). These capacities were computed by assigning the material properties $E = 22.9$ MPa and $\nu = 0.22$ as informed by the material tests. The local buckling stress used in Eq (2), was evaluated as $\sigma_{\text{buck,loc}} = \bar{P}_{\text{buck,loc}}/\bar{A}$.

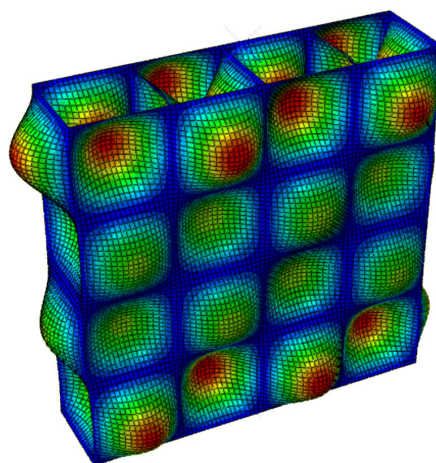


Figure 9: Visual representation of a typical local buckling failure mode in a wall member as calculated by finite element analysis. Shown for section type A.

The member capacity of the wall was evaluated from first principles by treating it as a column under eccentric loading with the potential for global buckling. In this treatment, the peak compressive stress σ_{\max} along on the section can be expressed as:

$$\sigma_{\max} = P \left[\frac{1}{A} + \frac{ec}{I} \sec \left(\frac{\pi}{2} \sqrt{\frac{P}{P_{\text{buck, glob}}}} \right) \right] \quad (3)$$

where P is the applied axial load; e is the net eccentricity of the applied load (described later); A and I are the section's area and moment of inertia; c is the distance from the centreline to the extreme compressive fibre, equal to $(d+t_{\text{in}})/2$. The critical global buckling load of the wall, $P_{\text{buck, glob}}$, was obtained by Euler's formula:

$$P_{\text{buck, glob}} = \frac{\pi^2 EI}{L_e^2} \quad (4)$$

where L_e is the effective length taken as the floor-to-floor or floor-to-roof height (see Figure 9), and other properties as defined previously.

The wall's unfactored load capacity was evaluated by assigning $\sigma_{c, \max}$ [from Eq (2)] to σ_{\max} in Eq (3) and solving for P . This solution was obtained numerically, since Eq (3) cannot be formulated explicitly in terms of P . The limit-state design capacity was obtained by applying the capacity-reduction factor $\phi = 0.5$ as per AS3700 (Standards Australia 2002), such that:

$$\phi N_c = \phi P . \quad (5)$$

4.1.4 Modelling an idealised low-rise building

To examine the feasibility of 3DP cob walls as load-bearing structural elements, the study considered an idealised 1- and 2-storey house. Schematic representations of the building's geometry are shown in Figure 10. In the case of a 1-storey house, the

walls carry only the roof load, while in the 2-storey house they carry loads from the roof and suspended floor. In each scenario, the total compressive force acting on the wall also incorporates self-weight as calculated at the ground level.

The forces imparted to the wall by the roof and the floor depend on their respective dead load (self-weight plus superimposed permanent load), live load, and span. The roof and floor are treated as one-way-spanning, so the load that they apply to the wall can be calculated as the total pressure load multiplied by a tributary width (L_{trib}). The tributary width depends on the configuration of the wall within building. In the case of an external wall, it is equivalent to half the span of the floor/roof beam [LW(1) or (3) in Figure 10]. For an internal wall, it includes the sum of the contributions from each side [LW(2) in Figure 10]. Further, if the wall contains an opening, a simplistic treatment can be to scale the tributary width pro-rata depending on the proportion of solid wall to openings. For instance, if half of the wall is perforated by openings, then the tributary width becomes twice what it would be if the wall were solid.

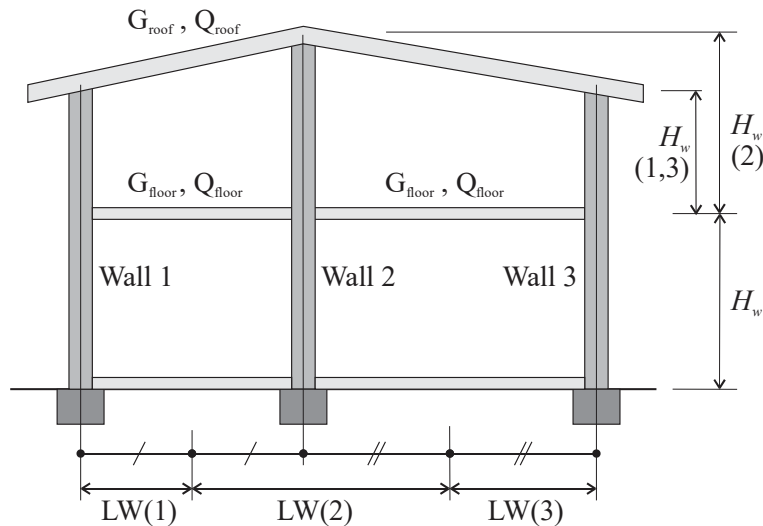


Figure 10: Overall building geometry, Two-storey ($n_s = 2$) double-bay building with internal and external walls, indicating the definition of wall height (H_w) and tributary width (denoted here as LW).

The gravity loads used in the analysis are representative of residential construction as prescribed by loading standards (e.g. (Standards Australia 2002)). The adopted unfactored loads are summarised in Table 4. The total dead load of the suspended floor is taken as 1.0 kPa, which allows for a timber joist plus timber deck floor (typically 0.5 kPa) in addition to a superimposed permanent load (0.5 kPa). The floor live load is taken as 1.5 kPa allowing for general residential occupancy. The dead load of the roof is taken as 0.9 kPa, making allowance for timber framing (rafters + purlins) with clay roof tiles. The live load on the roof is taken as 0.25 kPa.

The self-weight of the wall was calculated based on its section area, taking the weight density of the material as 18 kN/m³. Thus, the total design compressive load was evaluated as:

$$N_c^* = \begin{cases} P_{\text{roof}}^* + P_{\text{wall}}^* & \dots 1 \text{ storey} \\ P_{\text{roof}}^* + P_{\text{floor}}^* + 2P_{\text{wall}}^* & \dots 2 \text{ storey} \end{cases} \quad (6)$$

where P_{roof}^* is the load applied by the roof, P_{floor}^* by the suspended floor, and P_{wall}^* is the self-weight of the wall over a single storey height H_w . Each P^* is taken at the ultimate limit state using the load combination $1.2G+1.5Q$ (Standards Australia 2002), with G being the dead load and Q the live load component.

Table 4: Summary of constant inputs used in the feasibility study. Explanations are provided in the text.

Property	Value
<i>Cob material properties:</i>	
Elastic modulus, E	22.9 MPa
Characteristic compressive strength, f_c' (See note 1)	0.62 MPa
Weight density, γ	18 kN/m ³
Poisson's ratio, ν	0.22
<i>Unfactored loads:</i>	
Roof dead load, G_{roof}	0.9 kPa
Roof live load, Q_{roof}	0.25 kPa
Floor dead load, G_{floor}	1.0 kPa
Floor live load, Q_{floor}	1.5 kPa
<i>Limit state design factors:</i>	
Compressive strength capacity reduction factor, ϕ	0.5
Ultimate limit state design load combination	1.2G + 1.5Q
<i>Eccentricities (e) of applied load (w.r.t. wall centreline): (See note 2)</i>	
Load from roof	$0.1 \times D_{\text{out}}$
Load from floor	$0.25 \times D_{\text{out}}$
Self-weight of wall	$0.05 \times D_{\text{out}}$
<i>Notes:</i>	
1. Determined from mean strength $f_{cm} = 0.87$ MPa by assuming lognormal distribution and CoV = 20%.	
2. Where D_{out} is the full depth of the wall section measured between its outer edges (Figure 8).	

4.1.5 Connection details and load eccentricity

It is important to consider that the floor and roof will generally apply the resultant load eccentrically with respect to the wall's centreline, and this generates an out-of-plane bending moment that can have a major influence on the wall's load-carrying capacity. The eccentricity of the applied load is controlled by the connection detail. While the development of the connection details falls into the domain of detailed structural design and is outside the focus of this work, conceptual illustrations of the assumed connections are shown in Figure 11.

The connection between the roof and wall can be achieved by supporting the timber rafters using a timber bearing block, in turn resting on a spreader block that distributes the load onto the wall (Figure 11a). This detail is assumed to generate an eccentricity $e = 0.1 D_{\text{out}}$, with D_{out} as defined in Figure 8. The assumed wall-to-floor connection involves partial penetration of the joists into the wall and are supported by a bearing block and spreader block (Figure 11b), which is assumed to produce an eccentricity of $0.25 D_{\text{out}}$. It should be noted that a connection in which the floor is supported outside the extent of the wall is not advised, as it would generate an eccentricity $> 0.5 D_{\text{out}}$ and significantly diminish the load-bearing capacity. The aforementioned values of the assumed eccentricities are consistent with similar details for conventional clay brick masonry provided in AS3700 (Standards Australia 2018).



Figure 11: Potential connection details and definition of eccentricities (e) of the applied load (F).

Additionally, for sake of conservatism the self-weight of the wall is assumed to act at an eccentricity of $0.05 D_{out}$ to allow for any incidental geometric imperfection of the wall. The internal bending moment was calculated as the sum of each applied load P^* (i.e. P^*_{roof} , P^*_{floor} , P^*_{wall}) and its respective eccentricity, which dividing by the total compressive force N^*_c [from Eq. (6)] produces the net eccentricity:

$$e_{net} = \frac{\sum P_i^* e_i}{N_c^*} \quad (5)$$

The net eccentricity was used as the input value of e in Eq (3).

4.1.6 Optimisation methods

The 3D-printed sections in Figure 7 can be defined by two variables: the nominal wall depth (d) and average shell thickness (t). To determine the most efficient section needed for load-bearing functionality, an optimisation process was undertaken to minimise the material volume while ensuring that the load capacity remains sufficient to accommodate the applied design load. As a metric of the structural

adequacy, the limit state design formula [Eq (1)] can be rearranged and expressed as the capacity utilisation (u), i.e. the ratio of the design load to the design capacity:

$$u = \frac{N_c^*(t, d)}{\phi N_c(t, d)} \quad (5)$$

where both the capacity and design load are functions of the optimisation variables d and t .

As a proxy for the material volume, we can adopt the area per unit length of the wall (\bar{A}), since the two are directly proportional. Therefore, the optimisation process to determine the optimal t and d can be expressed as:

Minimise \bar{A} , by varying t and d , subject to the constraints:

- a. $u \leq 1$ (ensure structural adequacy),
- b. $t > 0, d > 0$ (positive values only),
- c. $d \geq t$ (for a section to be valid, shell thickness must not exceed effective depth).

To cater for varying architectural requirements on the building geometry, this optimisation was performed at different combinations of the wall height (H_w), tributary width (L_{trib}), and number of storeys (n_s). Constant inputs and their values are summarised in Table 4.

The optimisation problem was solved using two different methods, in order to provide a means of cross-verifying the results and to examine alternate approaches to the representation of results. The first approach used a continuous optimiser in MATLAB, in which t and d can adopt any values along a continuous domain. The second approach used the evolutionary optimiser Galapagos in the Rhino-Grasshopper package (McNeel 2020) (Figure 12). Galapagos relies on non-linear

optimisation (NLopt) and GUI algorithms (Johnson 2010). The continuous optimisation algorithm in MATLAB is the computationally faster of the two approaches; yet, implementing the optimisation in Grasshopper provides key advantages to the overall construction process, such as:

- 1) Direct link to the 3DP system (i.e. 3D printers and robotic arms), which enables an efficient fabrication process of the models.
- 2) An inclusive control over the design-to-fabrication framework, which includes geometry design and other performance optimisation aspects such as thermal, lighting and environmental impacts.
- 3) Better visual representation of the modelling results in real time, which facilitates envisaging the building geometry and its aesthetics (Figure 13).

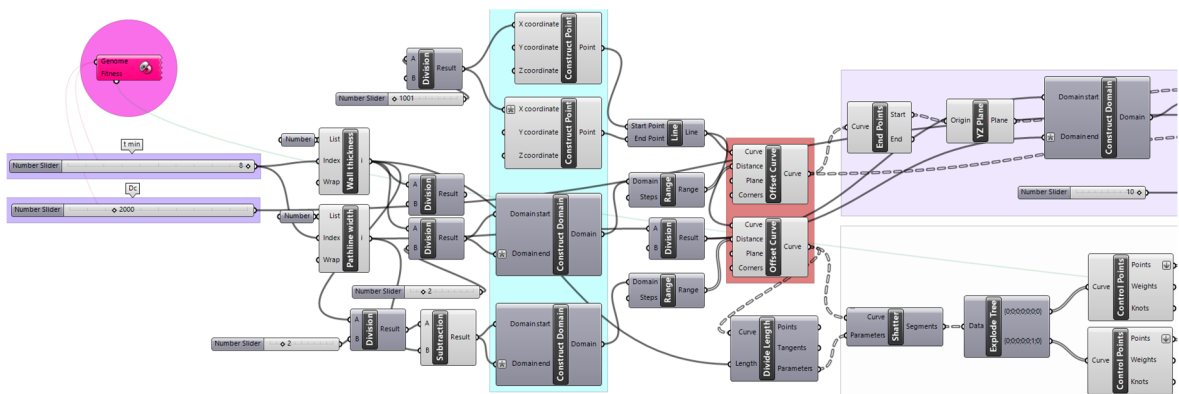


Figure 12: Part of the Grasshopper definition for the optimisation of the wall models.

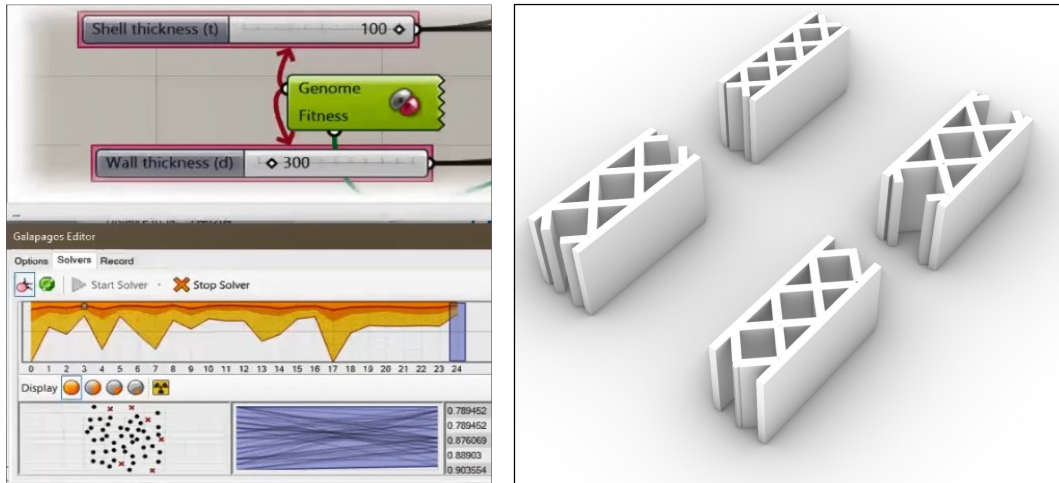


Figure 13: Visual representation of the optimisation process of Galapagos (left) and a sample of the visual generation of results for wall type C in Grasshopper (right).

4.2 Results

The typical relationship between capacity utilisation and the wall section is illustrated in Figure 14, which plots contour lines of equal utilisation (u) as a function of shell thickness (t) and nominal wall depth (d). The graph corresponds to a specific case where $H_w = 2.5$ m, $L_{trib} = 3.5$ m, and $n_s = 2$, but the general trends can be considered representative regardless of the exact values of these inputs. The thick black contour line corresponding to $u=1$ represents sections whose capacity exactly matches the design load. Thus, the grey shaded area above $u=1$ encompasses sections that are structurally adequate. The red dashed line delineates the zones where the section is compact (governed by the material crushing) as opposed to slender (governed by local buckling), as per Eq (2). The black dashed lines bound the range of t values that correspond to available nozzle sizes in the 3DP system used in the present experimental study.

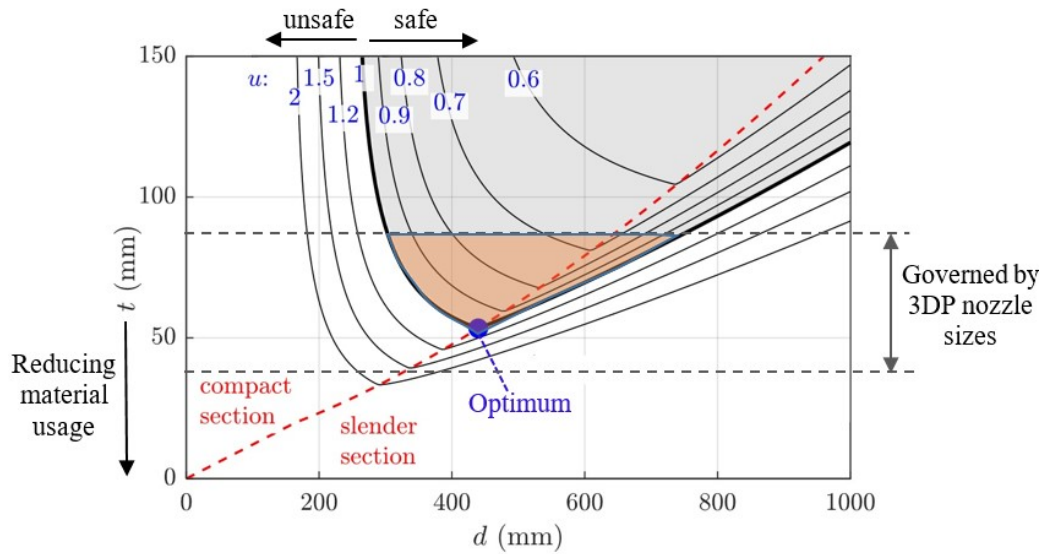


Figure 14: Typical utilisation contour plot for varied shell thickness (t) and nominal wall depth (d). Grey area indicates the zone where the wall's capacity is adequate for the design load. The dashed red line delineates compact sections (material stress failure) from slender sections (local buckling failure). In this example: $H_w = 2.5\text{m}$, $L_{trib} = 3.5\text{m}$, $n_s = 2$.

For any of the printed patterns (A, B, C) the area per unit length is approximately proportional to shell thickness (i.e. $t \propto \bar{A}$), which allows the shell thickness to be used as a proxy for material consumption. Therefore, in the graphical representation in Figure 14, the optimal section occurs at the trough of the contour line $u=1$, where t becomes minimised. Notably, the u contours follow distinct trajectories in the compact- and slender-section zones, and the optimal solution always occurs at the boundary that delineates them. In the compact-section zone, there is a roughly inverse relationship between t and d ; this is because a section with a reduced depth requires a thicker shell to maintain the necessary section area and moment of inertia. In the slender-section zone the capacity is governed by local buckling of the shell, and hence increasing the section depth requires an increase to the shell thickness to maintain the capacity. The existence of an optimal section also demonstrates that the hollow 3DP wall sections offer improved material efficiency compared to equivalent solid cob walls. Importantly these observations also highlight that in the practical

range of interest, the design capacity of the wall is governed both by the material’s compressive strength and elastic modulus.

4.2.1 Design charts using experimentally-quantified material properties

The load-bearing capability of 3DP cob walls is demonstrated in Figure 15 and Figure 16 through model ‘design charts’ that plot the t and d dimensions of the optimal wall section minimising material volume. These plots are based on the inputs in Table 4, which include the material properties as quantified through the tests in Section 3. Figure 15 keeps the wall height constant at 3.0 m while varying the tributary width up to a maximum of 6 m. Conversely, Figure 16 maintains a constant tributary width at 4.0 m while varying the wall height between 2.5 to 3.5 m. The range of wall height and tributary width was selected to reflect the practical range of interest in a typical residential building. Each figure considers the three alternate printed patterns (A, B, C), and a 1- or 2-storey building. The corresponding area per unit length (a proxy for the material consumption) of the optimal sections is plotted in Figure 17 and Figure 18, demonstrating the relative efficiency of the alternate sections.

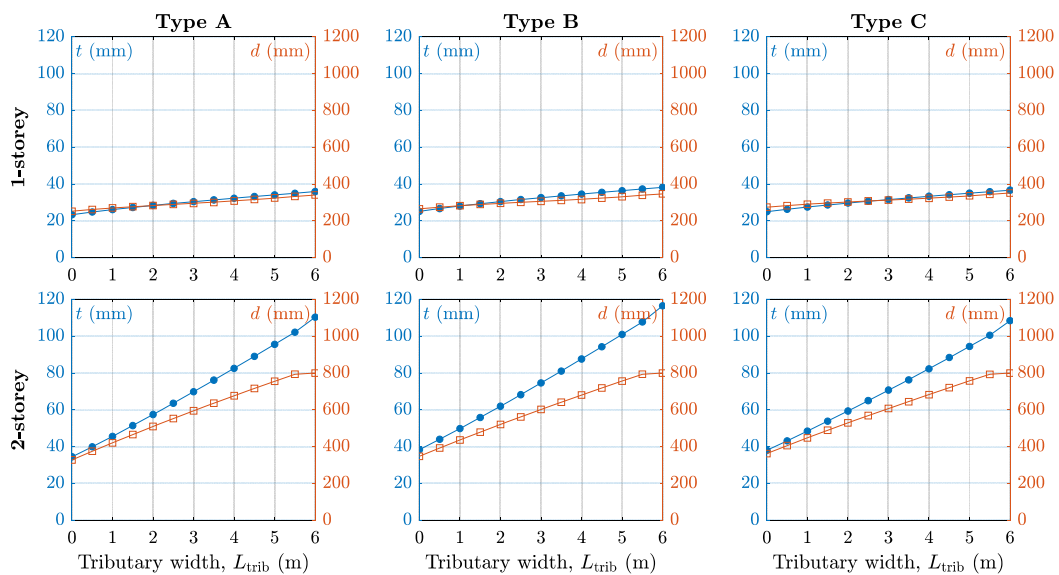


Figure 15: Dimensions t and d of optimised sections at varied tributary width and constant wall height of 3 m. Considers section types A, B, C. Top row is for single storey,

bottom row for double storey. Each graph shows t on the left y-axis and d on the right y-axis.

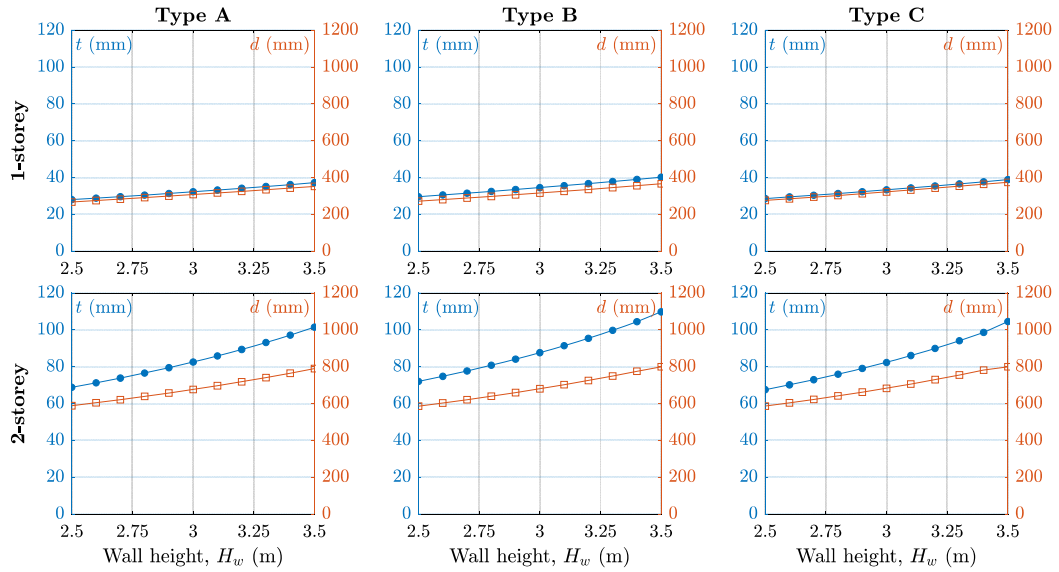


Figure 16: Dimensions t and d of optimised sections at varied wall height and constant tributary width of 4 m. Considers section types A, B, C. Top row is for single storey, bottom row for double storey. Each graph shows t on the left y-axis and d on the right y-axis.

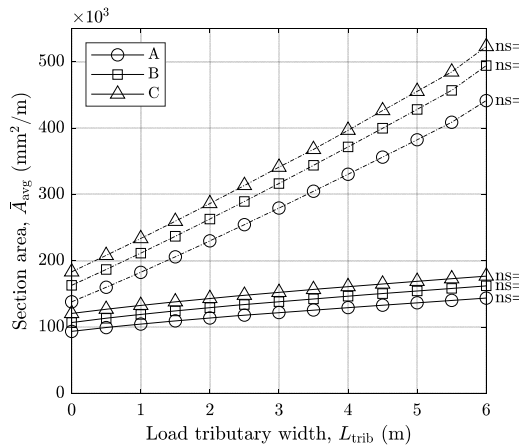


Figure 17: Cross-section area per unit metre for the optimised sections whose dimensions are plotted in Figure 15 (constant wall height of 3 m).

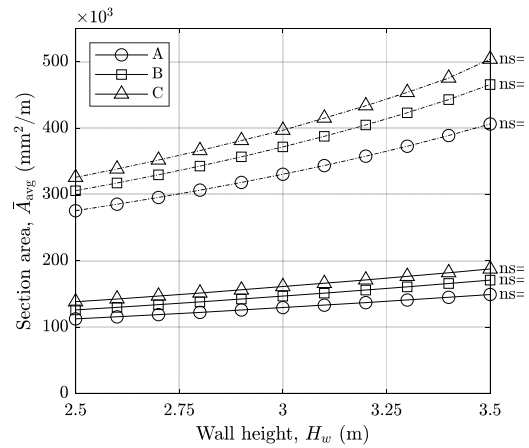


Figure 18: Cross-section area per unit metre for the optimised sections whose dimensions are plotted in Figure 16 (constant tributary width of 4 m).

5 Discussion

Application of established structural assessment principles in conjunction with the experimentally quantified properties has demonstrated that 3DP cob walls could safely sustain gravity loads in typical residential construction for up to a two-storey building with sufficient space sizes and reasonable thicknesses of walls. The design charts produced using this process (Figure 15 and Figure 16) describe the relationships between the different design variables so as to achieve the most efficient section (minimising material volume) while ensuring structural adequacy. Looking into the design charts, it is observed that a wall with a small section area A consumes less material in 3D printing. However, using small wall section area may also result in a less efficient architectural design with possibly compromised aesthetics and thermal performance, in addition to other workability challenges in the 3DP printing system to exert walls with small section area.

A previous study by Gomaa et al. (Gomaa et al. 2021) found that 3DP of large-scale cob walls require a nozzle of a size no less than 40 mm, resulting in an average shell thickness (t) that varies from 40 to 80 mm. Lower diameter sizes will slow down the printing process. They can also cause clogging problems inside the extrusion system. On the other hand, using larger nozzles leads to a higher consumption rate of material and less control over accuracy. Hence, for small load-carrying demands, not only is the wall section governed by structural requirements, it is also determined by other considerations such as thermal requirements, aesthetics, and the constraints of the 3DP apparatus.

The trends in the charts, as they are plotted now, present a range of the structurally acceptable values for the basic design variables of walls that affect the design and

fabrication process for the alternative section types (i.e. A, B, C). These variables, with their range of values, are summarised in Table 5.

Table 5: The suggested range values of the basic wall design variables in the design charts

	1 storey		2 stories	
	Min (mm)	Max. (mm)	Min (mm)	Max. (mm)
Shell thickness (t)	23	40	35	118
Wall thickness (d)	250	400	320	800

The results in general suggest that the Type A wall section is the most efficient for structural and material use considerations, followed by B then C. Nevertheless, it is essential to decide what kind of efficiency is at stake for a specific project. In other words, from a structural engineering viewpoint, ‘efficiency’ might refer only to achieving adequate structural performance with the minimal amount of material. Yet, from an architectural perspective, the notion of efficiency also combines aspects such as design function, thermal performance and environmental impacts. To elaborate further, the thermal performance efficiency of 3DP cob was explored thoroughly in a recent study by Gomaa et al. (Gomaa et al. 2019). The study proved that the voids within the 3DP cob walls dramatically improve thermal efficiency compared to solid cob walls. This means, when looking into the three wall types A, B and C in this study, their order of structural efficiency does not necessarily imply that they have the same order for thermal efficiency. Hence, it is highly recommended to consider analysing the holistic performance of the chosen wall type, including structural, thermal and environmental efficiency. This will be the subject of a future study.

5.1 Case study of a 3DP small house

As explained previously, the approach to leveraging the design charts depends greatly on the architectural design intentions and requirements. To elaborate this, a case study demonstrating an envisaged design process of a small cob house is presented and analysed in this section. The process starts with a simple floor plan indicating the zoning and the dimensions of spaces. For the purpose of this study, the house is designed to combine four spaces with different sizes and openings to represent typical design requirements. Spaces' dimensions vary from 2 m to 4 m wide, with constant wall heights of 3.0 m. The roof and the suspended floor in the 2-storey house alternative are treated as one-way spanning as shown in Figure 19. Each load-bearing wall (numbered 1–7 in Figure 18) has its characteristics detailed in Table 6 and Table 7 for 1- and 2-storey alternatives respectively. The non-loadbearing walls (unnumbered in Figure 19) can adopt the minimum required dimensions for each pattern (A, B, C), by treating it as a wall supporting zero tributary width ($L_{\text{trib}} = 0$). This case is analogous to a wall that needs to support only its own self-weight. However, assigning different L_{trib} for each wall can add complexity to the design and lower the efficiency of construction process. Therefore, non-loadbearing walls are recommended to be treated as case by case based on each design goals and requirements.

Table 6 and Table 7 indicate the process to assign the particular t and d to each wall in the building using the design charts from Figure 15. The process starts by defining the location of the wall (i.e. internal, external) and the direction of the floor and roof spans, which dictate the basic tributary width supported by each wall based on the gross dimensions. Then, if the wall has an opening, the basic tributary width was

upscaled in relation to the ratio of the openings (as described in section 4.1.4). For instance, a wall containing 50% openings (measured in the plan view) carries an effective tributary width equal to double the basic tributary width. The effective tributary width is then used to allocate t and d from the design charts for the particular wall type (A, B, C). Note that for simplicity, the effective tributary widths in Table 6 and Table 7 are rounded up to the nearest integer. Figure 20 demonstrates the finalised floor plan after assigning the selected t and d to each wall, adopting pattern type A for illustrative purposes.

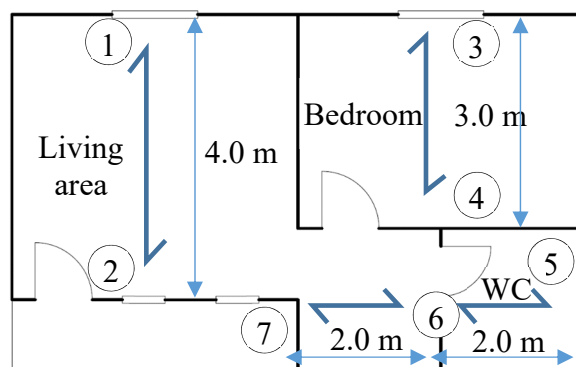


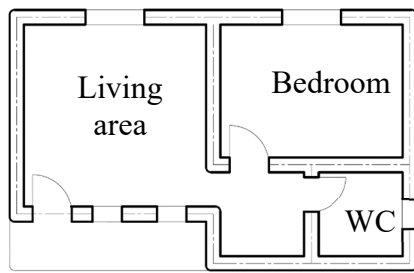
Figure 19: The floor plan of the idealised 3DP cob house. Half-headed arrows indicate the span direction of the suspended floor and roof in each space. Load-bearing walls are numbered from 1 to 7.

Table 6: Characteristics of each load-bearing wall in the 1-storey house alternative.

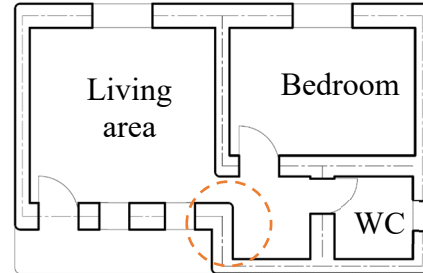
Wall code	Basic L_{trib} (m)	Opening ratio (%)	Tributary scale factor	Effective L_{trib} (m)	Corresponding t and d (mm)					
					Type A		Type B		Type C	
					t	d	t	d	t	d
1	2	25	1.5	3	30	300	35	310	35	320
2	2	50	2.0	4	35	310	35	320	35	330
3	1.5	30	1.6	3	30	300	35	310	35	320
4	1.5	15	1.3	2	30	290	35	300	35	310
5	1	5	1.1	1	30	280	30	290	30	300
6	2	30	1.6	3	30	300	35	310	35	320
7	1	40	1.8	2	30	290	35	300	35	310

Table 7: Characteristics of each load-bearing wall in the 2-storey house alternative.

Wall code	Basic L_{trib} (m)	Opening ratio (%)	Tributary scale factor	Effective L_{trib} (m)	Corresponding t and d (mm)					
					Type A		Type B		Type C	
					t	d	t	d	t	d
1	2	25	1.5	3	70	600	75	600	70	600
2	2	50	2.0	4	80	700	85	640	80	700
3	1.5	30	1.6	3	70	600	75	600	70	600
4	1.5	15	1.3	2	60	500	60	520	60	520
5	1	5	1.1	1	45	420	50	420	50	420
6	2	30	1.6	3	70	600	75	600	70	600
7	1	40	1.8	2	60	500	60	520	60	520



Adjusted walls for 3DP 1-storey house



Adjusted walls for 3DP 2-storey house

Figure 20: The finalised floor plan indicating the adjusted dimensions of walls for 3DP 1-storey house (left) and 2-storey house (right).

Based on Table 6, it can be seen that t and d vary minimally between the walls in the case of 1-storey house, regardless of the 3DP pattern (A, B, C). For example, in type A, t ranges between 30–35 mm, and d between 280–310 mm. This is because the wall dimensions are not overly sensitive to the tributary width in the case of a 1-storey building, as evident from Figure 15. In this instance, the designer may choose to standardise the walls sizes by simply adopting the largest t and d for every wall.

However, this is not the case for the 2-storey house as shown in Table 7, where the optimal sections vary substantially (e.g. for type A: $t = 45\text{--}80$ mm, $d = 420\text{--}700$ mm), thus affecting material quantity dramatically. Therefore, if the designer's ultimate aim is to save material, then it is recommended to find a suitable balance between standardising wall sizes and choosing optimal t and d using the design charts.

Figure 20 (right) shows the adjusted floor plan for the 2-storey example by assigning the minimum required section. It is immediately clear that the walls vary considerably in their sizes, especially for load-bearing versus non-loadbearing walls. These differences have a great effect on the overall quantity of materials considering the whole size of the building. It is also essential to notice that the adjusted wall thickness in the case of 2-storey building has an influence on the functionality of the space design. The aisle clearance linking the living area with the bedroom was severely narrowed down due to the increased thickness of the walls on both sides.

This previous discussion reveals the importance of the careful consideration of spanning direction in the design-to-construction process, which must cope with the functionality of the architectural design, as well as other efficiency aspects as previously suggested. To conclude, the following points are important to be considered when selecting the spanning direction:

- The function of the spaces,
- The openings location and clearance, and
- The thermal insulation aspects.

Also, when looking thoroughly into the impact of structural considerations, it becomes clear that the span direction of the floor/roof system and selection of which walls act as load-bearing can also play an important role in creating an efficient

balance between structural and architectural requirements. To elaborate this further, Figure 21 illustrates alternate options for the span direction of supporting beams (i.e. floor joists, rafters) comprising the floor/roof structure. The chosen layout influences the required wall sizes, since load-bearing walls (highlighted in red) will require a larger thickness. It is noted that consideration is given here only to gravity loads and not to out-of-plane loads due to wind or earthquake which are region-specific and not considered here.

Solution (1) in Figure 21 has four structural zones, leading to a small tributary width on each load-bearing wall, and thus enabling smaller wall thicknesses. However, this may create less freedom for design changes as the number of load-bearing walls is large. This can also reduce the functionality of the areas of the small spaces (i.e. toilets and storages) due to the thicker walls. On the other hand, solution (3) shows only two structural zones, which means only three walls in the whole house will act as load bearing. Despite the massive expected thickness of these main walls, this solution can provide high flexibility for the spacing design as the internal walls could be made of lightweight panels, while external walls only will be made of 3DP cob.

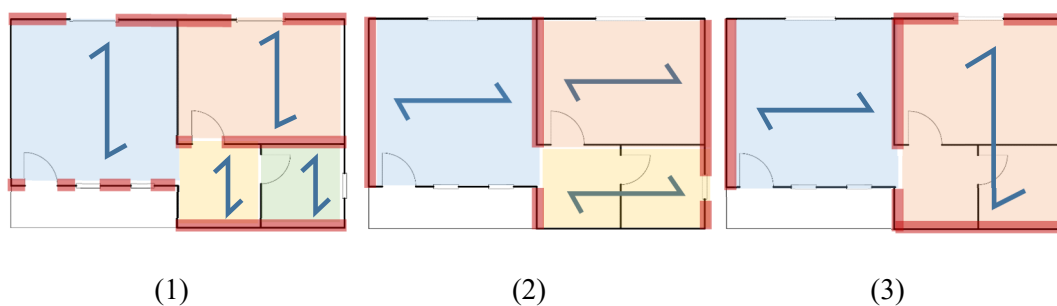


Figure 21. The possible approaches for defining the structural/spanning zones in a small 3DP cob house with indication for spanning direction. (1) Alternative with four structural zones; (2) Alternative with three structural zones; (3) Alternative with two structural zones. The load-bearing walls are highlighted in red.

6 Conclusion

The increased uptake of 3DP technologies in construction, accompanied with the quest for environmentally efficient materials, has led to leveraging earth-materials in a contemporary 3dp process. 3DP cob has been a subject of investigation for several years now; however, where those investigations mostly focused on the design aspects and environmental performance, it lacked proper testing to the 3DP cob's mechanical and structural properties.

This study has conducted a comprehensive structural feasibility investigation to the of 3DP cob walls under gravity loads. The study quantified the basic mechanical properties of 3DP cob using a standardised compression test. It then evaluated the expected member capacity of 3DP walls using established structural mechanics and design principles, and by doing so examined the feasibility of 3DP cob walls as load-bearing in typical residential construction. The testing demonstrated that 3DP cob could have very similar mechanical performance to conventional cob on the material scale. The feasibility modelling then demonstrated that 3DP cob walls have the capability to be utilised as structural load-bearing walls in up to 2-storey residential buildings.

The feasibility modelling also demonstrated the following:

- 3DP cob walls can sustain structural adequacy for less material consumption compared to conventional cob. That is due the incorporated voids inside the 3DP cob wall, which is hard to be performed in a conventional cob wall with the same thickness.
- The model design approach demonstrated in this paper provides a means for integrating 3DP cob into the design to construction framework. The generated design guidelines are directly linked to a Rhino-Grasshopper definition that enables adequate visual modelling and direct connection to 3DP system.

- The dimensions required for load-bearing functionality can be efficiently executed using the available 3DP technologies and extrusion systems.

The findings of this study complete a full feasibility investigation of 3DP cob for modern construction which combines other three aspects: 1) geometry & fabrication process; 2) thermal performance; and 3) life cycle assessment (LCA). The results lead to a conclusion that 3DP cob provides an excellent alternative to the contemporary digital construction. Also, 3DP cob can provide novel geometric and design opportunities, in addition higher precision when compared to manually constructed cob, especially in producing complex geometries. 3DP cob can substitute concrete-based constructions in small to medium size low-rise residential projects, especially as it provides higher environmental efficiency and rationalised energy use (Alhumayani et al. 2020). Moreover, 3DP cob construction can provide quick sheltering solutions with low cost and efficient use of local materials in expeditionary and hostile environments(Jagoda 2020).

It is however important to highlight, whilst promising, the findings presented herein are based on material-scale experimental tests combined with structural analysis. Therefore, future research is recommended into experimental testing at the wall member-scale to provide further verification of these findings. It is also highly recommended to consider the shrinkage aspect when experimenting construction scales. This research also initiates new opportunities for further research on exploring the emerging opportunities for workforce under the accelerating uptake of automation in construction, particularly under the declining workforce in the indigenous construction fields. This 3DP technology can potentially be a useful means for cob building repairs (e.g. crack filling, construction of pre-dried cob blocks), as well as providing some degree of adaptation and customisation for cob building design.

7. References

- 3D-WASP. 2020. "3D Printers | WASP | Leading Company in the 3d Printing Industry." 2020. <https://www.3dwasp.com/en/>.
- Akinkurolere, O. O., Cangru Jiang, A. T. Oyediran, O. I. Dele-Salawu, and A. K. Elensinnla. 2006. "Engineering Properties of Cob as a Building Material." *Journal of Applied Sciences*. <https://doi.org/10.3923/jas.2006.1882.1885>.
- Alhumayani, Hashem, Mohamed Gomaa, Veronica Soebarto, and Wassim Jabi. 2020. "Environmental Assessment of Large-Scale 3D Printing in Construction: A Comparative Study between Cob and Concrete." *Journal of Cleaner Production* 270 (June): 122463. <https://doi.org/10.1016/j.jclepro.2020.122463>.
- Ben-Alon, L, Vivian Loftness, K A Harries, and E Cochran Hameen. 2019. "Integrating Earthen Building Materials and Methods into Mainstream Construction Using Environmental Performance Assessment and Building Policy." *IOP Conference Series: Earth and Environmental Science* 323 (January): 012139. <https://doi.org/10.1088/1755-1315/323/1/012139>.
- Brunello, Gabi, Jose Espinoza, and Alex Golitz. 2018. "Cob Property Analysis." Santa Clara University.
- CEN. 2011. "EN 772-1. Methods of Test for Masonry Units - Part 1: Determination of Compressive Strength." https://infostore.saiglobal.com/en-us/Standards/EN-772-1-2011-A1-2015-331320_SAIG_CEN_CEN_761952/.
- Coventry, Kathryn Anne. 2004. "SPECIFICATION DEVELOPMENT FOR THE USE OF DEVON COB IN EARTHEN CONSTRUCTION . By KA University ö Plymouth A Thesis Ubmitt Fulfilment for the . In e of School of Earth , Ocean and Environmental Sciences Faculty of Science July 2004." University of Plymouth. <https://pearl.plymouth.ac.uk/handle/10026.1/1291>.
- CyBe. 2019. "3D Studio 2030 — CyBe Construction." 2019. <https://cybe.eu/case/3d-studio-2030/>.
- Damluji, Salma Samar. 2008. *The Architecture of Yemen: From Yafi to Hadramut*. London: Laurence King Publishing. <https://www.bcin.ca/bcin/detail.app?id=426855>.
- Earth Devon. 2008. "Cob Dwellings: Compliance with The Building Regulations." *Cob and Unbaked Earth Dwellings* 2000: 1–21.
- Fabbri, Antonin, Jean-Claude Morel, and Domenico Gallipoli. 2018. "Assessing the Performance of Earth Building Materials: A Review of Recent Developments." *RILEM Technical Letters* 3: 46–58. <https://doi.org/10.21809/rilemtechlett.2018.71>.
- Feng, Peng, Xinmiao Meng, Jian-Fei Chen, and Lieping Ye. 2015. "Mechanical Properties of Structures 3D Printed with Cementitious Powders." *Construction and Building Materials* 93: 486–97. <https://doi.org/10.1016/j.conbuildmat.2015.05.132>.

- Ford, Simon, and Mélanie Despeisse. 2016. "Additive Manufacturing and Sustainability: An Exploratory Study of the Advantages and Challenges." *Journal of Cleaner Production* 137: 1573–87. <https://doi.org/10.1016/j.jclepro.2016.04.150>.
- Fordice, John, and Lola Ben-Alon. 2017. "A Research Project Dedicated to Making Cob Legally Accessible to the Public."
- Gomaa, Mohamed, Jim Carfrae, Steve Goodhew, Wassim Jabi, and Alejandro Veliz Reyes. 2019. "Thermal Performance Exploration of 3D Printed Cob." *Architectural Science Review*, April, 1–8. <https://doi.org/10.1080/00038628.2019.1606776>.
- Gomaa, Mohamed, Wassim Jabi, Alejandro Veliz Reyes, and Veronica Soebarto. 2021. "3D Printing System for Earth-Based Construction: Case Study of Cob Walls." *Automation in Construction* 124: 103577. <https://doi.org/https://doi.org/10.1016/j.autcon.2021.103577>.
- Goodhew, Steve, P.C. Grindley, and S.D. Probeif. 1995. "Composition, Effective Thermal Conductivity And Specific Heat Of Cob Earth-Walling." *Transactions on The Built Environment* 15 (January): 205–13. <https://doi.org/10.2495/STR950231>.
- Hamard, Erwan, Bogdan Cazacliu, Andry Razakamanantsoa, and Jean Claude Morel. 2016. "Cob, a Vernacular Earth Construction Process in the Context of Modern Sustainable Building." *Building and Environment* 106: 103–19. <https://doi.org/10.1016/j.buildenv.2016.06.009>.
- Houben, H, and H Guillaud. 1994. *Earth Construction: A Comprehensive Guide*. London: Intermediate Technology Publications. https://scholar.google.com/eg/scholar?hl=en&as_sdt=0%2C5&q=%09Houben%2C+H.+and+Guillaud%2C+H.%2C+%281994%29+Earlh+Construction%2C+Intermedate+Technology+Publications&btnG=.
- Jagoda, Jenee A. 2020. "An Analysis of the Viability of 3D-Printed Construction as an Alternative to Conventional Construction Methods in the Expeditionary Environment." Air Force Institute of Technology. <https://scholar.afit.edu/etd/3240>.
- Jiménez Rios, Alejandro, and Dermot O'Dwyer. 2020. "Experimental Validation for the Application of the Flat Jack Test in Cob Walls." *Construction and Building Materials* 254. <https://doi.org/10.1016/j.conbuildmat.2020.119148>.
- Johnson, Steven G. 2010. "NLopt Documentation." 2010. <https://nlopt.readthedocs.io/en/latest/>.
- Kazemian, Ali, Xiao Yuan, Evan Cochran, and Behrokh Khoshnevis. 2017. "Cementitious Materials for Construction-Scale 3D Printing: Laboratory Testing of Fresh Printing Mixture." *Construction and Building Materials* 145: 639–47. <https://doi.org/10.1016/j.conbuildmat.2017.04.015>.
- Keefe, Laurence. 2005. *Earth Building : Methods and Materials, Repair and Conservation*. <https://books.google.com.au/books?hl=en&lr=&id=cCGAAgAAQBAJ&oi=fnd&p>

g=PR1&dq=Earth+Building+-
+Methods+and+Materials,+Repair+and+Conservation&ots=jZ3gR-
qkRd&sig=MYVBVS1ZW3-
ZXe0EjfwBku7b9i0&redir_esc=y#v=onepage&q=Earth Building – Methods and
Materials%2C R.

- Khoshnevis, Behrokh. 2004. “Automated Construction by Contour Crafting — Related Robotics and Information Technologies” 13: 5–19.
<https://doi.org/10.1016/j.autcon.2003.08.012>.
- Kianfar, Ehsan, and Vahab Toufigh. 2016. “Reliability Analysis of Rammed Earth Structures.” *Construction and Building Materials* 127: 884–95.
<https://doi.org/10.1016/j.conbuildmat.2016.10.052>.
- Le, T. T., S. A. Austin, S. Lim, R. A. Buswell, A. G.F. Gibb, and T. Thorpe. 2012. “Mix Design and Fresh Properties for High-Performance Printing Concrete.” *Materials and Structures/Materiaux et Constructions* 45 (8): 1221–32.
<https://doi.org/10.1617/s11527-012-9828-z>.
- McNeel, Robert. 2020. “Grasshopper - in Rhino 6.” 2020.
<https://www.rhino3d.com/6/new/grasshopper>.
- Miccoli, Lorenzo, Urs Müller, and Patrick Fontana. 2014. “Mechanical Behaviour of Earthen Materials: A Comparison between Earth Block Masonry, Rammed Earth and Cob.” *Construction and Building Materials* 61: 327–39.
<https://doi.org/10.1016/j.conbuildmat.2014.03.009>.
- Minke, Gernot. 2012. *Building with Earth: Design and Technology of a Sustainable Architecture*. Basel: Walter de Gruyter.
https://books.google.com.au/books?hl=en&lr=&id=DUbVAAAAQBAJ&oi=fnd&pg=PA7&ots=CDK0wx0OUL&sig=tPuVKZfCHEUL5OuczH1EHOx4gJk&redir_esc=y#v=onepage&q&f=false.
- Morton, Tom, Fionn Stevenson, Bruce Taylor, and Nicholas Charlton Smith. 2005. “Low Cost Earth Brick Construction: Monitoring & Evaluation.” Fife, UK.
<http://www.arc-architects.com/downloads/Low-Cost-Earth-Masonry-Monitoring-Evaluation-Report-2005.pdf>.
- Perrot, A., D. Rangeard, and E. Courteille. 2018. “3D Printing of Earth-Based Materials: Processing Aspects.” *Construction and Building Materials* 172: 670–76.
<https://doi.org/10.1016/j.conbuildmat.2018.04.017>.
- Perrot, A, D Rangeard, and A Pierre. 2016. “Structural Built-up of Cement-Based Materials Used for 3D- Printing Extrusion Techniques.” *Materials and Structures*, 1213–20. <https://doi.org/10.1617/s11527-015-0571-0>.
- Pullen, Quinn M., and Todd V. Scholz. 2011. “Index and Engineering Properties of Oregon Cob.” *Journal of Green Building* 6 (2): 88–106.
<https://doi.org/10.3992/jgb.6.2.88>.
- Quagliarini, Enrico, and Gianluca Maracchini. 2018. “Experimental and FEM

- Investigation of Cob Walls under Compression.” *Advances in Civil Engineering* 2018: 21–29. <https://doi.org/10.1155/2018/7027432>.
- Quagliarini, Enrico, Alessandro Stazi, Erio Pasqualini, and Evelina Fratolocchi. 2010. “Cob Construction in Italy: Some Lessons from the Past.” *Sustainability* 2 (10): 3291–3308. <https://doi.org/10.3390/su2103291>.
- Rizza, Michael, and Hana Bottger. 2015. “Effect of Straw Length and Quantity on Mechanical Properties of Cob.” San Francisco. http://umanitoba.ca/faculties/engineering/departments/ce2p2e/alternative_village/media/16th_NOCMAT_2015_submission_42.pdf.
- Saxton, R. H. 1995. “Performance of Cob as a Building Material.” *Structural Engineer London* 73 (7): 111–15.
- Shrubsole, C., I. G. Hamilton, N. Zimmermann, G. Papachristos, T. Broyd, E. Burman, D. Mumovic, Y. Zhu, B. Lin, and M. Davies. 2019. “Bridging the Gap: The Need for a Systems Thinking Approach in Understanding and Addressing Energy and Environmental Performance in Buildings.” *Indoor and Built Environment* 28 (1): 100–117. <https://doi.org/10.1177/1420326X17753513>.
- Standards Australia. 2002. *AS 1170.1–2002 (R2016) Structural Design Actions Part 1 : Permanent , Imposed and Other Actions. Australian / New Zealand Standard* TM. Sydney, NSW: Australian / New Zealand Standard TM.
- Veliz Reyes, Alejandro, Wassim Jabi, Mohamed Gomaa, Aikaterini Chatzivasileiadi, Lina Ahmad, and Nicholas Mario Wardhana. 2019. “Negotiated Matter: A Robotic Exploration of Craft-Driven Innovation.” *Architectural Science Review* 0 (0): 1–11. <https://doi.org/10.1080/00038628.2019.1651688>.
- Vinceslas, Théo, Erwan Hamard, Andry Razakamanantsoa, and Fateh Bendahmane. 2018. “Further Development of a Laboratory Procedure to Assess the Mechanical Performance of Cob.” *Environmental Geotechnics* 7 (3): 200–207. <https://doi.org/10.1680/jenge.17.00056>.
- Wang, Li, Hailong Jiang, Zhijian Li, and Guowei Ma. 2020. “Mechanical Behaviors of 3D Printed Lightweight Concrete Structure with Hollow Section.” *Archives of Civil and Mechanical Engineering* 20 (1): 1–17. <https://doi.org/10.1007/s43452-020-00017-1>.
- Weismann, Adam, and Katy Bryce. 2006. *Building with Cob: A Step-by-Step Guide*. Devon: Green Books Ltd.
- Zareiyani, Babak, and Behrokh Khoshnevis. 2017. “Interlayer Adhesion and Strength of Structures in Contour Crafting - Effects of Aggregate Size, Extrusion Rate, and Layer Thickness.” *Automation in Construction* 81 (June): 112–21. <https://doi.org/10.1016/j.autcon.2017.06.013>.

Chapter 6 Exploration of the Thermal properties of 3DP cob

6.1 Introduction

Determining the thermal properties of a material in buildings is essential for two reasons. First is to understand the heat transfer from outside to inside the building, or vice versa, through that material, and second, in the context of minimizing environmental impacts of building, to ensure an adequate level of comfort for occupants can be achieved while minimizing the energy demand for heating and cooling. Reducing the operational energy contributes greatly towards improving the overall environmental performance of buildings. Hence, this chapter explores the thermal properties of 3DP cob through conducting physical testing of the thermal conductivity using specimens that represent different types of 3DP cob walls. The chapter is expected to provide a fundamental understanding of the correlation between the basic designs of 3DP cob walls and their associated thermal performance. This will ultimately enable designers to conduct thermal performance and whole building energy simulations at the early design stage of 3DP cob houses, which is a step that goes side by side with the structural performance optimisation as detailed in the previous chapter.

6.2 List of manuscripts

This part of the research has been produced as a journal article, published in Architectural Science Review journal:

Gomaa, M., Carfrae, J., Goodhew, Jabi, W., Veliz, A., 2019. Thermal performance exploration of 3D printed cob. *Architectural Science Review*, pp. 1–8. Doi: <https://doi.org/10.1080/00038628.2019.1606776>

The paper is presented here in a reformatted version for consistency of the presentation of this thesis. The accepted manuscript can be found in Appendix III.

Statement of Authorship

Title of Paper	Thermal performance exploration of 3D printed cob
Publication Status	<input checked="" type="checkbox"/> Published <input type="checkbox"/> Accepted for Publication <input type="checkbox"/> Submitted for Publication <input type="checkbox"/> Unpublished and Unsubmitted work written in manuscript style
Publication Details	Mohamed Gomaa, Jim Carfrae, Steve Goodhew, Wassim Jabi & Alejandro Veliz Reyes (2019): Thermal performance exploration of 3D printed cob, <i>Architectural Science Review</i> , DOI: 10.1080/00038628.2019.1606776

Principal Author

Name of Principal Author (Candidate)	Mohamed Gomaa			
Contribution to the Paper	Physical prototyping of 3DP cob, Conceptualization, Methodology, Data curation, Investigation, Resources, Software, Validation, Visualization, Writing, review & editing, and acting as corresponding author.			
Overall percentage (%)	80 %			
Certification:	This paper reports on original research I conducted during the period of my Higher Degree by Research candidature and is not subject to any obligations or contractual agreements with a third party that would constrain its inclusion in this thesis. I am the primary author of this paper.			
Signature	<table border="1" style="width: 100%;"> <tr> <td style="text-align: center;"><i>Mohamed Gomaa</i></td> <td style="text-align: center;">Date</td> <td style="text-align: center;">14/09/2020</td> </tr> </table>	<i>Mohamed Gomaa</i>	Date	14/09/2020
<i>Mohamed Gomaa</i>	Date	14/09/2020		

Co-Author Contributions

By signing the Statement of Authorship, each author certifies that:

- i. the candidate's stated contribution to the publication is accurate (as detailed above);
- ii. permission is granted for the candidate to include the publication in the thesis; and
- iii. the sum of all co-author contributions is equal to 100% less the candidate's stated contribution.

Name of Co-Author	Jim Carfrae			
Contribution to the Paper	Methodology, Formal analysis, Resources, Editing and Reviewing			
Signature	<table border="1" style="width: 100%;"> <tr> <td style="width: 60%;"></td> <td style="text-align: center;">Date</td> <td style="text-align: center;">16 Sept 2020</td> </tr> </table>		Date	16 Sept 2020
	Date	16 Sept 2020		

Name of Co-Author	Steve Goodhew			
Contribution to the Paper	Methodology, Formal analysis, Resources, Editing and Reviewing			
Signature	<table border="1" style="width: 100%;"> <tr> <td style="width: 60%;"></td> <td style="text-align: center;">Date</td> <td style="text-align: center;">21st September</td> </tr> </table>		Date	21st September
	Date	21st September		

Name of Co-Author	Wassim Jabi		
Contribution to the Paper	Conceptualization, Methodolgy, Resources, Reviewing & Editing		
Signature		Date	3/12/2020

Name of Co-Author	Alejandro Veliz Reyes		
Contribution to the Paper	Resources, Reviewing & Editing		
Signature		Date	23.11.2020

Thermal Performance Exploration of 3D Printed cob

Abstract

This paper investigates the thermal properties of 3D printed Cob, a monolithic earth construction technique based on robotically extruded subsoil and locally available organic fibres. The relevance of 3D printed earthen construction materials and the transition from vernacular construction towards a digitally-enabled process are critically discussed. The use of robotic manufacturing is outlined and the methodology to produce the necessary samples for thermal measurement is detailed. The results of the 3D printed samples are compared with traditionally-constructed Cob material of the same dimensions. The assessment has revealed strong potential for 3D printed cob as compared to its manually constructed counterparts in terms of thermal conductivity. Moreover, the testing process has helped in identifying several challenges in the 3D printing process of cob and the assessment of its thermal properties, which will ultimately bring the work closer to full-scale applications.

Keywords:

robotics; 3d printing; cob construction; parametric design; thermal analysis; vernacular architecture.

1. Introduction

Conventional monolithic (e.g. concrete) construction has several associated shortcomings such as high CO₂ emissions, high embodied energy of construction process and depletion of natural resources (Goodhew and Griffiths 2005). In contrast, this paper presents cob construction as a viable alternative. Cob stands as the most used construction material around the world (Figure 1), and consists of subsoil (earth), water, fibrous material

(typically straw) and sometimes lime. Other mixtures can use an addition of sand and/or clay, if required, in order to improve the physical properties of the material mix (Hamard et al. 2016). Given the reliance of this material on localised modes of construction, its application in built elements can be found in a series of material configurations including adobe bricks or “quinchas” (clay-based soil mix applied onto a woven pattern of fibrous materials). Likewise, a series of geometric and formal configurations can be found in vernacular architecture which illustrate the versatility and structural characteristics of cob construction, including circular configurations in China and ovoid configurations in African vernacular architecture.

Cob is a sustainable material as compared with concrete, requires very limited resources to be sourced, mixed and constructed (Benardos, Athanasiadis, and Katsoulakos 2014). Moreover, Hamard et al. (2016) and Wanek, Smith, and Kennedy (2015) have demonstrated that re-using cob will have building performance and financial benefits, while it complies with modern UK building regulations.

In terms of design opportunities, cob provides higher freedom of design and ease of construction, while also it allows design modifications (cutting or adding material) easily at any time when the building element’s cob is still wet or dry (Melià et al. 2014; Hamard et al. 2016). This malleability, low cost and building performance suggest further work is required in order to understand the opportunities offered by cob in the new digital age, and particularly on novel and emergent frameworks of digital practice and design, such as robotic fabrication. Within this research territory, this paper explores the suitability of raw-earth in the research territory of robotically-assisted 3D printing. It is acknowledged that the consideration of raw-earth for 3D printing applications can reveal a series of potential lines of enquiry, such as mechanical and structural properties, new design and

formal opportunities, new local economies and skilled labour, or environmental and geological considerations. This report stems from the project "Computing craft" which aims at scoping the feasibility for robotically 3D printed cob structures at early stages of the technology development cycle, and further work is required to determine properties of larger scale cob construction. In response to this project's life cycle, we specifically introduce this area of enquiry by assessing the thermal performance of 3D printed cob in comparison with handmade cob samples.



Figure 1. Cob building in Totnes, UK (Veliz Reyes et al. 2018)

In order to critically situate this research within the broader area of 3D printing, cob must be defined in relation to its vernacular constructive expression, and particularly on how it can be adopted and modified in the context of emergent digital practices. Here, vernacular architecture and construction are not seen as primitive or historical, but instead as a series of local sophisticated material practices which engage with and address local

environmental and material conditions. It is acknowledged, then, that the perception of vernacular architecture has been evolving to reflect different environmental, technological and cultural contexts (Niroumand, Barceló Álvarez, and Saaly 2016). Aligned with this, earthen materials have received renewed interest within the modern construction industry for the past few years (Chandel, Sharma, and Marwah 2016; Veliz Reyes et al. 2018). As a result, it can be claimed that despite its vernacular development, cob is currently being subjected to a series of studies aiming at incorporating this local, material-based knowledge within established frameworks of practice and academic research and development (e.g. Veliz et al, 2019).

Much of the material performance outside the confines of life-cycle assessment relates to the thermal properties of earthen building techniques and subsequent materials (Houben and Guillaud 1994; Hurd and Gourley 2000; Walker et al. 2005). This has been assessed in a number of different design configurations, including different sequences of material layers and the inclusion of natural insulation (Steven Goodhew and Griffiths 2005; Griffiths and Goodhew 2012). Many of these proposed or measured material configurations specify appropriate thermal characteristics, such as thermal conductivity (W/mK) or specific heat capacity (J/kg/degC). Thermal conductivity is a property that is used to calculate (whether in the more raw form of a spreadsheet or more complex and animated use of dynamic thermal simulations) the ability for a building built from the material to perform as expected. This performance might be associated with the thermal comfort of the occupants or the energy use of the building (CIBSE 2015). Therefore, much interest is centred on the ability for an earthen material, that can be made from different subsoil types and mixed at different ratios with a range of different fibres, to fulfil technical and legislative requirements.

In the present era, cob construction techniques operate under established frameworks of practice often based on notions of hand-making, hand-assembling and localised material intelligence. This operational knowledge has been developed over many years outside the boundaries of academic, technological and professional disciplinary frameworks (Crysler, Cairns, and Heynen 2012). At the same time, the construction industry has been demanding more complex forms, faster processes, and lower labour costs, which are making traditional construction methods increasingly obsolete (Veliz Reyes et al. 2018). Hence, Digital construction of earthen materials could be instrumental to promoting the use of locally available natural construction materials as it expands the range of sustainable construction solutions that are adapted to local contexts (Hamard et al. 2016; Veliz Reyes et al. 2018), following the key precepts of vernacular architecture such as local, material-driven knowledge and practices.

The benefits of digitally augmented crafts have been examined broadly only on small-scale applications, yet the greater benefits for the design and construction industry are poorly explored. An early study that was conducted at ETH Zurich by Gramazio, Kohler, and Willmann in 2008 has revealed the ability of robotic technology to directly create informed design solutions based on materials and manufacturing restraints (Veliz Reyes et al. 2018). This early experimentation has raised the awareness of digital fabrication, and particularly additive manufacturing, within the AEC industries worldwide (Hague, Campbell, and Dickens 2003; Wu, Wang, and Wang 2016). The continuous experimentation with digital fabrication methods in recent years has created substantial enhancements to large-scale 3D printing techniques (Baumers et al. 2016; Ishak, Fisher, and Larochelle 2016). This dramatic increase in the amount of research on implementing 3D printing into large-scale processes has revealed several potential applications for

architecture and the construction industry (Agustí-Juan and Habert 2017a; Wu, Wang, and Wang 2016) , such as reductions in waste, material usage, and transportation costs in the supply chain. In this respect, both Hamard et al. (2016) and (Agustí-Juan et al. 2017b) highlight that the integration of digital fabrication techniques into vernacular architecture has revealed sustainability potentials for construction applications. However, this research has also revealed further challenges to be addressed that include not only the development of novel 3D printing robotic applications, but more broadly their implications for the AEC industry such as the need for skilled labour, new material configurations, or new design and geometric opportunities.

2. Methods and Materials

2.1 Prototypes design

This study is mainly assessing the thermal conductivity of four scaled prototypes of 3D printed cob specimens. Then the research compares the result to seven cob specimens of nearly the same dimensions that were constructed using manual techniques. The prototypes are scaled down to one fourth (1/4) the average real cob walls thickness. The geometries of prototypes are modelled in Rhinoceros via Grasshopper, while kuka PRC was the used tool for robotic simulation (Figure 2). Each model is designed on the basis of unidirectional tool paths then arrayed vertically to create the full height of the specimen. Some of the geometric constraints for toolpath design have been outlined as:

- The layer heights have been set to 18 mm. and the diameter of the nozzle in all experiments was 25 mm, yet, due to the fluid nature of the material, it was expected that a 35-40 mm thick cob path would be created.
- Printing speeds has been set at 10 mm/sec

- Initially all toolpaths have been created following a standard 3-axis contour crafting approach (X, Y, Z).

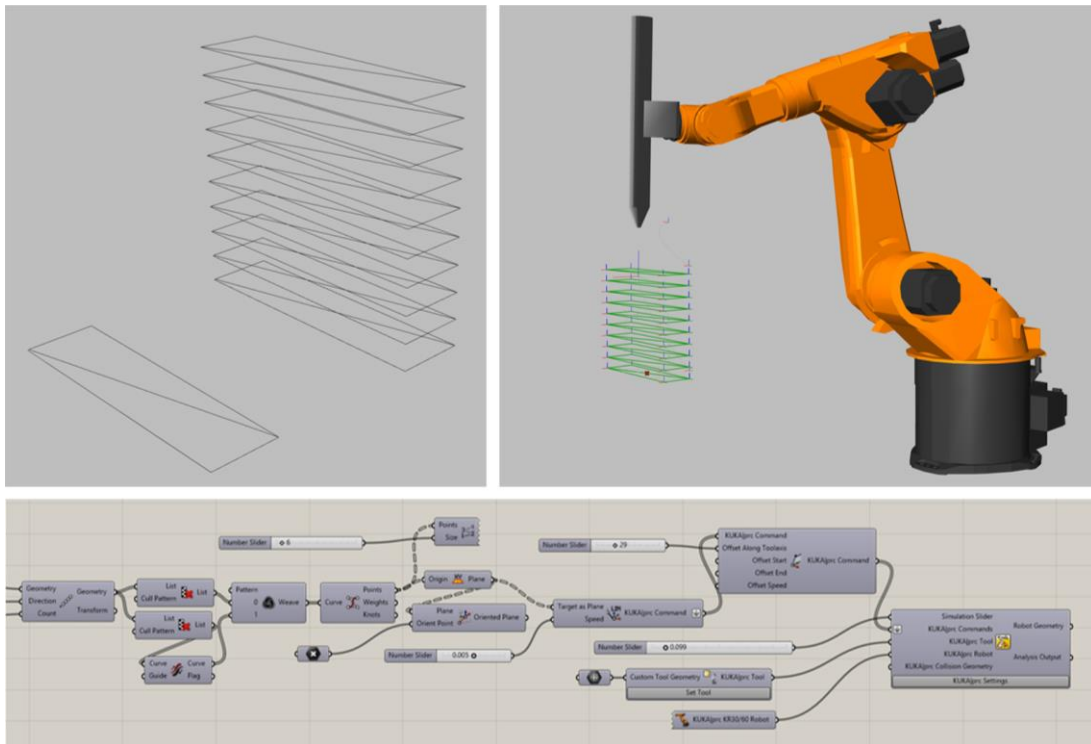


Figure 2. Creating the toolpath for cob prototypes in rhino via grasshopper and kuka PRC.

Virtual prototypes were then 3D printed at Cardiff University using a Kuka KR60HA robot and a custom designed material extrusion system (Figure 3). The extrusion system utilises a stepper motor with a worm gearbox and acme screw that pushes the wet cob mix through a tube with a 25mm nozzle at its end. The designed geometries are converted into multi-layered path lines of which the robotic arm can follow in a layer by layer fashion (Figure 4). Each of the four prototypes was designed to represent a different solution for better thermal insulation of walls (Figure 5).

- (1) The first prototype was designed as a solid wall (CF1).
- (2) The second prototype was design as a double-layered wall with a single continuous air gap (CF2).

- (3) The third prototype was designed as a triple-layered wall with air pockets (CF3).
- (4) The fourth prototype was designed as double-layered wall with pockets filled with straw (CF4).



Figure 3. The 3d printing set up in Cardiff University; KUKA KR60 HA robot with a custom designed material extrusion system



Figure 4. The Layer by layer technique of printing



Figure 5. Samples of the 3d printed cob. From left to right; solid, single gap with straw filling and double gap.

The 3D printed samples have dimensions of (300x300x90mm), while the manually constructed samples are (300x300x70mm) (Figure 6), both formed into blocks of a suitable size for the heat flow meter (Figure 7).



Figure 6. Samples of the manually constructed cob specimen in Plymouth University. The cob sample to the left uses UK subsoil in the mix, while the right one uses French subsoil

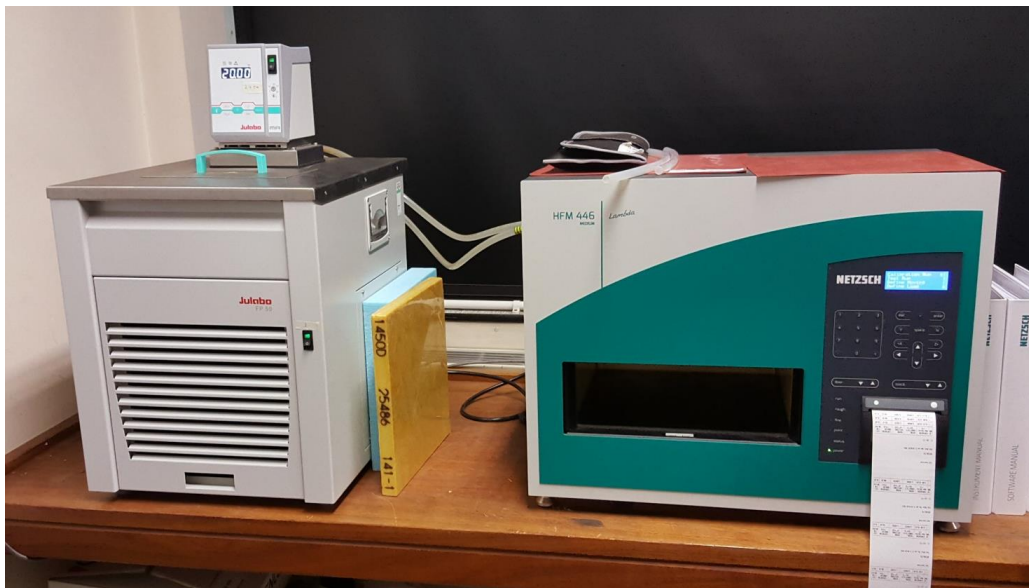


Figure 7. Heat flow meter (HFM 446) at Plymouth University

2.2 Materials

As stated earlier, cob basically is a mix of subsoil, fibre, and water. Weismann and Bryce (2006) recommended a generic ratio of water to subsoil as one part water to every five parts of dry ingredient. By converting this to weight, it means 2.0 Kg of water is added to each 8.0 Kg of subsoil. As for the straw, it is recommended to be 2 % by weight. Hamard et al. (2016) supported the previous statement in his extensive systematic review on cob by affirming the proportions of cob mixture (averages) to be 78 % subsoil, 20 % water and 2 % fibre (straw).

According to both Weismann and Bryce (2006) and Hamard et al. (2016), the recommendation for the subsoil formula itself is 15-25 % clay to 75-85 % aggregate/sand. Harrison (1999) also stated similar recommendation of 20 % clay to 80 percent aggregate/sand. Testing the subsoil properties is a critical step for the right determination of the cob formula. Testing occurs on the subsoil before water content is added. Subsoil contains different amount of clay, sand, silt and aggregate. This depends on the sourcing location and where the subsoil is being dug within that location. Based on several field testing of the subsoil, besides using a trial and error method, amendment to sand and clay ratios could be identified to achieve the right ingredient for cob. After examining the subsoil, the next step is to add the water and fibres, which is straw for this study. Other bindings fibres can be used such as seaweed and alginate (Perrot, Rangeard, and Courteille 2018).

2.2.1 3D printed cob samples

The subsoil for the 3D printed samples for this study was sourced from farmland near Barry in Cardiff, UK. Three subsoil specimens from three locations within the same field

were examined according to the recommended testing methods that are found in the literature (Goodhew, Grindley, and Probeif 1995; Harrison 1999; Weismann and Bryce 2006). These tests included simple field tests and in-depth laboratory tests. Both testing methods have revealed that the ingredients of the subsoil are matching the general recommendations for cob mixture without applying any additional aggregates or clay. The subsoil samples from Cardiff were found to have an average aggregate to clay ratio as 79.5 to 21.5 % respectively.

However, as cob is typically mixed in a nearly dry state, those proportions do not necessarily fit the purpose of 3D printing as a more viscous mix is required. An increase of water content can, however, affect negatively other material properties including shrinkage, drying time and mechanical/structural stability during the 3D printing process, limiting the layering height and overall quality of a printed prototype. Based on a number of 3D printing tests prior to this study, modified proportions of cob mixtures had been determined for 3D printing purposes (Veliz Reyes et al. 2018). The new mixture has a slight increase in the water content to 21% and a decrease in the straw ratio to 1%. Yet, the field tests of the subsoil properties are always recommended and required prior to determining the appropriate cob mix.

2.2.2 Manually constructed cob samples

The manually constructed cob samples were prepared at Plymouth University as part of the Interreg project ‘The CobBauge’ (The CobBauge Project 2018). These samples were prepared in the lab using a variety of sub-soils that had been identified as being suitable for use in cob construction without additional aggregates. The soils were then analysed for particle size distribution. These tests were carried out by wet sieving for the fraction

greater than 80 μm and by laser granulometry for elements smaller than 80 μm . The soils are identified as FR4, a sandy yellow French soil with a low clay content and UK3, a heavy red clay soil from mid Devon (UK). The subsoils had a variety of fibres added to them in different proportions based on the literature (Hamard et al. 2016), and the accumulated experience on several actual cob building projects.

The fibres used in these tests were hemp shiv, chopped reed and chopped straw in proportions of 8%, 4%, 2% and none (% by dry weight of soil). The soils were first oven dried at 40°C until they reached an equilibrium weight, where 3 subsequent weighing's at 24hour intervals were within 1% of each other (ISO, 2000), then a percentage of water was added: 28% to the FR4, and 31% to UK3 (the different amounts of water were added to give the same viscosity to the final mix). After allowing the clays to soak, the fibres were added and mixed manually.

2.3 Thermal performance testing

To establish the thermal performance of the material, a series of conductivity tests were undertaken using a Heat Flow Meter at Plymouth University. The four 3D printed cob samples were compared to seven manually-constructed cob samples. The heat flow meter used for the conductivity tests was a Netzsch HFM 446 (NETZSCH 2018). This machine is based on ASTM C518, ASTM C1784, ISO 8301, JIS A1412, DIN EN 12664, and DIN EN 12667 Method and Technique for the Characterization of Insulation Materials. The Netzsch was chosen because it takes a larger sample size and uses additional external thermocouples in conjunction with the hot and cold plates. This makes it suitable for measuring denser, more random materials like cob.

3. Results

Table 1 shows all the tested cob samples, listed in order of their conductivities. The close relation between density and conductivity could be also seen (Volhard and Reisenberger 2016). The graph in Figure 8 shows the relationship between conductivity and density of all the cob samples. Walls with lower conductivity and lower density, towards the left bottom corner of the figure, are more desirable due to their higher insulation value and lighter weight. The conductivity results show that all specimens conform to within 10% of each other. The dotted line shows an exponential trend in the relationship between the density and conductivity of the samples (Domínguez-Muñoz *et al.*, 2010). Of the four printed samples, the three that are not solid are all below this line. This indicates that the cavities in the samples are affecting their performance, and giving a relatively better conductivity in relation to their density (CIBSE, 2017).

Table 1 Results of the Conductivity analysis of the cob samples in relation to their density.

Sample	Method	Density (kg/ m ³)	Conductivity (W/mk)
UK3 8% reed	Manual	1047.6	0.25
UK3 8% shiv	Manual	1038.7	0.28
CF4 Straw fill	3d printed	1397.0	0.32
UK3 4% shiv	Manual	1206.5	0.33
CF2 Single-Gap	3d printed	1283.7	0.37
CF3 Double-Gap	3d printed	1495.5	0.40
UK3 2% shiv	Manual	1503.8	0.43
CF1 Solid	3d printed	1780.3	0.48
F4 2% straw	Manual	1564.5	0.63
F4 0% straw	Manual	1774.3	0.84
Cob Tile	Manual	1832.3	0.84

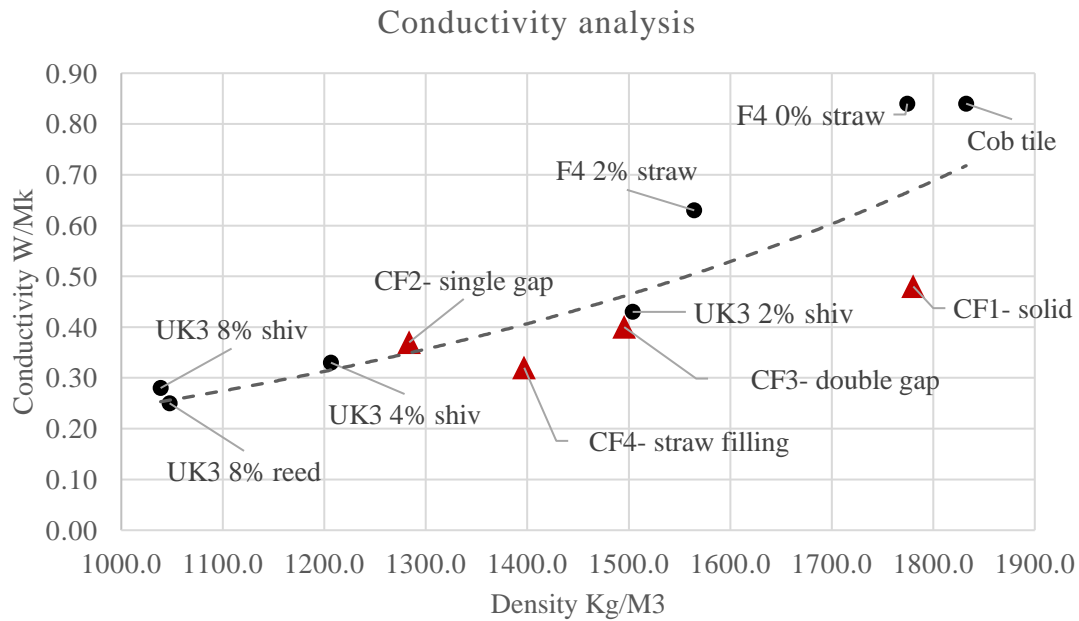


Figure 8. Conductivity of all the cob samples in relation to their density

The percentage of straw in the cob mixture of the 3D specimens was kept constant at 2%. The differences were in the design of the specimen cross-section and the addition of loosely packed straw in air cavities. The analysis indicates that the use of air cavities combined with the addition of straw into them significantly improves the conductivity of the 3D printed samples relative to their density. Specifically, CF4 (Air gap with straw) showed an improvement of 15.0% in conductivity and an increase of 8.0% in density when compared to CF2 (Air gap without straw). In terms of absolute conductivity, sample CF4, with the straw filling, gives the best result among the 3D printed samples. Within manually constructed samples, the higher percentage of fibres in the mix lead to lower density and consequently a lower conductivity.

Compared to all samples, CF4 represented the third best result. The significant thermal performance of the 3D printed samples is immediately recognised among their manually-structured counterparts. Even when comparing solid samples, the CF1 specimen out-

performed approximately half the manually-constructed samples.

4. Discussion and conclusions

The results detailed above reveal that 3D printer cob is comparable with hand-made counterparts. While the 3D printed samples do not outperform the hand-made samples significantly, the results suggest that 3D printing can be utilised for cob construction without compromising the building performance of the construction, thus revealing further opportunities for research by exploring additional benefits of robotic fabrication, including (among others):

- Novel geometric and design opportunities afforded by robotic fabrication as opposed as hand-made construction.
- Exploiting the capacities of robotic fabrication when compared to manual labour, including a higher precision and accuracy of the built element.
- Exploring emerging opportunities in the field of robotics in terms of skills automation, as well as to develop new skills in the construction workforce.
- Scope opportunities afforded by recent development in the fields of robotics and material sciences including human-robot collaboration, artificial intelligence and data-driven design processes.

5. Acknowledgement

We would like to acknowledge the continuous guidance and support of Professor Veronica Soebarto (University of Adelaide). We would also like to acknowledge the invaluable help of Lina Ahmad (Zayed University, UAE), Anas Lila, Aikaterini Chatzivasileiadi (Cardiff University).

6. Funding

This work is supported by the Engineering and Physical Sciences Research Council (EPSRC) and The University of Nottingham under the Network Plus: Industrial Systems in the Digital Age, Grant number: EP/P001246/1 (Feasibility study PI: Dr. Wassim Jabi, Cardiff University). Some measurements contained in this paper were conducted as part of the CobBauge project which is an Interreg programme, financed by the European Union.

7. References

- Agustí-Juan, Isolda, and Guillaume Habert. 2017. "Environmental Design Guidelines for Digital Fabrication." *Journal of Cleaner Production* 142. Elsevier Ltd: 2780–91. doi:10.1016/j.jclepro.2016.10.190.
- Agustí-Juan, Isolda, Florian Müller, Norman Hack, Timothy Wangler, and Guillaume Habert. 2017. "Potential Benefits of Digital Fabrication for Complex Structures: Environmental Assessment of a Robotically Fabricated Concrete Wall." *Journal of Cleaner Production* 154. Elsevier Ltd: 330–40. doi:10.1016/j.jclepro.2017.04.002.
- Baumers, Martin, Phill Dickens, Chris Tuck, and Richard Hague. 2016. "The Cost of Additive Manufacturing: Machine Productivity, Economies of Scale and Technology-Push." *Technological Forecasting and Social Change* 102. Elsevier Inc.: 193–201. doi:10.1016/j.techfore.2015.02.015.
- Benardos, A., I. Athanasiadis, and N. Katsoulakos. 2014. "Modern Earth Sheltered Constructions: A Paradigm of Green Engineering." *Tunnelling and Underground Space Technology* 41 (1). Elsevier Ltd: 46–52. doi:10.1016/j.tust.2013.11.008.
- Brunskill, R. W. 2000. *Houses and Cottages of Britain : Origins and Development of Traditional Buildings*. Gollancz.
- Chandel, S. S., Vandna Sharma, and Bhanu M. Marwah. 2016. "Review of Energy Efficient Features in Vernacular Architecture for Improving Indoor Thermal Comfort Conditions." *Renewable and Sustainable Energy Reviews* 65. Elsevier: 459–77. doi:10.1016/j.rser.2016.07.038.

- Crysler, C. Greig (Christopher Greig), Stephen. Cairns, and Hilde. Heynen. 2012. *The SAGE Handbook of Architectural Theory*. SAGE.
https://books.google.co.uk/books?hl=en&lr=&id=n354cBry_6EC&oi=fnd&pg=PP1&dq=Concepts+of+vernacular+architecture'+in+Crysler&ots=Pw24wWdCl-&sig=SNo-Gw-HqS2YldnJ573uAL73kXo&redir_esc=y#v=onepage&q=Concepts+of+vernacular+architecture'%2C+in+Crysler&f=false.
- Goodhew, Steve, P.C. Grindley, and S.D. Probeif. 1995. "Composition, Effective Thermal Conductivity And Specific Heat Of Cob Earth-Walling." *WIT Transactions on The Built Environment* 16 (January). WIT Press.
 doi:10.2495/STR950231.
- Goodhew, Steven, and Richard Griffiths. 2005. "Sustainable Earth Walls to Meet the Building Regulations." *Energy and Buildings*. Elsevier.
 doi:10.1016/j.enbuild.2004.08.005.
- Gramazio, F, M Kohler, and J Willmann. 2014. *Digital Materiality in Architecture*. Zurich: Park Books.
- Griffiths, Richard, and Steve Goodhew. 2012. "Sustainability of Solid Brick Walls with Retrofitted External Hemp-lime Insulation." *Structural Survey* 30 (4). Emerald Group Publishing Limited: 312–32. doi:10.1108/02630801211256661.
- Hague, R, I Campbell, and P Dickens. 2003. "Implications on Design of Rapid Manufacturing." *Proceedings of the Institution of Mechanical Engineers, Part C: Journal of Mechanical Engineering Science* 217 (1). SAGE PublicationsSage UK: London, England: 25–30. doi:10.1243/095440603762554587.
- Hamard, Erwan, Bogdan Cazacliu, Andry Razakamanantsoa, and Jean Claude Morel. 2016. "Cob, a Vernacular Earth Construction Process in the Context of Modern Sustainable Building." *Building and Environment* 106. Elsevier Ltd: 103–19.
 doi:10.1016/j.buildenv.2016.06.009.
- Harrison, Ray. 1999. *Earth: The Conservation and Repair of Bowhill, Exeter : Working with Cob*. London: James & James.
- "HFM 446 Lambda Series - NETZSCH Analyzing & Testing." 2018. Accessed October 18. <https://www.netzsch-thermal-analysis.com/en/products->

solutions/thermal-diffusivity-conductivity/hfm-446-lambda-series/.

- Houben, H, and H Guillaud. 1994. *Earth Construction: A Comprehensive Guide*. London: Intermediate Technology Publications.
https://scholar.google.com.eg/scholar?hl=en&as_sdt=0%2C5&q=%09Houben%2C+H.+and+Guillaud%2C+H.%2C+%281994%29+Earlh+Construction%2C+Intermediate+Technology+Publications&btnG=.
- Hurd, John., and Ben. Gourley. 2000. *Terra Britannica : A Celebration of Earthen Structures in Great Britain and Ireland*. Edited by ICOMOS/UK (Organization). Earth Structures Committee. London: James & James.
- Ishak, Ismayuzri Bin, Joseph Fisher, and Pierre Larochelle. 2016. “Robot Arm Platform for Additive Manufacturing Using Multi-Plane Toolpaths,” 1–7.
doi:10.1115/DETC2016-59438.
- Melià, Paco, Gianluca Ruggieri, Sergio Sabbadini, and Giovanni Dotelli. 2014. “Environmental Impacts of Natural and Conventional Building Materials: A Case Study on Earth Plasters.” *Journal of Cleaner Production* 80: 179–86.
doi:10.1016/j.jclepro.2014.05.073.
- Niroumand, Hamed, Juan Antonio Barceló Álvarez, and Maryam Saaly. 2016. “Investigation of Earth Building and Earth Architecture According to Interest and Involvement Levels in Various Countries.” *Renewable and Sustainable Energy Reviews* 57. Elsevier: 1390–97. doi:10.1016/j.rser.2015.12.183.
- Perrot, A., D. Rangeard, and E. Courteille. 2018. “3D Printing of Earth-Based Materials: Processing Aspects.” *Construction and Building Materials* 172. Elsevier Ltd: 670–76. doi:10.1016/j.conbuildmat.2018.04.017.
- “The CobBauge Project.” 2018. Accessed October 17.
<http://www.cobbauge.eu/en/cobbauge-2/>.
- Veliz Reyes, Alejandro, Mohamed Gomaa, Aikaterini Chatzivasileiadi, and Wassim Jabi. 2018. “Computing Craft: Early Stage Development Of a Robotically-Supported 3D Printing System for Cob Structures.” In *ECAADe- Computing for Better Tomorrow*, 1:791–800. Lodz: cuminCad.
- Volhard, Franz, and Julian Reisenberger. 2016. *Light Earth Building : A Handbook for*

Building with Wood and Earth. Birkhauser.

<https://www.ribabookshops.com/item/light-earth-building-a-handbook-for-building-with-wood-and-earth/86214/>.

Walker, Peter, Rowland Keable, Joe Martin, and Vasilios Maniatidis. 2005. “Rammed Earth : Design And.” IHS BRE.

<https://www.brebookshop.com/samples/148940.pdf>.

Wanek, C, M Smith, and JF Kennedy. 2015. *The Art of Natural Building: Design, Construction, Resources*. Edited by C Wanek, M Smith, and JF Kennedy. Vancouver, Canada: New Society Publishers.

Weismann, Adam, and Katy Bryce. 2006. *Building with Cob*. Devon: Green Books Ltd.

Wu, Peng, Jun Wang, and Xiangyu Wang. 2016. “A Critical Review of the Use of 3-D Printing in the Construction Industry.” *Automation in Construction* 68. Elsevier B.V.: 21–31. doi:10.1016/j.autcon.2016.04.005.

Chapter 7 Exploration of the Environmental Implications of 3DP Cob (LCA)

7.1 Introduction

Buildings play a critical role in improving the environmental conditions and reduce carbon emission globally. A building's external envelope, represented by the external walls, contributes greatly towards the overall environmental impacts of buildings. This chapter investigates the environmental impacts of 3DP cob walls compared to that of 3DP concrete, conventional concrete and conventional cob walls. The study utilized a standard LCA method, from cradle to site, with a focus on load-bearing walls in small/medium size houses. The chapter aims to provide an understanding of the environmental implications of using 3D printing methods in construction in general, and 3DP cob construction in specific. The findings empower the relevant stakeholders, such as designers and project owners to make an informed decision regarding construction methods and materials in relation to their environmental impacts.

7.2 List of manuscripts

This part of the research has been produced as a journal article, published in Journal of Cleaner Production:

Alhumayani, H., Gomaa, M., Soebarto, V., and Jabi, W. 2020. "Environmental Assessment of Large-Scale 3D Printing in Construction: A Comparative Study

between Cob and Concrete.” *Journal of Cleaner Production*, June.
<https://doi.org/10.1016/j.jclepro.2020.122463>

The paper is presented here in a reformatted version for consistency of the presentation of this thesis. The accepted manuscript can be found in Appendix IV.

Statement of Authorship

Title of Paper	Environmental Assessment of large-Scale 3D Printing in Construction: A Comparative Study between Cob and Concrete.
Publication Status	<input checked="" type="checkbox"/> Published <input type="checkbox"/> Accepted for Publication <input type="checkbox"/> Submitted for Publication <input type="checkbox"/> Unpublished and Unsubmitted work written in manuscript style
Publication Details	Hashem Alhumayani, Mohamed Gomaa, Veronica Soebarto and Wassim Jabi (2020). Environmental Assessment of large-Scale 3D Printing in Construction: A Comparative Study between Cob and Concrete. <i>Journal of Cleaner Production</i> . DOI: 10.1016/j.jclepro.2020.122463

Principal Author

Name of Principal Author (Candidate)	Hashem Alhumayani		
Contribution to the Paper	Conducting LCA assessment on 3DP concrete and conventional concrete. In addition, contributing to: Conceptualization, Methodology, Software, Resources for 3DP concrete, Data curation, Writing - review & editing, Visualization, Project administration		
Overall percentage (%)	45 %		
Certification:	This paper reports on original research I conducted during the period of my Higher Degree by Research candidature and is not subject to any obligations or contractual agreements with a third party that would constrain its inclusion in this thesis. I am the primary author of this paper.		
Signature		Date	15/10/2020

Co-Author Contributions

By signing the Statement of Authorship, each author certifies that:

- the candidate's stated contribution to the publication is accurate (as detailed above);
- permission is granted for the candidate to include the publication in the thesis; and
- the sum of all co-author contributions is equal to 100% less the candidate's stated contribution.

Name of Co-Author	Mohamed Gomaa		
Contribution to the Paper	Conducted the LCA analysis on 3DP cob and conventional cob, with percentage of contribution of 45 % equal to the principle author. I also acted as the corresponding author. In addition, I contributed to: Conceptualization, Methodology, Software, Resources for 3DP cob, Data curation, Writing - review & editing, Visualization, Project administration		
Signature		Date	14/10/2020

Name of Co-Author	Veronica Soebarto			
Contribution to the Paper	Reviewing & editing, Supervision			
Signature	Professor Veronica Soebarto	Digitally signed by Professor Veronica Soebarto DN: cn=Professor Veronica Soebarto, o=The University of Adelaide, ou=School of Architecture and Built Environment, email=veronica.soebarto@adelaide.edu.au, c=AU Date: 2020.12.02 19:32:37 +10'30'	Date	2/12/2020

Name of Co-Author	Wassim Jabi		
Contribution to the Paper	Reviewing & editing, Supervision		
Signature		Date	3/12/2020

Environmental Assessment of large-Scale 3D Printing in Construction: A Comparative Study between Cob and Concrete

Abstract

This paper explores the environmental impacts of large-scale 3D printing (3DP) construction in comparison to conventional construction methods using two different types of construction material: concrete and cob (a sustainable earth-based material). The study uses a standard Life Cycle Assessment (LCA) method, from cradle to site, to assess the environmental impacts of the construction materials and processes, with a focus on load-bearing walls in small/medium size houses. As expected, cob-based methods (conventional followed by 3DP) show lower overall environmental impacts and global warming potentials than the concrete-based methods. The study also shows that while the overall environmental impacts of 3DP concrete is higher than that of 3DP cob due to higher global warming potential, stratospheric ozone depletion and fine particulate matter formation, it has less impact on marine eutrophication, land use, and mineral resources scarcity. The environmental issues that remain to be overcome in relation to 3DP concrete is its high-cement content, while the issue in 3DP cob rises from the use of electricity for the 3D printing operation. The study indicates that the use of renewable energy resources and innovative material science can greatly increase the potentials of both 3DP cob and 3DP concrete respectively for future construction.

Keywords:

LCA; Robotic fabrication; 3D printing; Cob; Concrete; Sustainable construction

1. Introduction

In 2018, the International Energy Agency (IEA) reported that the average rate of growth of global energy consumption had increased almost two-fold since 2010. This high energy demand increased CO₂ emissions by 1.7% in 2018 alone, reaching a new record in its history (IEA, 2018). The building construction sector and its operations accounted for 40% of the CO₂ emissions and 36% of global fine energy use in 2018 (IEA and UNEP, 2018). At the same time, buildings play an important role in transitioning to a low-carbon economy (Shrubsole et al., 2019). The drive to improve environmental conditions and reduce carbon emissions has led to innovations in technology and construction techniques (Shrubsole et al., 2019). Digital fabrication technologies in the manufacturing industry are also being adopted in architecture and construction (Craveiro et al., 2019). 3D printing technologies, in particular, have become a focus of attention in a number of diverse fields, including the construction sector (Wang et al. 2014; Soliman et al. 2015).

3D printing involves producing three dimensional objects by layering different materials (ASTM International, 2013). 3D printing has developed dramatically in recent years and can now be done using a range of materials (Agustí-juan et al., 2017). Where originally the use of 3D printing was restricted to the creation of physical models to present concepts to stakeholders; it is now being used to build entire buildings (Geneidy & Ismaeel, 2018). A milestone in the development of 3D printing technology took place when “Contour Crafting”, a research project conducted at the University of Southern California, showed how layered extrusion technologies can work within large scale constructions (Khoshnevis et al., 2006).

The use of 3D printing in construction is gaining increased attention around the world. Several companies, such as Apis Cor, CyBe and Winsun, have upscaled technology intake over the past 5 years and have started tendering for 3D printed projects in Europe, Saudi Arabia, the United Arab Emirates and China (Apis-cor, 2019; CyBe, 2019; Winsun3d, 2019). In 2019, Apis Cor constructed the world's largest 3D Printed (3DP) building in the UAE for the Dubai Municipality. The building stands over an area of 640 square meters and has two-stories with an overall wall height of 9.5 meters. The walls were all 3D printed on site while the foundations and slabs were constructed conventionally (Apis-cor, 2019).

Although there have been numerous studies and many advancements in 3D printing of buildings, 3D printing applications in construction are still at an early stage and are still fairly limited in terms of project scale, materials, and the high cost of the technology (Wu et al., 2016; Berman, 2012). The other important aspect that remains insufficiently explored to date is the environmental impacts and the Life Cycle Assessment (LCA) of the 3DP technologies in construction (Veliz Reyes et al., 2018). There is, therefore, the need to investigate the environmental impact of 3D printed building design, materials, technology, regulations and codes (Dixit, 2019).

The Life Cycle Assessment (LCA) method, which is presented in the ISO 14040-44: 2006 Standards (ISO 2006), is an assessment method of the environmental impacts of products and processes. LCA has been used in the construction sector for the last twenty years (Singh et al., 2011; Buyle et al., 2013). LCA methods can evaluate and optimise the construction processes by taking a comprehensive and systemic approach to environmental assessment (Tulevech et al., 2018). LCA in construction has two main approaches, depending on the required level of depth of

assessment (Häfliger et al., 2017). The first approach involves a comprehensive level of detailing of the environmental impact of a building over its entire life cycle, including all the associated processes and materials (cradle to grave). The second approach assesses and compares only the environmental impact of the construction materials and/ or construction method (cradle to site). According to ISO14040, 2006, LCA involves four phases that work iteratively: The first phase is to define the goal and scope for launching the system boundaries and the quality criteria for the inventory data and functional unit. The second phase entails the inventory analysis (LCI), which focuses on the life cycle of the products in several steps. This phase deals with the production and collection of information on energy flows and physical material. The third phase is a life cycle impact assessment (LCIA), which uses the data collected from LCI and calculates their contribution to various environmental impact groups. The last phase is interpretation, which evaluates results to achieve conclusions, identifies important issues, gives recommendations, and describes limitations.

There are several impact assessment methods to calculate environmental performance, including CML, EDIP, ReCiPe, and TRACI (Cavalett et al., 2013) and each of these methods combines several impact indicators/ categories. The ReCiPe method, for instance, combines eighteen impact categories, as listed by Goedkoop et al. (2009), namely: global warming potential, ozone depletion potential, terrestrial acidification potential, freshwater eutrophication potential, marine eutrophication potential, human toxicity potential, photochemical oxidant formation potential, particulate matter formation potential, terrestrial ecotoxicity potential, freshwater ecotoxicity potential, marine ecotoxicity potential, ionising radiation potential, agricultural land occupation potential, urban land occupation potential, natural land

transformation potential, water depletion potential, mineral depletion potential, and fossil depletion potential. Each impact category has its weight and significance on the environment. Product Environmental Footprint Category Rules Guidance (PEFCR Guidance) provide recommendations for the most relevant impact categories to current global environmental concerns (European Commission, 2017). These recommendations are based on normalised and weighted factors, representing the level of importance per category based on its impact on the environment.

To date, a limited number of studies have been conducted to assess the environmental opportunities of applying digital fabrication and 3DP methods in construction (Soto et al. 2018; Dixit 2019). Researchers have generally focused on the environmental impact at a small scale, for example, Kreiger and Pearce (2013), who studied the environmental benefits of distributing conventional and 3D printing of polymer products. A study conducted by Faludi et al. (2015) compared the environmental impacts of two types of additive manufacturing machines versus traditional numerical (CNC) milling machines and showed that there is a reduction in energy use and waste in additive manufacturing machines when compared to CNC milling machines.

Recently, Yao et al. (2019) compared 3D printing geo-polymer technology and the use of ordinary concrete in four scenarios using a Life Cycle Assessment (LCA) method. The study revealed that 3D printing technologies perform better environmentally and possibly lead to a reduction in waste when creating complex construction components. However, ordinary concrete performed environmentally better than 3D printed geo-polymer when it came to building simple walls. Prior to this, Kafara et al. (2017) conducted a comparative study of 3D printing

manufacturing and conventional manufacturing of mould core making for carbon fiber reinforced polymer (CFRP) production. The results revealed that 3D printing manufacturing performed better on an environmental scale than conventional manufacturing. In recent years, researchers have started to explore 3D printing of earth-based materials, such as cob, as an eco-friendly substitute to 3D printed concrete (Perrot et al. 2018). It is claimed that 3D printing of earth materials can leverage the environmental potential of 3D printing techniques by reducing waste and the transportation and carbon footprint of the construction process (Gomaa et al., 2019; Veliz Reyes et al., 2018).

Concrete is one of the most used materials in conventional construction in the Middle East and Saudi Arabia (General Authority for Statistics, 2019). On the other hand, the Middle East region, including Saudi Arabia, is rich with earth materials and Cob houses (Ibrahim, 2018; NICDP, 2020). Saudi Arabia's national development plan (Vision 2030) envisages adopting and using new technologies, such as 3D printing, with the aim of becoming a global investment powerhouse (Saudi Vision 2030, 2018). Saudi's government aims to increase the percentage of ownership of houses by 60% (Housing Program, 2019). The fast-growing building industry in Saudi Arabia is pushing the government towards the adoption of advanced construction methods that can meet the new development agenda. The increasing demand is expected to substantially increase energy consumption with consequent environmental implications (Asif et al., 2017). This makes it even more imperative to study the environmental impact of the building industry.

Hence, the main aim of this study is to compare the environmental impact of the 3D printing construction method with conventional construction methods using two

different types of construction material: concrete and cob. Both materials are conventionally available worldwide with well-established knowledge of practice and historical performance. This approach is expected to provide a clearer understanding of the environmental implications of using 3D printing methods in construction, which should empower designers, project planners and stakeholders with the necessary data to make informed decisions regarding construction methods and materials. The study focuses on the construction market in the Middle East, particularly Saudi Arabia.

2. Methods and Materials

2.1. Life cycle assessment set up

The study used SimaPro 9.0.0.35 software (PRé 2019) to implement the LCA method. As recommended in ISO 14040 and 14044, the Ecoinvent v3.1 database was used because it is a compliant data source for studies and assessments. The ReCiPe Midpoint (H) v1.03 method for impact assessment was used as it provides a wide range of environmental categories, used in most scientific studies on LCA (Huijbregts et al., 2017; Agustí-Juan et al., 2017). For water use analysis, the study implemented the Available Water Remaining (AWARE) method, as recommended by the United Nations Environment Programme (UNEP/SETAC 2016). The chosen processes for the LCA of the constructed walls were raw material extraction, transport, material manufacturing, and the energy required for construction.

This study focuses on the most relevant impact categories, which are identified as all the impact categories that cumulatively contributed to at least 80% of the total environmental impacts (excluding toxicity related impact categories)(European-

Commission 2017). The seven most relevant impact categories, as advised by PEFCR Guidance, are: 1) global warming; 2) stratospheric ozone depletion; 3) fine particulate matter formation; 4) marine eutrophication; 5) land use; 6) mineral resource scarcity; and 7) water use (AWARE). The latest normalisation and weighting factors for this study were obtained through the European Commission Platform on Life Cycle Assessment (European Commission, 2017; Sala et al., 2018; European, Commission 2019).

2.2. Study goal and scope

Given the limited information about 3D printed constructions, the LCA carried out for the purposes of this thesis is a cradle to site, which includes raw materials, transportations, and construction process on site. The using phase and demolishing phase are not included in this study. LCA is applied to assess and compare the environmental impacts of two different construction methods: 3D printing and conventional construction methods. The materials used in both methods are concrete and cob. The conventional concrete method commonly used in Saudi Arabia involves reinforced concrete structures (column and beam) and blockwork walls while the 3DP method involves solely the concrete mix. On the other hand, cob ingredients are the same in both conventional and 3DP methods, but with different ratios.

The functional units of each construction method are chosen to represent a section of an external load bearing wall in a one-storey house. All the units share the same standing area of 1m^2 , while the thicknesses vary to reflect the differences in the physical/structural properties of each method. It is important to note that, despite both cob and concrete are constructed using the same technology of 3D printing,

each material has its own unique physical and structural characteristics. It is obvious that concrete has higher structural strength per unit area as compared to cob. Hence, the design of the wall section differs within the same structural function. Both Conventional and 3DP concrete require simpler wall design as compared to conventional and 3DP cob for the same wall unit in same building design. This means, when building a one-storey house, both concrete and cob walls will be designed to satisfy the same structural function.

The conventional method of building with cob requires a load bearing wall with a thickness that varies from 20 cm to 120 cm. An architect usually defines the thickness variation based on several factors, such as expected load, total wall height, and which part of the wall is being constructed (i.e. bottom or top of the wall). The most used thickness of straight cob walls (no tapering) is 62 cm on average. For tapered walls, this thickness varies from 120 cm at the bottom to 20 cm at the top (Hamard et al., 2016; Quagliarini et al., 2010). This study is based on straight cob walls with a thickness of 60 cm for use in a conventional cob functional unit.

The 3DP concrete wall was designed with a thickness of 40 cm, based on the walls used in a recent project in Saudi Arabia (CyBe, 2020). The 3DP cob was designed with a thickness of 60 cm similar to the standard used in straight cob walls and the thickness of similar walls constructed by researchers at Cardiff University and at 3D WASP (Veliz Reyes et al., 2018; 3D WASP, 2020). Both 3DP walls comprise an internal pattern filament (Figure 1).

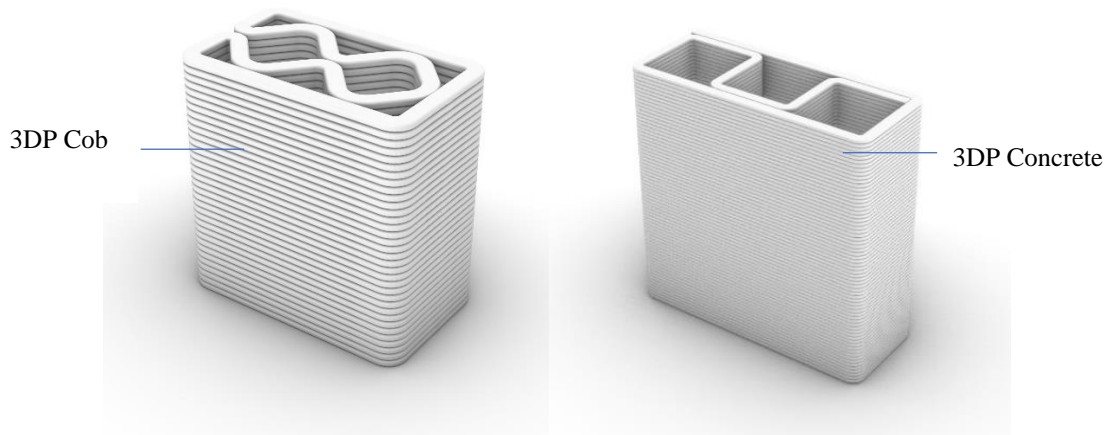


Figure 1. 3DP cob wall and 3DP concrete wall.

The selection of a comparable functional unit in a conventional concrete structure wall for this study requires a different approach, as the walls in this type of construction do not have uniform geometry (e.g. cube, parallelepiped). A structural “functional” wall unit in a concrete structure combines three components: columns, beams and blocks/ bricks (Figure 2). Hence, the study selected another transitional functional unit for the conventional concrete wall, i.e. 4 (L) x 3 (H) meters. This makes the standing area of this wall 12 m², which is 12 times the standing area of each of the other three functional units. Since the LCA comparison depends mainly on quantities, the calculated quantities in the 4 x 3 meter concrete wall were divided by 12 to represent the quantities in a 1 m² unit. Worth mentioning is the fact that it is possible to reverse this approach by upscaling the small functional units to 12m² walls. However, keeping the functional units as 1 m² will maintain a more generalised unit that will facilitate multiplication and reproduction of results.

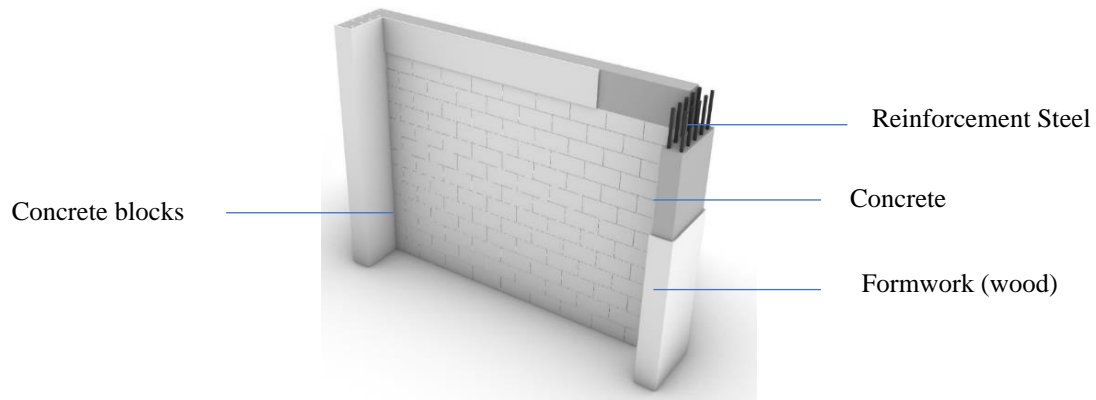


Figure 2. Conventional concrete construction wall.

Table 1. The specifications for each wall section per method.

Wall name	Method	Area m ²	Thickness	Type	Volume m ³
Conv. Concrete	Conventional	1	NA	solid	0.3 ¹
Conv. Cob	Conventional	1	0.6	solid	0.6
3DP Concrete	3D printed	1	0.4	patterned	0.16
3DP Cob	3D printed	1	0.5	patterned	0.31

As shown in Table 1, there are differences in volume between the 3D printed versions and the conventional method. The reason for this is that the 3D printed walls are combined with inner gaps in their design by default, which is a beneficial characteristic of the 3D printing technology that enables a reduction in the amount of construction material needed and an increase in the thermal performance of the walls (Veliz Reyes et al., 2018; Gomaa et al., 2019).

2.3. Electricity Consumption Calculation

2.3.1. Calculating the Electricity Consumption for 3DP Cob and Concrete

The electricity consumed for the robotic arm operation during the construction process can be estimated either practically or mathematically. The practical measure

¹ This volume includes concrete mix, framework, concrete block, reinforcement steel, and mortar.

of power consumption requires the use of electricity/power meters that only read the power source for the digital fabrication tools being used (i.e. in this case a robotic arm) or, if the tools are battery powered, a calculation of the number of full charges needed to finish the construction process. The mathematical method to estimate the electricity consumption depends on knowing the power ratings in Kilowatts (kWh) of the fabrication tools and the time required to complete the fabrication process. The total electricity consumption can then be obtained using the following equation

$$\text{Electricity consumption (kWh)} = \text{power demand (kW)} \times \text{Time (hrs)}$$

The fabrication tool used in the study is a KUKA KR60 HA robotic arm. This robot has a direct supply line of electricity but does not have an electricity meter. Therefore, the study used the mathematical estimation of power consumption. The robot operates 3D printing tasks with a payload of approximately 30 kg, and it has 6 motors on each of its axes; the motors have a collective power rating of 16.8 kW when working on maximum capacity, with 60 kg payload on the robot head. The motors are assumed to work initially at 50% of their full capacity, which is 8.4 kW. A sensitivity analysis has been conducted by examining another scenario where the robot runs on its full capacity.

To calculate the required time for the 3D printing process, two factors need to be defined: firstly, the 3D printing speed; and secondly, the perimeter length of the design pattern/path line for the wall, inclusive of all the layers. The operation time can be calculated by dividing the perimeter length over the 3D printing speed. The printing speed differs between 3DP in cob and a 3DP in concrete because of the different properties of the materials. The printing speed for 3DP cob was set at 0.05 m/sec. This speed was found to be appropriate for cob printing based on several tests

that took place at Cardiff University and the findings of Veliz Reyes et al. (2018). The 3DP concrete printing speed was set at 0.25 m/sec (BESIX, 2019).

The length of the perimeter/path line in 3D printing could be defined as the total length of all the layers that construct the wall unit, which equals the perimeter of a single layer multiplied by the number of layers. This study uses inner patterns for the 3DP walls as adopted in the industry. The selected pattern for the 3DP cob was inspired by 3DP WASP prototypes (3D-WASP), while the chosen pattern for the 3DP concrete was supplied by the CyBe project in Saudi Arabia (CyBe 2020)(Figure 3). The length of the total path line for the 3DP cob is 146.3 m and for the 3DP concrete 412 m. This noticeable difference in path line length between cob and concrete is due to the difference in the 3D printing settings. The printing layer height in the 3DP cob is 30 mm, while in the 3DP concrete it is 10 mm. Hence, more layers are required for the 3DP concrete to achieve the same required 1.0 m height wall. Increased number of layers means a longer total path line. By applying the previous calculations, the electricity consumption was found to be 6.8 kWh for 3DP cob and 3.9 kWh for 3DP concrete.



Figure 3. CyBe 3DP concrete pattern (left), 3D WASP 3DP cob pattern (right).

2.3.2. Electricity consumption for Conventional Cob and Concrete

In conventional constructions, the work is undertaken by manual labour. Nevertheless, in the environmental analysis, the energy requirements and emissions associated with human life are not counted usually (Agustí-juan et al., 2017). A study conducted by Alcott (2012) calculated the human factor, but the results showed that the impact was insignificant. Therefore, human factor is not included in this study, that is, this study does not include the energy consumption to manufacture conventional concrete because all the manufacturing processes were done manually.

2.4. Material Characterisation

2.4.1. Cob

Weismann and Bryce (2006) suggested a water to subsoil ratio of one part water to every four parts of soil. This converts to 20kg of water per each 80kg of subsoil by weight (20: 80 %). The recommended amount of straw to be included in the mix is 2% of the weight of the subsoil and water mix. A comprehensive systematic review by Hamard et al. (2016) affirmed the proportions of the cob mixture (78% subsoil, 20% water and 2% fibre i.e. straw). Hamard et al. (2016) also stated that the subsoil formula itself is 15–25% clay to 75–85% aggregate/sand. Similarly, Harrison (1999) recommended a subsoil formula of 20% clay to 80% aggregate/sand.

However, as cob is conventionally mixed in a near dry state due to the low water ratio, the commonly used proportions of water to subsoil do not fit the purpose of the 3D printing technique. The 3D printing technique involves a material extrusion process through tubes and/or hoses; therefore, less viscous material is always preferred to reduce the amount of friction inside the system, which then reduces the loads on the motors. Two comprehensive studies on 3DP cob have recommended a

new cob mix that has reduced viscosity. Based on a number of 3D printing tests, the water content in the 3DP cob mixture was increased to 23-25%, while the amount of straw was fixed at 2% (Gomaa et al., 2019) (Table 2).

Table 2. The components of 3DP and conventional cob.

	Subsoil		Water		Straw		Total (kg)
	%	Kg	%	Kg	%	Kg	
Cob conventional wall	78.0	748.8	20.0	192	2.0	19.2	960
Cob 3D printed wall	73.0	392.6	25.0	134.4	2.0	10.8	537.8

2.4.2. Concrete

3DP concrete is a mix of cement, fly ash, silica fume, sand, water, superplasticiser, and fibre (Le et al., 2012; Agustí-juan et al., 2017; Nerella et al., 2016; Anell 2015). Each of the previously cited studies suggested different ratios of material in the 3D printed concrete mix (Table 3). An extensive review of the literature revealed that Le et al. (2012) had carried out comprehensive testing of several 3DP concrete mixes to define which had the best workability and usability. Other studies used Le et al. (2012) as a main starting point to develop their new mixes (such as Labonnote et al., 2016; Ngo et al., 2018; Buswell et al., 2018; Wolfs 2015; Paul et al., 2018; Malaeb et al., 2015). Hence, this study conducted the LCA on the concrete mix recommended by Le et al. (2012). However, to further explore the differences in the environmental impacts of the 3DP concrete mixes, two more concrete mixes, taken from Nerella et al. (2016) and Anell (2015), will be used in the sensitivity analysis section.

This study used the 35MPa conventional concrete type and column size 60X20 cm² with 8 Ø 16 mm steel rods. The beam size was 40X20 cm² with 6 Ø 16 mm steel rods, each concrete block was 40 cm x 20 cm x 20 cm, and the formwork was

plywood. Plywood sheets have a thickness of 15 mm and are assumed to be used twice (one time per each side). All of the reinforced concrete properties used in the conventional wall were taken from the National Committee for the Saudi Building Code (Table 4).

Table 3. Different 3DP concrete mixes ingredients and their densities based on previous studies.

	(Nerella et al. 2016)		(Le et al. 2012b)		(Anell 2015)		(AgustíJuan et al. 2017)	
	Kg/m3	%	Kg/m3	%	Kg/m3	%	Kg/m3	%
Cement	430	19.5	579	25	659	30	500	20.5
Fly-ash	170	7.7	165	7.1	87	4	0	--
Silicafume	180	8.1	83	3.6	83	4	43.5	1.8
Sand/ aggregates	1240	56.1	1241	53.5	1140	52	1713	70.5
Water	180	8.1	232	10	228	10	169	7.
Superplasticiser	10	0.5	16.5	0.7	11.6	0.5	4.32	0.2
Fibre	0	--	1.2	0.05	1.2	0.05	0	--
Total density	2210		2318		2210		2430	

Table 4. The construction components of the conventional concrete method.

Concrete Conventional Wall	Percentage	Kg
Concrete blocks (main body)	50%	112.6
Formwork (wood)	16%	6.5
Reinforcement Steel	2%	12.3
Concrete mix	30%	206.1
Mortar	2%	12.5

3. Results and Discussion

This section discusses the results of the study in three steps. First, the overall outcome of the study, that is, the comparison of the four types of walls in terms of their environmental impacts. This step will also include a description of the results pertaining to the different properties of each material. The second step explores the breakdown of the impact of each wall type. This aim of this breakdown is to determine which material and/or process has the highest environmental impact within each wall type. Having defined the highest contributors, the third step will be to analyse the sensitivity of each contributor and describe the changes in the environmental impact.

The produced analyses in Simapro were initially in the form of characterised values that show the relative difference in the environmental performance between the four wall types, as can be seen in Figure 4. In order to obtain a holistic overview of the whole impact of the products, the characterised results must be normalised and weighted using special factors as indicated in the PEFCR guidance (European-Commission 2017). Normalised and weighted results can then be used as a real representation of the performance in all the impact categories collectively. For example, in Table 5, the characterised values were normalised using the normalisation factor (NF/person), then weighted using the weighting factor (WF/person) to produce the overall improvement in performance per wall type in all the impact categories combined, all as compared to the conventional concrete wall.

3.1. Primary comparison

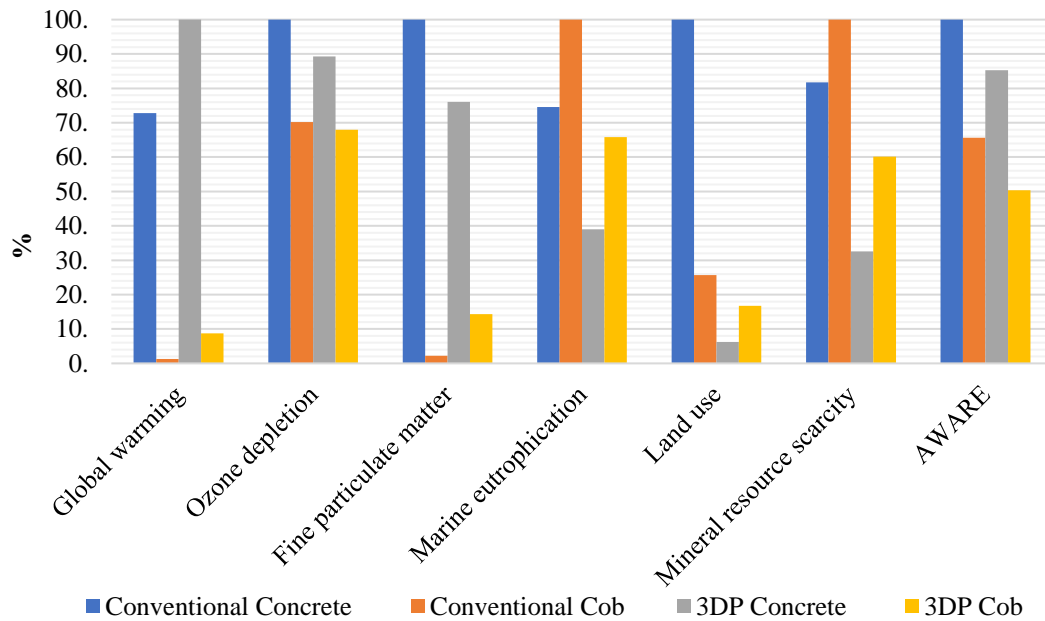


Figure 4. Chart shows the characterised overall outcome of comparing the four types of walls.

Table 5. Percentage of improvement in environmental performance of the wall types as compared to conventional concrete method. (NF: Normalisation factor; WF: Weighting Factor)

Impact categories	NF/ person	WF/ person	Conv. Cob	3DP Conc.	3DP Cob
Global warming	8095.53	22.19	98.2%	-27.2%	87.9%
Stratospheric ozone depletion	5.37E-2	6.75	29.8%	10.7%	32.0%
Particulate matter	5.95E-4	9.54	97.8%	23.9%	85.7%
Marine eutrophication	19.545	3.12	-34.0%	47.7%	11.7%
Land use	81.94E+4	8.42	74.3%	93.8%	83.3%
Mineral resource scarcity	6.36E-2	8.08	-18.3%	60.1%	26.4%
AWARE (water depletion)	11468.7	9.03	34.3%	14.7%	49.7%
Overall improvement	--	--	96%	24%	85%

The results generally align with the results of several other studies (including Agustí-juan et al., 2017; Kafara et al., 2017) which claimed better environmental performance for 3DP technologies when compared to conventional concrete construction. The novel added factor in this study is the introduction of cob as an alternative material in both the conventional and the 3D printing methods. The conventional concrete wall recorded the highest overall environmental impact out of all the other three walls. In addition, the 3DP concrete wall achieved a collective 24% improvement in all the seven relevant impact categories combined when compared to conventional concrete. However, in the global warming category, 3DP concrete performed 27.2% worse than conventional concrete. Unsurprisingly, the 3DP cob showed better environmental performance as compared to the concrete-based walls, with an overall improvement of 85% over the conventional concrete wall and 87.9% improvement in the global warming category only (Figure 4 and Table 5).

The study initially included the conventional cob wall as a base line as it was anticipated that this will yield the most efficient environmental performance. This was a correct assumption on a collective scale; interestingly, however, both the 3DP cob and the 3DP concrete performed better in comparison with the conventional cob wall in several impact categories, such as marine eutrophication, land use and mineral resources scarcity. These three categories are heavily related to the use of straw and subsoil, which are found in large amounts in conventional cob walls. However, conventional concrete performed better than conventional cob in the mineral resource scarcity category, again due to the huge presence of subsoil in conventional cob (Figure 4 and Table 5).

When focusing on concrete-based walls, the results revealed that 3DP concrete has an overall improvement in all categories collectively with 24%, except for the global warming category (European Commission, 2017). This is mainly due to the use of concrete and fly ash. Additionally, the reason for the poor performance of conventional concrete in the other impact categories is the presence of reinforcing steel and concrete which contribute highly to CO₂ emissions (Habert et al., 2013). These results could change if the comparisons were done on the basis of a whole building, including all structural elements, because 3D printing technology produces almost zero waste (Xia and Sanjayan, 2016)(Figure 5 and Table 6).

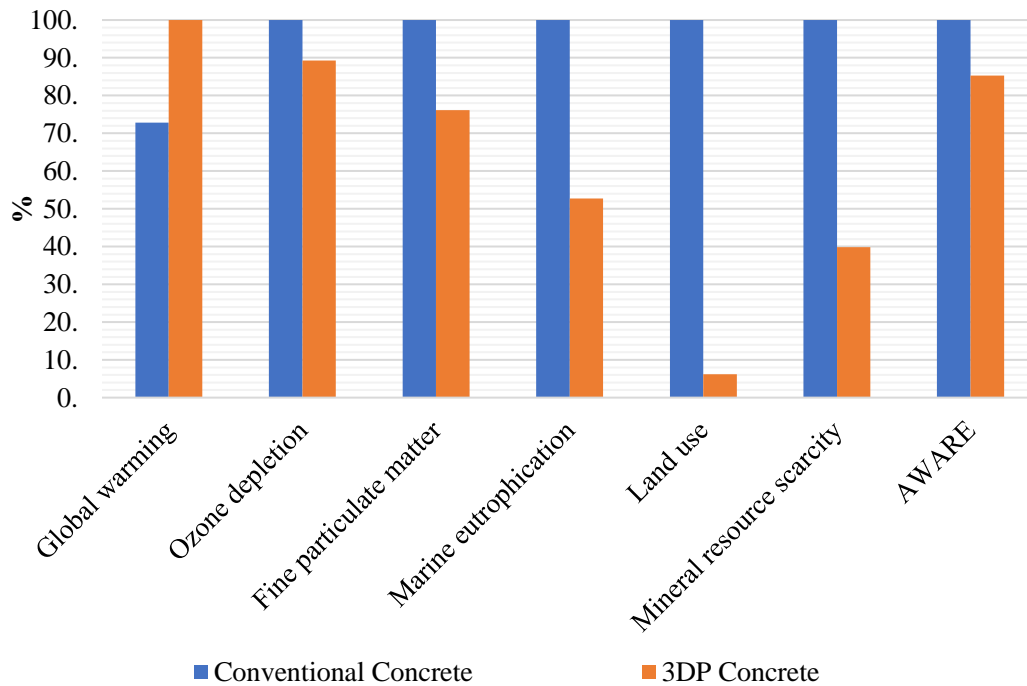


Figure 5. Comparison between 1 m² 3DP Concrete wall with 1 m² Conventional Concrete.

Table 6. Percentage of improvement between 3DP Concrete and Conventional Concrete.

	Conventional Concrete	3DP Concrete
Global Warming	27.2%	--
Stratospheric Ozone Depletion	--	11%
Fine Particulate Matter	--	24%
Marine Eutrophication	--	47%
Land Use	--	94%
Mineral Resource Scarcity	--	60%
Aware	--	15%
Overall Improvement	--	24.0%

On the other hand, despite the outperformance of 3DP cob over conventional cob in five of the seven impact categories, conventional cob has shown a much higher overall performance, with 83% improvement over 3DP cob (Figure 6 and Table 7). This is clearly down to the good performance of conventional cob in two of the most important and highly weighted impact categories: global warming and fine particulate matter formation (European Commission, 2017). It is also due to the high use of electricity in 3DP construction, which severely affects both global warming and fine particulate matter formation. The breakdown of both materials will be given in the following section.

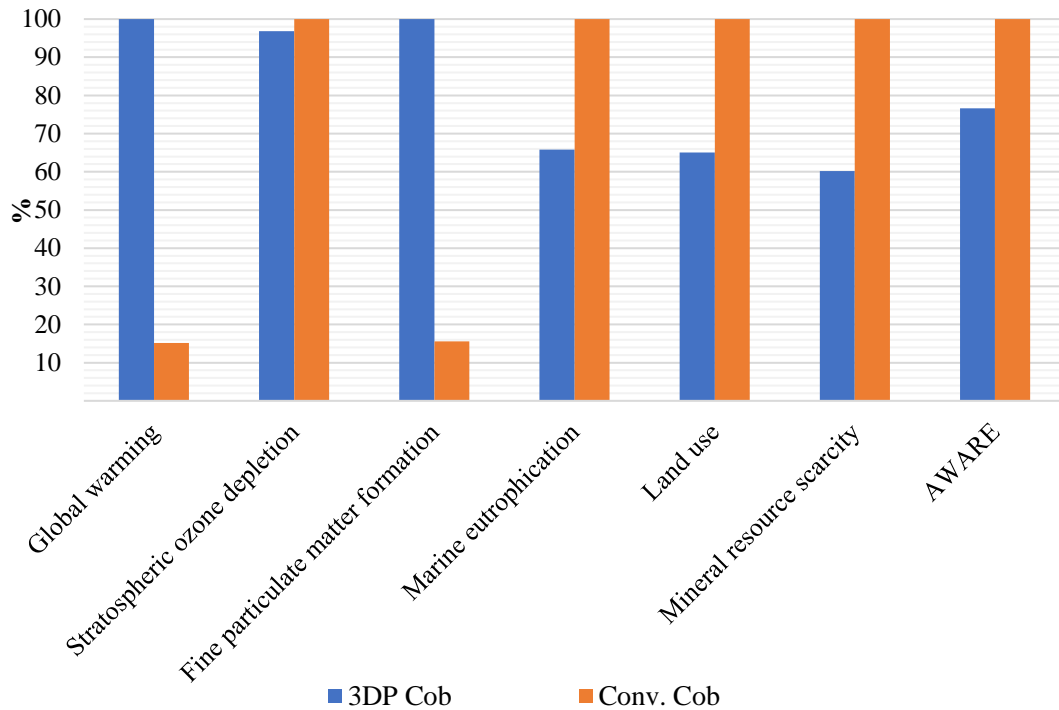


Figure 6. Comparison between 1 m² 3DP Cob wall with 1 m² conventional Cob.

Table 7. Percentage of improvement between 3D Cob and conventional Cob.

	Percentage of Improvement	
	3DP Cob	Conventional Cob
Global Warming	--	85%
Stratospheric Ozone Depletion	3%	
Fine Particulate Matter	--	84%
Marine Eutrophication	34%	
Land Use	35%	--
Mineral Resource Scarcity	40%	
Aware	23%	--
Overall improvement		83%

Since the focus of this study was 3DP technologies, a focused comparison on 3DP concrete and 3DP cob is provided in Figure 7 below. As seen in Table 8, the environmental performance of 3DP cob is 80.0% better than 3DP concrete in the seven impact categories. The graph below (Figure 5) shows that 3DP cob achieved

a better performance in global warming, stratospheric ozone depletion, and fine particulate matter formation, while 3DP concrete performed better in marine eutrophication, land use, and mineral resources scarcity.

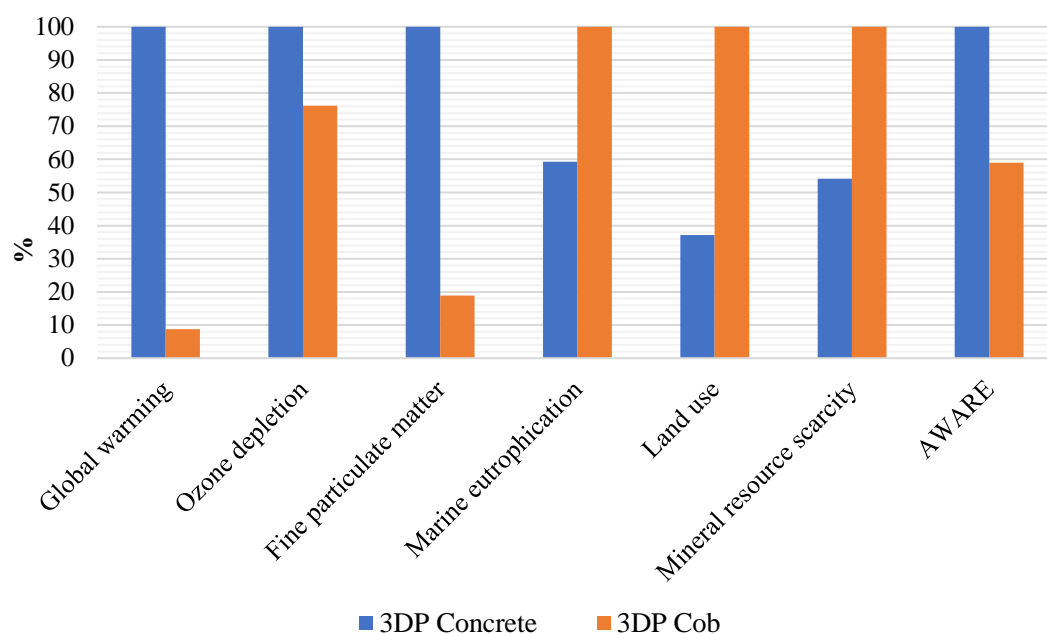


Figure 7. Comparing 1 m² 3DP Concrete with 1 m² 3DP Cob.

Table 8. Comparison of the environmental performance between 3DP Cob and 3DP Concrete.

	3DP Concrete	3DP Cob
Global Warming	--	91%
Stratospheric Ozone Depletion	--	24%
Fine Particulate Matter Formation	--	81%
Marine Eutrophication	41%	--
Land Use	63%	--
Mineral Resource Scarcity	46%	--
Aware	--	41%
Overall improvement	--	80.0%

3.2. The breakdown of impacts

For a deeper understanding of the results, each wall type was analysed separately through a breakdown of ingredients in order to identify the impact in relation to each sub-material. Also, the overall contribution of all categories will be analysed with a focus on global warming as the most important impact category. The results were normalised and weighted to give a better understanding of each impact category.

With regards to conventional concrete, it was found that 49% of the environmental impact was due to the reinforcing steel which scored the highest contribution out of all the categories, except land use where plywood scored the highest. Furthermore, concrete scores as the second highest contributor with an overall 19% contribution in all categories (Figure 8). This finding obviously puts 3DP techniques at an advantage as it does not require the use of formwork and reinforced steel (CyBe 2020). However, the high presence of cement in the 3DP concrete wall reduced its environmental performance, especially in the global warming impact category, where it obtained the worst environmental performance scores out of the three types of wall. The impact breakdown of 3DP concrete shows that cement and fly ash are collectively responsible for 70.8% of the environmental impact and obtained the highest contribution scores out of all the categories. Transportation achieved the next highest score with 12.8% contribution in all the categories (Figure 9).

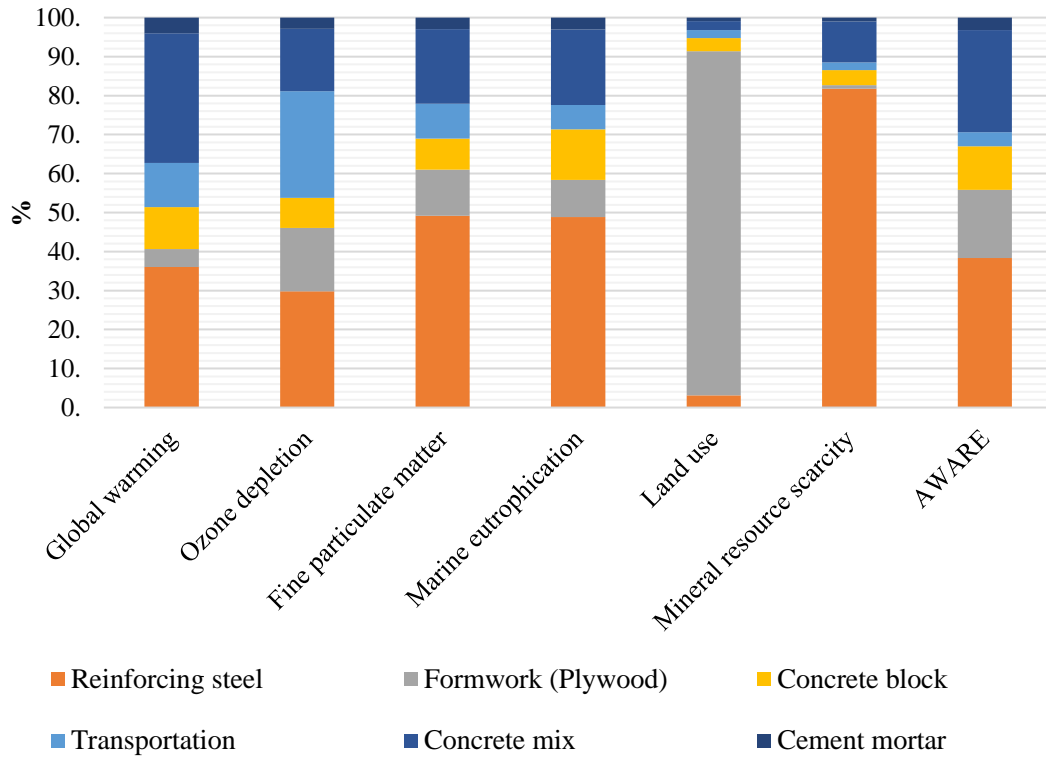


Figure 8. Breakdown analysis of 1 m² wall of Conventional Concrete type.

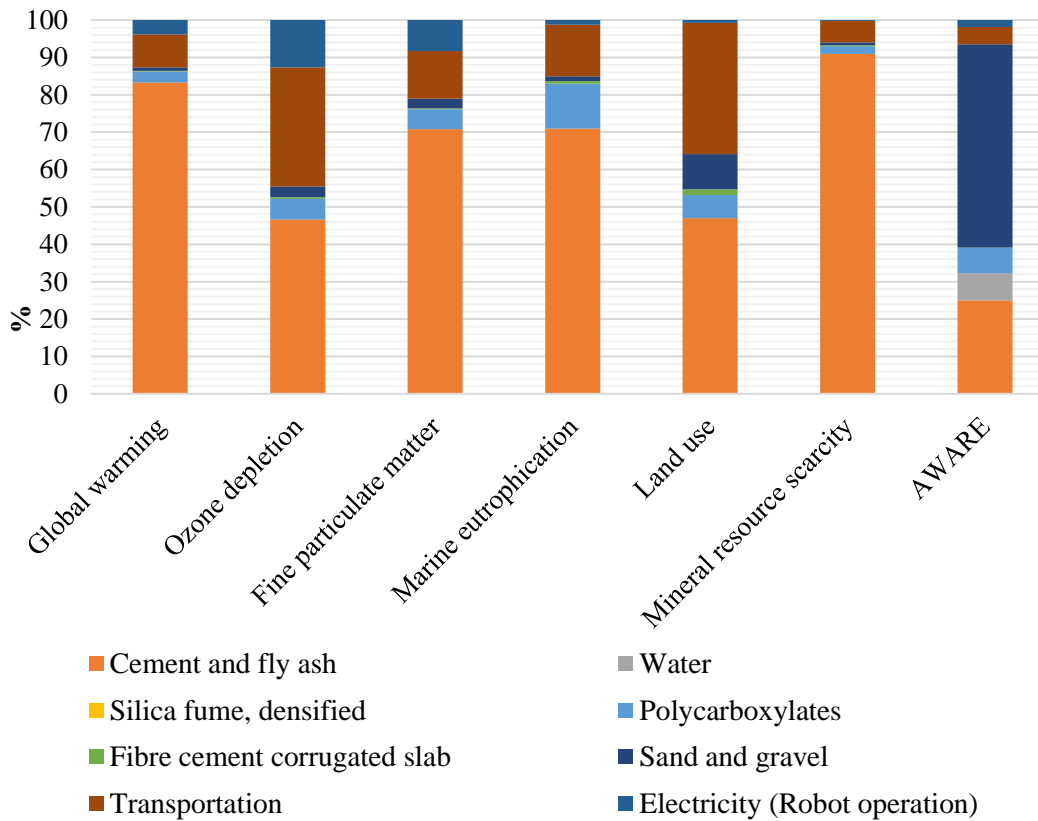


Figure 9. Breakdown analysis of 1 m² wall of 3DP Concrete.

In conventional cob construction, straw contributes 68% of the overall impact across all the categories, except mineral resource scarcity, where subsoil contributed the highest score (Figure 10). On the other hand, the electricity used in 3DP cob, mainly used in the operation of the robotic arm, contributed 83% of the impact across all the categories, followed by straw with an overall score of 7% (Figure 11). Considering the very low ratio of straw (2%) in the cob mixture, it can be concluded that straw has a significant effect on overall environmental performance. In addition, 3DP cob was proven to have the best collective environmental performance, even when compared to conventional cob. This is due to the massive reduction in the quantity of material and weights used in 3DP cob in comparison with conventional cob due to the integration of voids in the internal structures and the minimal amount of material used in the wall volume.

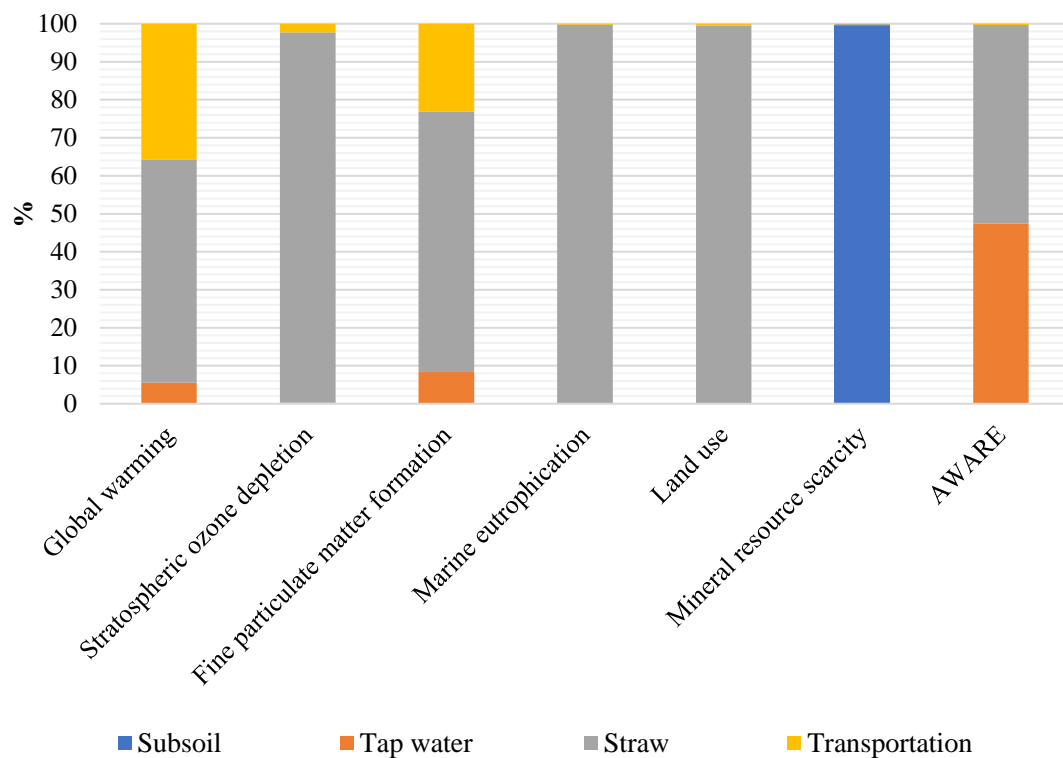


Figure 10. Breakdown analysis of 1m² wall of Conventional Cob.

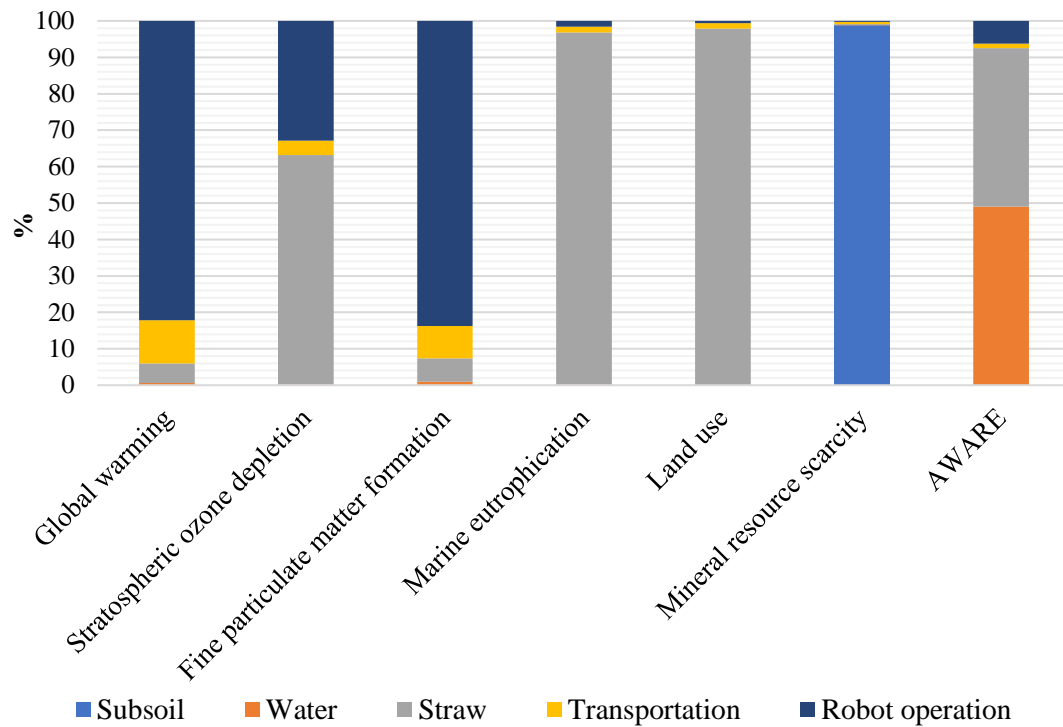


Figure 11. Breakdown analysis of 1m² wall of 3DP Cob.

3.3. Sensitivity analysis

Based on the previous observations, it is important to test the sensitivity of some materials that were identified to have a large environmental impact and explore how this impact can be improved or reduced. The sensitivity analysis for this study was carried out on the basis of three scenarios: (1) changing the percentage of steel reinforcement in conventional concrete; (2) changing the 3DP concrete mix; and (3) changing the robotic operation payload and geographical location. Conventional cob was excluded from the sensitivity analysis, as it had a significantly better environmental performance than all the other three types. Moreover, there is no demand for conventional cob for construction on the modern construction market.

3.3.1. Conventional concrete

As mentioned earlier, steel contributed the most to the environmental impact of conventional concrete. The quantity of steel used in the wall was originally calculated based on a reinforced 600x200 mm² column and 400x200 mm² beam which are used in a regular two-storey building. The amount of steel reinforcement and concrete were then reduced by nearly 20% and 22% respectively, to represent a smaller column of 400x200 mm² that can be used in a one-storey building, to mimic the walls that were used for the 3DP houses. This reduction in steel and concrete improved the performance of conventional concrete by an overall 17% and 16% in the global warming category when compared to the original concrete wall (Figure 12).

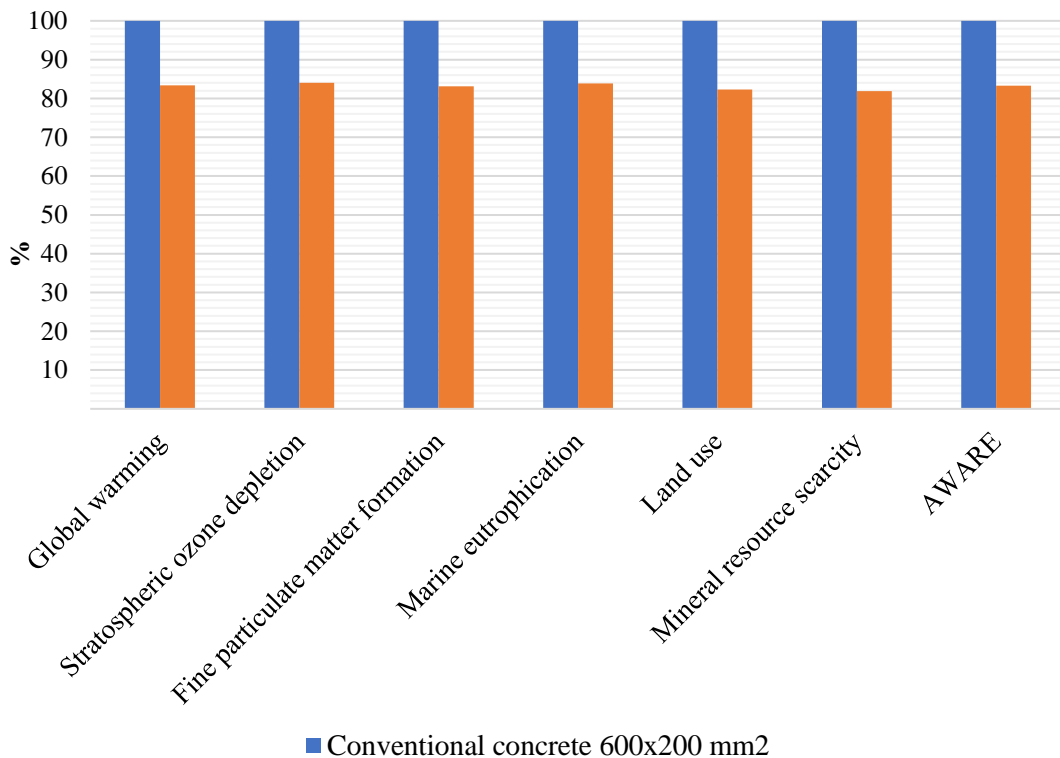


Figure 12. Comparing main Conventional Concrete wall to the reduced steel and concrete version.

3.3.2. 3DP concrete

As mentioned earlier, this study explored two more concrete mixes taken from Nerella et al. (2016) and Anell (2015) to better understand the variations in the environmental performance associated with changing mix ratios of the cement, fly ash and sand. The results demonstrated that there is no specific component to focus on, as each recipe has a different proportion of components (Table 9). However, as shown, reducing cement and fly ash in the mix does not necessarily guarantee an improvement in the environmental performance of the 3DP concrete (Table 9). It was observed that the reduction in cement and fly ash ratios in the 3DP concrete mix is usually accompanied by an increase in the sand and aggregate ratios, which then increases the overall quantities of material and consequently increases the environmental impacts of transportation. Therefore, it is concluded that it is important to analyse the main components of the 3DP concrete mix holistically.

It was found that, generally, all the three 3DP concrete mixes performed environmentally better than the conventional concrete wall, by 60.4%, 52.7% and 53.7% for the Nerella et al. (2016) mix, the Le et al. mix (2012) and the Anell mix (2015) respectively. However, the Nerella et al. (2016) mix had the lowest impact on global warming and all the categories when compared to the other mixes and conventional concrete (Table 10 and Figure 13). This may be an indicator that recently developed mixes can have the potential of performing better environmentally.

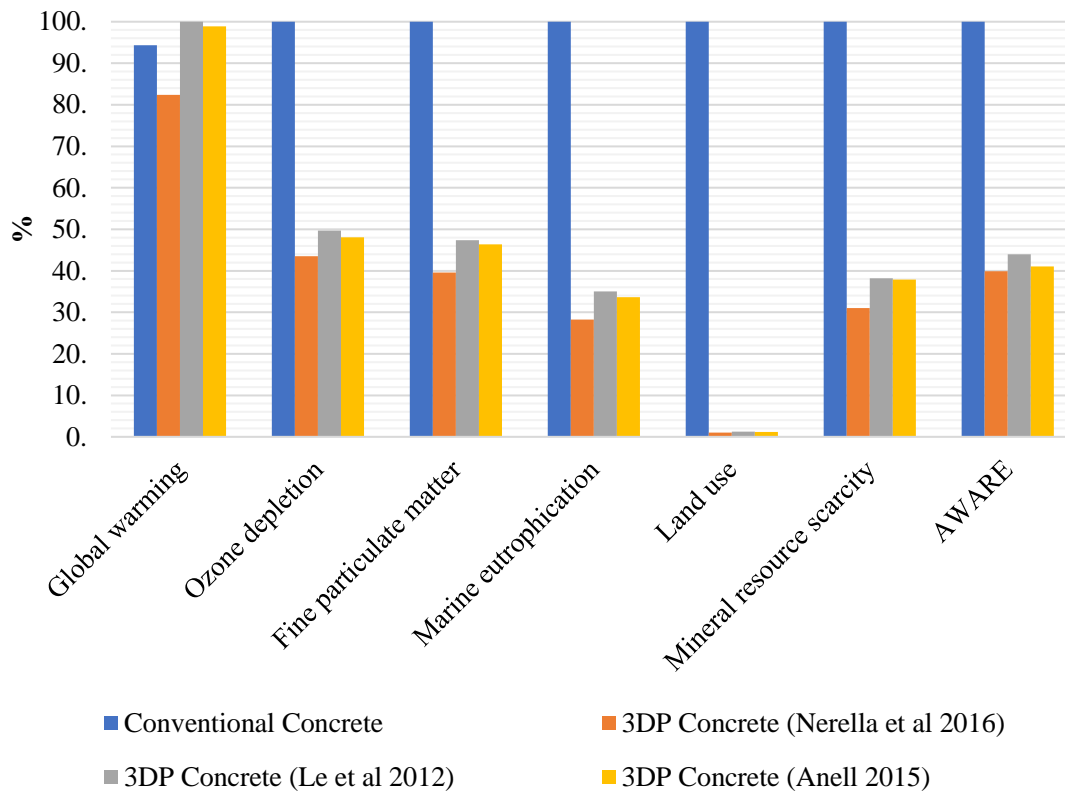


Figure 13. Comparison of the three 3DP mixes to conventional concrete wall mix.

Table 9. The percentage breakdown of contribution towards the environmental impacts for each component in the three 3DP concrete mixes.

	Cement and fly ash	Water	Polycarboxylates	Fibre cement	Sand and gravel	Transportation	Electricity (Robot operation)
(Le et al. 2012b)	71%	0.05%	5%	0.3%	2.6%	13%	8.3%
(Anell 2015)	72.5%	0.05%	4%	0.3%	2.4%	12.50%	8.5%
(Nerella et al. 2016)	68%	0.04%	4%	0.0%	3%	15%	10%

Table 10. The percentage of overall improvement in environmental performance of 3DP concrete mixes as compared to conventional concrete method.

	3DP Conc (Nerella et al. 2016)	3DP Conc. (Anell 2015)	3DP Conc (Le et al. 2012b)
Global warming	13%	- 4.6%	- 5.7%
Overall categories	60.4%	53.7%	52.7%

3.3.3. 3DP cob

A few changes were made in the robotic operation concerning electricity consumption and location. Firstly, the robotic operation capacity was changed from 50% to 100%. This means that the payload was changed from 8.4 kW to 16.8 kW. This change led to double the amount of electricity consumption that deteriorated the performance of 3DP cob by 55% in both overall and global warming levels (Figure 14).

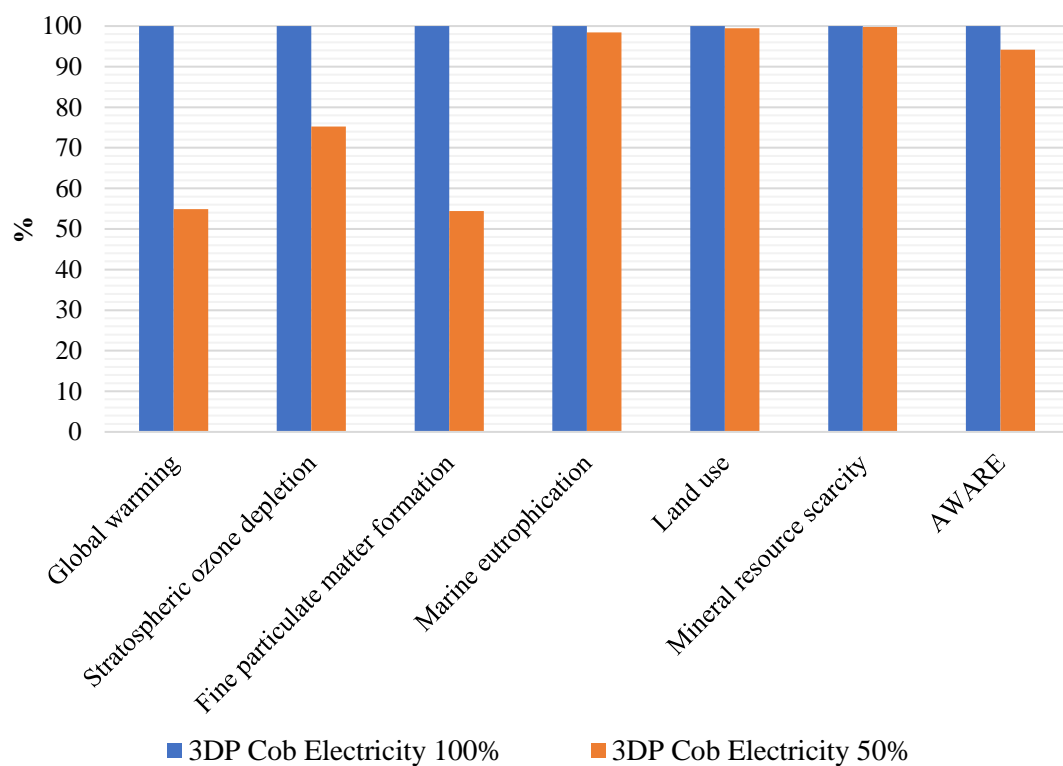


Figure 14. Comparing 3DP Cob 50% Electricity with 100% Electricity.

The impact of changing the geographical location from Saudi Arabia to Australia was also tested. The electricity in Saudi Arabia is totally produced from non-renewable energy resources (ERCA, 2018), while 19% of electricity generation in Australia comes from renewable energy sources (DEE, 2019). This study chose the state of South Australia (SA) as a case study for this sensitivity analysis as more than

50% of its electricity comes from renewable sources (DEE, 2019). Altering the location from Saudi Arabia to South Australia resulted in an improvement of the environmental performance by 52% overall and 36% in the global warming category (Figure 15).

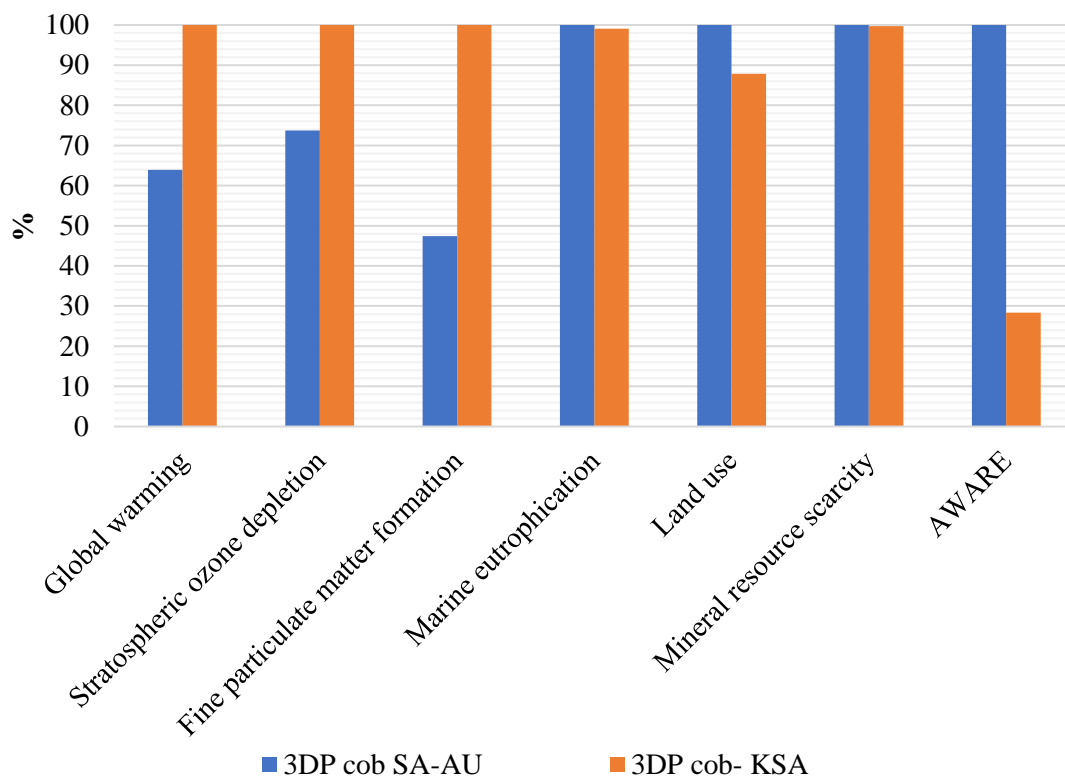


Figure 15. Comparison of 3DP Cob method in South Australia to 3DP Cob in Saudi Arabia.

4. Conclusion

Digital fabrication technologies have recently been adopted in architectural applications and constructions; however, the environmental impacts of such approaches have not been thoroughly investigated. This study compared the environmental impacts of constructing a wall using 3D printing construction methods with the impact of conventional construction methods. Four different types

of materials were tested: conventional concrete, conventional cob, 3D printed (3DP) concrete and 3DP cob.

The study had the following results:

- 1) Conventional cob has the least overall environmental impact and global warming potential, followed by 3DP cob. As expected, conventional concrete had the, highest environmental impact in all categories except global warming.
- 2) While 3DP concrete had a lesser overall environmental impact (by more than 50%) than conventional concrete, the performance of 3DP cob is still better than 3DP concrete due to its lesser global warming potential, stratospheric ozone depletion and fine particulate matter formation.
- 3) However, while the overall environmental impact of 3DP concrete is more than that of 3DP cob, it has less impact on marine eutrophication, land use, and mineral resources scarcity.
- 4) A detailed analysis shows that the high environmental impact of conventional concrete construction is mainly due to the use of reinforcing steel (49% contribution) and concrete (19%).
- 5) The absence of reinforcing steel bars in 3DP concrete is the main reason for its better environmental performance when compared to the performance of conventional concrete.
- 6) While conventional cob has a better environmental performance than the other three construction methods, the high content of straw in conventional cob contributes to its overall environmental impact while the use of subsoil contributes to mineral resource scarcity.

- 7) The consumption of electricity to operate the robotic arm in 3DP cob contributes to 83% of its overall environmental impact, while the very low straw content in the 3DP cob mixture contributes to its low environmental impact.

These results suggest that the environmental impact of conventional concrete is mostly due to its steel reinforcing bars as well as the concrete used. Changing the amount of steel reinforcement and concrete (but keeping it to the standards required for a one-story building) would reduce the environmental impact of conventional concrete. The environmental impact of 3DP concrete is mainly depending the ratio of the components of the mix, hence in the future modified mixes can reduce further the environmental impact of 3DP concrete.

On the other hand, the environmental performance of 3DP cob is not as affected by the material used as it is by the amount of electricity used to operate the robotic arm. Using renewable energy sources to generate electricity for the robotic operations would significantly reduce the environmental impacts of 3DP cob. The current global trends are moving towards renewable sources of energy (REN21 2019). Moreover, 3DP cob can generate complex shapes to meet the evolving demands of contemporary construction, which is difficult to achieve manually using conventional cob. In addition, 3DP facilitates modifications, repetitions, and maintenance if needed. However, 3DP cob still suffers some major limitations in terms of structural strength and productivity of the construction process as compared to 3DP concrete and other conventional construction methods. In the context of the limited available information regarding 3DP construction, this study aims to inspire

researchers to further investigate 3DP construction and assess its performance from cradle to grave.

5. Acknowledgments

The authors would like to acknowledge the help and assistance of Abbas Salhab and Ayman Mogahed for their technical support and guidance. Gratitude is also extended to Dr. Eshrar Latif at Cardiff University for his guidance on life cycle assessment topics.

6. References

- Agustí-juan, I. et al., 2017. Potential benefits of digital fabrication for complex structures : Environmental assessment of a robotically fabricated concrete wall. *Journal of Cleaner Production* 154, pp. 330–340. Available at: <http://dx.doi.org/10.1016/j.jclepro.2017.04.002> [Accessed: 15 December 2019].
- Ahmed, O. and Ibrahim, A. 2018. *The mud traditional architecture of the Sudan and Saudi Arabia : The difference in employment techniques*. Hail.
- Alcott, Blake. 2012. Mill’s Scissors: Structural Change and the Natural-Resource Inputs to Labour. *Journal of Cleaner Production* 21 (1): pp. 83–92. Available at: <https://doi.org/10.1016/j.jclepro.2011.08.012> [Accessed: 20 December 2019].
- Anell, L. 2015. *Concrete 3d Printer*. MA Thesis, Lund University.
- Apis Cor. 2019. *Dubai Municipality 3D printed building* [Online]. Available at: <https://www.apis-cor.com/dubai-project> [Accessed: 10 December 2019].
- Asif, M. et al. 2017. Life Cycle Assessment of a Three-Bedroom House in Saudi Arabia. *Environments* 4(3), p. 52. Available at: <http://www.mdpi.com/2076-3298/4/3/52> [Accessed: 12 January 2020].
- ASTM International 2013. ASTM f2792-12a. *Rapid Manufacturing Association*, pp. 1–3. Available at: <http://www.ciri.org.nz/nzrma/technologies.html> [Accessed: 10 January 2020].
- Berman, B. 2012. 3-D printing: The new industrial revolution. *Business Horizons*,

- 55(2), pp. 155–162. Available at: <http://dx.doi.org/10.1016/j.bushor.2011.11.003>.
- Besix, 2019. *BESIX Group* [Online]. Available at: <https://www.besix.com/en/about> [Accessed: 10 Aug 2019].
- Buswell, R.A. et al. 2018. 3D printing using concrete extrusion: A roadmap for research. *Cement and Concrete Research*, 112 (October 2017), pp. 37–49. doi: 10.1016/j.cemconres.2018.05.006.
- Buyle, M., Braet, J., and Audenaert, A. 2013. Life Cycle Assessment in the Construction Sector: A Review. *Renewable and Sustainable Energy Reviews*, 26: 379–88. <https://doi.org/10.1016/j.rser.2013.05.001>.
- Cavalett, O. et al. 2013. Comparative LCA of ethanol versus gasoline in Brazil using different LCIA methods. *International Journal of Life Cycle Assessment*, 18(3), pp. 647–658. doi: 10.1007/s11367-012-0465-0.
- Craveiro, F. et al. 2019. Additive manufacturing as an enabling technology for digital construction: A perspective on Construction 4.0. *Automation in Construction*, 103 (March), pp. 251–267. doi: 10.1016/j.autcon.2019.03.011.
- CyBe, 2018. *3D Studio 2030* [Online]. Available at: <https://cybe.eu/case/3d-studio-2030/> [Accessed: 15 Aug 2019].
- Dixit, M.K. 2019. 3-D Printing in Building Construction: A Literature Review of Opportunities and Challenges of Reducing Life Cycle Energy and Carbon of Buildings. *IOP Conference Series: Earth and Environmental Science* 290(1). doi: 10.1088/1755-1315/290/1/012012.
- 3D-WASP 2020. *3D Printers | WASP | Leading Company in the 3d printing industry*. Available at: <https://www.3dwasp.com/en/> [Accessed: 10 January 2020].
- ERCA 2018. *Annual Statistical Booklet For Electricity & Seawater Desalination Industries* [Online]. Available at: <https://www.ecra.gov.sa/en/us/MediaCenter/doclib2/Pages/SubCategoryList.aspx?categoryID=5> [Accessed: 11 Dec 2019].
- European Commission, 2017. Product Environmental Footprint Category Rules Guidance. *PEFCR Guidance document - Guidance for the development of*

- Product Environmental Footprint Category Rules (PEFCRs), version 6.3, December 2017*, p. 238.
- European Commission, 2019. European Platform on Life Cycle Assessment. Available at: <https://eplca.jrc.ec.europa.eu/LCDN/developerEF.xhtml> [Accessed: 15 January 2020].
- Faludi, J. et al. 2015. Comparing environmental impacts of additive manufacturing vs traditional machining via life-cycle assessment. *Rapid Prototyping Journal* 21(1), pp. 14–33. doi: 10.1108/RPJ-07-2013-0067.
- Geneidy, O. and Ismaeel, W.S.E. 2018. INVESTIGATING THE APPLICATION OF THE THREE DIMENSIONAL WALL BUILDING GREEN HERITAGE CONFERENCE 6-8 March. (March)
- Goedkoop, M. et al. 2009. ReCiPe_main_report_final_27-02-2009_web.pdf. doi: 10.029/2003JD004283.
- Gomaa, M. et al. 2019. Thermal Performance Exploration of 3D Printed Cob. *Architectural Science Review* 8628. <https://doi.org/10.1080/00038628.2019.1606776>.
- Geneidy, O. and Ismaeel, W.S.E. 2018. Investigating the application of the three dimensional wall building technology in Egypt. *Green Heritage Conference*. 6-8 March 2008. The British University in Egypt. Pp.681-696.
- Habert, G. et al. 2013. Lowering the global warming impact of bridge rehabilitations by using ultra high performance fibre reinforced concretes. *Cement and Concrete Composites* 38, pp. 1–11. Available at: <http://dx.doi.org/10.1016/j.cemconcomp.2012.11.008>.
- Häfliger, I.F. et al., 2017. Buildings environmental impacts' sensitivity related to LCA modelling choices of construction materials. *Journal of Cleaner Production*, 156, pp. 805–816. doi: 10.1016/j.jclepro.2017.04.052.
- Hamard et al. 2016. Cob, a Vernacular Earth Construction Process in the Context of Modern Sustainable Building. *Building and Environment*, 106, pp.103–19. <https://doi.org/10.1016/j.buildenv.2016.06.009>.

- Harrison, R. 1999. *Earth: the conservation and repair of Bowhill, Exeter : working with cob*. London: James & James.
- Housing Bulletin. 2019. *General Authority for statistics* [Online]. Available at: <https://www.stats.gov.sa/ar/911-0> [Accessed: 27 Jan 2020].
- Housing program. 2019. *Saudi Vision 2030* [Online]. Available at: <https://vision2030.gov.sa/en/programs/Housing> [Accessed: 14 Nov 2019].
- Huijbregts et al. 2017. ReCiPe2016: A Harmonised Life Cycle Impact Assessment Method at Midpoint and Endpoint Level. *International Journal of Life Cycle Assessment*, 22 (2), pp. 138–47. <https://doi.org/10.1007/s11367-016-1246-y>.
- IEA and UNEP 2018. International Energy Agency and the United Nations Environment Programme - Global Status Report 2018: Towards a zero-emission, efficient and resilient buildings and construction sector. p. 325. Available at: <http://www.ren21.net/status-of-renewables/global-status-report/>. [Accessed: 19 January 2020].
- International Energy Agency 2018. *Global Energy & CO2 Status Report*. Available at: <https://www.iea.org/publications/freepublications/publication/GECO2017.pdf> [Accessed: 9 December 2019].
- ISO. 2006. Environmental Management - Life Cycle Assessment - Principles and Framework. International Organization for Standardization. Vol. 3. <https://doi.org/10.1016/j.ecolind.2011.01.007>.
- Kafara, M. et al. 2017. Comparative Life Cycle Assessment of Conventional and Additive Manufacturing in Mold Core Making for CFRP Production. *Procedia Manufacturing*, 8 (October 2016), pp. 223–230. Available at: <http://dx.doi.org/10.1016/j.promfg.2017.02.028>.
- Khoshnevis, B. et al. 2006. Mega-scale fabrication by Contour Crafting. *International Journal of Industrial and Systems Engineering* 1(3), pp. 301–320. doi: 10.1504/IJISE.2006.009791.
- Kreiger, M. and Pearce, J.M. 2013. Environmental life cycle analysis of distributed

- three-dimensional printing and conventional manufacturing of polymer products. *ACS Sustainable Chemistry and Engineering*, 1(12), pp. 1511–1519. doi: 10.1021/sc400093k.
- Labonnote, N. et al. 2016. Additive construction: State-of-the-art, challenges and opportunities. *Automation in Construction* 72, pp. 347–366. Available at: <http://dx.doi.org/10.1016/j.autcon.2016.08.026>.
- Lau, M. et al. 2012. Digital fabrication. *Computer*, 45(12), pp. 76–79. doi: 10.1109/MC.2012.407.
- Le, T.T. et al. 2012a. Hardened properties of high-performance printing concrete. *Cement and Concrete Research* 42(3), pp. 558–566. doi: 10.1016/j.cemconres.2011.12.003.
- Le, T.T. et al. 2012b. Mix design and fresh properties for high-performance printing concrete. *Materials and Structures/Materiaux et Constructions* 45(8), pp. 1221–1232. doi: 10.1617/s11527-012-9828-z
- Malaeb, Z. et al. 2015. 3D Concrete Printing: Machine and Mix Design. *International Journal of Civil Engineering and Technology* 6(April), pp. 14–22.
- National Institute for Public Health and Environment. (2017, 11 26). *Country Factors ReCiPe*. Retrieved from National Institute for Public Health and Environment: <https://www.rivm.nl/en/life-cycle-assessment-lca/recipe>.
- Nerella, Venkatesh Naidu, and Viktor Mechtcherine. 2016. *Studying the Printability of Fresh Concrete for Formwork-Free Concrete Onsite 3D Printing Technology (CONPrint3D)*. 3D Concrete Printing Technology. Elsevier Inc. Available at: <https://doi.org/10.1016/b978-0-12-815481-6.00016-6>.
- Ngo, T.D. et al. 2018. Additive manufacturing (3D printing): A review of materials, methods, applications and challenges. *Composites Part B: Engineering* 143(December 2017), pp. 172–196. Available at: <https://doi.org/10.1016/j.compositesb.2018.02.012>.
- NICDP. 2019. *Natural Resources* [online], Available at: <https://www.ic.gov.sa/en/invest-in-saudi-arabia/natural-resources/> [Accessed: 28

Jan 2020].

- Paul, S.C. et al. 2018. A review of 3D concrete printing systems and materials properties: current status and future research prospects. *Rapid Prototyping Journal* 24(4), pp. 784–798. doi: 10.1108/RPJ-09-2016-0154.
- Perrot, A. et al. 2018. 3D printing of earth-based materials: Processing aspects. *Construction and Building Materials* 172, pp. 670–676. Available at: <http://linkinghub.elsevier.com/retrieve/pii/S0950061818308079>.
- PRéSustainability, SimaPro. 2019. *Software To Measure And Improve The Impact Of Your Product Life Cycle* [online], Available at: <https://www.pre-sustainability.com/sustainability-consulting/sustainable-practices/custom-sustainability-software> [Accessed: 13 Dec 2019].
- Quagliarini E. et al., 2010. Cob Construction in Italy: Some Lessons from the Past. *Sustainability*, 2 (10): 3291–3308. <https://doi.org/10.3390/su2103291>.
- REN21 2019. *Renewables 2019 Global Status Report*. Paris. Available at: <http://www.ren21.net/gsr-2019/>
- Sala, S. et al. 2018. *Development of a weighting approach for the Environmental Footprint*. Available at: <https://eplca.jrc.ec.europa.eu/LCDN/developerEF.xhtml>. [Accessed: 28 December 2019]
- Saudi Vision 2030. 2018. *Saudi Vision 2030* [online]. Available at: <http://vision2030.gov.sa/en> [Accessed: 29 Nov 2019].
- SBC 301-306. 2018. Saudi Building Code [Online]. Available at: https://www.sbc.gov.sa/En/BuildingCode/Pages/SBC_301.aspx [Accessed: 15 Nov 2019].
- Shrubsole, C. et al. 2019. Bridging the gap: The need for a systems thinking approach in understanding and addressing energy and environmental performance in buildings. *Indoor and Built Environment* 28(1), pp. 100–117. doi: 10.1177/1420326X17753513.
- Singh A. et al. 2011. Review of Life-Cycle Assessment Applications in Building

- Construction. *Journal of Architectural Engineering* 17 (March), pp. 15–23.
[https://doi.org/10.1061/\(ASCE\)AE.1943-5568.0000026](https://doi.org/10.1061/(ASCE)AE.1943-5568.0000026).
- Soliman, Y. et al. 2015. 3D Printing and Its Urologic Applications. *Reviews in Urology*, 17(1), pp.20–4. Available at:
<http://www.pubmedcentral.nih.gov/articlerender.fcgi?artid=4444770&tool=pmc-entrez&rendertype=abstract>.
- Soto, B.G. De et al. 2018. The potential of digital fabrication to improve productivity in construction : cost and time analysis of a robotically fabricated concrete wall. *Automation in Construction* 92(2018), pp. 297–311. Available at:
<https://doi.org/10.1016/j.autcon.2018.04.004>
- Tulevech, S. M., Hage, D. J. Spence, Jorgensen, K., Guensler, C. L., Himmler, R. and Gheewala, S. H. 2018. Life Cycle Assessment: A Multi-Scenario Case Study of a Low-Energy Industrial Building in Thailand. *Energy and Buildings* 168, pp. 191–200. <https://doi.org/10.1016/j.enbuild.2018.03.011>.
- UNEP/SETAC, 2016. *Global Guidance for Life Cycle Impact Assessment Indicators* Volume 1. Available at: <https://www.lifecycleinitiative.org/training-resources/global-guidance-lcia-indicators-v-1/>. [Accessed: 17 December 2019]
- Veliz, R. et al. 2018. Computing Craft: Early Development of a Robotically-Supported Cob 3D Printing System, pp.1–3.
- Veliz Reyes, A. et al. 2019. Negotiated matter: a robotic exploration of craft-driven innovation. *Architectural Science Review* 0(0), pp. 1–11. Available at:
<https://www.tandfonline.com/doi/full/10.1080/00038628.2019.1651688>.
- Wang, Q. et al. 2014. *Investigation of condensation reaction during phenol liquefaction of waste woody materials*. doi: 10.2495/SDP-V9-N5-658-668.
- Weismann, A. and Bryce, K. 2006. *Building with cob*. Devon: Green Books Ltd.
- Wolfs, R.J.M. 2015. 3D Printing of concrete structural. MA Dissertation, Eindhoven Univaersity of Technology.
- Wu, P. et al. 2016. A critical review of the use of 3-D printing in the construction industry. 68, pp. 21–31. *Automation in construction*. Available at: <https://ac.els->

cdn.com/S0926580516300681/1-s2.0-S0926580516300681-main.pdf?_tid=250f7c63-ec3d-4c30-88f0-b2763d3f5e6b&acdnat=1528375914_f48a2d599618a1e3277a7c39b42f2f90.

Xia, M. and Sanjayan, J. 2016. Method of formulating geopolymer for 3D printing for construction applications. *Materials and Design* 110, pp. 382–390. Available at: <http://dx.doi.org/10.1016/j.matdes.2016.07.136>.

Yao, Y. et al. 2019. Life cycle assessment of 3D printing geo-polymer concrete: An ex-ante study. *Journal of Industrial Ecology*, pp. 116–127. doi: 10.1111/jiec.12930.

Chapter 8 Discussion

8.1 Introduction

This chapter presents the overall discussion on the four preceding explorations in chapters 4 to 7. Since the detailed discussion on each exploration aspect has been presented in each chapter respectively, this chapter will focus only on the final remarks while revealing the interconnections between all the aspects. The chapter also offers a further exploration of relevant issues that could not be covered in the respective chapter.

8.2 The Geometry and Physical Characteristics

As presented in Chapter 4, this study has explored three main aspects of 3DP cob: material mixture, 3DP tools, and geometry. The study has been able to produce a revised cob recipe that fits the purpose of 3D Printing. The recipe adjustment involved increasing the water content in the mixture, which improved the rheological behaviour of the mix. However, increasing the water content also revealed concerns with regards to the structural stability of the freshly printed mix and the possibility of shrinkage. This was seen in testing the maximum lift height, where after achieving a height of 60 cm the structure started to become unstable (Figure 16). Hence, it is essential to either slow down or pause the 3DP process prior to reaching the 60 cm lift height to enable the printed geometry to harden and gain the necessary strength for the subsequent layers.

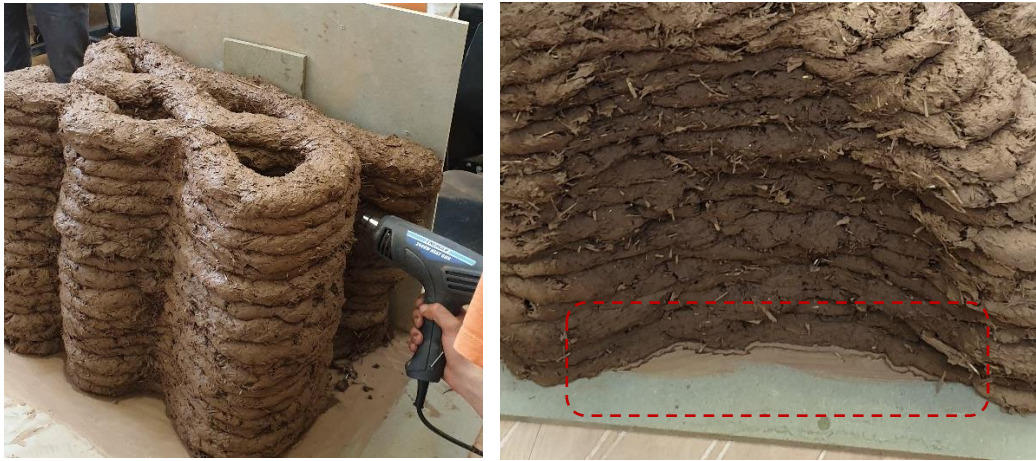


Figure 16. Problems with drying and shrinkage of the fresh cob mixtures.

It is also important to note that, while 3DP of cement-based materials may look like 3DP cob in terms of the viscosity nature, 3DP cob does not necessarily require advanced off-site lab testing of the mixture properties like concrete. Inspired and guided by the book “Building with cob: a step-by-step guide” (Weismann and Bryce 2006), this study aimed to provide an exploratory approach for 3DP cob system in construction, with minimal need for sophisticated lab testing in an attempt to mimic the traditional/ historical methods of building with cob, which suits most architects. This way the study generates several opportunities for future in-depth testing on 3DP cob.

On the aspect of 3DP tools, this research has developed an innovative bespoke extrusion that is able to tackle several challenges of 3DP cob as detailed in chapter 4. Nonetheless, despite the added benefits of the developed system, it is important to highlight the following:

- 1) The current proposed cartridge system does not suggest preparing all the required cartridges for large tasks (i.e. full-size wall) at once before the

printing, as it would require massive amounts of cartridges, which is not practical at all. Instead, the current cartridge system aims to create a transitional/ buffer time between the process of refilling and reloading. This means the printing process starts with a fully loaded cartridge rack with all its cartridges on the vehicle. Meanwhile, the mixing and refilling process will keep running separately. This way, the human role would be mixing the materials, refilling the empty cartridges, and reloading new full cartridges to both the rack and the extruder. So, if a task requires 100 cartridges, some of them would be ready on the rack at the start, while the rest are being prepared and transferred.

- 2) The proposed extrusion system, as it is now, does not exclude human interaction completely from the 3DP process. It is rather aiming to minimize human interference with the active 3D printing workspace through focusing the human role on material mix preparation, cartridge refilling and reloading.
- 3) For the future, automating the reloading process via a robotic arm (or any other special machine) can save time and increase the efficiency of the process. There is always room to expand the system for a completely automated 3DP site, where mixing, refilling and reloading are all undertaken by machines.

Moving to the geometry of 3DP cob, the study aims to develop a novel approach for an upscaled 3DP cob technique, with a special focus on the material behaviour under the developed 3DP extrusion system. Therefore, this study has prioritised exploring the geometries that form a basic cob construction as explained in chapter 4. Also, the

selection of the geometries carefully considered the possible 3D printing movement styles (i.e. conventional 3-axis printing and robotic 6-axis printing), which should reflect the material capabilities under different 3D printing processes. Establishing a fundamental understanding of the material potentials within a 3D printing system will possibly open a wider spectrum for further geometry explorations in the future, either by the current authors or others.

It is still true that more complex geometries would have been beneficial to exhibit further capabilities of the 3D printing process; yet, the study had some limitations in terms project time and the available funding, which affected conducting extended testing of the geometry with higher complexities or larger scale.

8.3 The Structural Performance

The study conducted a comprehensive feasibility investigation of the structural performance of 3DP cob walls under gravity loads. The basic mechanical properties of 3DP cob have been quantified, then used to produce a structural model to simulate the 3DP cob walls' load-bearing capacities in typical residential construction. The findings of the study have demonstrated promising capabilities of 3DP cob for use in low-rise buildings, where it can exhibit higher material efficiency and design flexibility as compared to traditional cob. It is, however, important to highlight the following:

- 1) The study findings are based on small-scale test specimens, combined with structural analysis. Therefore, future research is still required on the full-scale walls to provide further verification of these findings.

- 2) Whilst the study defines the 3DP cob wall dimensions using three parameters (i.e. t_{in} , t_{out} and t) as illustrated in Chapter 5, it is important to understand that an actual measurement of these values on a 3D printed geometry will vary slightly from the virtual model. In order to narrow the gap between the virtual and the physical model, further research is recommended into examining the change in model size from fresh to hardened mixture due to the shrinkage.
- 3) One of the general flows of the cob material/construction technique is that it is applied to build structural elements while still having relatively high water content (plastic consistency). This naturally causes shrinkage and cracks during the drying period of the material. Therefore, this natural behaviour must be carefully considered in designing the structural components of conventional cob. Since 3DP cob requires even higher water content as compared to conventional methods to facilitate its workability inside the extrusion system, it will become essential to understand and estimate the shrinkage behaviour of 3DP cob. Due to time constraints in conducting this doctoral research, the study did not manage to cover the aspect of shrinkage; therefore, further research on 3DP cob shrinkage behaviour is strongly recommended. It is worth mentioning that, despite the increased water content in the cob mixture prior to the printing process, the final printed cob (forming the geometry) tends to have a lower water content, which improves the structural stability of the printed layers. This favourable phenomenon was observed during the extrusion process, where the cob mixture loses some of its water while being compressed inside the cartridges and into the hose, as discussed in Chapter 4. The water came out in the form of minor leakage around the aluminium connections.

The study has demonstrated that 3DP cob can provide an adequate substitute for many of the current contemporary construction techniques. The incorporation of voids inside the wall design have made 3DP cob walls more material-efficient as compared to conventional cob, yet it is essential to assess the efficiency of the chosen 3D cob wall design holistically by also taking into consideration other performance aspects, such as the thermal performance and environmental impacts.

8.4 The Thermal properties

The study has investigated the thermal conductivity of four different types of 3DP cob walls. The results generally showed that 3DP cob walls exhibit a good thermal performance compared to the manually-constructed cob walls, with thermal conductivity of 0.32- 0.48 W/mK, which is lower than that of other traditional wall materials such as blockwork and concrete walls. This means 3D cob walls would conduct less heat from outside to inside or vice versa, potentially reducing the energy needed to cool or heat the building and improving thermal comfort of the occupants inside the building.

However, it is important to highlight the following:

- 1) Straw content plays a very important role in determining the thermal conductivity of cob, as cob mixtures with high straw content (4-8%) have less density, which leads to lower conductivity and an improved insulation performance. However, low-density cob has a reduced structural performance, which directly influences cob's capability for load bearing. In addition, as stated previously in the material testing in Chapter 4, a proper

3DP cob mixture should not contain high straw content as it leads to several extrusion problems.

- 2) Despite the variation in the tested 3DP cob walls with voids (i.e. single and double gap walls), the changes in the thermal conductivity values tend to be relatively small, where the single gap and the double gap walls have conductivity of 0.37 and 0.4 W/mK respectively. Nevertheless, this does not mean that the two wall types will exhibit similar performance when other performance aspects such as the structural and environmental performance are considered.
- 3) The thermal investigation was limited in scale, as the used heat flow meter accommodates small specimens only of 300 x 300 x 100 mm³. Therefore, future experiments would be needed on full-scale cob walls for verification of the results.

On the subject of environmental performance, the impact of 3DP cob walls on the operational energy performance of 3DP cob houses is also important, as it contributes to the overall environmental impacts. Whilst the intention of the thermal performance study as presented in Chapter 5 was solely to investigate the thermal conductivity of 3DP cob of various types, it is perceived important to explore the impact of using 3DP cob walls on the operating energy of the building, as shown below of a building using 3DP cob walls.

The selected wall types for this exploration is the single gap and the double gap walls, which were represented as Type A and Type B in the structural performance study in Chapter 5 (0). The exploration has been conducted through building performance

simulation by using Energy plus with Design Builder interface (DesignBuilder 2020). The simulation adopted an idealised one-story cob house from the structural performance study (Figure 17), while the location was set to Adelaide in Australia. The city is located on a latitude 34.9 south, longitude 138.6 east, and sits at an average elevation of 50 m above sea level. Adelaide has mild winter and a warm, dry summer, with an average temperature of 29°C in summer and 15°C in winter. Temperature in summer may soar occasionally to reach a maximum of 48°C (ABOM 2020).

The used wall thickness was fixed at 0.4 cm (400 mm). All other details about the building design can be found in Chapter 5. The building was modelled to be occupied with both mechanical and natural ventilation allowed. Heating and cooling setpoints were set as 21°C and 25°C respectively. As the study focuses on the thermal performance of the walls, roofs and floor were set as adiabatic to exclude their heat transfer in the analysis. Windows were modelled as single glazed with Al frames. The thermal properties of the walls were set based on the obtained conductivity values from the thermal performance experiments as in chapter 6. Table 1 below shows the basic setting of the thermal properties of each wall type. The simulation concentrated on the annual cooling and heating loads as a representation for the energy efficiency.

Table 1. Basic thermal properties the 3DP cob walls in the idealised building

	Type A wall (single gap)	Type B wall (double gap)
Conductivity (W/m.K)	0.37	0.4
Specific heat (J/ kg.K)	750	800
Density (kg/m ³)	1283	1496

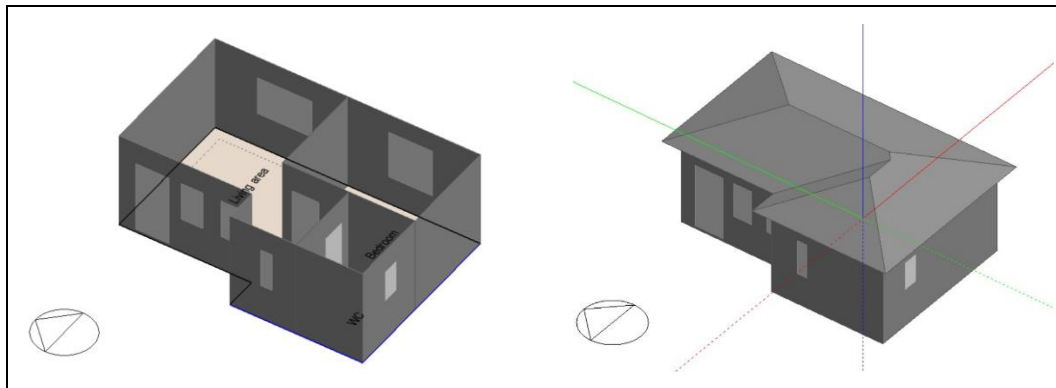


Figure 17. Modelling an idealised 3DP cob house in Designbuilder for operational energy simulation.

The energy simulation showed that the Type B wall with the double-gap design has slightly better annual performance as compared to the Type A single-gap wall (Table 2). This is despite the fact that single gap walls present lower conductivity, lower material consumption, and better structural efficiency. To explain this further, single gap walls exhibit lower heating loads due to its higher thermal insulation. However, having higher thermal insulation can lead to higher cooling loads, as more heat is trapped inside the building. On the contrary, walls with lower thermal insulation (higher conductivity) would lose the heat faster. In the context where cooling is more dominant than heating, using double gap wall seems to result in a lower overall energy use. This again stresses further on the importance of the holistic consideration of all the performance aspects before selecting a specific 3DP cob wall design for the desired project, including consideration of the impact of geographical location and climate on selecting the 3DP cob wall types for construction.

Table 2. Annual Energy loads for the 3DP cob walls in an idealised building

	Type A wall (single gap)	Type B wall (double gap)
Cooling loads (W/m ²)	28443	27591
Heating loads (W/m ²)	1903	1979
Total loads	55948	54391

8.5 The Environmental Implications

The study has explored the environmental implications of 3DP cob walls through a systematic comparison with three other types of wall construction: 3DP concrete, conventional concrete, and conventional cob walls. The study aims to focus on the environmental potentials that 3DP cob can provide over the widely spreading concrete construction, whether it is conventionally built or 3D printed. The explorations demonstrated that 3DP cob has superior environmental performance over its concrete counterparts due to its lesser global warming potential, stratospheric ozone depletion, and fine particulate matter formation. However, the study encountered several shortcomings which are important to highlight as follows:

- 1) Due to the limited information on 3DP cob construction on a real scale (i.e. actual built house), the scope of this study's LCA focused only on the cradle to site processes. It is important to consider further explorations on a full life cycle from cradle to grave.
- 2) The study had some limitations in materials and fabrication facilities, which made it difficult to construct a real size wall (e.g. 3 x 3 m² wall) for the 3DP cob. Therefore, the study used numerically calculated quantities on a 1 m² functional units based on previous experimentation on smaller scales.

Constructing a full-size wall may encounter slight variations in the actual quantities, whether in materials, transportation or in the energy/ electricity consumption in the fabrication process. Conducting future quantifications based on an actual built full-size 3DP cob wall will provide a better accuracy to the LCA.

- 3) While 3DP cob presents superior environmental performance over the concrete-based counterparts, it has poorer structural performance, as discussed in Chapter 5. This limits leveraging 3DP cob to certain types of projects, mostly small sized buildings with one to two storeys maximum. From an LCA perspective, this also limits the comparison of the environmental feasibility of 3DP cob with other construction techniques to the context of residential buildings. Moreover, the comparison between cob and concrete must consider other competitive aspects such as the lifespan and required maintenance. Cob buildings naturally exhibit shorter durability since it is more susceptible to damage from natural factors (e.g. rain, termites). Yet, on the other hand, concrete is more expensive to repair.

Finally, it is important to highlight that there is an increasing amount of research that eagerly pursues the improved environmental characteristics of 3DP concrete (Dixit 2019). This will create higher competency with 3DP cob, especially when holistically considering all the performance aspects that deals with workability, time, and structural integrity.

Chapter 9 Conclusions

The body of work presented in this thesis provides a comprehensive feasibility exploration of combining a low cost and sustainable material (Cob) with an innovative robotic 3D printing process. Originating from an aim to support the local building industry through integrating a dwindling traditional construction (cob) with an emerging technological sector (3D printing), a new work ethos has been established on a research model that embraces vernacular knowledge, local skillsets and materials as grounds for a new digital innovation.

The development of a robotic 3DP cob framework involves a standard innovation delivery process, from basic conceptions and research, up to proof of concept and physical prototyping. Although further development is required to industrialise 3DP cob on a wide scale, the research has managed to address the need to acknowledge the potentials of vernacular knowledge and buildings to expand the scope of additive manufacturing in construction beyond the concrete-based materials. This thesis has offered a roadmap capable of bringing 3DP cob construction closer to full-scale applications. The study has contributed to the disciplines of architectural design and construction by bridging the knowledge gap between earth construction and contemporary digital practice.

The thesis outcomes deliver practical guidelines for employing the 3DP cob technique in modern construction, which will enable architects and designers in the early stages of design to assess and compare the 3DP cob technique as a substitute

to other types of construction. These guidelines have been established by addressing the four fundamental aims of this work as follows:

- 1) Chapter 4 provides fundamental understanding of the rheological behaviour and workability aspects of a revised cob mixture under a developed 3DP system;
- 2) Chapter 5 establishes a structural design framework for 3DP cob buildings, allowing the optimisation of 3DP walls design based on structural performance and material efficiency;
- 3) Chapter 6 identifies the basic thermal performance properties of 3DP cob walls, allowing the optimisation of 3DP walls design based on their thermal efficiency; and
- 4) Chapter 7 provides a fundamental understanding of the associated environmental implications with 3DP cob construction, and how it compares to other conventional and 3DP techniques.

On a broader scale, this thesis has revealed several key contributions to the field of robotic fabrication in architecture. The introduced practical framework acknowledges the nuanced nature of a traditional craft and utilises it as a driver for robotic fabrication in architecture. In addition, the framework contributes not only to the design of new buildings, but also has the potential to be used in repairs and renovation of existing and historic cob buildings. In this way, the work approaches a new definition of craft that negotiates material behaviour under the framework of the contemporary digital practice. Following mixed assessment methods derived from a range of disciplines such as material science, design, architecture, robotics and

mechanical engineering, the study has demonstrated that interdisciplinary aspects of performance must be considered as an integral part of a contemporary architectural design and production process. This work's outcomes are expected to benefit architects, designers and researchers currently looking into craft as a source of material and design sophistication and knowledge.

Finally, this research has demonstrated its contributions to the areas of robotic material culture and human-robot collaboration. There are still limitations that prevent 3D Printing technologies from producing certain construction components on a large scale. However, as construction materials and methods are rapidly evolving, a constant pursuit for innovative hybrid solutions and mixed modes of construction is essential and needs to continue.

References (Excluding references in papers)

- 3D-WASP. 2020. “3D Printers | WASP | Leading Company in the 3d Printing Industry.” 2020. <https://www.3dwasp.com/en/>.
- ABOM. 2020. “Climate Data Online.” Australian Bureau of Meteorology. 2020. <http://www.bom.gov.au/climate/data/>.
- Acero, Aitor P, Cristina Rodríguez, and Andreas Ciroth. 2014. “LCIA Methods Impact Assessment Methods in Life Cycle Assessment and Their Impact Categories.” *OpenLCA*, no. February: 1–23.
- Agustí-Juan, Isolda, and Guillaume Habert. 2017. “Environmental Design Guidelines for Digital Fabrication.” *Journal of Cleaner Production* 142: 2780–91. <https://doi.org/10.1016/j.jclepro.2016.10.190>.
- Agustí-Juan, Isolda, Florian Müller, Norman Hack, Timothy Wangler, and Guillaume Habert. 2017. “Potential Benefits of Digital Fabrication for Complex Structures: Environmental Assessment of a Robotically Fabricated Concrete Wall.” *Journal of Cleaner Production* 154: 330–40. <https://doi.org/10.1016/j.jclepro.2017.04.002>.
- Alhumayani, Hashem, Mohamed Gomaa, Veronica Soebarto, and Wassim Jabi. 2020. “Environmental Assessment of Large-Scale 3D Printing in Construction: A Comparative Study between Cob and Concrete.” *Journal of Cleaner Production* 270 (June): 122463. <https://doi.org/10.1016/j.jclepro.2020.122463>.
- Andrew, Robbie M. 2019. “Global CO2 Emissions from Cement Production, 1928–2018.” *Earth System Science Data*. Vol. 11. <https://doi.org/10.5194/essd-11-1675-2019>.
- Apis-cor. 2019. “Apis Cor 3D Printed Project in Dubai.” 2019. <https://www.apis-cor.com/dubai-project>.
- Arrigoni, Alessandro, Christopher Beckett, Daniela Ciancio, and Giovanni Dotelli. 2017. “Life Cycle Analysis of Environmental Impact vs. Durability of Stabilised Rammed Earth.” *Construction and Building Materials* 142: 128–36. <https://doi.org/10.1016/j.conbuildmat.2017.03.066>.
- Bakens, Wim, Greg Foliente, and Mansi Jasuja. 2005. “Engaging Stakeholders in Performance-Based Building: Lessons from the Performance-Based Building

- (PeBBu) Network.” *Building Research and Information*. Routledge .
<https://doi.org/10.1080/0961321042000322609>.
- Balaji, N. C., Monto Mani, and B. V. Venkatarama Reddy. 2013. “Thermal Performance of the Building Walls.” *Building Simulation Applications* 2013-Janua (January): 151–59.
- Becker, Rachel. 2008. “Fundamentals of Performance-Based Building Design.” *Building Simulation* 1 (4): 356–71. <https://doi.org/10.1007/s12273-008-8527-8>.
- CEN. 2011. “EN 772-1. Methods of Test for Masonry Units - Part 1: Determination of Compressive Strength.” https://infostore.saiglobal.com/en-us/Standards/EN-772-1-2011-A1-2015-331320_SAIG_CEN_CEN_761952/.
- Chandel, S. S., Vandna Sharma, and Bhanu M. Marwah. 2016. “Review of Energy Efficient Features in Vernacular Architecture for Improving Indoor Thermal Comfort Conditions.” *Renewable and Sustainable Energy Reviews* 65: 459–77. <https://doi.org/10.1016/j.rser.2016.07.038>.
- CIB Working Commission. 1982. “CIB Report 64: Working with the Performance Approach to Building.” Rotterdam.
- Clarke, J A, P P Yaneske, and A A Pinney. 1990. “The Harmonisation of Thermal Properties of Building Materials.” *BEPAC Research Report*. Vol. 2.
- CyBe. 2019. “3D Studio 2030 — CyBe Construction.” 2019. <https://cybe.eu/case/3d-studio-2030/>.
- Deru, M, and P Torcellini. 2005. “Performance Metrics Research Project – Final Report.” Colorado.
- Ding, Grace K.C. 2008. “Sustainable Construction-The Role of Environmental Assessment Tools.” *Journal of Environmental Management* 86 (3): 451–64. <https://doi.org/10.1016/j.jenvman.2006.12.025>.
- Dixit, M. K. 2019. “3-D Printing in Building Construction: A Literature Review of Opportunities and Challenges of Reducing Life Cycle Energy and Carbon of Buildings.” *IOP Conference Series: Earth and Environmental Science* 290 (1). <https://doi.org/10.1088/1755-1315/290/1/012012>.
- Earth Devon. 2008. “Cob Dwellings: Compliance with The Building Regulations.” *Cob and Unbaked Earth Dwellings* 2000: 1–21.

- Ford, Simon, and Mélanie Despeisse. 2016. "Additive Manufacturing and Sustainability: An Exploratory Study of the Advantages and Challenges." *Journal of Cleaner Production* 137: 1573–87. <https://doi.org/10.1016/j.jclepro.2016.04.150>.
- Fox, Matthew, Harry Driver, Jim Carfrae, Kevin Owen, Karen Hood-Cree, and Steve Goodhew. 2019. "Waste-Paper Sludge and Shredded Sheet Additives . An Investigation into the Change in Thermal Properties of Cob Samples Using Waste-Paper Sludge and Shredded Sheet Additives Harry Driver Jim Carfrae Karen Hood-Cree Steve Goodhew." In . Santa Fe, NM: Earth USA 2019.
- Francis, Jack Stuart. 2018. "Re-Designing an Extrusion System for Accelerated Testing of 3D-Printing Earth- Based Construction Materials." Cardiff University.
- Freney, Martin. 2014. "Earthship Architecture: Post Occupancy Evaluation, Thermal Performance & Life Cycle Assessment." University of Adelaide. <http://hdl.handle.net/2440/91872>.
- Geneidy, Omar, Walaa S.E. Ismaeel, and Ayman Abbas. 2019. "A Critical Review for Applying Three-Dimensional Concrete Wall Printing Technology in Egypt." *Architectural Science Review* 0 (0): 1–15. <https://doi.org/10.1080/00038628.2019.1596066>.
- Gomaa, Mohamed, Jim Carfrae, Steve Goodhew, Wassim Jabi, and Alejandro Veliz Reyez. 2019. "Thermal Performance Exploration of 3D Printed Cob." *Architectural Science Review*, April, 1–8. <https://doi.org/10.1080/00038628.2019.1606776>.
- Häfliger, Ian Frederic, Viola John, Alexander Passer, Sebastien Lasvaux, Endrit Hoxha, Marcella Ruschi Mendes Saade, and Guillaume Habert. 2017. "Buildings Environmental Impacts' Sensitivity Related to LCA Modelling Choices of Construction Materials." *Journal of Cleaner Production* 156: 805–16. <https://doi.org/10.1016/j.jclepro.2017.04.052>.
- Hager, Izabela, Anna Golonka, and Roman Putanowicz. 2016. "3D Printing of Buildings and Building Components as the Future of Sustainable Construction?" In *Procedia Engineering*. Vol. 151. <https://doi.org/10.1016/j.proeng.2016.07.357>.

- Hague, R, I Campbell, and P Dickens. 2003. "Implications on Design of Rapid Manufacturing." *Proceedings of the Institution of Mechanical Engineers, Part C: Journal of Mechanical Engineering Science* 217 (1): 25–30. <https://doi.org/10.1243/095440603762554587>.
- Hall, Matthew, and David Allinson. 2009. "Assessing the Effects of Soil Grading on the Moisture Content-Dependent Thermal Conductivity of Stabilised Rammed Earth Materials | Elsevier Enhanced Reader." *Applied Thermal Engineering Journal* 29: 740–47. <https://reader.elsevier.com/reader/sd/pii/S1359431108001889?token=A79097E18362B0A49BB6C02E84736CE6000EAD0C46F421C2FDA82F0E9D561605683F2197627BFE78576E3DAD2F0A2402>.
- Hamard, Erwan, Bogdan Cazacliu, Andry Razakamanantsoa, and Jean Claude Morel. 2016. "Cob, a Vernacular Earth Construction Process in the Context of Modern Sustainable Building." *Building and Environment* 106: 103–19. <https://doi.org/10.1016/j.buildenv.2016.06.009>.
- Hartkopf, V, V Loftness, and P Mill. 1986. *The Concept of Total Building Performance and Building Diagnostics- In: Davis, G. Ed., Building Performance: Function, Preservation and Rehabilitation. Philadelphia. American Society for Testing and Materials.*
- Hitchcock, Rj. 2002. "High-Performance Commercial Building Systems Program Element 2 – Project 2.1 – Task 2.1.2." *Standardized Building Performance Metrics Final Report.* Berkeley. <http://scholar.google.com/scholar?hl=en&btnG=Search&q=intitle:High-Performance+Commercial+Building+Systems+Program+Standardized+Building+Performance+Metrics+Final+Report#2>.
- Hollberg, Alexander, and Jürgen Ruth. 2016. "LCA in Architectural Design—a Parametric Approach." *International Journal of Life Cycle Assessment* 21 (7): 943–60. <https://doi.org/10.1007/s11367-016-1065-1>.
- Iddon, Christopher R., and Steven K. Firth. 2013. "Embodied and Operational Energy for New-Build Housing: A Case Study of Construction Methods in the UK." *Energy and Buildings* 67 (2013): 479–88. <https://doi.org/10.1016/j.enbuild.2013.08.041>.

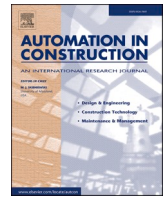
- IEA and UNEP. 2018. “International Energy Agency and the United Nations Environment Programme - Global Status Report 2018: Towards a Zero-emission, Efficient and Resilient Buildings and Construction Sector,” 325. <https://doi.org/978-3-9818911-3-3>.
- Joseph, Mathew, Victor Jose, and Anjuman Habeeb. 2015. “Thermal Performance of Buildings: Case Study and Experimental Validation of Educational Building.” *International Journal of Advanced Research in Electrical, Electronics and Instrumentation Engineering* 04 (06): 4968–74. <https://doi.org/10.15662/ijareeie.2015.0406011>.
- Kajaste, Raili, and Markku Hurme. 2016. “Cement Industry Greenhouse Gas Emissions e Management Options and Abatement Cost.” *Journal of Cleaner Production* 112: 4041–52. <https://doi.org/10.1016/j.jclepro.2015.07.055>.
- Kalo, Amar. 2020. “Amar Kalo [MS_DT].” 2020. <http://amarkalo.blogspot.com/>.
- Keefe, Laurence. 2005. *Earth Building: Methods and Materials, Repair and Conservation*. [https://books.google.com.au/books?hl=en&lr=&id=cCGAAgAAQBAJ&oi=fnd&pg=PR1&dq=Earth+Building+-+Methods+and+Materials,+Repair+and+Conservation&ots=jZ3gR-qkRd&sig=MYVBVS1ZW3-ZXe0EjfwBku7b9i0&redir_esc=y#v=onepage&q=Earth Building – Methods and Materials%2C R](https://books.google.com.au/books?hl=en&lr=&id=cCGAAgAAQBAJ&oi=fnd&pg=PR1&dq=Earth+Building+-+Methods+and+Materials,+Repair+and+Conservation&ots=jZ3gR-qkRd&sig=MYVBVS1ZW3-ZXe0EjfwBku7b9i0&redir_esc=y#v=onepage&q=Earth%20Building%20and%20Materials%20R).
- Khalfallah, Salah. 2018. *Structural Analysis 1: Statically Determinate Structures*. First eddi. Hoboken,: Wiley Blackwell.
- Kohler, Gramazio. 2006. “Gramazio Kohler.” 2006. https://www.aic-iac.org/editorial_n0/architectes/gramazio-kohler/.
- Kolarevic, Branko. 2001. “Digital Fabrication : Manufacturing Architecture in the Information Age.” *Proceedings of the Twenty First Annual Conference of the Association for Computer-Aided Design in Architecture / ISBN 1-880250-10-1*, 268–78.
- Kolarevic, Branko, and Ali Malkawi. 2005. *Performative Architecture: Beyond Instrumentality*. 1st editio. New York: Spon Press.
- Kothman, Ivo, and Niels Faber. 2016. “How 3D Printing Technology Changes the

- Rules of the Game Insights from the Construction Sector.” *Journal of Manufacturing Technology Management* 27 (7): 932–43. <https://doi.org/10.1108/JMTM-01-2016-0010>.
- Martín, Silvia, Fernando R. Mazarrón, and Ignacio Cañas. 2010. “Study of Thermal Environment inside Rural Houses of Navapalos (Spain): The Advantages of Reuse Buildings of High Thermal Inertia.” *Construction and Building Materials* 24 (5): 666–76. <https://doi.org/10.1016/j.conbuildmat.2009.11.002>.
- McNeel, Robert. 2020. “Grasshopper - in Rhino 6.” 2020. <https://www.rhino3d.com/6/new/grasshopper>.
- Micoli, Lorenzo, Urs Müller, and Patrick Fontana. 2014. “Mechanical Behaviour of Earthen Materials: A Comparison between Earth Block Masonry, Rammed Earth and Cob.” *Construction and Building Materials* 61: 327–39. <https://doi.org/10.1016/j.conbuildmat.2014.03.009>.
- Ngo, Tuan D., Alireza Kashani, Gabriele Imbalzano, Kate T.Q. Nguyen, and David Hui. 2018. “Additive Manufacturing (3D Printing): A Review of Materials, Methods, Applications and Challenges.” *Composites Part B: Engineering*. <https://doi.org/10.1016/j.compositesb.2018.02.012>.
- NRMCA. 2020. “The National Ready Mixed Concrete Association.” 2020. <https://www.nrmca.org/>.
- Ortiz, Oscar, Francesc Castells, and Guido Sonnemann. 2009. “Sustainability in the Construction Industry: A Review of Recent Developments Based on LCA.” *Construction and Building Materials* 23 (1): 28–39. <https://doi.org/10.1016/j.conbuildmat.2007.11.012>.
- Perrot, A., D. Rängeard, and E. Courteille. 2018. “3D Printing of Earth-Based Materials: Processing Aspects.” *Construction and Building Materials* 172: 670–76. <https://doi.org/10.1016/j.conbuildmat.2018.04.017>.
- Preiser, Wolfgang F.E., and Jacqueline C. Vischer. 2005. *Assessing Building Performance*. Burlington: Elsevier Butterworth-Heinemann. <https://doi.org/10.4324/9780080455228>.
- Pullen, Quinn M., and Todd V. Scholz. 2011. “Index and Engineering Properties of Oregon Cob.” *Journal of Green Building* 6 (2): 88–106. <https://doi.org/10.3992/jgb.6.2.88>.

- Quagliarini, Enrico, Alessandro Stazi, Erio Pasqualini, and Evelina Fratolocchi. 2010. "Cob Construction in Italy: Some Lessons from the Past." *Sustainability* 2 (10): 3291–3308. <https://doi.org/10.3390/su2103291>.
- Rajan, Subramaniam D. 2001. *Introduction to Structural Analysis & Design*. First. Wisley Blackwell. https://books.google.com.eg/books/about/Introduction_to_Structural_Analysis_Des.html?id=8eJRAAAAMAAJ&redir_esc=y.
- Schutter, Geert De, Karel Lesage, Viktor Mechtcherine, Venkatesh Naidu Nerella, Guillaume Habert, and Isolda Agusti-Juan. 2018. "Vision of 3D Printing with Concrete — Technical, Economic and Environmental Potentials." *Cement and Concrete Research*, no. June: 1–12. <https://doi.org/10.1016/j.cemconres.2018.06.001>.
- Shakor, Pshtiwan, Shami Nejadi, Gavin Paul, and Sardar Malek. 2019. "Review of Emerging Additive Manufacturing Technologies in 3d Printing of Cementitious Materials in the Construction Industry." *Frontiers in Built Environment* 4 (January). <https://doi.org/10.3389/fbuil.2018.00085>.
- Siddika, Ayesha, Md Abdullah Al Mamun, Wahid Ferdous, Ashish Kumer Saha, and Rayed Alyousef. 2019. "3D-Printed Concrete: Applications, Performance, and Challenges." *Journal of Sustainable Cement-Based Materials*. Taylor and Francis Ltd. <https://doi.org/10.1080/21650373.2019.1705199>.
- Soto, Borja García De, Isolda Agustí-juan, Jens Hunhevicz, Guillaume Habert, and Bryan Adey. 2018. "Productivity of Digital Fabrication in Construction: Cost and Time Analysis of a Robotically Built Wall." *Automation in Construction* 92 (2018): 297–311. <https://doi.org/10.1016/j.autcon.2018.04.004>.
- Veliz Reyes, Alejandro, Mohamed Gomaa, Aikaterini Chatzivasileiadi, and Wassim Jabi. 2018. "Computing Craft: Early Stage Development Ofa Robotically-Supported 3D Printing System for Cob Structures." In *ECAADe- Computing for Better Tomorrow*, 1:791–800. Lodz: cuminCad.
- Weismann, Adam, and Katy Bryce. 2006. *Building with Cob: A Step-by-Step Guide*. Devon: Green Books ltd.
- Wilde, Pieter de. 2018. *Building Performance Analysis. Building Performance Analysis*. First. Wiley Blackwell. <https://doi.org/10.1002/9781119341901>.

- Wu, Peng, Jun Wang, and Xiangyu Wang. 2016. "A Critical Review of the Use of 3-D Printing in the Construction Industry." *Automation in Construction* 68: 21–31. <https://doi.org/10.1016/j.autcon.2016.04.005>.
- Zabihi, Hossein, Farah Habib, and Leila Mirsaedie. 2012. "Sustainability in Building and Construction : Revising Definitions and Concepts." *International Journal of Emerging Sciences* 2 (December): 570–78. <http://ijes.info/2/4/42542406.pdf>.

Appendix I: Manuscript- Development of a 3D printing system for earth-based construction: case study of cob.



3D printing system for earth-based construction: Case study of cob

Mohamed Gomaa^{a,b,*}, Wassim Jabi^b, Alejandro Veliz Reyes^c, Veronica Soebarto^a

^a School of Architecture and Built Environment, Horace Lamb Building, University of Adelaide, Adelaide SA5005, Australia

^b Welsh School of Architecture, Bute Building, Cardiff University, Cardiff CF10 3NB, United Kingdom

^c School of Art, Design and Architecture, Roland Levinsky Building, University of Plymouth, PL4 8AA, United Kingdom

ARTICLE INFO

Keywords:

3D printing
Additive manufacturing
Robotic construction
Digital fabrication
Extrusion systems
Cob
Earth-based material

ABSTRACT

Despite the dramatic development in digital manufacturing technologies in the recent years, 3D printing of earth materials, such as cob, still presents several challenges to the market-available 3D printing systems. This paper describes the development process of a 3D printing system for cob that fits the contemporary requirements of digital construction. The study first described the methodology of producing a revised cob recipe for the purpose of 3D printing. Then, the study conducted thorough investigations into the properties of three types of extrusion systems using both electromechanical and pneumatic methods, leading eventually to the development of a new bespoke dual-ram extruder. The study then explored systematically the relationship between the new 3DP system and the rheological properties of cob, followed by an exploration to the new geometric opportunities the new system offers. The study findings show that the new extrusion system improves greatly the 3DP process of cob in terms of extrusion rate, continuity, consistency, and mobility. The findings are expected to bring 3D printed cob construction closer to full-scale applications. On a broader scale the study contributes to the disciplines of architectural design and construction by providing a framework capable of bridging the knowledge gap between vernacular modes of building production and contemporary digital practice.

1. Introduction

An increasing amount of research on implementing 3D printing (3DP) systems for large-scale formats has exposed multiple potential applications for architecture and the construction industry [1,2]. Concurrent research highlights the advantages of 3D printing in construction to achieve a higher degree of process optimisations (e.g. financial, construction time, staffing resource), the emergence of new digital processes associated to Building Information Modelling and potential for mass customisation, and environmental benefits towards the life cycle of 3D printed objects and building elements [2]. Additionally, research such as the review paper by Tay et al. [1] outlines environmental benefits of 3DP in construction as a result of a reduced use of formwork [3].

Cob stands as one of many types of earth construction methods and it had been utilized historically all over the world. Its mix consists of subsoil (earth), water, and fibrous material (typically straw). However, similarly to related construction methods, cob buildings embody a material mix, as well as its associated construction method. Cob walls are typically built using hand-made material deposition on top a plinth, then corrected (e.g. correction of vertical planes) with material added or

removed before or after drying [4]. As a result, building elements can comprise a variety of geometries, yet the builder is required to constantly negotiate the execution of an intended design with ever-changing material properties (e.g. water content, drying speed) necessary to achieve the design goals without the need for formwork or any mechanical compaction method (Fig. 1). As a result:

- Cob provides a high degree of design freedom and adaptability throughout the construction process, where the builder negotiates with the material (and its properties) as the building process proceeds (Veliz [5]), challenging the normalised view of robotic 3D printing as a linear process from design to production.
- Cob can be reutilised throughout the construction process, providing the opportunity for testing and prototyping design solutions [6], reducing the amount of waste material and enabling low-cost project corrections and modifications on-site.
- Recent research demonstrates that cob complies with modern regulations such as UK building performance standards [7].
- When compared to other massing construction materials and methods (e.g. concrete), cob has lower CO₂ emissions, low embodied

* Corresponding author.

E-mail addresses: mohamed.gomaa@rmit.edu.au (M. Gomaa), jabiw@cardiff.ac.uk (W. Jabi), alejandro.velizreyes@plymouth.ac.uk (A. Veliz Reyes), veronica.soebarto@adelaide.edu.au (V. Soebarto).

<https://doi.org/10.1016/j.autcon.2021.103577>

Received 24 February 2020; Received in revised form 6 January 2021; Accepted 18 January 2021

Available online 25 January 2021

0926-5805/© 2021 Elsevier B.V. All rights reserved.



Fig. 1. Exposed cob construction in Totnes, UK.

energy [8] and requires a lower degree of depletion of natural resources [7].

These criteria suggest that a 3D printing system of cob warrants further investigation as a potential pathway towards more sustainable 3DP practices, with a lesser environmental impact when compared to concrete 3D printing [9]. Recent evidence supports this observation; an early study conducted on small material samples [10] provides evidence that 3D printed cob elements have competitive thermal performance standards when compared to other materials such as concrete, brickwork, and conventional cob construction.

Hamard et al. [4] and Agustí-Juan et al. [11] highlight that the integration of digital fabrication techniques with vernacular modes of architectural production can reveal sustainability potentials for construction applications as compared to other cement-based 3D printing methods. This, mainly due to existing forms of cob knowledge production (e.g. vernacular construction techniques), emerges from long-lasting local environmental, material, social and skills contexts of construction practice. This research recognises the potential of developing building technologies associated with vernacular knowledge and building practices, generating a research and development process highly grounded on responsible innovation by leveraging local industries and technologies, utilising local materials and workforce [12]. Moreover, the study challenges normalised models of design-to-fabrication research by incorporating local, vernacular and material knowledge as a methodological consideration and engagement process throughout the study. This negotiation between disparate frameworks of material practice (detailed in Veliz [5]), established both in R&D research and in vernacular construction, not only results in emergent material opportunities within a standard design-engineering professional delivery framework but also enables novel methodological approaches to architectural tectonics, local materials and skillsets, digital discourses and building technologies.

A substantial share of recent research on 3DP for construction addresses 3D printing of cement and mortar-like materials. As a result, there has been a huge development in 3D printing systems for cement-based materials in recent years [13,14]. Different types of extrusion systems are currently used for 3D printing; varying from pneumatic pumps and electromechanical ram extruders. In spite of these developments, 3D printing of earth-based materials, such as cob, still presents several challenges to the market-available 3D printing systems such as material granularity, material properties and mix ratios, or the use of local organic fibres, which must be addressed through extensive experimental research before delivering a feasible construction method (Veliz [15]). These requirements highlight the opportunities of

vernacular knowledge as a source of digital innovation, as it has already tested, iterated and perfected mix ratios and earthen architecture production typologies around the world.

Following early studies of cob 3DP technology (e.g. Veliz [15]) the sensitivity of the printing process to the material mix is currently a major limiting factor in the development of construction-scale 3D printing with cob. The hardening property of the material mix creates a critical constraint on the speed of the 3D printing process [16,17]. The interrelation between hardening time and printing velocity must be monitored carefully, as each printed layer must be hard enough to support the weight of the successive layers. At the same time, the material mix must sustain a certain rheological behaviour that enables it to be extruded smoothly through the 3DP printing system ([18]; [15]), despite its irregular granularity and addition of organic material. Moreover, effective design of material delivery systems may offset some irregularities that may be unavoidable in a commercial application, particularly considering the effect of specific geological, environmental or geographic conditions on the quality of 3DP cob mix.

Panda and Tan [19] demonstrated the importance of establishing a clear understanding of the rheological behaviour of highly viscous 3D printed materials such as concrete. One of the major issues with 3D printing of such materials is to balance between the fluidity level and sufficient viscosity simultaneously in a way to ensure smooth flow of material through the extrusion system without clogging while maintaining the extruded material shape during the printing process. In concrete 3D printing, the developed mixtures must be thixotropic in nature, which means it should have high yield stress and low viscosity [20]. Other studies by Lipscomb and Denn [21], Le et al. [22] and Choi, Kim, and Kim [23] also highlighted the critical influence of mixture components, such as particle size, gradation, surface area and paste/aggregate volume on the flow property of the material as they govern the yield stress and viscosity. In his study, Perrot et al. [18] proposed a theoretical framework for the structural built-up of 3DP of cement-based materials. His proposal showed the correlation between vertical stress acting on the first deposited layer with the critical stress related to plastic deformation that is linked to the material yield stress.

In earth construction, the rheology of the material is the key to control the quality of the structures. Historically, adjusting the consistency of cob mixtures depended greatly on the on the local know-how, simply though controlling the water to soil ratios, or by adding other ingredients such as fibres or lime [24]. As the construction industry shows a growing interest in earth materials via 3D printing, the need to develop simple and rapid testing for estimating earth material workability and rheological properties has increased [25,26]. According to Perrot, Rangeard, and Lecompte [24], field-oriented tests can be leveraged to estimate material parameters such as the yield stress, which will provide important information to describe the rheological behaviour of the earth material. Weismann and Bryce [27] demonstrated in their book “Building with cob: a step-by-step guide” detailed the methods for simple field tests of subsoil and cob characteristics. The recommended testing procedures were established on historical methods for building with cob, all aiming to provide clear understanding of the subsoil workability and rheology properties.

This research leverages the qualities of cob construction to utilise it as a groundwork for digital innovation through robotic 3D printing of building elements. This line of research has maintained the craft quality of cob as a source of innovative knowledge, often developed outside the boundaries of professional and academic frameworks - a “vernacular” understanding of the material usually communicated through making and practice instead of standard academic communication pathways [28]. This evolutionary approach of vernacular architecture as a driver for novel environmental, technological and cultural discourses is exploited in this study through an iterative design research method, which has developed a material mix for cob 3D printing applications, an innovative extrusion system for cob 3D printing applications, and a series of tests attempting to outline emerging large-scale design

opportunities resulting from this technology.

2. Methods and material

2.1. Material

In cob construction, printing material properties must be considered and formulated carefully according to both its wet and hardened states. Wet properties are those related to the material in its fresh, or 'green' state, i.e. the state that the material is in from initial mixing to the point at which it is deployed on site, before drying or hardening [17]. According to Le, Austin, Lim, Buswell, Law, Gibb, and Thorpe [16], three basic criteria must be met to ensure a successful 3D printing process; extrudability, buildability, and workability with time. This means that the material must flow efficiently through the system without excessive force and be deposited in layers with minimal deformations. At the same time it must be able to support the loads of subsequent layers before hardening and reaching some degree of structural integrity. The transition from printing to hardening must occur within a time frame considering the material hardening rate while meeting the overall construction requirements such as tolerances for deformation. A similar process is conducted during hand constructed cob, as the builder must skillfully negotiate water contents, structural integrity and building design throughout the construction process.

In the context of this study, mix ratios have been reached through an iterative process of testing and material characterisation. Weismann and Bryce [27] and Hamard et al. [4] recommended that the composition of a cob mixture (averages) to be 78% subsoil, 20% water and 2% fibre (straw) by weight. The recommendation for the subsoil formula itself is 15–25% clay to 75–85% aggregate/sand. This mix, however, requires adaptation for 3D printing applications that maximises its fluidity, while maintaining printability properties (e.g. layer definition) and structural cohesion (e.g. layer height). This study used subsoil sourced from a farmland near Cardiff, UK, for the cob specimens. Subsoil specimens were examined according to the recommended testing methods in the literature (Steve [27,29]): shake test, brick test, sausage test, ball drop test. These tests utilized simple deposition tests in order to acknowledge typically utilized on-site tests as well as to eventually simplify the material characterisation process should this method be used in different contexts with little or no access to material testing facilities (Fig. 2).

However, as cob is traditionally mixed in a nearly dry state, the recommended compositions above do not necessarily fit the purpose of 3DP applications where a less viscous rheology is required. Lower water content in the mix leads to higher friction between the material and extrusion cycle parts, creating massive pressure on the extrusion mechanisms, resulting in increasing wear rate of the parts and reduce the long-term efficiency and printing quality. Goma et al. [10]

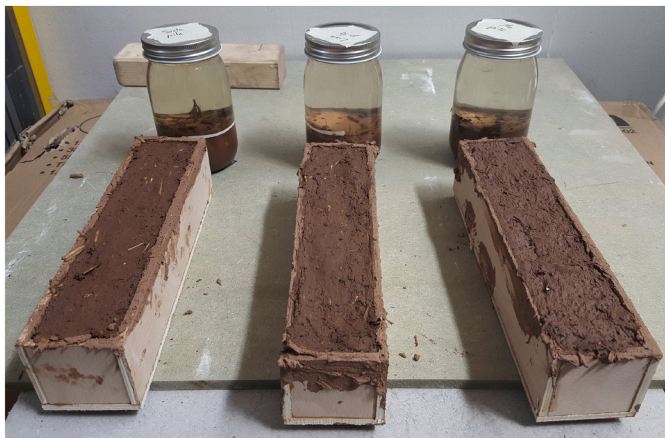


Fig. 2. Shake and brick tests to the three subsoil samples from Cardiff.

conducted a number of systematic tests to reach suitably modified proportions of cob mixtures for 3D printing purposes. The testing process included systematic alteration of several factors. Water contents of 22, 24, 26, and 28% were tested. The study concluded that the water content in the 3D printed cob mixture should be increased to an average of 25% while straw remains at 2%, resulting in a subsoil percentage of 73% (by weight).

It was anticipated that the increase in the water content will alter the rheology of the cob mix during and after the extrusion process. Therefore, it was important to examine the behaviour of the cob mix under the extrusion force. This examination seeks a systematic understanding of the variation in the printed path size in relation to the extrusion rate through the nozzle and motion speed on one side, and nozzle size and layer height on the other. Extrusion rate is usually used to express the volume of material passing through a given cross sectional nozzle area per unit time (mm^3/s). Linear extrusion rate, on the other hand, represents the passing length of the material over unit time (mm/s) [30,31]. The study at first examined the synchronization process between linear extrusion rate and motion speed. Linear extrusion is chosen so that changes in the cross sections of different nozzles will not alter the outcome. Yet, the study focused on understanding the vital relation between the layer height and nozzle size, and their impact on the printed outcome. Understanding this relation is essential during the process of transforming the designed geometry into accurate contours and path lines for the 3D printing framework. The correct, and accurate, estimation of the 3D printed size of path lines and the geometry in total increases the quality of the outcome.

A series of tests were conducted to define this relationship mathematically. The tests set the nozzle diameter and the motion speed as constants at 45 mm and 80 mm/s respectively, with a synchronised linear extrusion rate at 105% of the nozzle motion speed (approximately 85 mm/s). The printed file consisted of five path lines. Each line had a different layer height, starting from 15 mm and ending at 35 mm with 5 mm intervals. Each printed line was then measured and assigned to its respective height. This test was repeated three times to observe any possible variation to the outcome and increase credibility of estimations.

2.2. Equipment

A complete 3D Printing (3DP) system consists of two separate devices: a motion controller and a material delivery system. The two must be designed in coordination to realise the final 3D printed outcome: the weight of the extrusion system can affect the motion controller, or the accuracy of the motion controller can affect the tolerance and deformation of the final printed element. The study used a 6-axes KUKA KR60 HA robotic arm as the motion controller. The computer software package for robotic control was Rhinoceros via Grasshopper and KUKA PRC®. The material delivery system is the part of the printer setup which stores, transports, and deposits the print medium. The design of the material delivery system is vital to successful printing, as the material must be layered with enough accuracy, at a consistent and synchronised extrusion rate with the robot motion. Not meeting these needs can easily jeopardise the resulting print quality, which could significantly affect the shape and the structural integrity of a printed element. The material delivery tool (i.e. the extrusion system) replicated commercial clay extruders that exist in the market, which usually use both pneumatic and electromechanical techniques. The study then developed a new bespoke extrusion system which will be detailed later in the paper.

2.3. Extrusion system

Two types of material extrusion methods were tested in this research; 1) Screw-pump, and 2) Ram extrusion. The screw pump is a method that utilises an auger screw in order to transport and compress the material to a specific point, which in the case of 3D printing is the nozzle. Upon

rotation, the screw acts as a type of rotational positive displacement pump, transporting material in the axial direction of the screw (Fig. 3). Auger extrusion systems may be vertically or horizontally oriented. The screw sits within a material hopper, which is filled with material to be extruded. The rotating screw then pulls the material through the system. This method is used by the WASP Company in their Delta 3MT and 12MT printers, which they used to experiment with 3D printing of earth-based materials (Fig. 4) [32].

In ram extruders, a linear force is applied on a piston inside a cylinder ram filled with the material. The generated pressure then forces the material through the nozzle once a threshold of pressure is reached. These systems are also commercially known as linear actuators. The exerted force in linear actuators is generated by two methods (Fig. 5);

- 1) Pneumatic, using air/gas, by increasing the pressure on one side of a pneumatic cylinder, leading to linear motion and an applied force on the plunger of the extrusion device.
- 2) Electromechanical, using lead screw or screw-jack, which translates circular motion from a motor into the linear motion and force exertion required to extrude the material.

2.4. Prototyping and geometry

The prototyping process included two stages; the first stage is the calibration of the 3D printing settings, and the second stage is geometry prototyping. The calibration of settings is an important step to enhance the relationship between the robotic arm and the extrusion system. The calibration process was designed as a set of 3D printed path lines with variable layer heights and speeds. An understanding of the material behaviour is pursued through observing the relationship between the layer height, extrusion rate and nozzle dimension. The applied changes in the layer heights varied from 15 to 35 mm. These heights are chosen to represent a range of ratios in relation to the nozzle size, which has a diameter of 45 mm.

The second stage of prototyping focused on the geometry potentials and limitations. The main aim of this step is to examine several geometrical challenges that encounter the robotically assisted 3D printing of cob such as the inclined surfaces, arch based shapes and maximum height per printing period. The maximum height per printing period reflects the achieved geometry height before pausing the printing process until the printed geometry gain structural strength through the transformation process from wet to dry state [33]. Additionally, it must be acknowledged that cob can be reutilised after printing, either through the modification of a printed object (while still wet) or through trimming excess cob from already set built elements. As a result, the geometric and prototyping processes of cob 3D printing comprise an iterative quality which facilitates testing.



Fig. 4. Screw pump extruder by WASP.

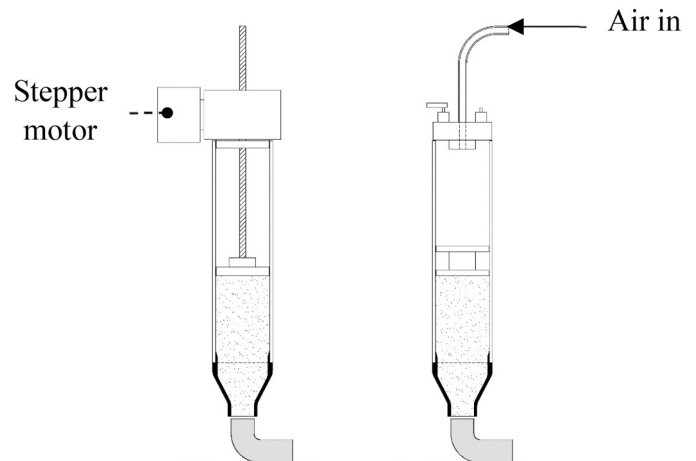


Fig. 5. Scheme of the Pneumatic (right) and electromechanical (left) ram extruders.

3. Results and discussion

3.1. Extrusion system

3.1.1. Bespoke screw pump

Inspired by the vertical screw extrusion system in the commercial Delta12MT WASP® (Fig. 4), the research team developed a screw pump based on an auger bit device. The initial concept was to create a more robot-friendly extruder, where the material feed point was stationary and the extruded material was delivered to the robot arm end-effector point through a hose. This design concept aimed to provide a higher freedom of movement for the robot, besides an improved practicality of material feeding technique as compared to the available cob and clay extrusion system in the market, which requires regular human interference with the extruder for material feeding while on the move.

The used device for this testing was a repurposed auger conveyor, originally designed to transport sand. Alterations were made in order to make it suitable for cob extrusion (Fig. 6). The initial testing of the

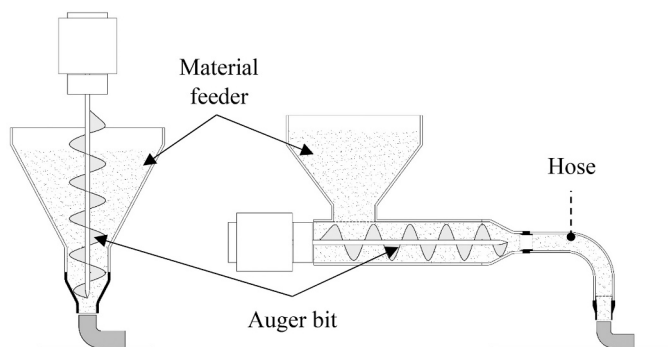


Fig. 3. Two types of the screw pump: vertical screw (left) and horizontal screw (right).



Fig. 6. The prototype of the bespoke screw pump.

device showed remarkable improvement in terms of extrusion rate, consistency and scale of the printed outcome. It was able to achieve a maximum extrusion rate of 80 mm/s with a 50 mm nozzle diameter. However, this system revealed several major shortcomings that required further stage of developments:

- The extruder jammed consistently due to the build-up of straw and rough aggregate at two points in the system; one at the interface between the auger tip and the nozzle and another at the interface between the hopper (feed point) and the auger.
- It still required constant human interaction to feed the material through the hopper.
- The whole mechanism was heavy and relatively large, which compromised the freedom of movement of the robot, and consequently limiting the complexity level of the geometry designs.
- The attempt of making the screw device stationary and install a hose at the screw end (as shown in Fig. 3- right) was unsuccessful. Installation of the hose increased both the load and the material travel distance beyond the auger direct contact surface. The increase in hose length has an inverse proportional relation with the extrusion rate, accompanied by noticeable material retraction at the feeding point.

3.1.2. Pneumatic

The experimentation of this extrusion type was inspired by most of the industrial clay and concrete extruders, which are based on exerting linear force by using pneumatic pumps. The study used a pneumatic linear ram extruder, in which the pressure was manually controlled. The ram cylinder had a maximum capacity of 4000 ml and the used nozzle size was 30 mm Fig. 7. The system was compact enough to be mounted easily on the robot arm and enable remote control of system at the same time. Despite the acquired strength from this extruder, the use of pneumatic system for a dense material like cob revealed a series of challenges in terms of controlling the extrusion rate, quality and consistency of extrusion. Furthermore, it required consistent human interaction throughout the print process to adjust the extrusion rate, fix faults and prevent collapses.

3.1.3. Electromechanical

In order to overcome the drawbacks of the pneumatic system, the study switched again to the use of the electromechanical extrusion method in its third phase. This phase used a commercial small size screw-jack extruder provided by 3D potter® (Fig. 8). The benefit of a screw-jack is that it includes a gearbox, providing extra torque at a lower speed. The new system provided a better control over the extrusion rate and consistency due to the use of a stepper electric motor, which resulted in a higher print quality. However, this extruder by 3D potter is



Fig. 7. The pneumatic linear ram extruder.

designed to execute small-medium size prototypes of clay-based materials, as the standard maximum nozzle size was 16 mm. The system had to be modified by attaching a larger 25 mm bespoke nozzle to be more suitable for cob extrusion. Despite the dramatic increase in the printing quality, the new system suffered from a slow printing speed limited to 5 mm/s due to the increased nozzle size. This rate of 3D printing had restricted the progress of the experimentation, while it also restricted the scale of the printed outcome which may represent actual wall in a building. Furthermore, the capacity of the material container was too small (3000 ml) for a large print to be made without refilling, and the process of refilling the device was slow as it required almost a partial

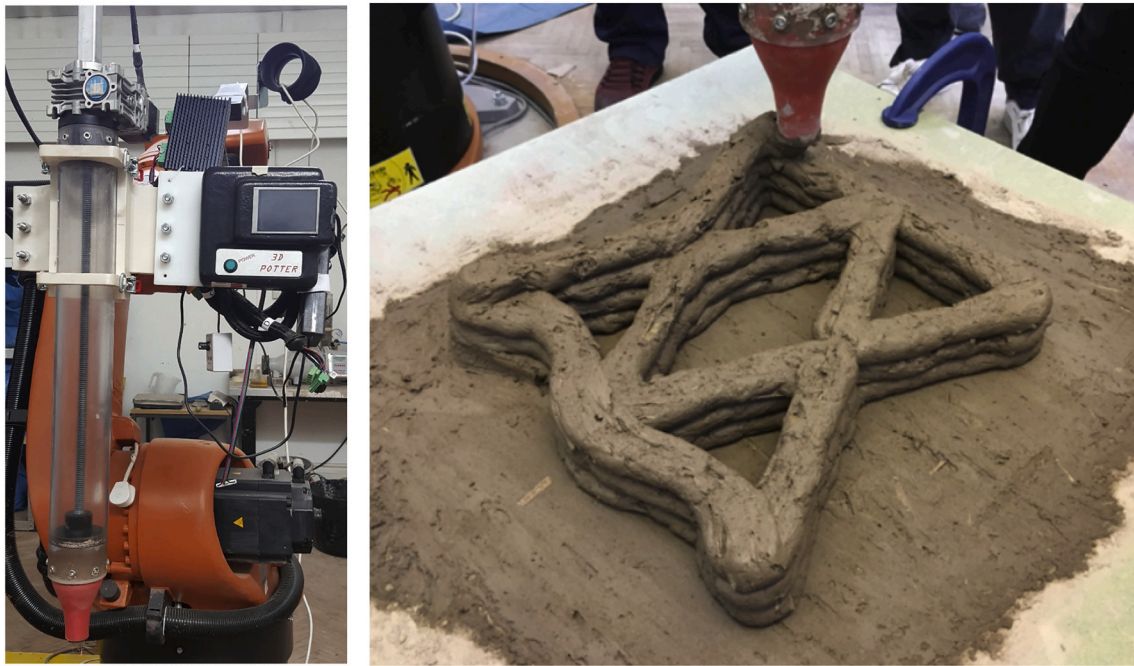


Fig. 8. The electromechanical linear ram extruder and its 3D printed outcome.

disassembly of the whole extruder (Veliz [15]).

3.1.4. Bespoke electromechanical dual ram extruder

All the previous experimentations of different extrusion methods have led to the development of a completely new extrusion method that can accelerate the creation of prototypes, leading to an increased productivity and greater research potentials. The previous three experimentations have exposed five critical challenges that face robotically assisted 3D printing of cob:

- 1) Continuity of printing process.
- 2) Maximum extrusion rate.
- 3) Consistency and quality of outcome.
- 4) The freedom of movement.
- 5) Reduction of human interaction (remote control).

Each tested extrusion system exhibited a number of advantages and limitations. Table 1 summarises the efficiency level of each tested extrusion system based on the five previous criteria. The efficiency levels are expressed as Low, Medium and High, where low refers to limitations and high refers to advantages.

These criteria are crucial challenges to improve the workability and productivity of 3D printed cob research and practice. The successful encounter of these issues will open the window for more sophisticated explorations on both the 3DP cob mix properties and the geometry design aspects. Out of all the previous three introduced extruding systems, the electromechanical linear ram has shown promising potentials in overcoming the five challenges. However, it suffered mainly from the slow extrusion speed and the lengthy process of material reloading. Therefore, it has become important to build a new -off the shelf-extrusion system, inspired by the core concept of electromechanical

screw jacks and capable of tackling the limitations of the previous systems.

The design process of the new system went through different iterations of trials and failures before reaching the final design. The initial concept started with the aim of building a simple upscaled version of the existing electromechanical screw jacks, shifting it from a single 2000 ml cartridge to a single 8000 ml, while adding a quick release system to accelerate the refill process. However, while this partially solved the issue of material quantity, it did not solve the continuity issue as the system still required to be on hold while the cartridges were being replaced. To solve this problem, an auxiliary cartridge was added in order to cover the hold time for the main cartridge to be replaced, but with the two cartridges working sequentially. The concept was inspired by small scale PLA and ceramic dual extruder by Leu et al. [34] and 3D-WASP [32]. The first trials were proofs of concept, where preliminary prototypes of the system were made in 1:4 scale using 3D printed plastic parts. These trials used the standard 2000 ml cartridges from the existing

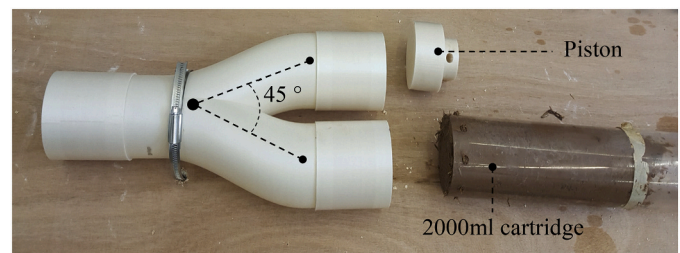


Fig. 9. Initial proof of concept of the system in 1:4 scale using the 45 degrees dual joint.

Table 1
Efficiency level of the tested criterions of each extrusion systems.

	Continuity	Extrusion rate	Consistency	Movement freedom	Human interaction
Screw pump	Medium	High	Medium	Low	Low
Pneumatic	Low	Medium	Low	Medium	Medium
Electromechanical	Low	Low	High	Medium	Medium

3D potter electromechanical screw jack (Fig. 9). The dual joint tested two different angles (45° and 22.5°) to ensure a smooth merge of the material between the two channels. The lower angle (22.5°) showed a smoother merge, hence it was selected to be applied in the full-scale prototype.

The full-scale prototype initially used 3D printed plastic joints and fixtures. The whole system was then fixed on a mobile plywood platform (Fig. 10). The first set of tests of the prototype showed success in terms of proving the workability of dual extrusion concept, yet it revealed two critical flaws which affected the extrusion process. The plastic parts were receiving a huge amount of pressure externally from the screw jacks and internally from the material flow, which eventually led to a quick wear and destruction of the parts at the mounting points (Fig. 11-left). In addition, the accumulating pressure along the axis between the screw jack mounting point and the dual joint mounting point made the plywood platform buckle from the middle. This buckling forced the cartridge to bend, leading to a material leakage then eventually a massive crack in the plastic cartridge (Fig. 11-right and Fig. 12). Therefore, to avoid these flaws in the final prototype, it was obvious that the system components must be fabricated from stronger materials such as aluminium, whereas the platform must be reinforced with a metal structure to prevent bending. The extrusion system can then be mobile by mounting the whole platform on a mobile table.

The final system prototype introduces a bespoke extrusion system with a unique dual-cartridge design (Fig. 13, Fig. 14). Each cartridge has a capacity of 8000 ml (total of 16,000 ml both) and powered by a heavy-duty electric screw jack. The screw jacks are supplied by ZIMM® with 25

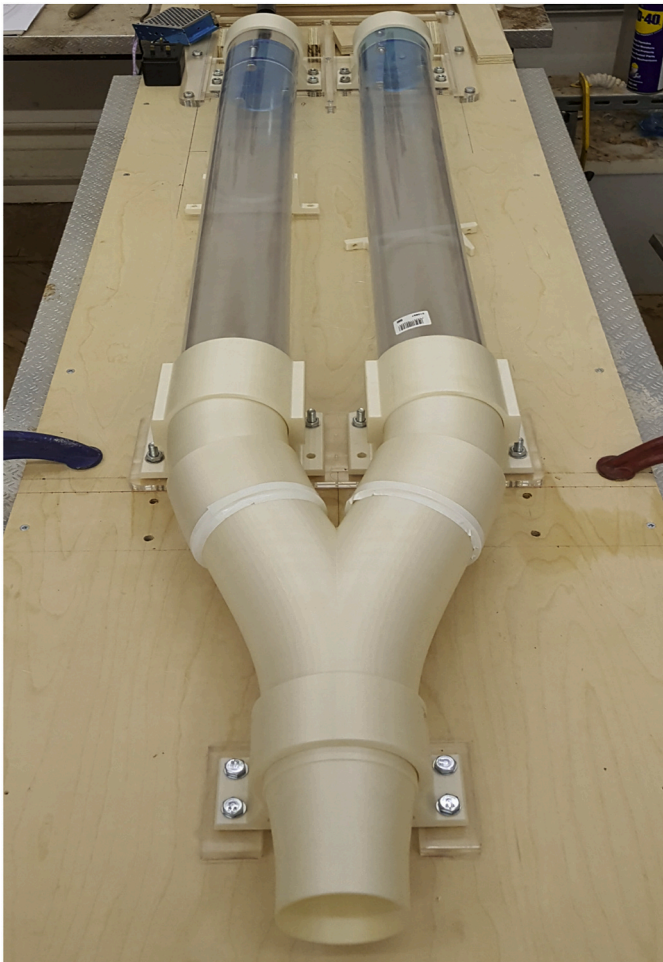


Fig. 10. The initial full-scale prototype using 3DP PLA joints and fixtures on a plywood platform.

kN nominal capacity, leveraging a 1000 mm stroke and capable of delivering 80 mm/s operating travel speed. The screw jacks are powered by two 3-phase motors, 0.75 kW each. The motors combine electromagnetic braking system that ensures immediate stop to the stroke, which minimises the dynamic response. These specs were specially requested based on calculations of the expected loads in the system, considering factors such as the material weight inside the system and the desired extrusion rate. As budget was limited, some adjustment to the system design were applied to simplify the manufactured parts and reduce the cost without affecting the targeted efficiency. Fig. 13 shows a scheme of the bespoke dual extruder different components.

Material cartridges and screw jacks are connected together by bespoke aluminium parts, which are designed to provide smooth and fast reloading process. The most distinctive aluminium part is the Y-shaped joint that merges the material dual flow from both cartridges into a single flow then feed it to a hose. The used hose is 3-m-long, made from PVC with a steel-wire reinforcement. The complete system is mounted on a mobile platform, allowing transitions around the robotic arm.

The new system was tested extensively through sequence of calibrations and prototyping process, which took place as part of an experiential studio on 3D printing of cob at the Welsh School of Architecture in Cardiff University. The system proved to be successful in overcoming the five previous challenges as follows:

1- Continuity of printing process:

The new system adopts a sequential process of extrusion based on dual lines of cartridges. This process can be described in 6 steps as shown in Fig. 15:

Step 1: The process preparation starts by loading two filled cob cartridges on the platform. Each cartridge, with its attached screw jack, form a line of extrusion. Few other cartridges are filled with the required amount of cob for the whole print and kept in a rack, ready to be loaded on the system later.

Step 2: The printing process starts by pumping cob through one cartridge at a time using one screw jack (line 1), simultaneously with initiating the robotic arm motion to exert the required design.

Step 3: As the operating screw jack on line 1 reaches its stroke end, it stops and immediately triggers the second screw jack to start pumping cob through the second cartridge on line 2 while the first screw jack is retracting. After the complete retraction of the first screw jack, the empty cartridge is removed and a full cartridge is reloaded.

Step 4: By the time the first cartridge is reloaded, the operating cartridge will be reaching its end of stroke, which then releases the stopping brakes and triggers the first screw jack to start pumping cob through the first cartridge while the second screw jack is retracting.

Step 5: After the complete retraction of the second screw jack, the empty cartridge is removed and a full cartridge is reloaded on line 2.

Step 6: The process then repeats sequentially until the end of the required 3D printed outcome.

It is recommended to estimate the whole required amount of material before the printing process, then preparing either the exact number of cartridges (for small tasks) or just a few extra cartridges and store them in a rack. This will create a buffer margin between the process of refilling and reloading, which will ensure continuity of the process and constant flow of cob throughout the whole process, with no need to interfere, stop or slow it down. The special design of the aluminium parts also enhances the continuity of the process as they combine rails with latching mechanism, offering smooth reloading of cartridges on the platform.

2- Maximum extrusion rate:

The upgraded screw jacks can deliver up to 80 mm/s operating travel speed. Using this travel speed with a 45 mm diameter nozzle elevates the extrusion rate of cob on the nozzle to 120 mm/s, which is nearly 20 times faster than the previous small linear ram extruder



Fig. 11. Destruction of the 3DP PLA joints due to pressures caused by the cob mix (left) and the destruction of the cartridge due to pressures caused by the bending plywood platform (right).

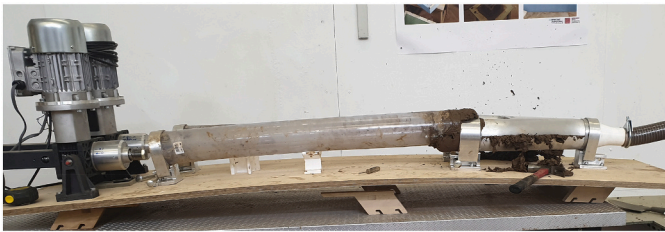


Fig. 12. Buckling of the plywood platform due to accumulated pressures on multiple points.

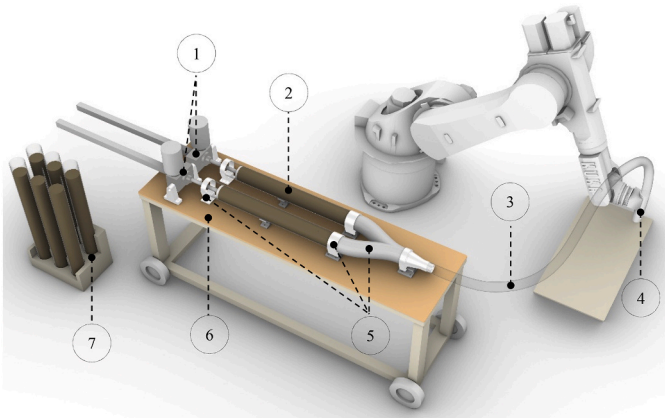


Fig. 13. Scheme of the new bespoke dual extruder components: 1) Screw jack, 2) Cob Cartridge, 3) Steel-wired PVC hose, 4) Nozzle, 5) Aluminium parts, 6) Mobile platform, 7) Cartridges Rack.

with 30 mm nozzle. However, based on calibration tests, it was found that 50 to 80 mm/s extrusion rate is sufficient for most of the geometry testing in this project. Moderate speeds offer a relaxed reloading process and gives time to extruded layer of cob to strengthen slightly before receiving the subsequent layers.

3- Consistency and quality of outcome:

The new screw jack by ZIMM leverages a 25KN ball screw gearbox and 3-phase motor controlled by variant frequency driver (VFD). This enables a steady operational torque and an accurate control over travel speed, which provides a consistent flow of cob. This consistent flow dramatically improves the quality of the printed outcome as compared to the previous extruders.

4- Freedom of movement

The new system uses a hose to link between the main body of the extruder on the platform and the nozzle point. This minimises the mounted mass/ load on the robot's end-effector, as now it only carries the nozzle joint with the hose instead of carrying the whole extruder as in the previous pneumatic and small electromechanical linear ram extruders. Minimising the contact size between extruder and robot enables more degrees of freedom for the robot to move, resulting on broader complexity levels in the geometry design if needed. Moreover, the platform itself is mobile and can be easily moved around the robot if required to compensate the possible limitation in the hose length.

5- Reduction of human interaction (remote control)

The new system is designed to separate between the material feeding point on the platform and the extrusion point on the robot's end-effector. This separation enables the reloading of the cartridges without the need to interrupt (stopping or slowing down) the robot movement. The cartridges system and the simple latching mechanism of aluminium parts also minimise the time required for reloading and reduce human interaction time consequently.

3.1.5. Remarks on the dual extrusion system

Besides the five previous advantages, the simple, yet innovative, design of the new extrusion system made it replicable and also affordable to build as compared to the available commercial options. Moreover, the design enables the system to operate either as a single or dual extruder with different nozzle sizes. This facilitates the 3D printing process for small and medium size prototypes without the need to operate the full system. In addition, the new system has potential for successful implementation into full autonomous large-scale 3D printing process. The study suggests leveraging two on-site 3D printing concepts for that purpose; first one is inspired by mobile crane 3DP system by ContourCrafting [35] Fig. 16-left, where the robotic arm and the extrusion system can be combined in the crane system. The second is inspired by the mobile robotic vehicles which is presented in a study by Zhang et al. [36] Fig. 16- right. A revised design for mobile robot vehicle that can combine both the extruder and the collaborative robotic station is suggested as in Fig. 17.

It is however important to state that the system is an initial prototype that also requires some enhancements and future upgrades. The current design still depends on human interaction to initiate and terminate the 3D printing process, in addition to preparing the cob mixtures, refilling and reloading the cartridges on the platform. It is also very important to follow good practice while filling the cartridges to avoid air pockets and inconsistency, which causes high dynamic response. Also, the current material capacity is limited to 12.0 kg/cartridge, which forces large number of refills to print a real scale wall. For example, $1 \times 1 \times 0.5$ m cob wall would require nearly 45 cartridges. Another current limitation

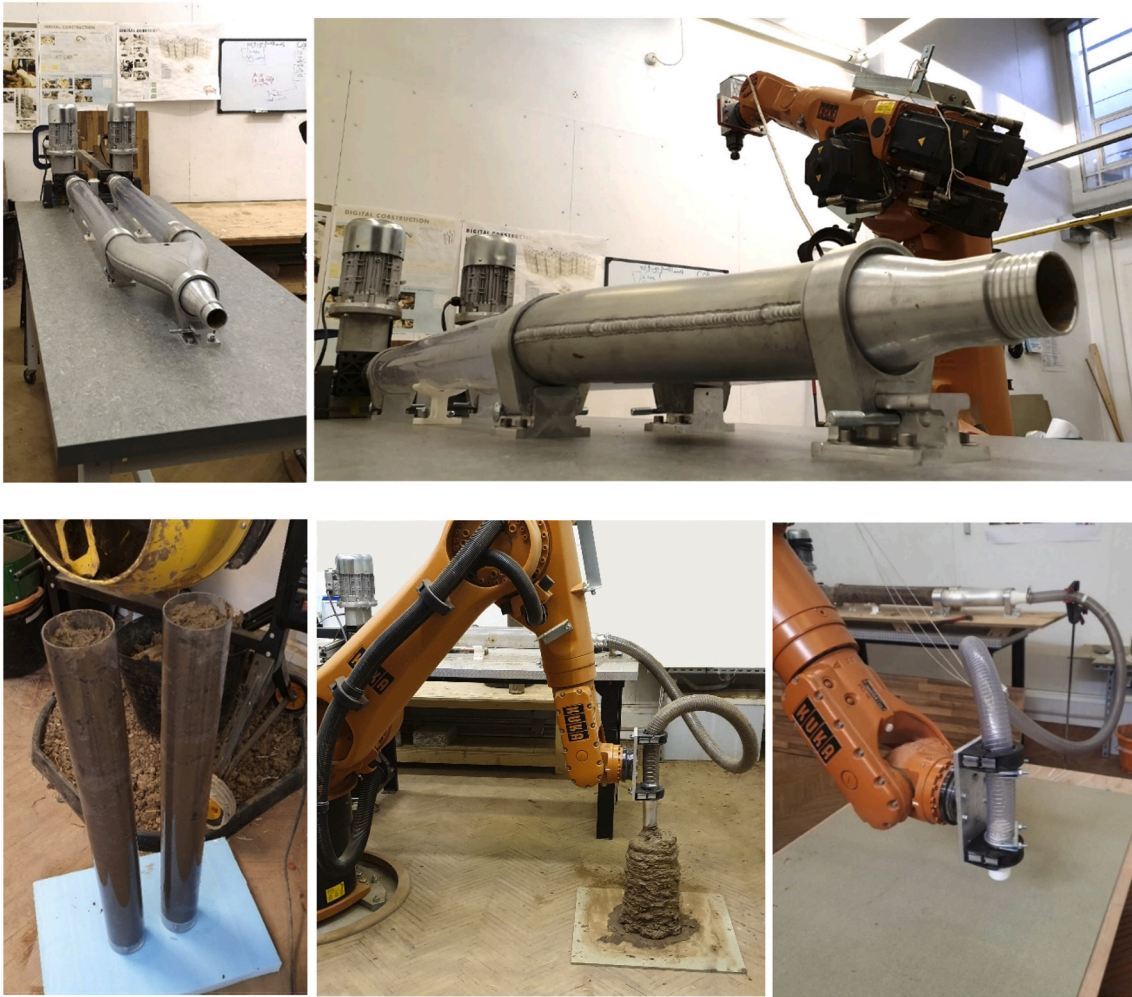


Fig. 14. The components of the bespoke dual extruder.

is associated with the hose length. Increasing the hose length over 3 m was found to be harder to mount on the robot and creates higher resistance towards moving and bending. Longer hose is also harder to be cleaned from cob leftovers after each printing process. Therefore, several planned upgrades will involve:

- Connecting the VFDs (controllers) of the screw jacks directly to the Robot controller unit, where the extruder will be operated simultaneously with the robot using the same code file.
- Increasing the material capacity of the system through upgrading the screw jack power and the cartridges volume. Moreover, the current dual-piston design could be redesigned to combine four pistons, capable of accommodating four cartridges at a time.
- The introduction of a collaborative robotic process, where a smaller robot arm will be part of the extruder platform to execute the cartridge reloading task. The required amount of material will be calculated ahead of the process, then translated into a number of cartridges. Another machine will be dedicated for mixing and refilling the empty cartridges while the prefilled cartridges are being used in the extruder.
- Implementing a shutter mechanism over the main dual Al connections can add extra layer of controllability as it will prevent any possible backflow of material during the cartridge reloading process. The current system design, however, does not suffer from material backflow due to the acute angle (45 degrees) of the dual Al piece and the relatively high viscous nature of the cob mix.

3.2. Material mix properties

The increased water content to 25% in the new 3DP cob composite, instead of 20% for conventional cob composite, has shown satisfactory extrusion in terms of consistency and quality of extrusion. It was naturally anticipated that the increase in fluidity has proportional relation to the rheology of the cob mix during and after the extrusion process. First set of tests explored the synchronization process between extrusion rate and robot motion speed. It was clear from the start that the extrusion rate must be synchronised with the motion speed of the robotic arm on a 1:1 rate at least. Slower rate of extrusion will result in an intermittent printed outcome as can be seen in Fig. 18-left. On the contrary, increasing the extrusion rate in relation to the robot motion speed (using a constant layer height) will result in a more consistent print and wider path lines. In Fig. 18-right, the path lines A and B reflect a ratio of 1.15:1, while path lines C and D reflect a ratio of 1.05:1. The increased ratio of extrusion rate to motion speed results in wider path lines under a constant layer height. Table 2 below describe the relationship between extrusion rate and robot arm motion speed.

The study concluded after several trials that 3D printing with a liner extrusion rate of 105–110% of the robot motion speed (1.1:1) considered favourable due to the nature of the cob mix, where there are chances of having inconsistent sections of materials inside the cartridges that cause slight interruptions in the extrusion rate from time to time. It is possible to overcome this issue by installing an extrusion rate sensor at the nozzle end that can give live feedback to the variant frequency driver (VFD) of the actuator to make the proper adjustments to power. Worth

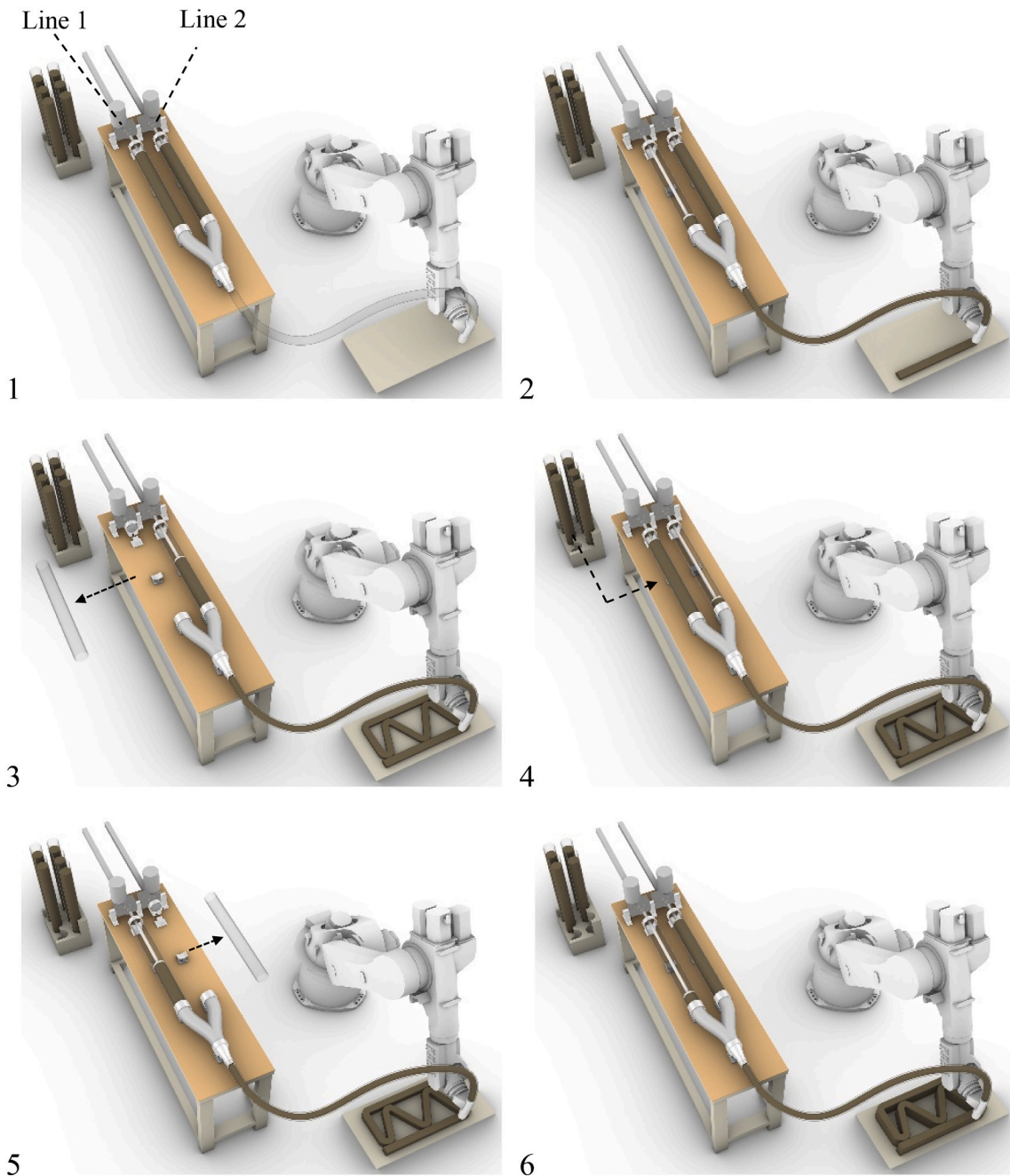


Fig. 15. The six steps of the extrusion process in the bespoke dual extruder.

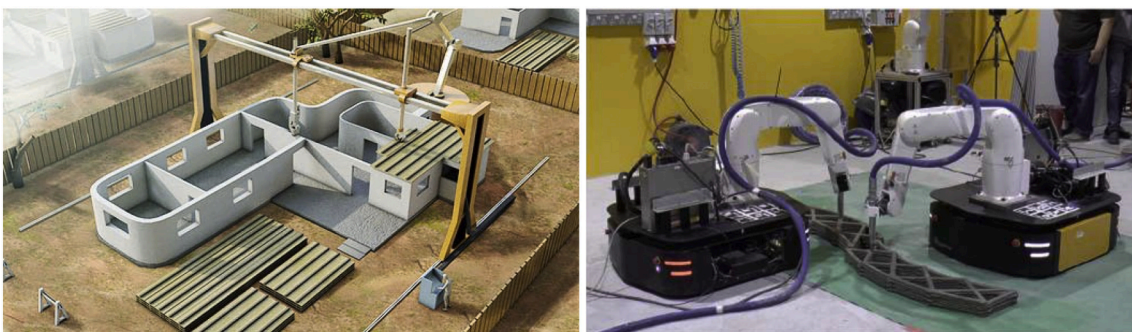


Fig. 16. Mobile crane system for 3DP by Contour crafting (left), mobile robotic vehicles by Zhang et al. [36] (Right).

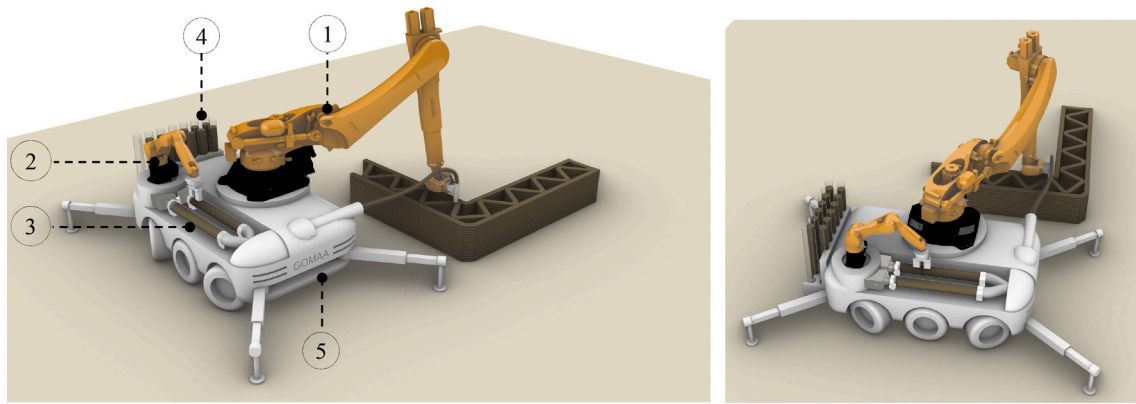


Fig. 17. Design of mobile robot vehicle combining both the cob extruder and the collaborative robotic station. 1)Primary robot for printing. 2) Secondary robot for cartridges reloading. 3) Cob extruder. 4) Cartridges rack. 5) Autonomous robotic vehicle.



Fig. 18. Explorations of the synchronization process between extrusion rate and robot motion speed (left & right).

Table 2
Relationship between extrusion rate and robot arm motion speed.

Path line code	A-B	C-D	Unit
Nozzle diameter (D)	45	45	mm
Layer height (h)	15	15	mm
Extrusion rate	92	85	mm/s
Robot motion speed	80	80	mm/s
Path width (w)	88	70	mm
Extrusion rate to motion speed ratio	115	105	%

mentioning that the study also observed that the slightly higher extrusion rate has a “ramming effect” on the printed outcome, where the printed path lines becomes denser and gain more structural strength with each new printed layer.

The second set of tests on the relationship between the layer height, nozzle size and path line width has improved the understanding of their influence on the 3D printed outcome and printing process in general. As can be seen in Fig. 19, each printed path line (A to E) is designed to reflect the relation between a specific layer height and its respective path width, where the extrusion rate to robot motion speed ratio is set to 110% as advised previously, and the nozzle size is fixed at 45 mm. The layer heights started with 15 mm at path line A, then the heights were increased discretely with 5 mm increment per each path line, ending with 35 mm layer height at path line E. Each increase in the layer height exhibited a decrease in the path line width. These relationships between the change in layer heights and path line width has been recorded and described as the expansion factor in Table 3. This test eventually resulted in a model that can estimate the path line width in accordance



Fig. 19. Exploring the relationship between layer height and nozzle size.



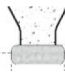
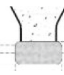
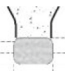
to the layer height and the nozzle size (Fig. 20).

The linear relationship presented in Fig. 20 can be described using the following equation:

$$\text{Estimated path line width (mm)} = \text{Nozzle size (mm)} \times \text{Expansion factor}$$

where the expansion factor can be obtained from the chart. To explain further; for example; under a synchronised motion speed and linear extrusion rate, with a 45 mm in diameter extrusion nozzle and 25 mm

Table 3
Description of the testing on the relationship between layer height, nozzle size and path line width.

Path line code	A	B	C	D	E	Unit
Scheme of path line cross section						--
Nozzle diameter (D)	45	45	45	45	45	mm
Layer height (h)	15	20	25	30	35	mm
Path width (w)	88	79	70	62	52	mm
Layer height to nozzle D ratio	33	44	56	67	78	%
Path width multiplication factor	1.96	1.76	1.56	1.36	1.16	--

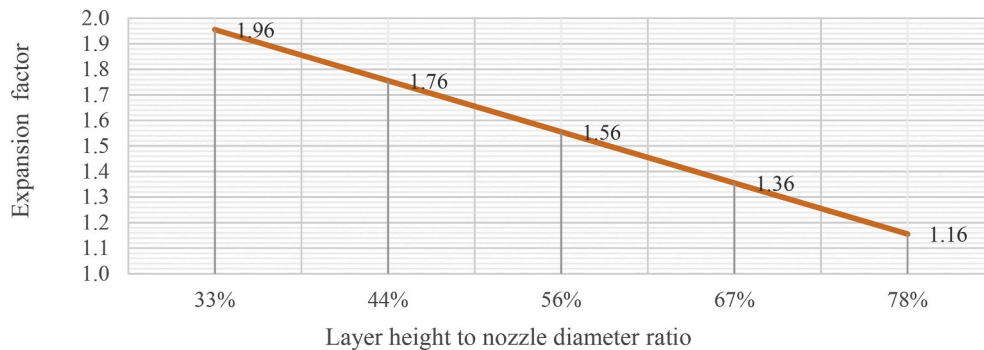


Fig. 20. Path line width estimation chart.

layer height (layer height is 56% of the nozzle size) and an expansion factor of 1.6:

$$\text{Estimated path line width (mm)} = 45 \times 1.6 = 70 \text{ mm}$$

The early estimation of path line's printed width has enabled the study team to implement a code in the Grasshopper definition as part of the 3D model files to estimate the printed outcome to provide informed decisions for geometry planning. For example, when planning to print a cob wall that has a thickness of 500 mm, using a layer height of 25 mm would require a distance of 430 mm between the two path lines creating the inner and outer sides of the wall. Increasing the layer height to 30 mm (while using the added definition in the 3D models) will then

automatically update the distance between the wall path lines to 448 mm.

In addition to the previous changes in path line width due to the extrusion process and the forced height by the nozzle, 3D printed cob encounters another cause of lateral deformation due to the accumulative loads of each added layer. As the 3D printing process continues, more printed layers accumulate on top of each other to create the desired height of the geometry. This increase in loads leads to further slight lateral and longitudinal deformation as compared to the original virtual model, where it is mostly seen in the bottom layers (Fig. 21, left & right). It was observed during all experiments that the level of deformation depends primarily on the water content in the cob mix, as lower water



Fig. 21. Prototypes showing the longitudinal deformation due to accumulative weight of layers (lower water content to left, higher water content to the right).

content minimises the deformation to a negligible level (Fig. 21- left), which was an early prototype with 22% water content. The higher water content of 24–25% leads to a noticeable deformation as in Fig. 21- the prototype to the right, where the gradual increase in layer heights is slightly noticeable from the bottom to the top layers. Further exploration for the deformation aspects will be tested and presented in future work.

3.3. Geometry exploration

An exploration of various geometries was conducted to examine the capabilities of the 3D printing system. The study experimented with three types of geometries. The criteria of geometry selection were established on exploring the geometrical challenges that face the robotic 3D printing of a simple cob wall with an opening. Fig. 22 suggests a traditional cob wall with arch-shaped opening to represent possible challenges while 3D printing cob walls, without using form work to create the openings. The challenges were found to be as follow:

- A. Lift height (Max. height of continuous 3D printing)
- B. Inclined 3-axis 3D printing (horizontal corbelling)
- C. Inclined 6-axis 3D printing (radial corbelling)

3.3.1. Lift height

Cob walls are conventionally built of successive monolithic layers of earth called lifts. Each lift must be dry enough to a degree that enables it to bear the loads from the subsequent lifts. Lift height has an average of 60 cm. [4,27,37]. Hence, the first geometry exploration aimed to examine the maximum height per lift (Fig. 23). The geometry footprint was designed to have a rectangular footprint of 60×40 cm, with a serpentine printing path line that creates the inner pattern of the wall. A serpentine path line was selected for two reasons; first is to improve the structural performance of the wall [38]; second is to extend the printing time per each path line as this should give more time for each layer to start drying and gain rigidity before receiving the successive layers.

This test showed that the maximum stable height of the lift was 58 cm, very similar to the traditional cob method. Exceeding this height increasingly jeopardised the stability of the geometry and it starts showing toppling signs. This finding is also supported by the prototypes by WASP [33]. This finding highlighted the importance of pausing or reducing the 3D printing speed to give a chance to the freshly printed layers to settle properly and gain more structural strength throughout the drying process.

3.3.2. Inclined 3-axis 3D printing (horizontal corbelling)

The Second geometry exploration aimed to examine inclined 3-axis

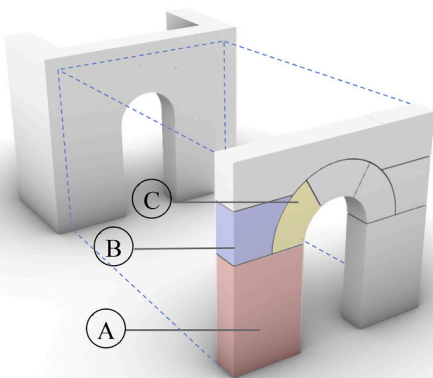


Fig. 22. Geometry challenges in a regular cob wall with an opening. 1) Lift height- 3 axis 3D printing; 2) Inclined 3-axis printing (corbelling); 3) Inclined 6-axis 3D printing.



Fig. 23. Testing the maximum height per printing period.

3D printing, where the corbelling happens in the horizontal XY plane only. The study examined two main approaches, straight and gradual inclination (Fig. 24, left-right). Based on several trials, it was found that cob can sustain up to 40 degrees of straight inclination with 1:1.25 slope as shown in Fig. 24-left. This was possible to achieve without using inner patterns but with slow printing speed of 30 mm/s. Based on several trials, it was observed that high inclinations (more than 40 degrees) are less stable and require denser design for inner patterns. On the other hand, using gradual inclination required the addition of inner patterns to the geometry, but it showed a possibility to achieve nearly 90 degrees of inclination as shown in Fig. 24- left. However, the increase of the inner pattern, in addition to the serpentine path line, caused a dramatic consumption of material per unit volume.

3.3.3. Inclined 6-axis 3D printing (radial corbelling)

The third exploration aimed to exercise a more complex style of movement that involved all the six axes of the robotic arm. Such added complexity can be leveraged to construct arch-based shapes, like catenary vaults and arches Fig. 22-C. The test was able to achieve 45 degrees of radial inclination in a one continuous print (Fig. 25). It was possible to continue achieving higher degree of inclination, however, the geometry started to show instability due to its relatively small footprint (40×40 cm). It is worth mentioning that 75 degrees of inclination were successfully achieved in a previous study under this project using the small scale nozzle and less water content (Veliz [15]). During the printing process of the arch prototype, the study observed that the 3D printed cob can gain structural strength from the ramming process, which is created by the extrusion forces and robotic arm compression. Also, similar to the previous two tests, it was necessary to add an inner pattern to geometry to increase the structural rigidity and the printing time per layer.

3.3.4. Remarks on geometry testing

Generally, the previous prototypes generated a record that has become useful to the planning of the future work on 3DP cob. Table 4 shows the different characteristics for each 3DP geometry. In addition, the testing process have revealed other factors which influence the

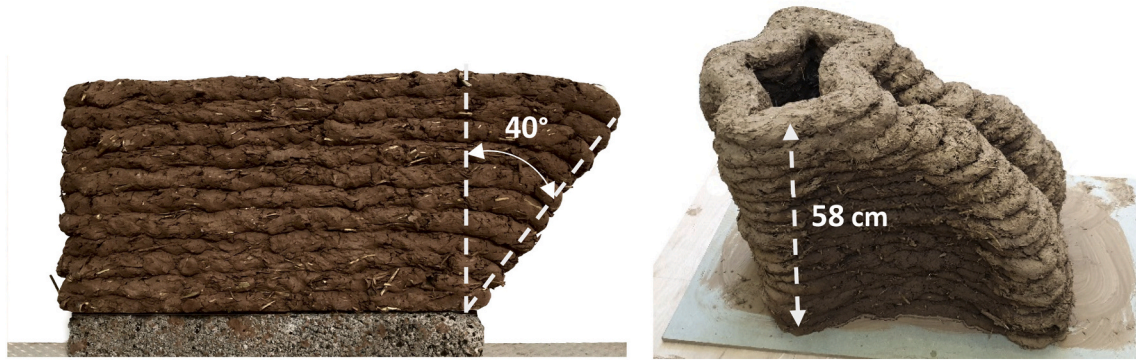


Fig. 24. Examining the inclined 3-axis 3D printing; straight inclination (left) and gradual inclination (right).



Fig. 25. Testing complex movement through 3D printing arch-based geometry.

Table 4
The different characteristics for each 3DP geometry in the three tests.

	Test 1	Test 2	Test 3	Unit
Printing speed	50	50	50	mm/s
Volume of printed cob	0.11	0.1	0.08	m ³
Weight of printed cob	198	182	132	kg
Number of used cartridges	16	15	11	
Total printing time	30	27	20	min
Extrusion rate	6.7	6.7	6.7	Kg/min

geometry formation and its achieved quality. These factors are as follow:

- The overall footprint of the printed geometry: As longer foot prints, such as the external walls of a small house for instance, means more time is spent in each layer, which consequently enables the fresh 3D printed layers of cob to gain further strength as they dry. The footprint of the geometries (e.g. Walls), can be also increased by designing denser inner patterns inside the walls, which increase the stability of the printed structure, and also improve the thermal performance [10].
- Layer height to path line ratio: As discussed earlier in Section 3.2, lower layer height creates wider path line. The increased footprint of path line offers greater stability to the geometry. However, reducing the layer height means additional material is consumed due to the increased number of required layers to reach the desired total height of the geometry. This also will increase the overall printing time.

- The relation between printing velocity and hardening time: where this study did not test systematically the competition between printing velocity and material hardening, the study observed that shorter printing paths per layer jeopardise the ability of each printed layer to harden sufficiently in order to sustain the loads of the successive layers. For instance, in geometry 2, the small squared footprint created shorter printing path per layer, which consequently required slower printing velocity, while in geometry 1, the larger rectangular footprint enabled higher printing velocity. However, this issue can be compensated by reducing the printing velocity or design the printing process to follow longer paths. This explains why the extrusion rates as per Table 4 were all maintained at 6.7 kg/ min while testing the current geometries despite the ability of system to reach a flow rate of up to 11 kg/min. Worth mentioning that replacing the empty cartridge manually takes nearly 30 s, which is less than the time needed to extrude the other full cartridge This means that the extrusion does not stop at any moment during the total printing process.

4. Conclusion

This paper presents a systematic study leveraging a traditional material and its associated embodied knowledge as a driver for digital innovation, specifically to develop a low-cost and sustainable alternative robotic 3D printing process and hardware (an extrusion system). The construction industry has done substantial strides in the 3DP area since the development of large-scale digital fabrication technologies (e.g.

contour crafting). Several case studies and prototypes greatly illustrate the potentials of these technologies beyond standard procurement and standard building delivery models by integrating new knowledge into the building delivery from areas such as manufacturing and robotics. In that context, this article advocates that historical, traditional or vernacular material systems are a rich source of knowledge for further research and innovation in the built environment sector, and provides a groundwork of material resourcing, building knowledge and local skills with the potential for more sustainable construction data-driven processes. The impact of this study can be outlined in three key areas:

- 1) The development of an innovative extrusion system for earth-based materials.
- 2) The development of a robotic 3DP system that provides the opportunity to prototype new models of earth materials in the context of industrial frameworks of practice;
- 3) The leverage of vernacular material knowledge and skills to develop new technology in the digital sector.

The system presented here involves material studies and printing characterisation parameters as well as its associated hardware (an extrusion mechanism), and its implementation on small scale tests. The development of this system involved building a series of prototypes through a standard innovation delivery process, from basic ideation and research, up to proof of concept and prototyping stages. Building upon standard liquid deposition modelling 3DP 3-axis strategies, this system allows for more complex geometric configurations with more than 3 axis, and in contrast to traditional cob building processes, it allows for cob building elements to be produced on the basis of a filament (forming a hollow geometry) instead of bulk mass-based components, leading to higher geometrical flexibility, reduced material use and better thermal efficiency as a result of air cavities.

This paper also contributes to architectural design research, as it acknowledges the material cultural context as a springboard for digital and technological innovation delivery. This multi-disciplinary approach reflects on the applicability of this technology in professional practice. This project poses the concept of “material negotiation” to enable more flexible, open ended and multi-disciplinary relationships between design and fabrication by using a recyclable and reusable material prone to on-site modifications and adaptation. For instance, the dual extrusion system allows for a decentralised production model by pre-packaging and procuring cob cartridges from local suppliers and materials, reducing even further the construction’s carbon footprint and involving knowledgeable local suppliers in the delivery plan.

The research suggests, however, further work to develop this system into an industrial demo (and, even further, into a commercially viable system). Broadly, the research sets out a more ambitious agenda addressing the need to acknowledge and further investigate the potential of vernacular knowledge and buildings to facilitate material and digital manufacturing studies. For instance, further work can explore the applicability of machine learning, material feedback and computer vision approach for the robotic fabrication of building elements, as well as the observation of craft and making practices as a way to develop more intelligent and responsive manufacturing systems. Specifically to this study, the extrusion system would benefit from a higher degree of automation by developing a feeding system where cartridges are loaded and unloaded into the extrusion mechanism, ready to deliver material for 3D printing and where empty tubes can be collected and re-filled. A simple computation of printing speed, volume, and daily schedule can inform the size of buffer needed for pre-filled tubes and the required rate of exchange and delivery, which will greatly improve the degree of automation of the system enabling larger continuous prints. Also, in terms of local markets and the need to refurbish and repair existing cob structures, we envisage this technology as a useful alternative for cob building maintenance (e.g. crack filling, construction of pre-dried cob blocks), in alignment with recent strides on the use of robotic technology

and intelligent computer vision for building maintenance applications, such as autonomous crack detection.

Funding sources

This work was supported financially by the Engineering and Physical Sciences Research Council (EPSRC) and The University of Nottingham under the Network Plus: Industrial Systems in the Digital Age, Grant number: EP/P001246/1.

This work is also partially supported financially by the University of Adelaide through the Research Abroad Scholarship scheme.

Declaration of Competing Interest

The authors declare that they have no known competing financial interests or personal relationships that could have appeared to influence the work reported in this paper.

Acknowledgements

We would like to acknowledge Jack Francis and Dr. Peter Theobald for their valuable collaboration and support (Cardiff University). We also extend our gratitude to Aikaterini Chatzivasileiadi and Anas Lila (Cardiff University) for their invaluable help. Special thanks also must be made to EMAR Engineering Services in Egypt for their technical support.

References

- [1] Yi Wei Daniel Tay, Biranchi Panda, Suvash Chandra Paul, Nisar Ahamed Noor Mohamed, Ming Jen Tan, Kah Fai Leong, 3D printing trends in building and construction industry: a review, *Virtual Phys. Prototyp.* 12 (3) (2017) 261–276, <https://doi.org/10.1080/17452759.2017.1326724>.
- [2] Peng Wu, Jun Wang, Xiangyu Wang, A critical review of the use of 3-D printing in the construction industry, *Autom. Constr.* 68 (2016) 21–31, <https://doi.org/10.1016/j.autcon.2016.04.005>.
- [3] Ivo Kothman, Niels Faber, How 3D printing technology changes the rules of the game insights from the construction sector, *J. Manuf. Technol. Manag.* 27 (7) (2016) 932–943, <https://doi.org/10.1108/JMTM-01-2016-0010>.
- [4] Erwan Hamard, Bogdan Cazaciu, Andry Razakamanantsoa, Jean Claude Morel, Cob, a vernacular earth construction process in the context of modern sustainable building, *Build. Environ.* 106 (1) (2016) 103–119, <https://doi.org/10.1016/j.buildenv.2016.06.009>.
- [5] Veliz Reyes, Alejandro, Wassim Jabi, Mohamed Goma, Aikaterini Chatzivasileiadi, Lina Ahmad, Nicholas Mario Wardhana, Negotiated matter: a robotic exploration of craft-driven innovation, *Archit. Sci. Rev.* 0 (0) (2019) 1–11, <https://doi.org/10.1080/00038628.2019.1651688>.
- [6] Joseph F. Kennedy, Michael G. Smith, Catherine Wanek, in: C. Wanek, M. Smith, J. F. Kennedy (Eds.), *The Art of Natural Building*, New Society Publishers, Vancouver, Canada, 2015 (ISBN: 0865714339).
- [7] Steven Goodhew, Richard Griffiths, Sustainable Earth walls to meet the building regulations, *Energy Build.* 37 (2005) (2005) 451–459. Elsevier, <https://doi.org/10.1016/j.enbuild.2004.08.005>.
- [8] A. Benardos, I. Athanasiadis, N. Katsoulakos, Modern earth sheltered constructions: a paradigm of green engineering, *Tunn. Undergr. Space Technol.* 41 (1) (2014) 46–52, <https://doi.org/10.1016/j.tust.2013.11.008>.
- [9] Hashem Alhumayani, Mohamed Goma, Veronica Soebarto, Wassim Jabi, Environmental assessment of large-scale 3D printing in construction: a comparative study between cob and concrete, *J. Clean. Prod.* 270 (June) (2020) 122463–122488, <https://doi.org/10.1016/j.jclepro.2020.122463>.
- [10] Mohamed Goma, Jim Carfrae, Steve Goodhew, Wassim Jabi, Alejandro Veliz Reyez, Thermal performance exploration of 3D printed cob, *Architect. Sci. Rev.* (April) (2019) 1–8, <https://doi.org/10.1080/00038628.2019.1606776>.
- [11] Isolda Agustí-Juan, Florian Müller, Norman Hack, Timothy Wangler, Guillaume Habert, Potential benefits of digital fabrication for complex structures: environmental assessment of a robotically fabricated Concrete Wall, *J. Clean. Prod.* 154 (2017) 330–340, <https://doi.org/10.1016/j.jclepro.2017.04.002>.
- [12] Banning Garrett, 3D printing: new economic paradigms and strategic shifts, *Global Policy* 5 (1) (2014) 70–75, <https://doi.org/10.1111/1758-5899.12119>.
- [13] Omar Geneidy, Walaa S.E. Ismael, Ayman Abbas, A critical review for applying three-dimensional Concrete Wall printing technology in Egypt, *Archit. Sci. Rev.* 0 (0) (2019) 1–15, <https://doi.org/10.1080/00038628.2019.1596066>.
- [14] Pshtiwan Shakor, Shami Nejadi, Gavin Paul, Sardar Malek, Review of emerging additive manufacturing technologies in 3d printing of cementitious materials in the construction industry, *Front. Built Environ.* 4 (85) (2019) 1–17, <https://doi.org/10.3389/fbuil.2018.00085>.

- [15] Veliz Reyes, Alejandro, Mohamed Goma, Aikaterini Chatzivasilieadi, Wassim Jabi, Computing craft: early stage development of a robotically-supported 3D printing system for cob structures, in: Proceedings of the 34th Conference of Education in Computer Aided Architectural Design in Europe (eCAADe)-Computing for Better Tomorrow 1, Lodz: cuminCad, 2018, pp. 791–800. <https://pea.rli.plymouth.ac.uk/handle/10026.1/12769>.
- [16] T.T. Le, S.A. Austin, S. Lim, R.A. Buswell, R. Law, A.G.F. Gibb, T. Thorpe, Hardened properties of high-performance printing concrete, *Cem. Concr. Res.* 42 (3) (2012) 558–666, <https://doi.org/10.1016/j.cemconres.2011.12.003>.
- [17] A. Perrot, D. Rangeard, E. Courteille, 3D printing of earth-based materials: processing aspects, *Constr. Build. Mater.* 172 (2018) 670–676, <https://doi.org/10.1016/j.conbuildmat.2018.04.017>.
- [18] A. Perrot, D. Rangeard, A. Pierre, Structural built-up of cement-based materials used for 3D-printing extrusion techniques, *Mater. Struct.* 49 (2016) 1213–1220, <https://doi.org/10.1617/s11527-015-0571-0>.
- [19] Biranchi Panda, Ming Jen Tan, Experimental study on mix proportion and fresh properties of Fly ash based Geopolymer for 3D concrete printing, *Ceram. Int.* 44 (9) (2018) 10258–10265, <https://doi.org/10.1016/j.ceramint.2018.03.031>.
- [20] Biranchi Panda, Cise Unluer, Ming Jen Tan, Investigation of the rheology and strength of Geopolymer mixtures for extrusion-based 3D printing, *Cem. Concr. Compos.* 94 (November 2017) (2018) 307–314, <https://doi.org/10.1016/j.cemconcomp.2018.10.002>.
- [21] G.G. Lipscomb, M.M. Denn, Flow of Bingham fluids in complex geometries, *J. Non-Newtonian Fluid Mech.* 14 (C) (1984) 337–346, [https://doi.org/10.1016/0377-0257\(84\)80052-X](https://doi.org/10.1016/0377-0257(84)80052-X).
- [22] H.D. Le, E.H. Kadri, S. Aggoun, J. Vierendeels, P. Troch, G. De Schutter, Effect of lubrication layer on velocity profile of concrete in a pumping pipe, *Mater. Struct.* 48 (12) (2015) 3991–4003, <https://doi.org/10.1617/s11527-014-0458-5>.
- [23] Myoung Sung Choi, Young Jin Kim, Jin Keun Kim, Prediction of concrete pumping using various rheological models, *Int. J. Concrete Struct. Mater.* 8 (4) (2014) 269–278, <https://doi.org/10.1007/s40069-014-0084-1>.
- [24] A. Perrot, D. Rangeard, T. Lecompte, Field-oriented tests to evaluate the workability of cob and adobe, *Mater. Struct.* 51 (2) (2018) 1–10, <https://doi.org/10.1617/s11527-018-1181-4>.
- [25] Agostino Walter Bruno, Domenico Gallipoli, Céline Perlot, Joao Mendes, Mechanical behaviour of hypercompacted earth for building construction, *Mater. Struct.* 50 (2) (2017) 160–175, <https://doi.org/10.1617/s11527-017-1027-5>.
- [26] H. Khelifi, A. Perrot, T. Lecompte, G. Ausias, Design of Clay/cement mixtures for extruded building products, *Mater. Struct.* 46 (6) (2013) 999–1010, <https://doi.org/10.1617/s11527-012-9949-4>.
- [27] Adam Weismann, Katy Bryce, *Building With Cob: A Step-by-step Guide*, Green Books Ltd., Devon, 2006 (ISBN: 1903998727).
- [28] Hamed Niroumand, Juan Antonio Barceló Álvarez, Maryam Saaly, Investigation of earth building and earth architecture according to interest and involvement levels in various countries, *Renew. Sust. Energ. Rev.* 57 (2016) 1390–1397, <https://doi.org/10.1016/j.rser.2015.12.183>.
- [29] Steve Goodhew, P.C. Grindley, S.D. Probeif, Composition, effective thermal conductivity and specific heat of cob earth-walling, *WIT Trans. Built Environ.* 15 (1) (1995) 205–217, <https://doi.org/10.2495/STR950231>.
- [30] Khan Academy, What is volume flow rate?, in: Fluids Khan Academy, 2015, 2015, <https://www.khanacademy.org/science/physics/fluids/fluid-dynamics/a/what-is-volume-flow-rate> (accessed 01-09-2020).
- [31] Babak Zareian, Behrokh Khoshnevis, Interlayer adhesion and strength of structures in contour crafting - effects of aggregate size, extrusion rate, and layer thickness, *Autom. Constr.* 81 (June) (2017) 112–121, <https://doi.org/10.1016/j.autcon.2017.06.013>.
- [32] 3D-WASP, 3D Printers | WASP | Leading Company in the 3D Printing Industry, 2020, <https://www.3dwasp.com/en/>, 2020 (accessed 31-08-2020).
- [33] 3D WASP, The Clay and Straw Wall by The 3 M| Stampanti 2D | WASP, 2016, <https://www.3dwasp.com/en/il-muro-di-terra-e-paglia-alle-soglie-dei-3-metri/>, 2016 (accessed 31-08-2020).
- [34] Ming C. Leu, Lie Tang, Brad Deuser, Robert G. Landers, Gregory E. Hilmars, Shi Zhang, Jeremy Watts, Freeze-form extrusion fabrication of composite structures, in: 22nd Annual International Solid Freeform Fabrication Symposium - An Additive Manufacturing Conference, (2011, Aug. 8–10, Austin, TX), University of Texas at Austin, 2011, pp. 111–124. <https://www.researchgate.net/publication/266522915>.
- [35] ContourCrafting, Building Construction - CC-Corp, 2020, <https://contourcrafting.com/building-construction/>, 2020 (accessed 08-02-2020).
- [36] Xu Zhang, Mingyang Li, Jian Hui Lim, Yiwei Weng, Yi Wei Daniel Tay, Hung Pham, Quang Cuong Pham, Large-scale 3D printing by a team of Mobile robots, *Autom. Constr.* 95 (August) (2018) 98–106, <https://doi.org/10.1016/j.autcon.2018.08.004>.
- [37] Clarke Snell, Tim Callahan, *Building Green : A Complete how-to Guide to Alternative Building Methods : Earth Plaster, Straw Bale, Cordwood, Cob, Living Roofs*, Lark Books, 2005 (ISBN: 9781579905323).
- [38] Stephen Emmitt, Christopher A. Gorse, Barry's Introduction to Construction of Buildings, Blackwell Publishing Ltd., Cornwall, 2005 (ISBN 1-4051-1055-4).

**Appendix II: Manuscript- Feasibility of 3DP cob walls
under compression loads in low-rise construction.**

Construction and Building Materials

Feasibility of 3DP cob walls under compression loads in low-rise construction --Manuscript Draft--

Manuscript Number:	
Article Type:	Research Paper
Keywords:	Additive manufacturing; 3D printing; Vernacular architecture; Cob; Compression test; Limit state design; Structural performance optimisation
Corresponding Author:	Jaroslav Vaculik University of Adelaide Adelaide, AUSTRALIA
First Author:	Mohamed Gomaa, MSc
Order of Authors:	Mohamed Gomaa, MSc Jaroslav Vaculik, PhD Veronica Soebarto, PhD Michael Griffith, PhD Wassim Jabi, PhD
Abstract:	<p>This paper presents an investigation of the structural feasibility of 3D printed (3DP) cob to be used in low-rise buildings. Cob is a traditional earth-based building material. The investigation includes conducting a compression test on 3DP cob samples to obtain its mechanical properties. The obtained values were then used for structural analyses of three types of 3DP cob walls to evaluate their load-carrying capacity based on a Limit State (LS) design framework. Results from the analyses were implemented in modelling an idealised low-rise cob building. The study found that 3DP cob has very similar mechanical performance to conventional cob on the material scale but with less material consumption, which makes 3DP cob a more attractive construction from the point of view of resource efficiency. An important outcome of the study is a structural design framework for low-rise 3DP cob buildings, which will allow designers to optimize the design of the 3DP wall construction based on its structural performance and material efficiency.</p>
Suggested Reviewers:	<p>Charles Augarde, PhD Professor, Durham University charles.augarde@durham.ac.uk Charles's main research interest is numerical modelling of geotechnical and structural engineering problems. Charles is also interested in unsaturated soil mechanics particularly applied to sustainable earthen construction materials.</p> <p>Kevin Klinger, PhD Professor, Ball State University krklinger@bsu.edu Prof Klinger has extended experience in the engagement between material exploration and architectural forms production, especially using digitally-driven design processes.</p> <p>Arnaud Perrot, PhD Assistant Professor, Universite de Bretagne-Sud arnaud.perrot@univ-ubs.fr Dr Perrot has extended experience in the experimentation of 3D printing of earth materials, especially on the rheology and mechanical properties.</p> <p>Enrico Quagliarini, PhD Professor, Universita Politecnica delle Marche e.quagliarini@univpm.it Prof Quagliarini skills are focused on the protection, retrofitting and conservation of Historic constructions. He is oriented to investigating the behavioural design/assessment of the built environment and of building components for risk reduction.</p>

Feasibility of 3DP cob walls under compression loads in low-rise construction

Mohamed Gomaa^a, Jaroslav Vaculik^{b,c*}, Veronica Soebarto^a, Michael Griffith^{b,c}, Wassim Jabi^d

^a School of Architecture and Built Environment, Horace Lamb Building, University of Adelaide, Adelaide SA5005, Australia.

^b The School of Civil, Environmental and Mining Engineering, Engineering North Building, University of Adelaide, Adelaide SA5005, Australia.

^c Bushfire and Natural Hazards Cooperative Research Centre, Melbourne, Australia

^d The Welsh School of Architecture, Bute Building, Cardiff University, Cardiff CF10 3NB, UK.

*Corresponding Author

Postal address: The School of Civil, Environmental and Mining Engineering, Engineering North Building, University of Adelaide, Adelaide SA5005, Australia.

Phone: (+61 8 8313 5451)

Abstract

This paper presents an investigation of the structural feasibility of 3D printed (3DP) cob to be used in low-rise buildings. Cob is a traditional earth-based building material. The investigation includes conducting a compression test on 3DP cob samples to obtain its mechanical properties. The obtained values were then used for structural analyses of three types of 3DP cob walls to evaluate their load-carrying capacity based on a Limit State (LS) design framework. Results from the analyses were implemented in modelling an idealised low-rise cob building. The study found that 3DP cob has very similar mechanical performance to conventional cob on the material scale but with less material consumption, which makes 3DP cob a more attractive construction from the point of view of resource efficiency. An important outcome of the study is a structural design framework for low-rise 3DP cob buildings, which will allow designers to optimize the design of the 3DP wall construction based on its structural performance and material efficiency.

Key words:

Additive manufacturing; 3D printing; Vernacular architecture; Cob; Compression test; Limit state design; Structural performance optimisation.

1. Introduction

Digital fabrication technologies, especially 3D printing (3DP), have been witnessing an increasing intake in many areas of industry [1]. The construction industry has been adopting a scaled-up version of 3DP over the past two decades. The increased demand for 3DP technologies in construction industry has encouraged researchers to develop novel ideas for a fully automated construction process. Several studies have proven that a well-developed digital-based process of construction offers various benefits such as higher design freedom, accelerated productivity, higher degree of customization and improved security of workers [2], [3]. Among the developed techniques of digital fabrication in construction, 3DP has been the most studied, with concentrated focus on cement-based materials in its focal point [4]–[6].

41 Nowadays, there is a rapid spread of prototypes of 3DP buildings around the world, as several
42 institutions and companies have been competing to upscale the 3DP technology intake over the
43 past few years [7]. The year 2019 only witnessed the construction of two of the largest 3DP
44 concrete buildings in the world. In UAE, the Russian company Apis-Cor constructed the world
45 largest 3DP building for the Municipality of Dubai. The building consists of two-storey with
46 an area of 640 m² and 9,5 m overall height [8] (Figure 1). In Saudi Arabia, the Dutch company
47 CyBe constructed an 80 m² house as part of their contract with the Saudi Arabia Ministry of
48 Housing. This project came as a milestone in an ambitious goal by the Saudi government to
49 build 1.5 million houses using innovative technologies such as 3D concrete printing and fast-
50 brick robotics before 2030 [9] (Figure 1).



51
52 Figure 1. 3DP building in Dubai by Apis-cor (Left) and 3DP house in Saudi Arabia by CyBe
53 (Right).

54 This continuous advancement in construction technology has increased the productivity of
55 the building sector, which consequently, has associated implications on the environment. The
56 building sector is one of the largest contributors towards climate change, as it is responsible for
57 40% of the CO₂ emissions and 36% of global fine energy use [10], [11]. Luckily, the
58 implementation of digital technology in construction offers great potentials for sustainability
59 [12]. According to Ford and Despeisse [13], the adoption of additive manufacturing (i.e. 3D
60 printing) in construction has three significant sustainability benefits: Firstly, an improved
61 efficiency of resources implementation during production and use phase. Secondly, an
62 extended product life as processes like repair, refurbishment and re-manufacture become easier
63 from a technical perspective. Third, reconfigured value chains, as it provides shorter, simpler
64 and more localised production and supply chains.

65 The increased willingness of reducing the environmental impact of building industry has
66 renewed the interest in earth construction after many decades of neglect [11],[14]. Nearly one
67 third of world's population has used earth buildings for construction, especially in developing
68 countries [15]. Earth constructions have very low embodied energy and are highly recyclable
69 with very limited waste production. Furthermore, earth materials proved to have high thermal
70 performance, leading to an improved thermal insulation and indoor comfort [11], [16], [17]. In
71 addition, earth materials are significantly cheap compared to standardized building materials
72 [14]. Studies by Hamard et al. [11] and Agustí-Juan et al. [18] have revealed that sustainability
73 potentials can be achieved through the integration of digital fabrication techniques into earth-
74 based materials in construction.

75 In this respect, the feasibility of 3DP earth-based materials have been under investigation over
76 the past few years by institutions such as IAAC and Cardiff University [19]. WASP 3D is an
77 Italian company that has taken this investigation further and managed to produce prototypes of
78 3D printed earth-based houses [20] (Figure 2).



79
80 Figure 2. 3DP earth house by WASP 3D.

81 Despite these recent studies, there is a lack of definitive information on the construction of
82 3DP cob buildings, which would create reluctance in approving the technique by practitioners
83 and the regulating authorities. Cob is a type of earth construction, traditionally made of soil,
84 water and straw. To date, very little scientific research has been conducted to investigate the
85 engineering properties of 3DP cob. Moreover, to the authors' knowledge, there are no
86 published studies on the analytical/numerical modelling of 3DP cob walls.

87 This paper intends to complete an essential part of larger overarching research by the authors
88 on the feasibility of 3DP cob for modern construction. To date three main studies have been
89 conducted: 1) geometry & fabrication process [21] ; 2) thermal performance [22] and 3) life
90 cycle assessment (LCA) [7]. This paper focuses on the fourth part, i.e. investigation of the
91 structural feasibility of 3D printed cob structures. Together, these studies holistically aim to
92 establish a design guideline for 3D printed cob buildings.

93 2. Cob construction

94 Earth construction has three famous forms: cob, adobe, and rammed earth. Cob, which is the
95 focus of this study, is a traditional technique of building with earth and straw (or other fibers).
96 It differs from adobe and rammed earth with its wet-based technique of construction, where it
97 gives freedom of design and disregard the use of formwork and keeps excellent maintenance
98 characteristics through add-ons or cuts-out, even after the cob is dry [23]–[25]. Cob buildings
99 are well-known historically for their durability and resistance to weathering [26]. In two-storey
100 cob houses, the structural systems for the floors and roofs usually comprise timber framing
101 (primary and secondary beams, as designed specifically by the engineer). In the case of the
102 floor, the joist beams are typically overlaid with timber decking. The roof is usually sloped,
103 with eaves to protect the walls from rain. Cob walls thickness has an average of 60 cm, and
104 traditionally they are thicker at the ground floor as compared to the first floor [14], [27].

105 According to both Miccoli et al. [28] and Earth Devon [29], the mechanical properties of cob
106 walls depend greatly on a number of factors: subsoil properties, the water and straw content,
107 the degree of compaction and the general quality of the workmanship. Compressive strength
108 can be considered to be the fundamental engineering property of earthen material structures, as

109 it controls their load-bearing capacity under gravity loads [14], [30]. The compressive strength
 110 of cob walls is relatively low when compared to other traditional construction materials such
 111 as conventional masonry and rammed earth. However, using greater wall thicknesses in cob
 112 compensates the load-bearing capacity [27], [29].

113 Despite the historical widespread use of cob construction around the world, the structural
 114 behaviour of conventional cob for modern construction is poorly documented, especially when
 115 compared to the available literature of other construction materials such as masonry and
 116 concrete. Only few works can be found in the literature on the structural performance of cob.
 117 These studies are reported in Table 1. The studies show that cob compressive strength (f_c) varies
 118 from 0.1 MPa for a single story cob dwelling [31] and can reach up to 1.59 as in Miccoli et al.
 119 [28]. Cob, compared to all the earthen materials, has the lowest modulus of elasticity (E), its
 120 typical values ranging within 200–500 MPa. Existing data on the Poisson’s ratio of cob is very
 121 limited in literature; the only published test results to the authors’ knowledge come from
 122 Quagliarini and Maracchini [32] who reported a value of 0.21.

123 In general, cob has been found to exhibit considerably higher material ductility than rammed
 124 earth and adobe [28], [32], as characterised by the material’s ability to maintain substantial
 125 stress resistance well into the post-peak phase of stress-strain response. In his study, Miccoli
 126 et al. [28] demonstrated this to be the case under both compressive and shear loading. The
 127 observed ductility can be attributed to the presence of the fibres, which are absent in other
 128 earthen materials such as rammed earth and adobe. This favourable behaviour implies the
 129 ability of cob to outperform the alternate earthen materials under deformation-controlled
 130 loading such as earthquake; however, this still warrants further investigation.

131 Table 1. Values of compressive strength (f_c) and elastic modulus (E) of conventional cob as
 132 reported in the literature.

Source	f_c (MPa)	E (MPa)
Houben and Guillaud (1994) [31]	0.1 (one story)	--
Akinkulore et al. (2006) [23]	0.6	--
Weismann and Bryce (2006) [27]	0.77	--
Quagliarini et al. (2010) [14]	0.24-0.4 (CoV 23%)	--
Pullen and Scholz (2011) [30]	0.44-0.89 (CoV 22%)	75.84
Miccoli et al. (2014) [28]	1.59	--
Rizza and Bottger (2015) [33]	0.6	71.5
Brunello et al. (2018) [34]	0.86	--
Quagliarini and Maracchini (2018) [32]	1.12	16.9
Wright (2019) [35]	1.35 (CoV 21%)	--

133 Recently, research on the performance of digitally manufactured cob has started to emerge,
 134 most famously on 3D printed cob. In addition to studies by a team of researchers at Cardiff
 135 University mentioned above [7], [19], [22], [36], a study by Perrot et al. [37] explored the
 136 structural performance of a cob-like material. The material in this study was made from a mix
 137 of earth material and alginate seaweed biopolymer (as a substitute for straw). The study showed
 138 that 3DP earth with alginate has a compressive strength between 1.2 and 1.77 MPa. These

139 results demonstrate that 3DP earth material can exhibit compressive strength similar to those
140 of the conventional cob construction. The study also suggests that an improved extrusion system
141 can enhance strongly the structural performance of 3DP cob. Until the present day, Perrot's
142 study is the first and only published work on exploring the structural performance of 3DP earth-
143 based material.

144 The pursuit of fully implementing 3DP cob in modern construction requires ensuring
145 structural safety through engineering design. Every type of construction must have design
146 guidelines or standards to provide assurance of the structural stability [28], [29]. The growing
147 interest in large-scale 3DP techniques in general urges for establishing a new code of practice
148 that can provide quick and firm testing process of the workability and buildability of 3DP
149 materials. Understanding the material's mechanical performance and developing the necessary
150 design tools for structural design are key steps necessary for the systematic integration of 3DP
151 materials in construction. This integration can then help practitioners to efficiently plan, design
152 and print the desired structures [1], [17], [22], [38].

153 **3. Aim and objectives**

154 The present study aims to provide insights into the feasibility of 3DP cob walls in terms of
155 their expected structural load-bearing capability. The study approaches this aim through two
156 steps: The first is by conducting an experimental compression test on 3DP cob samples to
157 obtain the basic mechanical properties of 3DP cob including compressive strength, Young's
158 modulus, and Poisson's ratio. The second step is to evaluate the wall section geometries
159 necessary to perform a load-bearing function in typical residential construction for alternate
160 3DP patterns, by applying established engineering design and modelling principles. This will
161 be combined with an optimisation process to examine the relationship between structural
162 efficiency and several design variables such as variable room size, floor heights, number of
163 storeys, and wall section properties. The results are expected to empower architects and
164 engineers with the necessary information for design and construction process of 3DP cob.

165 **4. Material Properties Experimentation**

166 **4.1. Test Specimens**

167 **4.1.1. Material mix preparation**

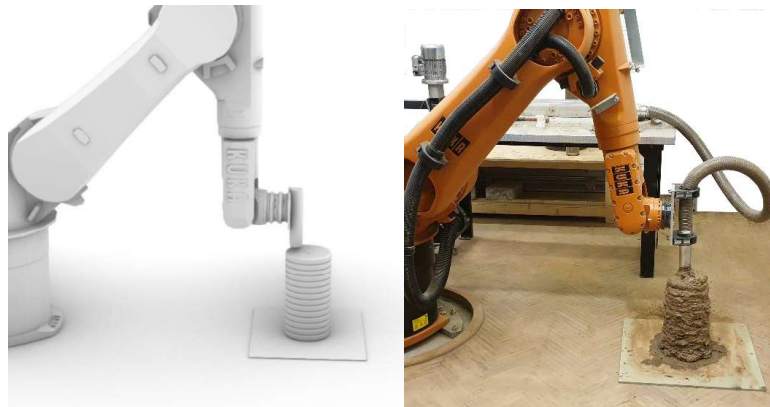
168 According to Weismann and Bryce [27] and Hamard et al. [11], the composition of a
169 traditional cob mixture is 78% subsoil, 20% water and 2% fibre (straw) by weight. The proper
170 subsoil formula stated as 15-25 % clay to 75-85 % aggregate/sand. This study sourced the
171 subsoil from Cardiff, UK, for the cob specimens. Subsoil specimens were examined following
172 the recommended methods in the literature [27], [39] and were found to match the general
173 recommendations for cob mixture.

174 The properties of 3D printed materials must be formulated carefully considering both its wet
175 and hardened states. Wet properties of material relates to its fresh, or 'green' state, before
176 drying or hardening [37]. In a 3D printing process, the material must flow efficiently through
177 the system, be deposited as layers and harden properly to reach a structural integrity threshold
178 within an acceptable time frame that meets the construction requirements [5]. Hence, this study

179 has developed a new cob mixture to meet the purpose of 3D printing process. Cob is
180 traditionally mixed in a nearly dry state, which does not fit the purpose of 3D printing where a
181 less viscous rheology is required. Based on a number of systematic 3D printing tests conducted
182 prior to this study by Gomaa et al. [22], the water content in the 3D printed cob mixture was
183 increased to an average of 25% while straw was maintained at 2%, resulting in a subsoil
184 percentage of 73% (by weight).

4.1.2. 3D printing and robotic tools

186 Robotic 3D printing platform consists of two main tools: the robotic arm that controls all the
187 movements and an extruder that controls the material delivery within the system. Both tools
188 must work collaboratively in synchronised to ensure high level of precision and efficiency of
189 the 3D printing process. The study used a 6-axes KUKA KR60 HA robotic arm (Figure 3). The
190 software package for robotic control was Rhinoceros via Grasshopper® and KUKA PRC®.
191 An electromechanical dual ram extruder, developed by Gomaa et al. [21], was used for the
192 material delivery.



194
195 Figure 3. Robotic 3D printing of the cob specimens, with the virtual model on Rhino (left)
196 and the real output (right)

4.2. Test Arrangement and Method

198 The compressive test on cob specimens was undertaken in a universal compression testing
199 machine (Figure 4) following the standardised procedure in EN 772-1 [40]. The specimens
200 comprised printed cob cylinders of 400 mm tall and 200 mm in diameter as shown in Figure 4.
201 Each specimen was subjected to a uniformly distributed axial load by the two steel loading
202 platens that were coated with grease to minimise confinement due to friction. The rate of
203 applied load was approximately 0.077 MPa/min, which meant that each test took about 10
204 minutes to perform. A total of three samples were tested.

205 The test apparatus monitored the applied load and axial (longitudinal) displacement between
206 the two platens using a built-in linear variable differential transformer (LVDT). Since it was
207 not practical to apply strain gauges to the specimens due to their irregular surface, horizontal
208 deformation (necessary to evaluate the Poisson's ratio) was determined in post-processing by
209 the digital image correlation technique.



Figure 4. Compression test set up and the specimen design.

4.3.Results

The measured stress-strain behaviour is shown in Figure 5, demonstrating consistent response for each of the three tested samples. The plotted stress was calculated as $\sigma = P/A$, where P is the applied force and A is the cross-sectional area of the specimen ($31,400 \text{ mm}^2$). Axial strain was computed as $\epsilon_{\text{axial}} = \Delta/L$, where Δ is the displacement measured between platen-to-platen, and L is the length of the specimen (400 mm).

Key parameters derived from the test are summarised in Table 2. The maximum compressive stress (σ_{max}) was obtained directly as the peak measured value. To account for the influence of the specimen's aspect ratio and size on its load capacity, EN 772-1 defines the unconfined compressive strength of a test sample as $f_c = k \sigma_{\text{max}}$, where k is a correction factor which for the given specimen geometry is equal to 1.25. The resulting unconfined compressive strength has a mean of 1.08 MPa and coefficient of variation (CoV \equiv standard deviation / mean) of 4%. The mean value sits within the range of values measured in existing studies as shown in Table 1.

The elastic modulus (E) was evaluated as the slope of the σ - ϵ curve along the initial rising branch before the onset of nonlinearity, its mean value equal to 22.9 MPa. As seen from Table 1, this is comparable to the value of Quagliarini and Maracchini [32], but only 30% of the value measured by Pullen and Scholz [30] and Rizza and Bottger [33] as will be seen later, E can have significant influence on wall loadbearing capacity as it controls the local buckling capacity of the printed patterns. Poisson's ratio (ν) was calculated as $\nu = \epsilon_{\text{lateral}} / \epsilon_{\text{axial}}$, with $\epsilon_{\text{lateral}}$ being determined from video capture of the test using digital image correlation.

Table 2. Key results derived from compression test, including peak stress (σ_{max}), unconfined compressive strength (f_c), elastic modulus (E), and Poisson's ratio (ν).

Sample	σ_{max} (MPa)	f_c (MPa)	E (MPa)	ν
1	0.88	1.10	22.7	0.16
2	0.83	1.04	25.3	0.28
3	0.89	1.11	20.6	0.21
Mean value	0.87	1.08	22.9	0.22
CoV	4%	4%	10%	28%

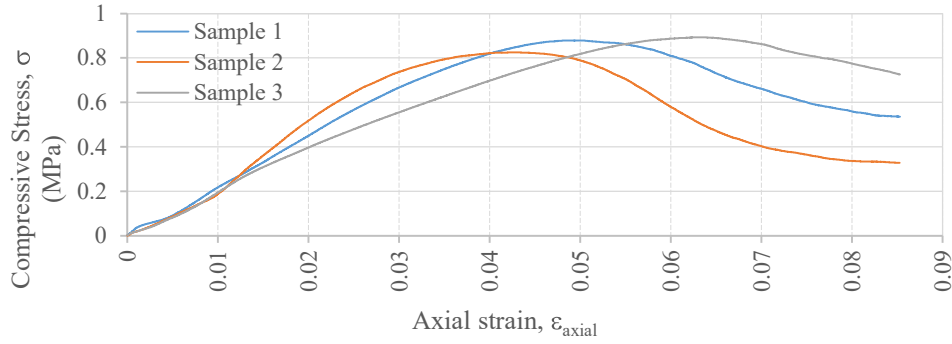


Figure 5. Stress-strain behaviour observed under compression.

5. Evaluation of the feasibility of loadbearing 3DP cob walls

This section examines the feasibility of using 3DP cob as loadbearing walls in low-rise residential buildings by applying limit-state design (LSD) framework. The design actions considered here are from gravity loads only, excluding possible loads from the wind or earthquake, which can be highly region-specific.

5.1. Method of Structural Analysis

Because current design codes are intended predominantly toward conventional construction materials, they are not necessarily applicable to performing the required structural adequacy checks for 3DP cob walls. Therefore, the approach adopted here is to evaluate the wall's load-carrying capacity by applying first principles while adhering to the general concepts of limit state design. This involves the use of characteristic values (rather than mean values) of material stress capacity, applying load factors to upscale the design loads, and applying capacity reduction factors to downgrade the design capacity.

5.1.1. Limit state design

Capacity adequacy checks were performed according to a limit state (LS) design framework. With reference to the compressive strength, the design check can be expressed using the generalised form

$$N_c^* < \phi N_c \quad (1)$$

In Eq. (1), N_c^* is the design compressive force acting on the wall, determined as γS , with S being the unfactored working load and γ being the load factor greater than 1. In turn, ϕN_c is the design compressive capacity of the wall, determined as the basic capacity N_c multiplied by the capacity reduction factor ϕ (less than 1). To account for the fact that the material stress capacities exhibit stochastic variability, capacity N_c is calculated using the characteristic compressive strength of the material, f_c' , defined as the lower 5th percentile value (rather than the mean value).

5.1.2. Selection of wall sections

Three different types of printed patterns were considered as part of this feasibility study; these are referred to as A, B and C, as shown in Figure 7. These three designs align carefully with the wall sections in two previous studies that investigated the thermal performance and life cycle

analysis (LCA) of 3D printed cob by Gomaa et al. [22] and Alhumayani et al. [7] respectively. The criteria for choosing these wall sections are based on meeting variable design requirements such as adequate thermal insulation, efficient use of material and structural integrity. A generic vertical cross section of a wall is shown in Figure 8. Because the 3D printing process in this study dispenses the cob material in circular cross sections while being flattened down into wider layers, the resulting vertical shells do not have a constant thickness (Figure 8); rather its thickness ranges between an inner value, t_{in} , and outer value, t_{out} , as shown. On the basis of typical printed patterns, we take $t_{out} - t_{in} = 20$ mm, and from this also define the average thickness, t , as $t = (t_{in} + t_{out})/2$. For each type of section, d is the nominal wall depth as measured from the centrelines of the two external shells, while a refers to distance between the pattern cycles (Figure 6). a was taken equal to d .

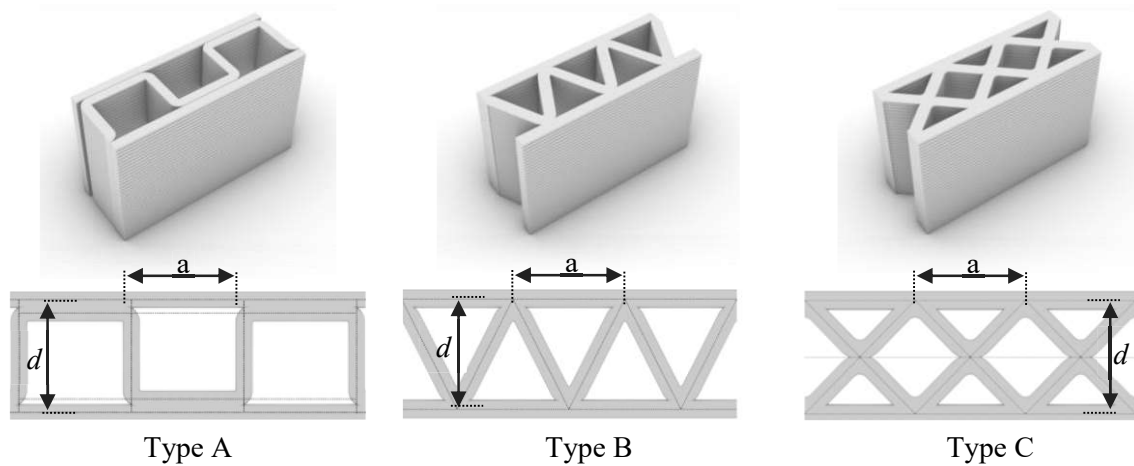


Figure 7: Alternate printed patterns considered in this study.

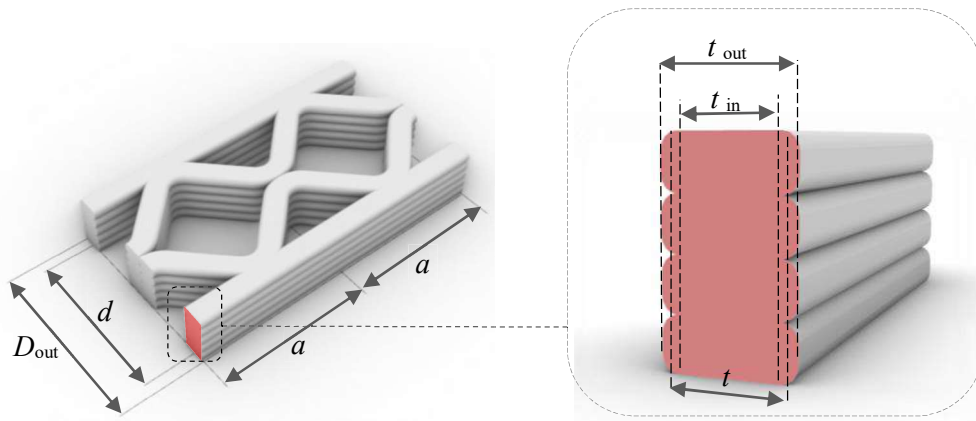


Figure 8: Definition of geometric properties used in the analysis along a vertical cross section. d (wall thickness), a (distance between the pattern cycles).

Evaluation of the wall's compressive capacity requires fundamental section properties including the wall's area (A), out-of-plane moment of inertia (I). These were calculated for each type of section by conservatively treating the shell thickness in the resisting section as t_{in} . For comparative purposes, the sectional properties of the three types of patterns are provided in Table 3.

283 Table 3. Section properties for the alternate printed patterns. Each uses $t_{in} = 50\text{mm}$ and $d = 500\text{mm}$.
 284 Properties accentuated by bar (\bar{X}) denote the value per unit length run of the wall.

Wall Type	t_{in} (mm)	t (mm)	d (mm)	\bar{A} (mm ² /m)	\bar{I} (mm ⁴ /m)	$\bar{P}_{\text{buck,loc}}$ (kN/m)
A	50	60	500	200,000	9.32×10^9	145
B	50	60	500	212,000	8.60×10^9	137
C	50	60	500	241,000	9.23×10^9	181

285 5.1.3. Wall compressive strength

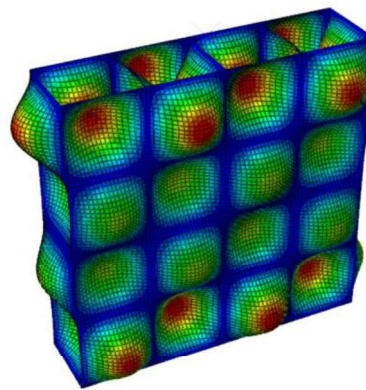
286 The compressive load capacity of a wall was evaluated by considering the combined stress
 287 axial load and eccentricity moment, with allowance for local buckling of the shell structure and
 288 global buckling of the wall member. This involved firstly calculating the compressive stress
 289 capacity of the section ($\sigma_{c,\text{max}}$) as:

$$\sigma_{c,\text{max}} = \min(\sigma_{\text{mat}}, \sigma_{\text{buck,loc}}) \quad (2)$$

290 i.e., as the lesser of the stress to cause material crushing (σ_{mat}) and local buckling ($\sigma_{\text{buck,loc}}$).

291 Eq. (2) adopts the material crushing limit (σ_{mat}) as the characteristic compressive strength of
 292 the material, f_c' , defined as the lower 5th percentile value. The characteristic value was
 293 estimated on the basis of the mean value of 1.08 MPa (Table 1) by assuming that f_c follows a
 294 lognormal distribution and has a CoV of 20%. This gives $f_c' = 0.77$ MPa.

295 The resistance of the shell structure to local buckling was determined by finite element
 296 analysis (FEA) using the package ABAQUS (Version 6.13). The model analysed for each type
 297 of printed section represented the full-sized wall with its length and height made sufficiently
 298 large so as not to influence the local buckling stress. A typical local buckling mode shape of a
 299 wall is shown in Figure 9. The computed values of the buckling load per unit length of the wall
 300 ($\bar{P}_{\text{buck,loc}}$) are summarised in the last column of Table 3. These values were computed by taking
 301 $E = 22.9$ MPa and $\nu = 0.22$ as informed by the material tests. The local buckling stress inputted
 302 into Eq (2), was evaluated as $\sigma_{\text{buck,loc}} = \bar{P}_{\text{buck,loc}}/\bar{A}$.



303 Figure 9: Visual representation of a typical local buckling failure mode in a wall member
 304 as calculated by finite element analysis. Shown for section type A.

304 The member-scale load capacity of the wall with the potential for global buckling was
 305 evaluated from first principles, by treating the wall as a column under eccentric loading. In this
 306 treatment, the peak compressive stress σ_{\max} acting on the section can be expressed as:

$$\sigma_{\max} = P \left[\frac{1}{A} + \frac{ec}{I} \sec \left(\frac{\pi}{2} \sqrt{\frac{P}{P_{\text{buck, glob}}}} \right) \right] \quad (3)$$

307 where P is the applied axial load; e is the applied load's net eccentricity (quantified as
 308 described later); A , I are the section area and moment of inertia; c is the distance from the
 309 centreline to the extreme compressive fibre, equal to $(d+t_{\text{in}})/2$. $P_{\text{buck, glob}}$ is the critical global
 310 buckling load of the wall, obtained from Euler's formula:

$$P_{\text{buck, glob}} = \frac{\pi^2 EI}{L_e^2} \quad (4)$$

311 where L_e is the effective length, taken as the floor-to-floor or floor-to-roof height (see Figure
 312 9), and other properties as defined previously.

313 The wall's unfactored load capacity was evaluated by assigning section stress capacity $\sigma_{c, \max}$
 314 from Eq (3) to σ_{\max} in Eq (2), and solving Eq (2) for P . This solution was obtained numerically,
 315 since Eq (2) cannot be formulated explicitly in terms of P . The limit state design capacity was
 316 then obtained by applying the capacity-reduction factor $\phi = 0.5$ as per AS3700 [41], such that:

$$\phi N_c = \phi P \quad (5)$$

317 with P being the solution obtained from Eq (3).

318 5.1.4. Modelling an idealised low-rise building

319 To examine the feasibility of using 3DP cob walls as loadbearing structural elements, the
 320 study considered an idealised 1- and 2-storey house. Schematic representations of the
 321 building's geometry are shown in Figure 10. In the case of a 1-storey house, the walls carry only
 322 the roof load, while in the 2-storey house, they carry loads from the roof and suspended floor.
 323 In each scenario, the total compressive force in the wall also incorporates the wall self-weight
 324 and is calculated at the ground level.

325 The roof load and the suspended floor structures depend on these elements' dead load (self-
 326 weight plus any superimposed permanent load), carried live load, and the dimension of their
 327 span. The roof and floor are treated as one-way-spanning in the direction perpendicular to the
 328 wall, so the load that they apply to the wall can be calculated as the total pressure load
 329 multiplied by a tributary load width (LW). The tributary load width depends on the
 330 configuration of the wall within building. In the case of an external wall, it is equivalent to half
 331 the span of the floor/roof beam. For an internal wall, it includes the sum of the respective
 332 contributions from each side (Figure 10). Further, in the case where the wall contains an
 333 opening, in a simplistic treatment the load width could be scaled pro-rata depending on the
 334 proportion of solid wall to openings. For instance, if half of the wall is perforated by openings,
 335 then the load width becomes twice what it would be if the wall were solid.

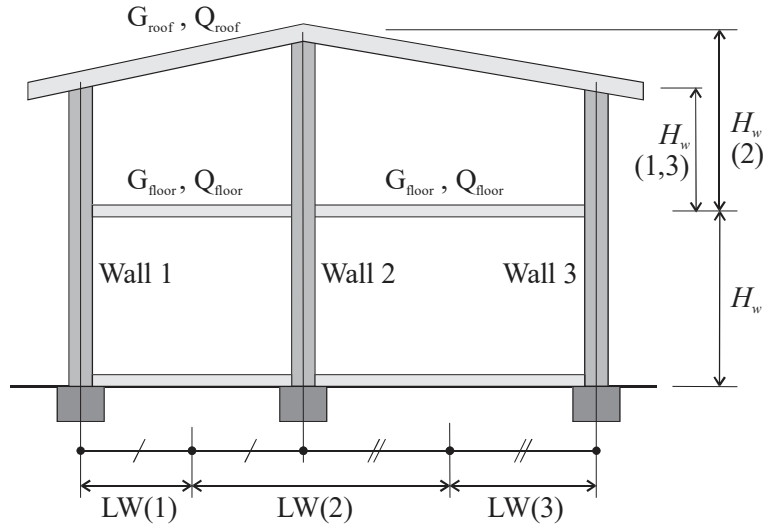


Figure 10: Overall building geometry, Two-storey ($n_s = 2$) double-bay building with internal and external walls, indicating the definition of wall height (H_w) and tributary load width (LW).

The gravity loads adopted in the analysis are representative of values for residential construction, which are consistent with typical loads stipulated in design standards [e.g. Australian loading code AS1170.1 [41]]. The adopted values are summarised under ‘unfactored loads’ in Table 4. The total dead load of the suspended floor is taken as 1.0 kPa, which allows for a timber joist and timber deck floor (typically 0.5 kPa), as well as a superimposed permanent load (0.5 kPa). The general occupancy floor live load is taken as 1.5 kPa, consistent with residential dwellings. The total dead load of the roof is taken as 0.9 kPa. This makes allowance for timber framing (rafters + purlins) with clay roof tiles. Note that in comparison, a sheet metal finish (as opposed to clay tile) would reduce the total load to 0.5 kPa total. The live load acting on the roof is taken as 0.25 kPa.

The self-weight of the wall was calculated in proportion to its section area, taking the weight density of the material as 18 kN/m³. Thus, the total design compressive load was taken as:

$$N_c^* = \begin{cases} P_{\text{roof}}^* + P_{\text{wall}}^* & \dots 1 \text{ storey} \\ P_{\text{roof}}^* + P_{\text{floor}}^* + 2P_{\text{wall}}^* & \dots 2 \text{ storey} \end{cases} \quad (6)$$

where P_{roof}^* is the load applied by the roof, P_{floor}^* by the suspended floor, and P_{wall}^* is the self-weight of the wall over a single storey (height H_w). Each load P^* is taken ultimate limit state load combination $1.2G+1.5Q$, with G being the dead load and Q the live load.

Table 4: Summary of constant input parameters used in the feasibility study. Explanations are provided in the text.

Property	Value
<i>Cob material properties:</i>	
Elastic modulus, E	22.9 MPa
Characteristic compressive strength, f_c' (See note 1)	0.77 MPa
Weight density, γ	18 kN/m ³
Poisson's ratio, ν	0.22

Unfactored loads:

Roof dead load, G_{roof}	0.9 kPa
Roof live load, Q_{roof}	0.25 kPa
Floor dead load, G_{floor}	1.0 kPa
Floor live load, Q_{floor}	1.5 kPa

Limit state design factors:

Compressive strength capacity reduction factor, ϕ	0.5
Ultimate limit state design load combination	$1.2G + 1.5Q$

Eccentricities (e) of applied load (w.r.t. wall centreline): (See note 2)

Load from roof	$0.1 \times D_{\text{out}}$
Load from floor	$0.25 \times D_{\text{out}}$
Self-weight of wall	$0.05 \times D_{\text{out}}$

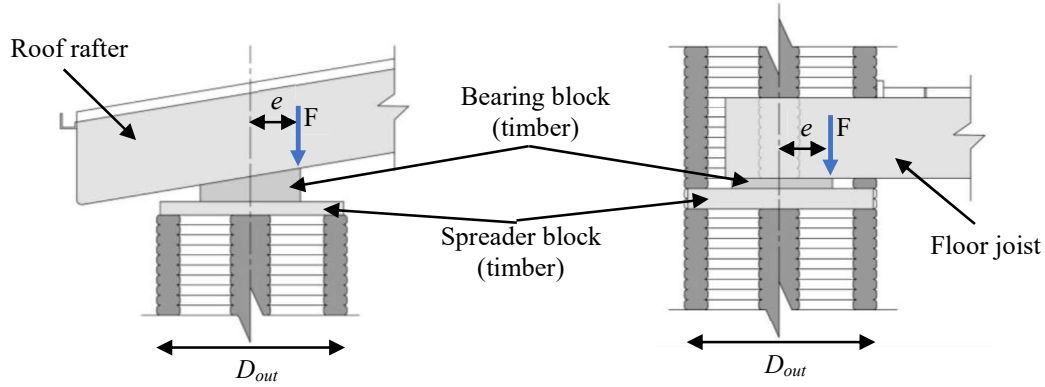
Notes:

1. Determined from mean strength ($f_c = 1.08$ MPa) by assuming lognormal distribution and CoV = 20%.
2. Where D_{out} is the full depth of the wall section measured between its outer edges.

5.1.5. Connection details and load eccentricity

It is important to consider that the floor and roof will generally apply the resultant load eccentrically (i.e. offset with respect to the wall's centreline), and this generates an out-of-plane bending moment that can ultimately have a major influence on the wall's load-carrying capacity. The eccentricity of the applied load is largely influenced by the connection detail. While the development of the connection details falls into the domain of detailed structural design and is outside the focus of this work, conceptual illustrations of possible connections are shown in Figure 11.

The connection between the roof and wall can be achieved by supporting the timber rafters using a timber bearing block, in turn resting on a spreader block that distributes the load onto the wall (Figure 11a). This detail is assumed to generate an eccentricity $e = 0.1 D_{\text{out}}$, with D_{out} being the full depth of the wall measured between its outer edges. The wall-to-floor connection (Figure 11b) involves a detail in which the joists penetrate partially into the wall and are supported by a bearing block and spreader block. The assumed eccentricity of this connection is $0.25 D_{\text{out}}$. It should be noted that a connection in which the floor is supported outside the extent of the wall would generate an eccentricity $> 0.5 D_{\text{out}}$, and is not advised as this would significantly diminish the loadbearing capacity. The aforementioned values of the assumed eccentricities are consistent with similar details for conventional clay brick masonry provided in AS3700 [42].



(a) Wall-to-roof connection (section view). (b) Wall-to-floor connection (section view).

Figure 11: Potential connection details and definition of eccentricities (e) of the applied load (F).

Additionally, for sake of conservatism the self-weight of the wall is assumed to act at an eccentricity of $0.05 D_{out}$ to allow for any incidental geometric imperfection of the wall. The internal bending moment was calculated as the sum of each applied load P^* (i.e. P^*_{roof} , P^*_{floor} , P^*_{wall}) and its respective eccentricity, which dividing by the total compressive force N^*_c [from Eq. (6)] produces the net eccentricity:

$$e_{net} = \frac{\sum P_i^* e_i}{N_c^*} \quad (5)$$

The net eccentricity was used as the input value of e in Eq (3).

5.1.1. Optimisation methods

The 3D printed sections in Figure 7 can be defined by two variables: the nominal wall depth (d) and average shell thickness (t). In order to determine the most efficient section needed for load-bearing functionality, an optimisation process was undertaken to minimise the material volume while ensuring that the load capacity remains sufficient to accommodate the applied design load. As a metric of the structural adequacy, the limit state design formula [Eq (1)] can be rearranged and expressed as the capacity utilisation (u), i.e. the ratio of the design load to the design capacity:

$$u = \frac{N_c^*(t, d)}{\phi N_c(t, d)} \quad (5)$$

where both the capacity and design load are functions of the optimisation variables d and t .

As a proxy for the material volume, we can adopt the area per unit length of the wall (\bar{A}), since the two are directly proportional. Therefore, the optimisation process to determine the optimal t and d can be expressed as:

Minimise \bar{A} , by varying t and d , subject to the constraints:

- $u \leq 1$ (ensure structural adequacy),
- $t > 0, d > 0$ (positive values only),
- $d \geq t$ (for a section to be valid, shell thickness must not exceed section depth).

To cater for varying architectural requirements on the building geometry, this optimisation was performed at different combinations of the wall height (H_w), load width (LW), and number of storeys (n_s). Constant inputs and their values are summarised in Table 4.

Two types of optimisation approaches were adopted in this study. Both solvers were leveraged collaboratively for two reasons: first, to ensure the integrity of the results through verification; and second, to provide two different approaches to results representation. The first approach used a continuous optimiser in MATLAB®, where t and d can adopt any values along a continuous domain. The second approach utilized Galapagos, an evolutionary optimiser in Rhino- Grasshopper® package by McNeel [43] (Figure 12). Galapagos relies on Non Linear Optimization (NLopt) and GUI algorithms [44]. Implementing the optimisation within MATLAB provides a simple and quick process of optimisation compared to Galapagos; yet, using the Grasshopper package provides essential key advantages to the whole construction process, such as:

- 1) Direct link to the 3DP system (i.e. 3D printers and robotic arms), which enables an efficient execution of models.
- 2) An inclusive control over the design-to-fabrication framework, which includes geometry design and other performance optimisation aspects such as thermal, lighting and environmental impacts.
- 3) Better visual representation of the modelling results in real time, which facilitates envisaging the building geometry and its aesthetics (Figure 13).

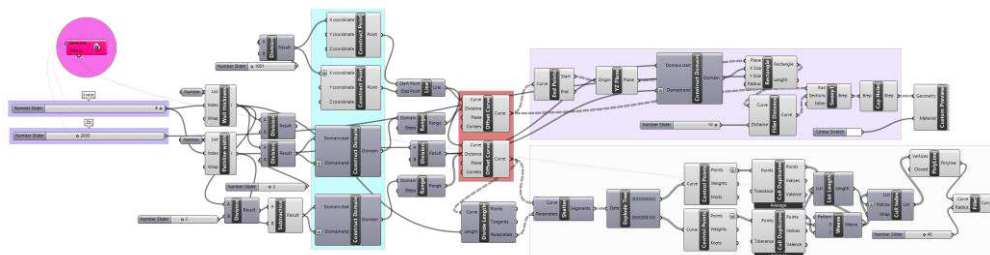


Figure 12. Grasshopper definition for the optimisation of the wall models.

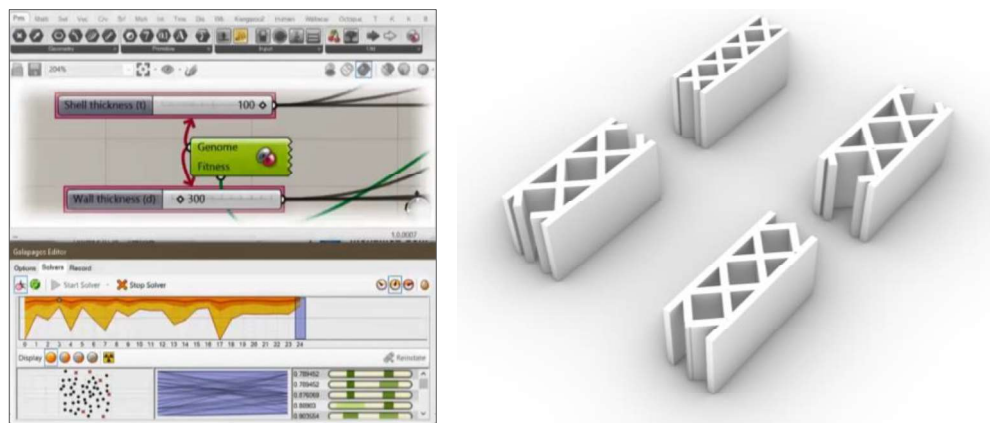


Figure 13. Visual representation of the optimisation process of Galapagos (left) and a sample of the visual generation of results for wall type C in Grasshopper (right).

419 5.2.Results

420 The relationship between capacity utilisation and the wall section is illustrated in Figure 14,
 421 which plots contour lines of equal utilisation (u) as a function of shell thickness (t) and nominal
 422 wall depth (d). The graph corresponds to a specific case where the wall height (H_w) = 2.5 m,
 423 the load width (LW) = 3.5 m, and the building having two-stories ($n_s = 2$). It is important to
 424 note that the presented trends in Figure 14 are representative of general trends, regardless of
 425 the actual values of these inputs. The thick black contour line indicates utilisation of unity
 426 ($u=1$), i.e. the locus of points where the capacity is equal to the design load. The shaded grey
 427 area encompasses wall sections that are structurally adequate. The red dashed line delineates
 428 the zones where the section is compact (governed by the material crushing) as opposed to
 429 slender (governed by local buckling), as per Eq (2). The black dashed lines determine the range
 430 of the t values (and their associated d values) that are governed by the available nozzle sizes in
 431 the used 3DP system.

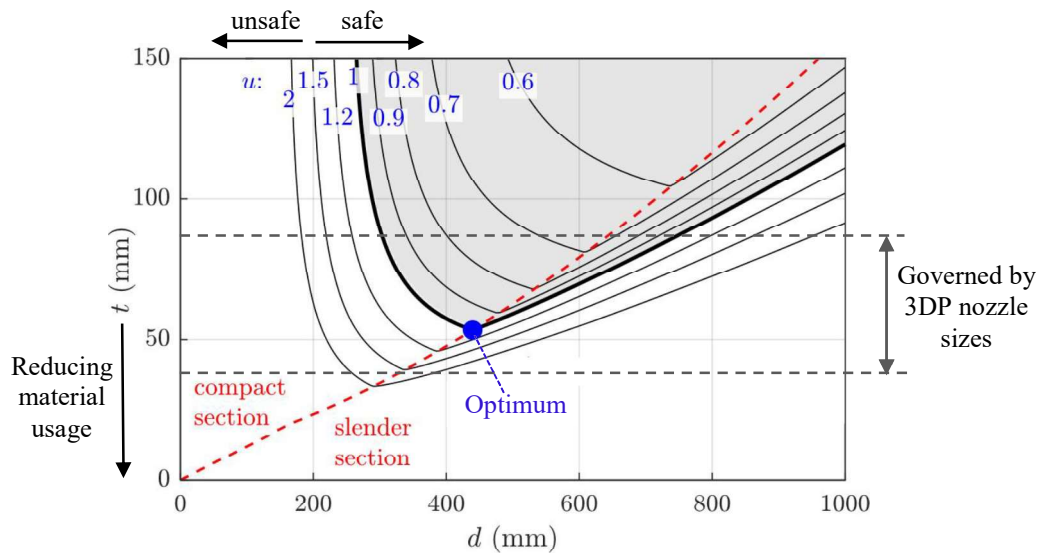


Figure 14: Typical utilisation contour plot for varied shell thickness (t) and the nominal wall depth (d). Grey area indicates the zone where the capacity is adequate for the design load. The dashed red line delineates compact sections (material stress failure) from slender sections (local buckling failure). Calculated for $H_w = 2.5\text{m}$, $LW = 3.5\text{m}$, $n_s = 2$.

432 Figure 14 demonstrates that since material usage (and \bar{A}) is proportional to the shell thickness
 433 (t). Sections with a small depth (d) are inefficient in terms of material usage, because they
 434 require an uneconomically thick shell (t) to maintain the necessary stress bearing area and
 435 moment of inertia. The optimal section in terms of material volume is one that minimises the
 436 shell thickness along the line $u = 1$. This indicates that 3DP cob walls can offer improved
 437 material efficiency compared to equivalent solid cob walls.

438 Notably, the u contours follow distinctly different trajectories in the compact- and slender-
 439 section zones, and consequently the optimal solution occurs at the boundary that delineates
 440 them. In the compact section zone, there is a roughly inverse relationship between t and d
 441 at any constant utilisation; this is because of the trade-off between t and d while maintaining a
 442 sufficient bearing area and moment of inertia. However, as the shell thickness is continually

reduced (with the aim of making the section more economical), the section compressive capacity [Eq. (2)] eventually begins to be governed by local buckling, at which point the section's efficiency drastically diminishes. This can be explained by the fact that if a section is already slender, increasing its depth d would make it more prone to local buckling (d being analogous to the effective length in the context of local buckling). Therefore, a larger t would be required to compensate for this, resulting in a progressively less economical section in terms of material volume.

These observations highlight the importance of reliably quantifying both the material crushing strength (f_c) and the elastic modulus (E) of the cob material, since both properties govern the design capacity of the section in the practical range of interest. The results shown in Figure 14 have also led to a narrowed down scope of values for the optimisation process of t and d , which helped accelerating process and producing concise design charts.

5.2.1. Design charts

The results of the optimisation process are shown in the form of model 'design charts' as in Figure 15 and Figure 16. Each figure plots the t and d dimensions of the optimal wall section design. Figure 15 keeps the wall height constant at 3.0 m while varying the load width on the horizontal axis to a maximum of 6 m width. Figure 16 maintains a constant load width at 4.0 m while varying the wall height on the horizontal axis between 2.5 to 3.5 m. Each figure considers the three alternate printed patterns (A, B, C), and a 1- or 2-storey building. The corresponding area per unit length (proxy for the material volume) of the optimal sections is plotted in Figure 17 and Figure 18. Both figures demonstrate the relative efficiency of the sections to maintain the same structural adequacy. The selected constant values of wall height (H_w) and load width (LW) at 3 m and 4 m in Figure 15 and Figure 16 respectively were intended to reflect an idealised size of a room in a typical residential building (i.e. $4 \times 4 \times 3$ m).

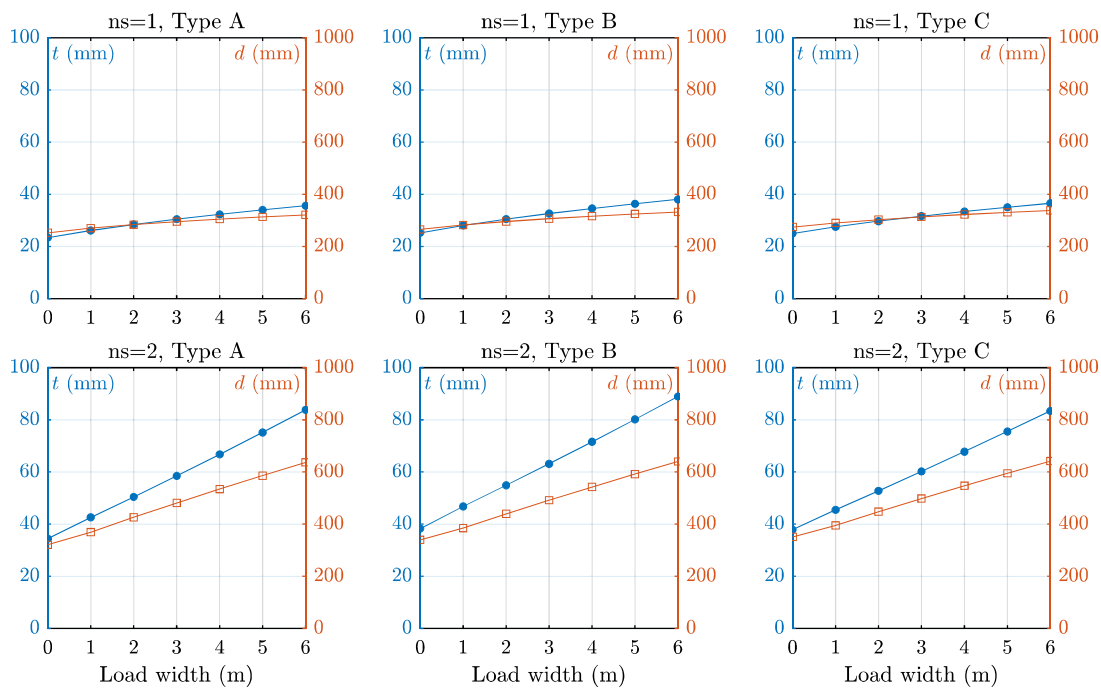


Figure 15: Dimensions t and d for optimised sections at varied load width (horizontal axis of each plot) and constant wall height of 3 m. Considers section types A, B, C. Top row is for single storey, bottom row for double storey. Each graph shows t on the left y-axis and d on the right y-axis.

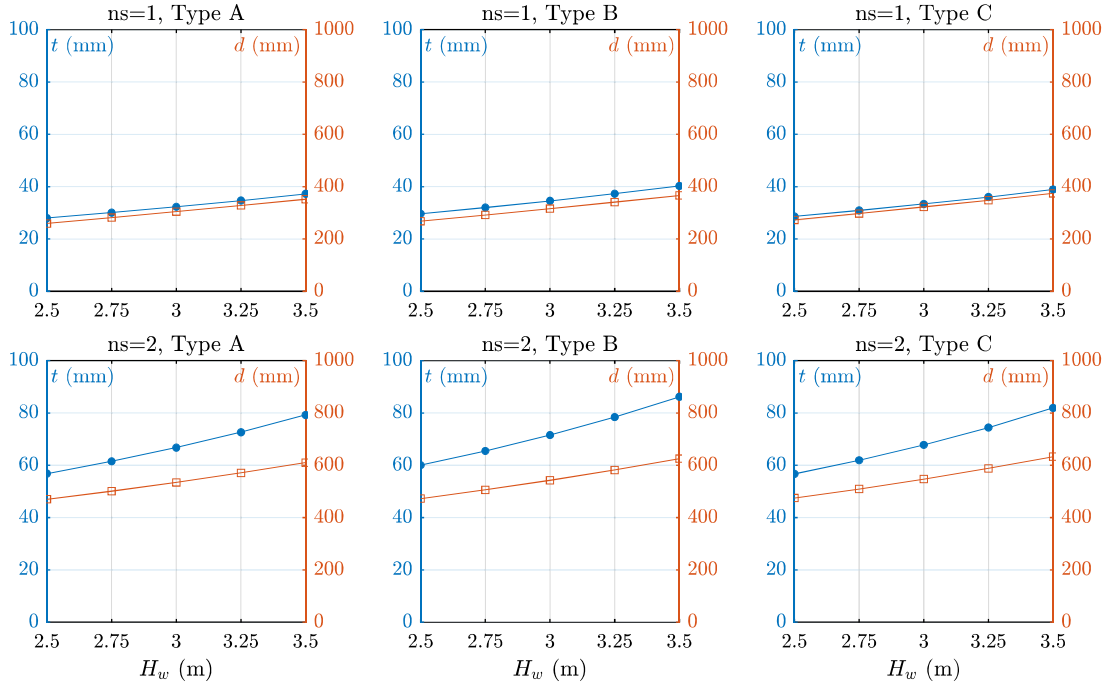


Figure 16: Dimensions t and d for optimised sections at varied wall height (horizontal axis of each plot) and constant load width of 4 m. Considers section types A, B, C. Top row is for single storey, bottom row for double storey. Each graph shows t on the left y-axis and d on the right y-axis.

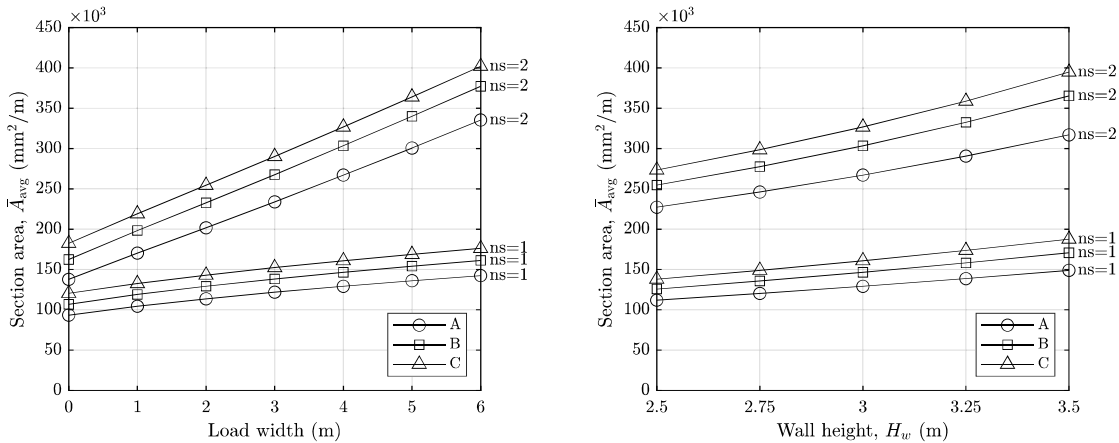


Figure 17: Cross-section area per unit metre for the optimised sections whose dimensions are plotted in Figure 15 (varied load width and constant wall height of 3 m).

Figure 18: Cross-section area per unit metre for the optimised sections whose dimensions are plotted in Figure 15 (varied wall height and constant load width of 4 m).

6. Discussion

Starting with the material properties examination: the tested 3DP cob samples (Table 2) show generally comparable mechanical performance to conventional cob (Table 1) under axial compression testing. The measured compression strength (f_c) is within the higher range of reported values for conventional cob. Similarly, the Poisson's ratio of the 3DP cob was matching the reported value in the literature. However, the elasticity modulus of the 3DP cob was toward to lower end of reported values. Yet, all the quantified properties were deemed to be satisfactory, to proceed with the next phase of the feasibility evaluation.

Moving to the structural analysis: application of established structural assessment principles in conjunction with the experimentally quantified properties has demonstrated that 3DP cob walls could safely sustain gravity loads in typical residential construction for up to a two-storey building with sufficient space sizes and reasonable thicknesses of walls. The design charts produced using this process (Figure 15 and Figure 16) describe the relationships between the different design variables so as to achieve the most efficient section (minimising material volume) while ensuring structural adequacy. Looking into the design charts, it is obvious that a wall a small section area A consumes less material in 3d printing. However, using small wall section area may also result in a less efficient architectural design with possibly compromised aesthetics and thermal performance, in addition to other workability challenges in the 3DP printing system to exert walls with small section area.

A previous study by Gomaa et al. [21] found that 3DP of large-scale cob walls require a nozzle of a size no less than 40 mm, resulting in an average shell thickness (t) that varies from 40 to 80 mm. Lower diameter sizes will slow down the printing process. They can also cause clogging problems inside the extrusion system. On the other hand, using larger nozzles leads to a higher consumption rate of material and less control over accuracy. Hence, for small load-carrying demands, not only is the wall section governed by structural requirements, it is also determined by other considerations such as thermal requirements, aesthetics, and the constraints of the 3DP apparatus.

The trends in the charts, as they are plotted now, present a spectrum of the structurally functional values for the basic design variables of walls that affect the design and fabrication process, regardless of the chosen wall section type (i.e. A, B or C). These variables, with their range of values, are summarised in Table 5.

Table 5. The suggested range values of the basic wall design variables in the design charts

	1 storey		2 stories	
	Min (mm)	Max. (mm)	Min (mm)	Max. (mm)
Shell thickness (t)	25	40	35	90
Wall thickness (d)	250	380	320	640

The results in general suggest that the Type A wall section is the most efficient for structural and material use considerations, followed by B then C. Nevertheless, it is essential to decide what kind of efficiency is at stake for a specific project. In other words, from a structural engineering viewpoint, 'efficiency' might refer only to achieving adequate structural performance with the minimal amount of material. Yet, from an architectural perspective, the

505 notion of efficiency also combines aspects such as design function, thermal performance and
1 506 environmental impacts. To elaborate further, the thermal performance efficiency of 3DP cob
2
3 507 was explored thoroughly in a recent study by Gomaa et al. [22] . The study proved that the
4 508 voids within the 3DP cob walls dramatically improve thermal efficiency compared to solid cob
5
6 509 walls. This means, when looking into the three wall types A, B and C in this study, their order
7 510 of structural efficiency does not necessarily imply that they have the same order for thermal
8
9 511 efficiency. Hence, it is highly recommended to consider analysing the holistic performance of
10 512 the chosen wall type, including structural, thermal and environmental efficiency. This will be
11 513 the subject of a future study.

13 514 6.1. Case study of a 3DP small house

15 515 As explained previously, the approach to leveraging the design charts depends greatly on the
16 516 architectural design intentions and requirements. To elaborate this, a case study demonstrating
17 517 an envisaged design process of a small cob house is presented and analysed in this section. The
18 518 process starts with a simple floor plan indicating the zoning and the dimensions of spaces. For
19 519 the purpose of this study, the house is designed to combine four spaces with different sizes and
20
21 520 openings to represent typical design requirements. Spaces' dimensions vary from 2 m to 4 m
22 521 wide. The roof and the suspended floor in the 2-storey house alternative are treated as one-way
23 522 spanning as shown in Figure 19. Each loadbearing wall (numbered 1–7 in Figure 18) has its
24 523 characteristics detailed in Table 6 and Table 7 for 1- and 2-storey alternatives respectively. The
25 524 non-loadbearing walls (unnumbered in Figure 19) can adopt the minimum required dimensions
26 525 for each pattern (A, B, C), by treating it as a wall supporting zero load width. $LW=0$ is
27 526 analogous to a wall that needs to support only its own self-weight. However, assigning different
28 527 LW for each wall can add complexity to the design and lower the efficiency of construction
29 528 process. Therefore, non-loadbearing walls are recommended to be treated as case by case based
30 529 on each design goals and requirements.

36 530 Table 6 and Table 7 indicate the process to assign the particular t and d to each wall in the
37 531 building using the design charts from Figure 15. The process starts by defining the location of
38 532 the wall (i.e. internal, external) and the direction of the floor and roof spans, which dictate the
39 533 basic tributary load width supported by each wall based on the gross dimensions. Then, if the
40 534 wall has an opening, the basic load width was upscaled in relation to the ratio of the openings
41 535 (as described in section 5.1.4). For instance, a wall containing 50% openings (measured in the
42 536 plan view) carries an effective load width equal to double the basic load width. The effective
43 537 load width is then used to allocate t and d from the design charts for the particular wall type
44 538 (A, B, C). Note that for simplicity, the effective load widths in Table 6 and Table 7 are rounded
45 539 up to the nearest integer. Figure 20 demonstrates the finalised floor plan after assigning the
46 540 selected t and d to each wall, adopting pattern type A for illustrative purposes.

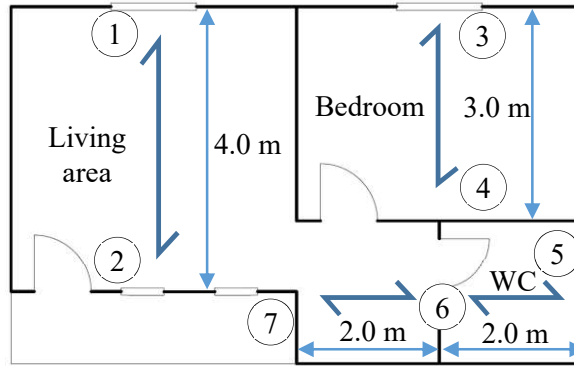


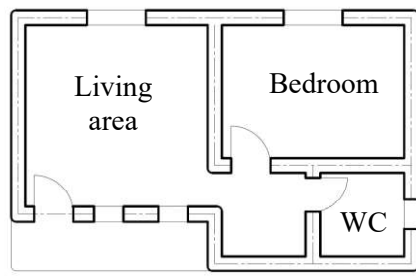
Figure 19. The floor plan of the idealised 3DP cob house. Half-headed arrows indicate the span direction of the suspended floor and roof in each space. Load-bearing walls are numbered from 1 to 7.

Table 6. Characteristics of each loadbearing wall in the 1-storey house alternative.

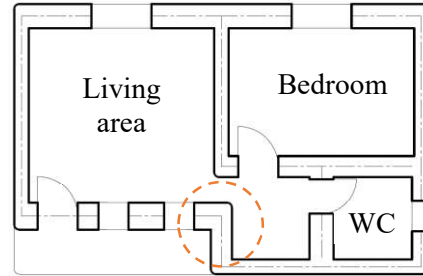
Wall code	Basic LW (m)	Opening ratio (%)	LW scale factor	Effective LW (m)	Corresponding t and d (mm)					
					Type A		Type B		Type C	
					t	d	t	d	t	d
1	2	25	1.5	3	30	300	35	310	35	320
2	2	50	2.0	4	35	310	35	320	35	330
3	1.5	30	1.6	3	30	300	35	310	35	320
4	1.5	15	1.3	2	30	290	35	300	35	310
5	1	5	1.1	1	30	280	30	290	30	300
6	2	30	1.6	3	30	300	35	310	35	320
7	1	40	1.8	2	30	290	35	300	35	310

Table 7. Characteristics of each loadbearing wall in the 2-storey house alternative.

Wall code	Basic LW (m)	Opening ratio (%)	LW scale factor	Effective LW (m)	Corresponding t and d (mm)					
					Type A		Type B		Type C	
					t	d	t	d	t	d
1	2	25	1.5	3	60	480	65	490	60	500
2	2	50	2.0	4	70	535	75	540	70	550
3	1.5	30	1.6	3	60	480	65	490	60	500
4	1.5	15	1.3	2	50	430	55	440	55	450
5	1	5	1.1	1	45	375	50	390	50	400
6	2	30	1.6	3	60	480	65	490	60	500
7	1	40	1.8	2	50	430	55	440	55	450



Adjusted walls for 3DP 1-storey house



Adjusted walls for 3DP 2-storey house

Figure 20. The finalised floor plan indicating the adjusted dimensions of walls for 3DP 1-storey house(left) and 2-storey house (right).

Based on Table 6, it can be seen that the t and d vary minimally between the walls in the case of 1-storey house, regardless of the 3DP pattern (A, B, C). For example, in type A, t ranges between 30–35 mm, and d between 280–310 mm. This is because the wall dimensions are not overly sensitive to the load width in the case of a 1-storey building, as evident from Figure 15. In this instance, the designer may choose to standardise the walls sizes by simply adopting the largest t and d for every wall.

However, this is not the case for the 2-storey house as shown in Table 7, where the optimal sections vary substantially (e.g. for type A: $t = 45\text{--}70$ mm, $d = 375\text{--}535$ mm), thus affecting material quantity dramatically. Therefore, if the designer's ultimate aim is to save material, then it is recommended to find a suitable balance between standardising wall sizes and choosing optimal t and d using the design charts.

Figure 20 (right) shows the adjusted floor plan for the 2-storey example by assigning the minimum required section. It is immediately clear that the walls vary considerably in their sizes, especially for loadbearing and non-loadbearing walls. These differences have a great effect on the overall quantity of materials considering the whole size of the building. It is also essential to notice that the adjusted wall thickness in the case of 2-storey building has an influence on the functionality of the space design. The aisle clearance linking the living area with the bedroom was severely narrowed down due to the increased thickness of the walls on both sides.

This previous discussion reveals the importance of the careful consideration of spanning direction in the design-to-construction process, which must cope with the functionality of the architectural design, as well as other efficiency aspects as previously suggested. To conclude, the following points are important to be considered when selecting the spanning direction:

- The function of the spaces,
- The openings location and clearance, and
- The thermal insulation aspects.

Also, when looking thoroughly into the impact of structural considerations, it becomes clear that the span direction of the floor/roof system and selection of which walls act as load-bearing can also play an important role in creating an efficient balance between structural and architectural requirements. To elaborate this further, Figure 21 illustrates alternate options for the span direction of supporting beams (i.e. floor joists, rafters) comprising the floor/roof

579 structure. The chosen layout influences the required wall sizes, since load-bearing walls
580 (highlighted in red) will require a larger thickness.

581 Solution (1) in Figure 21 has four structural zones, leading to a small load width on each
582 loadbearing wall, and thus enabling smaller wall thicknesses. However, this may create less
583 freedom for design changes as the number of loadbearing walls is large. This can also reduce
584 the functionality of the areas of the small spaces (i.e. toilets and storages) due to the thicker
585 walls. On the other hand, solution (3) shows only two structural zones, which means only three
586 walls in the whole house will act as load bearing. Despite the massive expected thickness of
587 these main walls, this solution can provide high flexibility for the spacing design as the internal
588 walls could be made of lightweight panels, while external walls only will be made of 3DP cob.

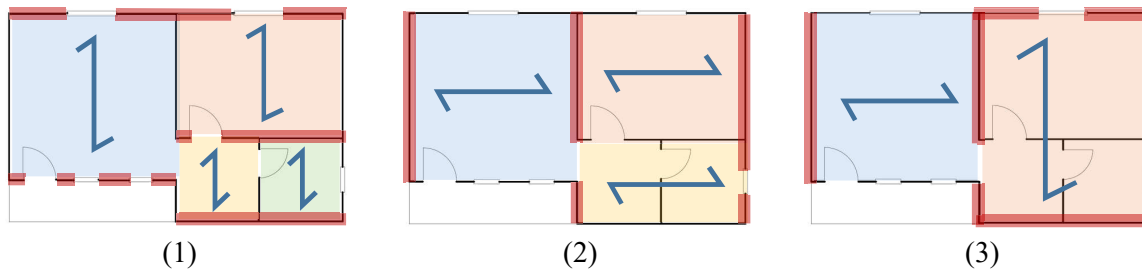


Figure 21. The possible approaches for defining the structural/spanning zones in a small 3DP cob house with indication for spanning direction. (1) Alternative with four structural zones; (2) Alternative with three structural zones; (3) Alternative with two structural zones. The load-bearing walls are highlighted in red.

7. Conclusion

589 The increased intake of 3DP technologies in construction, accompanied with the quest for
590 environmentally efficient materials, has led to leveraging earth-materials in a contemporary
591 3dp process. 3DP cob has been a subject of investigation for several years now; however, where
592 those investigations mostly focused on the design aspects and environmental performance, it
593 lacked proper testing to the 3DP cob's mechanical and structural properties.

594 This study has conducted a comprehensive structural feasibility investigation to the of 3DP
595 cob walls under gravity loads. The study quantified the basic mechanical properties of 3DP cob
596 using a standardised compression test. It then evaluated the expected member capacity of 3DP
597 walls using established structural mechanics and design principles, and by doing so examined
598 the feasibility of 3DP cob walls as load-bearing in typical residential construction. The testing
599 demonstrated that 3DP cob could have very similar mechanical performance to conventional
600 cob on the material scale. The feasibility modelling then demonstrated that 3DP cob walls have
601 the capability to be utilised as structural load-bearing walls in up to 2-storey residential
602 buildings.

603 The feasibility modelling also revealed the following results:

- 604 • 3DP cob walls can sustain structural adequacy for less material consumption compared to
605 conventional cob. That is due the incorporated voids inside the 3DP cob wall, which is hard
606 to be performed in a conventional cob wall with the same thickness.
607

- 608 • The model design approach demonstrated in this paper provides a means for integrating 3DP
609 cob into the design to construction framework. The generated design guidelines are directly
610 linked to a Rhino-Grasshopper definition that enables adequate visual modelling and direct
611 connection to 3DP system.
612 • The dimensions required for load-bearing functionality can be efficiently executed using the
613 available 3DP technologies and extrusion systems.

614 The findings of this study completed a final milestone in full feasibility investigation of 3DP
615 cob for modern construction which combines other three aspects: 1) geometry & fabrication
616 process; 2) thermal performance; and 3) life cycle assessment (LCA). The results lead to a
617 conclusion that 3DP cob provides an excellent alternative to the contemporary digital
618 construction. Also, 3DP cob can provide novel geometric and design opportunities, in addition
619 higher precision when compared to manually constructed cob, especially in producing complex
620 geometries.

621 It is however important to highlight, whilst promising, the findings presented herein are based
622 on material-scale experimental tests combined with structural analysis. Therefore, future
623 research is recommended into experimental testing at the wall member-scale to provide further
624 verification of these findings. This research also initiates new opportunities for further research
625 on exploring the emerging opportunities for workforce under the accelerating intake of
626 automation in construction, particularly under the declining workforce in the indigenous
627 construction fields. This 3DP technology can potentially be a useful mean for cob building
628 repairs (e.g. crack filling, construction of pre-dried cob blocks), as well as providing some
629 degree of adaptation and customisation for cob building design.

630 8. Acknowledgements

631 We would like to acknowledge Dr Alejandro Veliz Reyes for his valuable collaboration and
632 support (University of Plymouth). We also extend our gratitude to Aikaterini Chatzivasileiadi
633 and Anas Lila (Cardiff University) for their invaluable help.

634 9. Funding Resources

635 This work was supported financially by the Engineering and Physical Sciences Research
636 Council (EPSRC) and The University of Nottingham under the Network Plus: Industrial
637 Systems in the Digital Age, Grant number: EP/P001246/1. This work is also partially supported
638 by the University of Adelaide through the Research Abroad Scholarship scheme.

639 10. References

- 640 [1] P. Feng, X. Meng, J.-F. Chen, and L. Ye, “Mechanical properties of structures 3D printed with
641 cementitious powders,” *Constr. Build. Mater.*, vol. 93, pp. 486–497, 2015, doi:
642 10.1016/j.conbuildmat.2015.05.132.
643 [2] A. Kazemian, X. Yuan, E. Cochran, and B. Khoshnevis, “Cementitious materials for
644 construction-scale 3D printing: Laboratory testing of fresh printing mixture,” *Constr. Build.
645 Mater.*, vol. 145, pp. 639–647, 2017, doi: 10.1016/j.conbuildmat.2017.04.015.
646 [3] B. Zareiyan and B. Khoshnevis, “Interlayer adhesion and strength of structures in Contour
647 Crafting - Effects of aggregate size, extrusion rate, and layer thickness,” *Autom. Constr.*, vol.
648 81, no. June, pp. 112–121, 2017, doi: 10.1016/j.autcon.2017.06.013.
649 [4] B. Khoshnevis, “Automated construction by contour crafting — related robotics and

- 650 information technologies,” vol. 13, pp. 5–19, 2004, doi: 10.1016/j.autcon.2003.08.012.
- 1 651 [5] T. T. Le, S. A. Austin, S. Lim, R. A. Buswell, A. G. F. Gibb, and T. Thorpe, “Mix design and
2 652 fresh properties for high-performance printing concrete,” *Mater. Struct. Constr.*, vol. 45, no. 8,
3 653 pp. 1221–1232, 2012, doi: 10.1617/s11527-012-9828-z.
- 4 654 [6] A. Perrot, D. Rängeard, and A. Pierre, “Structural built-up of cement-based materials used for
5 655 3D- printing extrusion techniques,” *Mater. Struct.*, pp. 1213–1220, 2016, doi: 10.1617/s11527-
6 656 015-0571-0.
- 7 657 [7] H. Alhumayani, M. Gomaa, V. Soebarto, and W. Jabi, “Environmental Assessment of large-
8 658 Scale 3D Printing in Construction: A Comparative Study between Cob and Concrete,” *J.
9 659 Clean. Prod.*, p. 122463, Jun. 2020, doi: 10.1016/j.jclepro.2020.122463.
- 10 660 [8] Apis-cor, “Apis Cor 3D printed project in Dubai,” 2019. [https://www.apis-cor.com/dubai-
11 661 project](https://www.apis-cor.com/dubai-project) (accessed Nov. 20, 2019).
- 12 662 [9] CyBe, “3D Studio 2030 — CyBe Construction,” 2019. [https://cybe.eu/case/3d-studio-2030/
13 663](https://cybe.eu/case/3d-studio-2030/) (accessed Nov. 20, 2019).
- 14 664 [10] IEA and UNEP, “International Energy Agency and the United Nations Environment
15 665 Programme - Global Status Report 2018: Towards a zero- emission, efficient and resilient
16 666 buildings and construction sector,” p. 325, 2018, doi: 978-3-9818911-3-3.
- 17 667 [11] E. Hamard, B. Cazacliu, A. Razakamanantsoa, and J. C. Morel, “Cob, a vernacular earth
18 668 construction process in the context of modern sustainable building,” *Build. Environ.*, vol. 106,
19 669 pp. 103–119, 2016, doi: 10.1016/j.buildenv.2016.06.009.
- 20 670 [12] C. Shrubsole *et al.*, “Bridging the gap: The need for a systems thinking approach in
21 671 understanding and addressing energy and environmental performance in buildings,” *Indoor
22 672 Built Environ.*, vol. 28, no. 1, pp. 100–117, 2019, doi: 10.1177/1420326X17753513.
- 23 673 [13] S. Ford and M. Despeisse, “Additive manufacturing and sustainability: an exploratory study of
24 674 the advantages and challenges,” *J. Clean. Prod.*, vol. 137, pp. 1573–1587, 2016, doi:
25 675 10.1016/j.jclepro.2016.04.150.
- 26 676 [14] E. Quagliarini, A. Stazi, E. Pasqualini, and E. Fratolocchi, “Cob construction in Italy: Some
27 677 lessons from the past,” *Sustainability*, vol. 2, no. 10, pp. 3291–3308, 2010, doi:
28 678 10.3390/su2103291.
- 29 679 [15] F. Pacheco-Torgal and S. Jalali, “Earth construction: Lessons from the past for future eco-
30 680 efficient construction,” *Constr. Build. Mater.*, vol. 29, pp. 512–519, 2012, doi:
31 681 10.1016/j.conbuildmat.2011.10.054.
- 32 682 [16] T. Morton, F. Stevenson, B. Taylor, and N. C. Smith, “Low Cost Earth Brick Construction:
33 683 Monitoring & Evaluation,” Fife, UK, 2005. [Online]. Available: [http://www.arc-
34 684 architects.com/downloads/Low-Cost-Earth-Masonry-Monitoring-Evaluation-Report-2005.pdf](http://www.arc-architects.com/downloads/Low-Cost-Earth-Masonry-Monitoring-Evaluation-Report-2005.pdf).
- 35 685 [17] L. Ben-Alon, V. Loftness, K. A. Harries, and E. Cochran Hameen, “Integrating Earthen
36 686 Building Materials and Methods into Mainstream Construction Using Environmental
37 687 Performance Assessment and Building Policy,” *IOP Conf. Ser. Earth Environ. Sci.*, vol. 323,
38 688 no. January, p. 012139, 2019, doi: 10.1088/1755-1315/323/1/012139.
- 39 689 [18] I. Agustí-Juan, F. Müller, N. Hack, T. Wangler, and G. Habert, “Potential benefits of digital
40 690 fabrication for complex structures: Environmental assessment of a robotically fabricated
41 691 concrete wall,” *J. Clean. Prod.*, vol. 154, pp. 330–340, 2017, doi:
42 692 10.1016/j.jclepro.2017.04.002.
- 43 693 [19] A. Veliz Reyes, W. Jabi, M. Gomaa, A. Chatzivasileiadi, L. Ahmad, and N. M. Wardhana,
44 694 “Negotiated matter: a robotic exploration of craft-driven innovation,” *Archit. Sci. Rev.*, vol. 0,
45 695 no. 0, pp. 1–11, 2019, doi: 10.1080/00038628.2019.1651688.
- 46 696 [20] 3D-WASP, “3D Printers | WASP | Leading Company in the 3d printing industry,” 2020.
47 697 <https://www.3dwasp.com/en/> (accessed Jan. 10, 2020).
- 48 698 [21] M. Gomaa, W. Jabi, A. Veliz Reyes, and V. Soebarto, “Development of a 3D Printing System
49 699 for Earth-based construction: Case Study of Cob Walls,” *Autom. Constr.*, 2020.
- 50 700 [22] M. Gomaa, J. Carfrae, S. Goodhew, W. Jabi, and A. Veliz Reyez, “Thermal performance
51 701 exploration of 3D printed cob,” *Archit. Sci. Rev.*, pp. 1–8, Apr. 2019, doi:
52 702 10.1080/00038628.2019.1606776.
- 53 703 [23] O. O. Akinkurolere, C. Jiang, A. T. Oyediran, O. I. Dele-Salawu, and A. K. Elensinnla,
54 704 “Engineering properties of Cob as a building material,” *Journal of Applied Sciences*, vol. 6,

- no. 8. pp. 1882–1885, 2006, doi: 10.3923/jas.2006.1882.1885.
- [24] J. Fordice and L. Ben-Alon, “A research project dedicated to making cob legally accessible to the public,” 2017.
- [25] E. Kianfar and V. Toufigh, “Reliability analysis of rammed earth structures,” *Constr. Build. Mater.*, vol. 127, pp. 884–895, 2016, doi: 10.1016/j.conbuildmat.2016.10.052.
- [26] L. Keefe, *Earth building : methods and materials, repair and conservation*. 2005.
- [27] A. Weismann and K. Bryce, *Building with cob: a step-by-step guide*. Devon: Green Books Ltd, 2006.
- [28] L. Miccoli, U. Müller, and P. Fontana, “Mechanical behaviour of earthen materials: A comparison between earth block masonry, rammed earth and cob,” *Constr. Build. Mater.*, vol. 61, pp. 327–339, 2014, doi: 10.1016/j.conbuildmat.2014.03.009.
- [29] Earth Devon, “Cob Dwellings: Compliance with The Building Regulations,” *Cob Unbaked Earth Dwellings*, vol. 2000, pp. 1–21, 2008.
- [30] Q. M. Pullen and T. V. Scholz, “Index and engineering properties of Oregon Cob,” *J. Green Build.*, vol. 6, no. 2, pp. 88–106, 2011, doi: 10.3992/jgb.6.2.88.
- [31] H. Houben and H. Guillaud, *Earth construction: a comprehensive guide*. London: Intermediate Technology Publications, 1994.
- [32] E. Quagliarini and G. Maracchini, “Experimental and FEM Investigation of Cob Walls under Compression,” *Adv. Civ. Eng.*, vol. 2018, pp. 21–29, 2018, doi: 10.1155/2018/7027432.
- [33] M. Rizza and H. Bottger, “Effect of Straw Length and Quantity on Mechanical Properties of Cob,” San Francisco, 2015. [Online]. Available: http://umanitoba.ca/faculties/engineering/departments/ce2p2e/alternative_village/media/16th_NOCMAT_2015_submission_42.pdf.
- [34] G. Brunello, J. Espinoza, and A. Golitz, “Cob Property Analysis,” Santa Clara University, 2018.
- [35] D. J. Wright, “BUILDING FROM THE GROUND UP : UNDERSTANDING AND PREDICTING THE STRENGTH OF COB , AN EARTHEN CONSTRUCTION MATERIAL,” 2019.
- [36] A. Veliz Reyes, M. Gomaa, A. Chatzivasileiadi, and W. Jabi, “Computing Craft: Early stage development of a robotically-supported 3D printing system for cob structures,” in *eCAADe-Computing for better tomorrow*, 2018, vol. 1, pp. 791–800.
- [37] A. Perrot, D. Rangeard, and E. Courteille, “3D printing of earth-based materials: Processing aspects,” *Constr. Build. Mater.*, vol. 172, pp. 670–676, 2018, doi: 10.1016/j.conbuildmat.2018.04.017.
- [38] A. Perrot, D. Rangeard, and T. Lecompte, “Field-oriented tests to evaluate the workability of cob and adobe,” *Mater. Struct. Constr.*, vol. 51, no. 2, pp. 1–10, 2018, doi: 10.1617/s11527-018-1181-4.
- [39] S. Goodhew, P. C. Grindley, and S. D. Probeif, “Composition, Effective Thermal Conductivity And Specific Heat Of Cob Earth-walling,” *WIT Trans. Built Environ.*, vol. 16, Jan. 1995, doi: 10.2495/STR950231.
- [40] CEN, “EN 772-1. Methods of test for masonry units - Part 1: Determination of compressive strength,” 2011. [Online]. Available: https://infostore.saiglobal.com/en-us/Standards/EN-772-1-2011-A1-2015-331320_SAIG_CEN_CEN_761952/.
- [41] Standards Australia, *AS 1170.1–2002 (R2016) Structural design actions Part 1 : Permanent , imposed and other actions*. Sydney, NSW: Australian / New Zealand Standard TM, 2002.
- [42] Standards Australia, *Australian Standard for Masonry structures (AS 3700:2018)*. Sydney, NSW: Australian / New Zealand Standard TM, 2018.
- [43] R. McNeel, “Grasshopper - in Rhino 6,” 2020. <https://www.rhino3d.com/6/new/grasshopper> (accessed Jul. 30, 2020).
- [44] S. G. Johnson, “NLOpt Documentation,” 2010. <https://nlopt.readthedocs.io/en/latest/> (accessed Jul. 30, 2020).

Highlights

- Basic mechanical properties of 3D printed cob were experimentally quantified.
- Mechanical properties of 3DP cob are similar to traditional cob.
- A model technique for compression design is demonstrated using a limit state framework.
- Loadbearing 3DP cob wall are shown to be feasible for residential construction up to 2 stories.

Declaration of interests

The authors declare that they have no known competing financial interests or personal relationships that could have appeared to influence the work reported in this paper.

The authors declare the following financial interests/personal relationships which may be considered as potential competing interests:

CRediT author statement

Mohamed Gomaa: Conceptualization, Methodology, Data curation, Formal analysis, Investigation, Resources, Software, Validation, Visualization, Writing - original draft, Writing - review & editing, Project administration, Funding acquisition

Jaroslav Vaculik: Conceptualization, Methodology, Data curation, Formal analysis, Investigation, Resources, Software, Validation, Visualization, Writing - original draft, Writing - review & editing.

Veronica Soebarto: Conceptualization, Writing - review & editing, Supervision

Michael Griffith: Methodology, Writing - review & editing, Supervision

Wassim Jabi: Resources, review & editing, funding acquisition

**Appendix III: Manuscript- Thermal performance
exploration of 3D printed cob.**

Thermal performance exploration of 3D printed cob

Mohamed Gomaa ^{a,c}, Jim Carfrae^b, Steve Goodhew ^b, Wassim Jabi ^c and Alejandro Veliz Reyes ^b

^aSchool of Architecture and built environment, University of Adelaide, Adelaide, Australia; ^bSchool of Art, Design and Architecture, University of Plymouth, Plymouth, UK; ^cWelsh School of Architecture, Cardiff University, Cardiff, UK

ABSTRACT

This paper investigates the thermal properties of 3D printed Cob, a monolithic earth construction technique based on robotically extruded subsoil and locally available organic fibres. The relevance of 3D printed earthen construction materials and the transition from vernacular construction towards a digitally-enabled process are critically discussed. The use of robotic manufacturing is outlined and the methodology to produce the necessary samples for thermal measurement is detailed. The results of the 3D printed samples are compared with traditionally-constructed Cob material of the same dimensions. The assessment has revealed strong potential for 3D printed cob as compared to its manually constructed counterparts in terms of thermal conductivity. Moreover, the testing process has helped in identifying several challenges in the 3D printing process of cob and the assessment of its thermal properties, which will ultimately bring the work closer to full-scale applications.

ARTICLE HISTORY

Received 21 October 2018
Accepted 8 April 2019

KEYWORDS

Robotics; 3d printing; cob construction; parametric design; thermal analysis; vernacular architecture

Introduction



Conventional monolithic (e.g. concrete) construction has several associated shortcomings such as high CO₂ emissions, high embodied energy of construction process and depletion of natural resources (Goodhew and Griffiths 2005). In contrast, this paper presents cob construction as a viable alternative. Cob stands as the most used construction material around the world (Figure 1), and consists of subsoil (earth), water, fibrous material (typically straw) and sometimes lime. Other mixtures can use an addition of sand and/or clay, if required, in order to improve the physical properties of the material mix (Hamard et al. 2016). Given the reliance of this material on localized modes of construction, its application in built elements can be found in a series of material configurations including adobe bricks or 'quinchas' (clay-based soil mix applied onto a woven pattern of fibrous materials). Likewise, a series of geometric and formal configurations can be found in vernacular architecture which illustrate the versatility and structural characteristics of cob construction, including circular configurations in China and ovoid configurations in African vernacular architecture.

Cob is a sustainable material as compared with concrete, requires very limited resources to be sourced, mixed and constructed (Benardos, Athanasiadis, and Katsoulakos 2014). Moreover, Hamard et al. (2016) and Wanek, Smith, and Kennedy (2015) have demonstrated that re-using cob will have building performance and financial benefits, while it complies with modern UK building regulations.

In terms of design opportunities, cob provides higher freedom of design and ease of construction, while also it allows design modifications (cutting or adding material) easily at any

time when the building element's cob is still wet or dry (Melià et al. 2014; Hamard et al. 2016). This malleability, low cost and building performance suggest further work is required in order to understand the opportunities offered by cob in the new digital age, and particularly on novel and emergent frameworks of digital practice and design, such as robotic fabrication. Within this research territory, this paper explores the suitability of raw-earth in the research territory of robotically-assisted 3D printing. It is acknowledged that the consideration of raw-earth for 3D printing applications can reveal a series of potential lines of enquiry, such as mechanical and structural properties, new design and formal opportunities, new local economies and skilled labour, or environmental and geological considerations. This report stems from the project 'Computing craft' which aims at scoping the feasibility for robotically 3D printed cob structures at early stages of the technology development cycle, and further work is required to determine properties of larger scale cob construction. In response to this project's life cycle, we specifically introduce this area of enquiry by assessing the thermal performance of 3D printed cob in comparison with handmade cob samples.

In order to critically situate this research within the broader area of 3D printing, cob must be defined in relation to its vernacular constructive expression, and particularly on how it can be adopted and modified in the context of emergent digital practices. Here, vernacular architecture and construction are not seen as primitive or historical, but instead as a series of local sophisticated material practices which engage with and address local environmental and material conditions. It is acknowledged, then, that the perception of vernacular architecture has been

CONTACT Mohamed Gomaa  mohamed.gomaa@adelaide.edu.au  School of Architecture and built environment, University of Adelaide, Adelaide, Australia
Welsh School of Architecture, Cardiff University, Cardiff, UK

This article has been republished with minor changes. These changes do not impact the academic content of the article.

© 2019 The Author(s). Published by Informa UK Limited, trading as Taylor & Francis Group

This is an Open Access article distributed under the terms of the Creative Commons Attribution License (<http://creativecommons.org/licenses/by/4.0/>), which permits unrestricted use, distribution, and reproduction in any medium, provided the original work is properly cited.



Figure 1. Cob building in Totnes, UK (Veliz Reyes et al. 2018).

evolving to reflect different environmental, technological and cultural contexts (Niroumand, Barceló Álvarez, and Saaly 2016). Aligned with this, earthen materials have received renewed interest within the modern construction industry for the past few years (Chandel, Sharma, and Marwah 2016; Veliz Reyes et al. 2018). As a result, it can be claimed that despite its vernacular development, cob is currently being subjected to a series of studies aiming at incorporating this local, material-based knowledge within established frameworks of practice and academic research and development (e.g. Veliz et al. 2018).

Much of the material performance outside the confines of life-cycle assessment relates to the thermal properties of earthen building techniques and subsequent materials (Houben and Guillaud 1994; Hurd and Gourley 2000; Walker et al. 2005). This has been assessed in a number of different design configurations, including different sequences of material layers and the inclusion of natural insulation (Steven Goodhew and Griffiths 2005; Griffiths and Goodhew 2012). Many of these proposed or measured material configurations specify appropriate thermal characteristics, such as thermal conductivity (W/mK) or specific heat capacity (J/kg/degC). Thermal conductivity is a property that is used to calculate (whether in the more raw form of a spreadsheet or more complex and animated use of dynamic thermal simulations) the ability for a building built from the material to perform as expected. This performance might be associated with the thermal comfort of the occupants or the energy use of the building (CIBSE 2015). Therefore, much interest is centred on the ability for an earthen material, that can be made from different subsoil types and mixed at different ratios with a range of different fibres, to fulfil technical and legislative requirements.

In the present era, cob construction techniques operate under established frameworks of practice often based on notions of hand-making, hand-assembling and localized material intelligence. This operational knowledge has been developed over many years outside the boundaries of academic, technological and professional disciplinary frameworks (Crysler, Cairns, and Heynen 2012). At the same time, the construction industry has been demanding more complex forms, faster processes, and lower labour costs, which are making traditional construction methods increasingly obsolete (Veliz Reyes et al. 2018). Hence, Digital construction of earthen materials could be instrumental to promoting the use of locally available natural construction materials as it expands the range of sustainable construction solutions that are adapted to local contexts (Hamard et al. 2016; Veliz Reyes et al. 2018), following the key precepts of vernacular architecture such as local, material-driven knowledge and practices.

The benefits of digitally augmented crafts have been examined broadly only on small-scale applications, yet the greater benefits for the design and construction industry are poorly explored. An early study that was conducted at ETH Zurich by Gramazio, Kohler, and Willmann in 2008 has revealed the ability of robotic technology to directly create informed design solutions based on materials and manufacturing restraints (Veliz Reyes et al. 2018). This early experimentation has raised the awareness of digital fabrication, and particularly additive manufacturing, within the AEC industries worldwide (Hague, Campbell, and Dickens 2003; Wu, Wang, and Wang 2016). The continuous experimentation with digital fabrication methods in recent years has created substantial enhancements to large-scale 3D printing techniques (Baumers et al. 2016; Ishak, Fisher, and Larochelle 2016).

This dramatic increase in the amount of research on implementing 3D printing into large-scale processes has revealed several potential applications for architecture and the construction industry (Agustí-Juan and Habert 2017; Wu, Wang, and Wang 2016), such as reductions in waste, material usage, and transportation costs in the supply chain. In this respect, both Hamard et al. (2016) and (Agusti-Juan et al. 2017) highlight that the integration of digital fabrication techniques into vernacular architecture has revealed sustainability potentials for construction applications. However, this research has also revealed further challenges to be addressed that include not only the development of novel 3D printing robotic applications, but more broadly their implications for the AEC industry such as the need for skilled labour, new material configurations, or new design and geometric opportunities.

Methods and materials

Prototypes design

This study is mainly assessing the thermal conductivity of four scaled prototypes of 3D printed cob specimens. Then the research compares the result to seven cob specimens of nearly the same dimensions that were constructed using manual techniques. The prototypes are scaled down to one fourth (1/4) the average real cob walls thickness. The geometries of prototypes are modelled in Rhinoceros via Grasshopper, while kuka PRC was

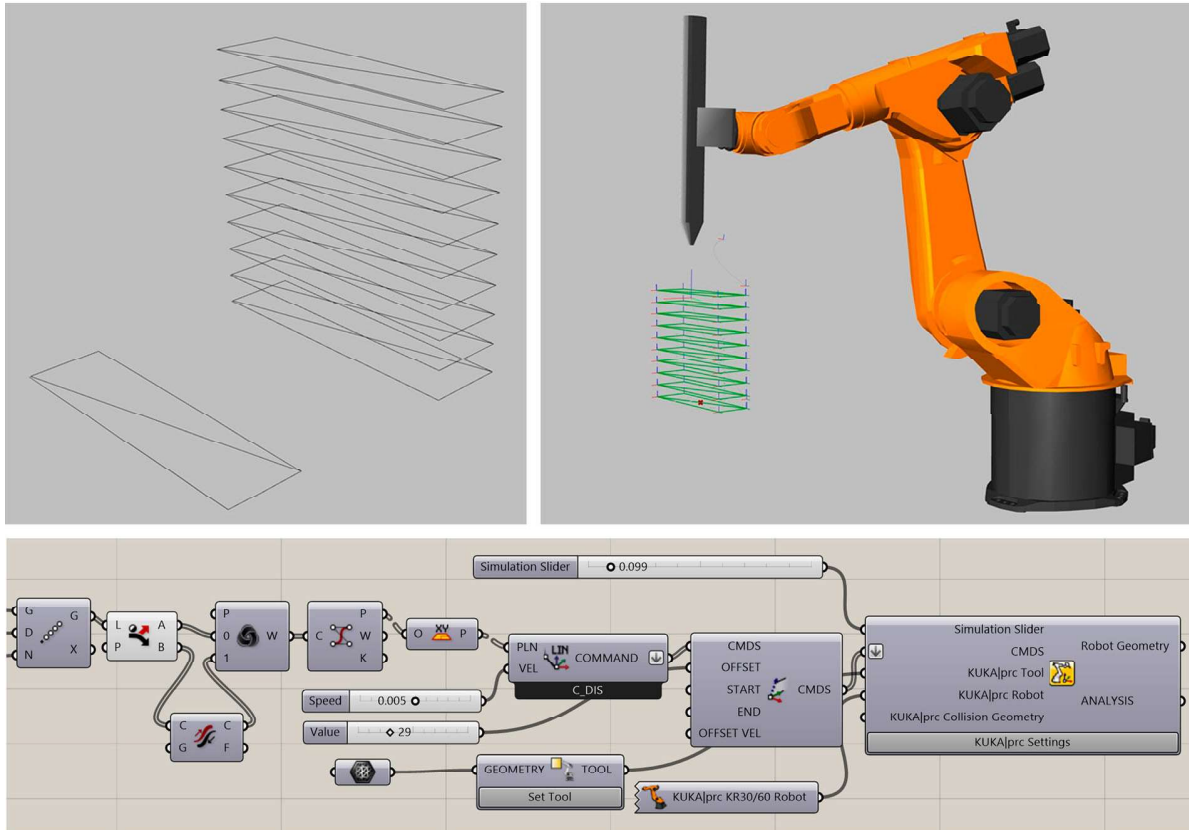


Figure 2. Creating the toolpath for cob prototypes in rhino via grasshopper and kuka PRC.

the used tool for robotic simulation (Figure 2). Each model is designed on the basis of unidirectional tool paths then arrayed vertically to create the full height of the specimen. Some of the geometric constraints for toolpath design have been outlined as:

- The layer heights have been set to 18 mm. and the diameter of the nozzle in all experiments was 25 mm, yet, due to the fluid nature of the material, it was expected that a 35–40 mm thick cob path would be created.
- Printing speeds has been set at 10 mm/sec
- Initially all toolpaths have been created following a standard 3-axis contour crafting approach (X, Y, Z).

Virtual prototypes were then 3D printed at Cardiff University using a Kuka KR60HA robot and a custom designed material extrusion system (Figure 2). The extrusion system utilizes a stepper motor with a worm gearbox and acme screw that pushes the wet cob mix through a tube with a 25 mm nozzle at its end. Each 3D printed sample consumed nearly two hours for production (including the time to replace the cob cartridge). The designed geometries are converted into multi-layered path lines of which the robotic arm can follow in a layer by layer fashion (Figure 3). Each of the four prototypes was designed to represent a different solution for better thermal insulation of walls (Figure 4).

- (1) The first prototype was designed as a solid wall (CF1).
- (2) The second prototype was design as a double-layered wall with a single continuous air gap (CF2).

- (3) The third prototype was designed as a triple-layered wall with air pockets (CF3).
- (4) The fourth prototype was designed as double-layered wall with pockets filled with straw (CF4).

The 3D printed samples have dimensions of (300 × 300 × 90 mm), while the manually constructed samples (Figure 5) are (300 × 300 × 70 mm), both formed into blocks of a suitable size for the heat flow metre (Figure 6). The air gaps in the 3d printed cob samples is a natural result of the 3D printing technique and design workflow, while they are created without the use of formwork. This eventually leads to a reduction in time, the overall weight and used raw material while maintain the same volume as compared to conventional cob.

Materials

As stated earlier, cob basically is a mix of subsoil, fibre, and water. Weismann and Bryce (2006) recommended a generic ratio of water to subsoil as one part water to every five parts of dry ingredient. By converting this to weight, it means 2.0 Kg of water is added to each 8.0 Kg of subsoil. As for the straw, it is recommended to be 2% by weight. Hamard et al. (2016) supported the previous statement in his extensive systematic review on cob by affirming the proportions of cob mixture (averages) to be 78% subsoil, 20% water and 2% fibre (straw).

According to both Weismann and Bryce (2006) and Hamard et al. (2016), the recommendation for the subsoil formula itself is 15–25% clay to 75–85% aggregate/sand. Harrison (1999)



Figure 3. The 3D printing set up in Cardiff University; KUKA KR60 HA robot with a custom designed material extrusion system.

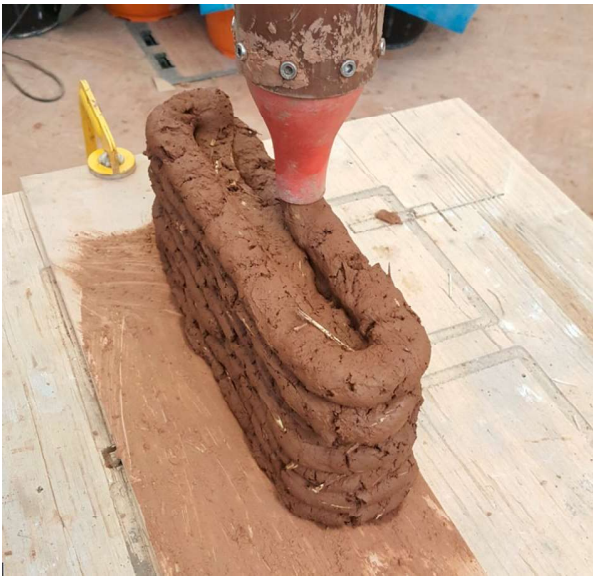


Figure 4. The Layer by layer technique of printing.

also stated similar recommendation of 20% clay to 80% aggregate/sand. Testing the subsoil properties is a critical step for the right determination of the cob formula. Testing occurs on the subsoil before water content is added. Subsoil contains different amount of clay, sand, silt and aggregate. This depends on the

sourcing location and where the subsoil is being dug within that location. Based on several field testing of the subsoil, besides using a trial and error method, amendment to sand and clay ratios could be identified to achieve the right ingredient for cob. After examining the subsoil, the next step is to add the water and fibres, which is straw for this study. Other bindings fibres can be used such as seaweed and alginate (Perrot, Rängeard, and Courteille 2018).

3D Printed cob samples

The subsoil for the 3D printed samples for this study was sourced from farmland near Barry in Cardiff, UK. Three subsoil specimens from three locations within the same field were examined according to the recommended testing methods that are found in the literature (Goodhew, Grindley, and Probeif 1995; Harrison 1999; Weismann and Bryce 2006). These tests included simple field tests and in-depth laboratory tests. Both testing methods have revealed that the ingredients of the subsoil are matching the general recommendations for cob mixture without applying any additional aggregates or clay. The subsoil samples from Cardiff were found to have an average aggregate to clay ratio as 79.5 to 21.5% respectively.

Since cob is typically mixed in a nearly dry state, the previous proportions do not fit the purpose of 3D printing. The relatively low water content of the mix creates massive friction in the extrusion circuit, which then generates enormous pressure on the extrusion system joints. This continues pressure leads to the destruction of the holding parts and it increases the wear rate of the electric actuators. Hence, a more viscous mix is required. However, the increase of water content can affect negatively other material properties including shrinkage, drying time and mechanical/structural stability during the 3D printing process, leading consequently to limitations in the layering heights and the overall quality of a printed prototype (Veliz Reyes et al. 2018).

Several 3D printing tests were conducted to reach a modified proportions of cob mixtures for 3D printing purposes. These tests mainly examined how the cob mix rheology is influenced by the following factors:

- (a) Water content in the cob mix
- (b) Extrusion speed (relative to the robot speed)
- (c) Layer height (relative to the nozzle diameter)

Testing process included systematic alteration of each factor. Water content was tested as 22, 24, 26, and 28%. Extrusion speed was tested on a range from 0.01 to 0.1 m/sec, while layer height was tested as 30, 60 and 90% of the nozzle size. Worth mentioning that the layer height always preferred to be less than the used nozzle diameter in order to create a flat surface that can support the following layer. The new mixture has an increase in the water content to 25–26%, a subsoil ratio of 72–73% and a straw ratio to 2%. In all cases, field tests of the subsoil properties are always recommended and required prior to determining the appropriate cob mix.

Manually constructed cob samples

The manually constructed cob samples were prepared at Plymouth University as part of the Interreg project 'The CobBauge'



Figure 5. Samples of the 3d printed cob. From left to right; solid, single gap with straw filling and double gap.



Figure 6. Samples of the manually constructed cob specimen in Plymouth University. The cob sample to the left uses UK subsoil in the mix, while the right one uses French subsoil.

(The CobBauge Project 2018). These samples were prepared in the lab using a variety of sub-soils that had been identified as being suitable for use in cob construction without additional aggregates. The soils were then analyzed for particle size distribution. These tests were carried out by wet sieving for the fraction greater than 80 μm and by laser granulometry for elements smaller than 80 μm . The soils are identified as FR4, a sandy yellow French soil with a low clay content and UK3, a heavy red clay soil from mid Devon (UK). The subsoils had a variety of fibres added to them in different proportions based on the literature (Hamard et al. 2016), and the accumulated experience on several actual cob building projects.

The fibres used in these tests were hemp shiv, chopped reed and chopped straw in proportions of 8%, 4%, 2% and none (% by dry weight of soil). The soils were first oven dried at 40°C until they reached an equilibrium weight, where 3 subsequent weighing's at 24 hour intervals were within 1% of each other, then a percentage of water was added: 28% to the FR4, and 31% to UK3 (the different amounts of water were added to give the same viscosity to the final mix). After allowing the clays to soak, the fibres were added and mixed manually.

Thermal performance testing

To establish the thermal performance of the material, a series of conductivity tests were undertaken using a Heat Flow Meter at Plymouth University (Figure 7). The four 3D printed cob samples were compared to seven manually-constructed cob samples.

The heat flow metre used for the conductivity tests was a Netzsch HFM 446 (NETZSCH 2018). This machine is based on ASTM C518, ASTM C1784, ISO 8301, JIS A1412, DIN EN 12664, and DIN EN 12667 Method and Technique for the Characterization of Insulation Materials. The Netzsch was chosen because it takes a larger sample size and uses additional external thermocouples in conjunction with the hot and cold plates. This makes it suitable for measuring denser, more random materials like cob.

The thermal measuring process requires samples of a certain size and geometry. Thus, the results are influenced by the thermal measurement technique and the geometry produced via the 3d printing process. Comparability of samples could be improved by using the same cob mix in both conventional and 3d printing technique. Yet, the cob mix used for 3d printing purposes needs to combine a higher water content at 25–26% and low straw ratio at 2% as compared to conventional cob mix.

Results

Table 1 shows all the tested cob samples, listed in order of their conductivities. The close relation between density and conductivity could be also seen (Volhard and Reisenberger 2016). The graph in Figure 8 shows the relationship between conductivity and density of all the cob samples. Walls with lower conductivity and lower density, towards the left bottom corner of the figure, are more desirable due to their higher insulation value and lighter weight. The conductivity results show that all specimens conform to within 10% of each other. The dotted line

Table 1. Results of the Conductivity analysis of the cob samples in relation to their density.

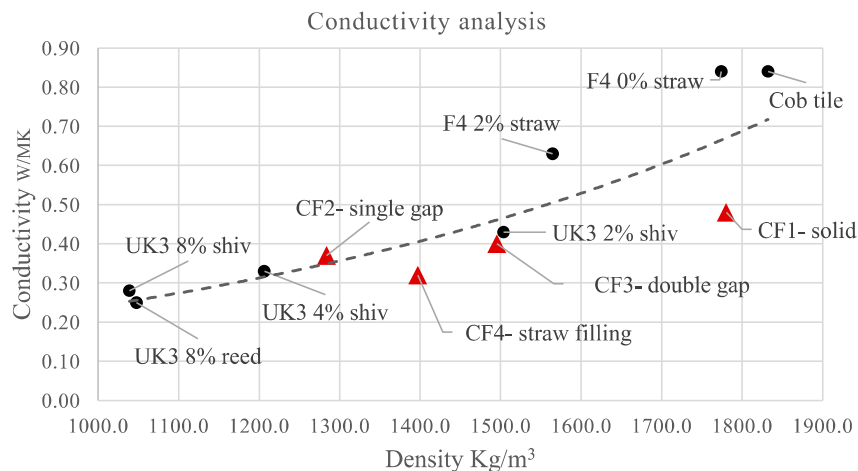
Sample	Method	Density (kg/m ³)	Conductivity (W/mk)
UK3 8% reed	Manual	1047.6	0.25
UK3 8% shiv	Manual	1038.7	0.28
CF4 Straw fill	3d printed	1397.0	0.32
UK3 4% shiv	Manual	1206.5	0.33
CF2 Single-Gap	3d printed	1283.7	0.37
CF3 Double-Gap	3d printed	1495.5	0.40
UK3 2% shiv	Manual	1503.8	0.43
CF1 Solid	3d printed	1780.3	0.48
F4 2% straw	Manual	1564.5	0.63
F4 0% straw	Manual	1774.3	0.84
Cob Tile	Manual	1832.3	0.84

shows an exponential trend in the relationship between the density and conductivity of the samples (Domínguez-Muñoz et al. 2010). Of the four printed samples, the three that are not solid are all below this line. This indicates that the cavities in the samples are affecting their performance, and giving a relatively better conductivity in relation to their density).

The percentage of straw in the cob mixture of the 3D specimens was kept constant at 2%. The differences were in the

design of the specimen cross-section and the addition of loosely packed straw in air cavities. The analysis indicates that the use of air cavities combined with the addition of straw into them significantly improves the conductivity of the 3D printed samples relative to their density. Specifically, CF4 (Air gap with straw) showed an improvement of 15.0% in conductivity and an increase of 8.0% in density when compared to CF2 (Air gap without straw). In terms of absolute conductivity, sample CF4, with the straw filling, gives the best result among the 3D printed samples due to its lower conductivity regardless of density. Within manually constructed samples, the higher percentage of fibres in the mix lead to lower density and consequently a lower conductivity.

Compared to all samples, CF4 represented the third best result. The significant thermal performance of the 3D printed samples is immediately recognized among their manually-structured counterparts. Even when comparing solid samples, the CF1 specimen out-performed approximately half the manually-constructed samples. The relationship between density and conductivity is plotted for a range of conventionally mixed soil and fibre mixes. There is no reference for an extruded material, so further work will be needed to establish the appropriate relationship.

**Figure 7.** Heat flow metre (HFM 446) at Plymouth University.**Figure 8.** Conductivity of all the cob samples in relation to their density.

Conclusions

the results detailed above reveal that 3D printed cob is comparable with hand-made counterparts. While the 3D printed samples do not outperform the hand-made samples significantly, the results suggest that 3D printing can be utilized for cob construction without compromising the building performance of the construction, thus revealing further opportunities for research by exploring additional benefits of robotic fabrication, including (among others):

- Novel geometric and design opportunities.
- Higher precision and accuracy of the built element when compared to manual labour, specially in producing complex geometries
- Exploring emerging opportunities in the field of robotics in terms of skills automation, as well as to develop new skills in the construction workforce.
- Scoping new opportunities afforded by recent development in the fields of robotics and material sciences including human-robot collaboration, artificial intelligence and data-driven design processes.

This study, on the other hand, has exposed major challenges of cob 3D printing during the early stage of experimentation. Three main challenges were specified: extrusion speed, consistency of extrusion, and continuity of extrusion. Hence, the project team has been developing an innovative bespoke large-scale cob extruder that has improved dramatically the preceding challenges. The new extrusion system is capable of achieving variable high speeds up to 0.3 m/sec, while combining an enhanced cartridges system that allows a continuous extrusion of material. The details of the new system will be introduced as part of a future study. Another line of future studies will focus on establishing a viable business model, utilizing robotically fabricated building components for small-scale building solutions.

Acknowledgments

We would like to acknowledge the continuous guidance and support of Professor Veronica Soebarto (University of Adelaide). We would also like to acknowledge the invaluable help of Lina Ahmad (Zayed University, UAE), Anas Lila, Aikaterini Chatzivasilieiadi (Cardiff University).

Disclosure statement

No potential conflict of interest was reported by the authors.

Funding

This work is supported by the Engineering and Physical Sciences Research Council (EPSRC) and The University of Nottingham under the Network Plus: Industrial Systems in the Digital Age, Grant number: EP/P001246/1 (Feasibility study PI: Dr. Wassim Jabi, Cardiff University). Some measurements contained in this paper were conducted as part of the CobBauge project which is an Interreg programme, financed by the European Union.

ORCID

Mohamed Goma  <http://orcid.org/0000-0001-9463-4888>

Steve Goodhew  <http://orcid.org/0000-0003-1227-217X>

Wassim Jabi  <http://orcid.org/0000-0002-2594-9568>

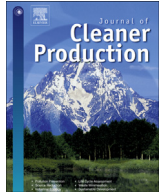
Alejandro Veliz Reyes  <http://orcid.org/0000-0002-5044-1782>

References

- Agustí-Juan, Isolda, and Guillaume Habert. 2017. "Environmental Design Guidelines for Digital Fabrication." *Journal of Cleaner Production* 142 (Elsevier Ltd): 2780–2791. doi:10.1016/j.jclepro.2016.10.190.
- Agustí-Juan, Isolda, Florian Müller, Norman Hack, Timothy Wangler, and Guillaume Habert. 2017. "Potential Benefits of Digital Fabrication for Complex Structures: Environmental Assessment of a Robotically Fabricated Concrete Wall." *Journal of Cleaner Production* 154 (Elsevier Ltd): 330–340. doi:10.1016/j.jclepro.2017.04.002.
- Baumers, Martin, Phill Dickens, Chris Tuck, and Richard Hague. 2016. "The Cost of Additive Manufacturing: Machine Productivity, Economies of Scale and Technology-Push." *Technological Forecasting and Social Change* 102 (Elsevier Inc.): 193–201. doi:10.1016/j.techfore.2015.02.015.
- Benardos, A., I. Athanasiadis, and N. Katsoulakos. 2014. "Modern Earth Sheltered Constructions: A Paradigm of Green Engineering." *Tunnelling and Underground Space Technology* 41 (1): Elsevier Ltd: 46–52. doi:10.1016/j.tust.2013.11.008.
- Chandel, S. S., Vandna Sharma, and Bhanu M. Marwah. 2016. "Review of Energy Efficient Features in Vernacular Architecture for Improving Indoor Thermal Comfort Conditions." *Renewable and Sustainable Energy Reviews* 65 (Elsevier): 459–477. doi:10.1016/j.rser.2016.07.038.
- CIBSE. 2015. *Guide A: Environmental Design*. London: CIBSE
- Crysler, Christopher Greig, Stephen Cairns, and Hilde Heynen. 2012. *The SAGE Handbook of Architectural Theory*. SAGE. https://books.google.co.uk/books?hl=en&lr=&id=n354cBry_6EC&oi=fnd&pg=PP1&dq=Concepts+of+vernacular+architecture'+in+Crysler&ots=Pw24wWdCl-&sig=SNo-Gw-HqS2YldnJ573uAL73kXo&redir_esc=y#v=onepage&q=Concepts+of+vernacular+architecture'%2C+in+Crysler&f=false.
- Dominguez-Muñoz, Fernando, Brian Anderson, José M. Cejudo-López, and Antonio Carrillo-Andrés. 2010. "Uncertainty in the thermal conductivity of insulation materials." *Energy and Buildings* 42 (11): 2159–2168. doi:10.1016/j.enbuild.2010.07.006.
- Goodhew, Steven, and Richard Griffiths. 2005. "Sustainable Earth Walls to Meet the Building Regulations." *Energy and Buildings* 37 (Elsevier): 451–459. doi:10.1016/j.enbuild.2004.08.005.
- Goodhew, Steve, P. C. Grindley, and S. D. Probeif. 1995. "Composition, Effective Thermal Conductivity And Specific Heat Of Cob Earth-Walling." *WIT Transactions on The Built Environment* 16 (January). WIT Press. doi:10.2495/STR950231.
- Griffiths, Richard, and Steve Goodhew. 2012. "Sustainability of Solid Brick Walls with Retrofitted External Hemp-Lime Insulation." *Structural Survey* 30 (4): Emerald Group Publishing Limited: 312–332. doi:10.1108/02630801211256661.
- Hague, R., I. Campbell, and P. Dickens. 2003. "Implications on Design of Rapid Manufacturing." *Proceedings of the Institution of Mechanical Engineers, Part C: Journal of Mechanical Engineering Science* 217 (1): SAGE Publications Sage UK: London, England: 25–30. doi:10.1243/095440603762554587.
- Hamard, Erwan, Bogdan Cazacliu, Andry Razakamanantsoa, and Jean Claude Morel. 2016. "Cob, a Vernacular Earth Construction Process in the Context of Modern Sustainable Building." *Building and Environment* 106 (Elsevier Ltd): 103–119. doi:10.1016/j.buildenv.2016.06.009.
- Harrison, Ray. 1999. *Earth: The Conservation and Repair of Bowhill, Exeter: Working with Cob*. London: James & James.
- "HFM 446 Lambda Series – NETZSCH Analyzing & Testing." 2018. Accessed October 18. <https://www.netzsch-thermal-analysis.com/en/products-solutions/thermal-diffusivity-conductivity/hfm-446-lambda-series/>.
- Houben, H., and H. Guillaud. 1994. *Earth Construction: A Comprehensive Guide*. London: Intermediate Technology Publications. https://scholar.google.com/eg/scholar?hl=en&as_sdt=0%2C5&q=%09Houben%2C+H.+and+Guillaud%2C+H.%2C+%281994%29+Earlh+Construction%2C+Intermediate+Technology+Publications&btnG=.
- Hurd, John, and Ben Gourley. 2000. *Terra Britannica: A Celebration of Earthen Structures in Great Britain and Ireland*. Edited by ICOMOS/UK (Organization). Earth Structures Committee. London: James & James.
- Ishak, Ismayuzri Bin, Joseph Fisher, and Pierre Larochelle. 2016. "Robot Arm Platform for Additive Manufacturing Using Multi-Plane Toolpaths." 1–7. doi:10.1115/DETC2016-59438.
- Melià, Paco, Gianluca Ruggieri, Sergio Sabbadini, and Giovanni Dotelli. 2014. "Environmental Impacts of Natural and Conventional Building Materials:

- A Case Study on Earth Plasters." *Journal of Cleaner Production* 80: 179–186. doi:10.1016/j.jclepro.2014.05.073.
- Niroumand, Hamed, Juan Antonio Barceló Álvarez, and Maryam Saaly. 2016. "Investigation of Earth Building and Earth Architecture According to Interest and Involvement Levels in Various Countries." *Renewable and Sustainable Energy Reviews* 57 (Elsevier): 1390–1397. doi:10.1016/j.rser.2015.12.183.
- Perrot, A., D. Rangeard, and E. Courteille. 2018. "3D Printing of Earth-Based Materials: Processing Aspects." *Construction and Building Materials* 172 (Elsevier Ltd): 670–676. doi:10.1016/j.conbuildmat.2018.04.017.
- "The CobBauge Project." 2018. Accessed October 17. <http://www.cobbauge.eu/en/cobbauge-2/>.
- Veliz Reyes, Alejandro, Mohamed Gomaa, Aikaterini Chatzivasileiadi, and Wassim Jabi. 2018. "Computing Craft: Early Stage Development of a Robotically-Supported 3D Printing System for Cob Structures." In *ECAADe-Computing for Better Tomorrow*, 1, 791–800. Lodz: cuminCad.
- Volhard, Franz, and Julian Reisenberger. 2016. *Light Earth Building: A Handbook for Building with Wood and Earth*. Birkhauser. <https://www.ribabookshops.com/item/light-earth-building-a-handbook-for-building-with-wood-and-earth/86214/>.
- Walker, Peter, Rowland Keable, Joe Martin, and Vasilios Maniatidis. 2005. "Rammed Earth: Design And." *IHS BRE*. <https://www.brebookshop.com/samples/148940.pdf>.
- Wanek, C., M. Smith, and J. F. Kennedy. 2015. *The Art of Natural Building: Design, Construction, Resources*. Edited by C. Wanek, M. Smith, and J. F. Kennedy. Vancouver, Canada: New Society Publishers.
- Weismann, Adam, and Katy Bryce. 2006. *Building with Cob*. Devon: Green Books Ltd.
- Wu, Peng, Jun Wang, and Xiangyu Wang. 2016. "A Critical Review of the Use of 3-D Printing in the Construction Industry." *Automation in Construction* 68 (Elsevier B.V.): 21–31. doi:10.1016/j.autcon.2016.04.005.

Appendix IV: Environmental assessment of large-scale 3D printing in construction: a comparative study between cob and concrete.



Environmental assessment of large-scale 3D printing in construction: A comparative study between cob and concrete

Hashem Alhumayani ^{a, c}, Mohamed Gomaa ^{b, *}, Veronica Soebarto ^b, Wassim Jabi ^a

^a Welsh School of Architecture, Cardiff University, Bute Building, Cardiff, CF10 3NB, United Kingdom

^b School of Architecture and Built Environment, University of Adelaide, Horace Lamb Building, North Tce, Adelaide, SA, 5005, Australia

^c Taibah University, Janadah Bin Umayyah Road, Tayba, Medina, 42353, Saudi Arabia

ARTICLE INFO

Article history:

Received 11 March 2020

Received in revised form

21 May 2020

Accepted 22 May 2020

Available online 1 June 2020

Handling editor: Prof. Jiri Jaromir Klemes

Keywords:

LCA

Robotic fabrication

3D printing

Cob

Concrete

Sustainable construction

ABSTRACT

This paper explores the environmental impacts of large-scale 3D printing (3DP) construction in comparison to conventional construction methods using two different types of construction material: concrete and cob (a sustainable earth-based material). The study uses a standard Life Cycle Assessment (LCA) method, from cradle to site, to assess the environmental impacts of the construction materials and processes, with a focus on load-bearing walls in small/medium size houses. As expected, cob-based methods (conventional followed by 3DP) show lower overall environmental impacts and global warming potentials than the concrete-based methods. The study also shows that while the overall environmental impacts of 3DP concrete is higher than that of 3DP cob due to higher global warming potential, stratospheric ozone depletion and fine particulate matter formation, it has less impact on marine eutrophication, land use, and mineral resources scarcity. The environmental issues that remain to be overcome in relation to 3DP concrete is its high-cement content, while the issue in 3DP cob rises from the use of electricity for the 3D printing operation. The study indicates that the use of renewable energy resources and innovative material science can greatly increase the potentials of both 3DP cob and 3DP concrete respectively for future construction.

© 2020 Elsevier Ltd. All rights reserved.

1. Introduction

In 2018, the International Energy Agency (IEA) reported that the average rate of growth of global energy consumption had increased almost two-fold since 2010. This high energy demand increased CO₂ emissions by 1.7% in 2018 alone, reaching a new record in its history (International Energy Agency, 2018). The building construction sector and its operations accounted for 40% of the CO₂ emissions and 36% of global fine energy use in 2018 (IEA and UNEP, 2018). At the same time, buildings play an important role in transitioning to a low-carbon economy (Shrubsole et al., 2019). The drive to improve environmental conditions and reduce carbon emissions has led to innovations in technology and construction techniques (Shrubsole et al., 2019). Digital fabrication technologies

in the manufacturing industry are also being adopted in architecture and construction (Craveiro et al., 2019). 3D printing technologies, in particular, have become a focus of attention in a number of diverse fields, including the construction sector (Wang et al., 2014; Soliman et al., 2015).

3D printing involves producing three dimensional objects by layering different materials (ASTM International, 2013). 3D printing has developed dramatically in recent years and can now be done using a range of materials (Agusti-juan et al., 2017). Where originally the use of 3D printing was restricted to the creation of physical models to present concepts to stakeholders; it is now being used to build entire buildings (Geneidy and Ismaeel, 2018). A milestone in the development of 3D printing technology took place when “Contour Crafting”, a research project conducted at the University of Southern California, showed how layered extrusion technologies can work within large scale constructions (Khoshnevis et al., 2006).

The use of 3D printing in construction is gaining increased attention around the world. Several companies, such as Apis Cor, CyBe and Winsun, have upscaled technology intake over the past 5 years and have started tendering for 3D printed projects in Europe,

* Corresponding author. School of Architecture and Built environment, Horace Lamb Building, University of Adelaide, Adelaide, SA, 5005, Australia.

E-mail addresses: alhumayanih@cardiff.ac.uk (H. Alhumayani), mohamed.gomaa@adelaide.edu.au (M. Gomaa), veronica.soebarto@adelaide.edu.au (V. Soebarto), jabiw@cardiff.ac.uk (W. Jabi).

Saudi Arabia, the United Arab Emirates and China (Apis Cor, 2019; CyBe, 2018; Winsun3d, 2019). In 2019, Apis Cor constructed the world's largest 3D Printed (3DP) building in the UAE for the Dubai Municipality. The building stands over an area of 640 square meters and has two-stories with an overall wall height of 9.5 m. The walls were all 3D printed on site while the foundations and slabs were constructed conventionally (Apis Cor, 2019).

Although there have been numerous studies and many advancements in 3D printing of buildings, 3D printing applications in construction are still at an early stage and are still fairly limited in terms of project scale, materials, and the high cost of the technology (Wu et al., 2016; Berman, 2012). The other important aspect that remains insufficiently explored to date is the environmental impacts and the Life Cycle Assessment (LCA) of the 3DP technologies in construction (Veliz et al., 2018). There is, therefore, the need to investigate the environmental impact of 3D printed building design, materials, technology, regulations and codes (Dixit, 2019).

The Life Cycle Assessment (LCA) method, which is presented in the ISO 14040- 44: 2006 Standards (ISO, 2006), is an assessment method of the environmental impacts of products and processes. LCA has been used in the construction sector for the last twenty years (Singh et al., 2011; Buyle et al., 2013). LCA methods can evaluate and optimise the construction processes by taking a comprehensive and systemic approach to environmental assessment (Tulevech et al., 2018). LCA in construction has two main approaches, depending on the required level of depth of assessment (Häfliger et al., 2017). The first approach involves a comprehensive level of detailing of the environmental impact of a building over its entire life cycle, including all the associated processes and materials (cradle to grave). The second approach assesses and compares only the environmental impact of the construction materials and/or construction method (cradle to site). According to ISO14040, 2006, LCA involves four phases that work iteratively: The first phase is to define the goal and scope for launching the system boundaries and the quality criteria for the inventory data and functional unit. The second phase entails the inventory analysis (LCI), which focuses on the life cycle of the products in several steps. This phase deals with the production and collection of information on energy flows and physical material. The third phase is a life cycle impact assessment (LCIA), which uses the data collected from LCI and calculates their contribution to various environmental impact groups. The last phase is interpretation, which evaluates results to achieve conclusions, identifies important issues, gives recommendations, and describes limitations.

There are several impact assessment methods to calculate environmental performance, including CML, EDIP, ReCiPe, and TRACI (Cavalett et al., 2013) and each of these methods combines several impact indicators/categories. The ReCiPe method, for instance, combines eighteen impact categories, as listed by Goedkoop et al. (2009), namely: global warming potential, ozone depletion potential, terrestrial acidification potential, freshwater eutrophication potential, marine eutrophication potential, human toxicity potential, photochemical oxidant formation potential, particulate matter formation potential, terrestrial ecotoxicity potential, freshwater ecotoxicity potential, marine ecotoxicity potential, ionising radiation potential, agricultural land occupation potential, urban land occupation potential, natural land transformation potential, water depletion potential, mineral depletion potential, and fossil depletion potential. Each impact category has its weight and significance on the environment. Product Environmental Footprint Category Rules Guidance (PEFCR Guidance) provide recommendations for the most relevant impact categories to current global environmental concerns (European Commission,

2017). These recommendations are based on normalised and weighted factors, representing the level of importance per category based on its impact on the environment.

To date, a limited number of studies have been conducted to assess the environmental opportunities of applying digital fabrication and 3DP methods in construction (Soto et al., 2018; Dixit, 2019). Researchers have generally focused on the environmental impact at a small scale, for example, Kreiger and Pearce (2013), who studied the environmental benefits of distributing conventional and 3D printing of polymer products. A study conducted by Faludi et al. (2015) compared the environmental impacts of two types of additive manufacturing machines versus traditional numerical (CNC) milling machines and showed that there is a reduction in energy use and waste in additive manufacturing machines when compared to CNC milling machines.

Recently, Yao et al. (2019) compared 3D printing geo-polymer technology and the use of ordinary concrete in four scenarios using a Life Cycle Assessment (LCA) method. The study revealed that 3D printing technologies perform better environmentally and possibly lead to a reduction in waste when creating complex construction components. However, ordinary concrete performed environmentally better than 3D printed geo-polymer when it came to building simple walls. Prior to this, Kafara et al. (2017) conducted a comparative study of 3D printing manufacturing and conventional manufacturing of mould core making for carbon fiber reinforced polymer (CFRP) production. The results revealed that 3D printing manufacturing performed better on an environmental scale than conventional manufacturing. In recent years, researchers have started to explore 3D printing of earth-based materials, such as cob, as an eco-friendly substitute to 3D printed concrete (Perrot et al., 2018). It is claimed that 3D printing of earth materials can leverage the environmental potential of 3D printing techniques by reducing waste and the transportation and carbon footprint of the construction process (Gomaa et al., 2019; Veliz et al., 2018).

Concrete is one of the most used materials in conventional construction in the Middle East and Saudi Arabia (General Authority for Statistics, 2019). On the other hand, the Middle East region, including Saudi Arabia, is rich with earth materials and Cob houses (Ibrahim, 2018; NICDP, 2019). Saudi Arabia's national development plan (Vision, 2030) envisages adopting and using new technologies, such as 3D printing, with the aim of becoming a global investment powerhouse (Saudi Vision, 2030; 2018). Saudi's government aims to increase the percentage of ownership of houses by 60% (Housing program, 2019). The fast-growing building industry in Saudi Arabia is pushing the government towards the adoption of advanced construction methods that can meet the new development agenda. The increasing demand is expected to substantially increase energy consumption with consequent environmental implications (Asif et al., 2017). This makes it even more imperative to study the environmental impact of the building industry.

Hence, the main aim of this study is to compare the environmental impact of the 3D printing construction method with conventional construction methods using two different types of construction material: concrete and cob. Both materials are conventionally available worldwide with well-established knowledge of practice and historical performance. This approach is expected to provide a clearer understanding of the environmental implications of using 3D printing methods in construction, which should empower designers, project planners and stakeholders with the necessary data to make informed decisions regarding construction methods and materials. The study focuses on the construction market in the Middle East, particularly Saudi Arabia.

2. Methods and materials

2.1. Life cycle assessment set up

The study used SimaPro 9.0.0.35 software (PRé, 2019) to implement the LCA method. As recommended in ISO 14040 and 14044, the Ecoinvent v3.1 database was used because it is a compliant data source for studies and assessments. The ReCiPe Midpoint (H) v1.03 method for impact assessment was used as it provides a wide range of environmental categories, used in most scientific studies on LCA (Huijbregts, 2017; Agustí-juan et al., 2017). For water use analysis, the study implemented the Available Water Remaining (AWARE) method, as recommended by the United Nations Environment Programme (UNEP/SETAC, 2016). The chosen processes for the LCA of the constructed walls were raw material extraction, transport, material manufacturing, and the energy required for construction.

This study focuses on the most relevant impact categories, which are identified as all the impact categories that cumulatively contributed to at least 80% of the total environmental impacts (excluding toxicity related impact categories) (European Commission, 2017). The seven most relevant impact categories, as advised by PEFGR Guidance, are: 1) global warming; 2) stratospheric ozone depletion; 3) fine particulate matter formation; 4) marine eutrophication; 5) land use; 6) mineral resource scarcity; and 7) water use (AWARE). The latest normalisation and weighting factors for this study were obtained through the European Commission Platform on Life Cycle Assessment (European Commission, 2017, 2019; Sala et al., 2018).

2.2. Study goal and scope

Given the limited information about 3D printed constructions, the LCA carried out for the purposes of this thesis is a cradle to site, which includes raw materials, transportations, and construction process on site. The using phase and demolishing phase are not included in this study. LCA is applied to assess and compare the environmental impacts of two different construction methods: 3D printing and conventional construction methods. The materials used in both methods are concrete and cob. The conventional concrete method commonly used in Saudi Arabia involves reinforced concrete structures (column and beam) and blockwork walls while the 3DP method involves solely the concrete mix. On the other hand, cob ingredients are the same in both conventional and 3DP methods, but with different ratios.

The functional units of each construction method are chosen to represent a section of an external load bearing wall in a one-storey house. All the units share the same standing area of 1 m², while the thicknesses vary to reflect the differences in the physical/structural properties of each method. It is important to note that, despite both cob and concrete are constructed using the same technology of 3D printing, each material has its own unique physical and structural characteristics. It is obvious that concrete has higher structural strength per unit area as compared to cob. Hence, the design of the wall section differs within the same structural function. Both Conventional and 3DP concrete require simpler wall design as compared to conventional and 3DP cob for the same wall unit in same building design. This means, when building a one-storey house, both concrete and cob walls will be designed to satisfy the same structural function.

The conventional method of building with cob requires a load bearing wall with a thickness that varies from 20 cm to 120 cm. An architect usually defines the thickness variation based on several factors, such as expected load, total wall height, and which part of the wall is being constructed (i.e. bottom or top of the wall). The

most used thickness of straight cob walls (no tapering) is 62 cm on average. For tapered walls, this thickness varies from 120 cm at the bottom to 20 cm at the top (Hamard, 2016; Quagliarini et al., 2010). This study is based on straight cob walls with a thickness of 60 cm for use in a conventional cob functional unit.

The 3DP concrete wall was designed with a thickness of 40 cm, based on the walls used in a recent project in Saudi Arabia (CyBe, 2018). The 3DP cob was designed with a thickness of 60 cm similar to the standard used in straight cob walls and the thickness of similar walls constructed by researchers at Cardiff University and at 3D WASP (Veliz et al., 2018; Veliz Reyes et al., 2019; 3D WASP, 2020). Both 3DP walls comprise an internal pattern filament (Fig. 1).

The selection of a comparable functional unit in a conventional concrete structure wall for this study requires a different approach, as the walls in this type of construction do not have uniform geometry (e.g. cube, parallelepiped). A structural "functional" wall unit in a concrete structure combines three components: columns, beams and blocks/bricks (Fig. 2). Hence, the study selected another transitional functional unit for the conventional concrete wall, i.e. 4 (L) x 3 (H) meters. This makes the standing area of this wall 12 m², which is 12 times the standing area of each of the other three functional units. Since the LCA comparison depends mainly on quantities, the calculated quantities in the 4 x 3 m concrete wall were divided by 12 to represent the quantities in a 1 m² unit. Worth mentioning is the fact that it is possible to reverse this approach by upscaling the small functional units to 12 m² walls. However, keeping the functional units as 1 m² will maintain a more generalised unit that will facilitate multiplication and reproduction of results.

As shown in Table 1, there are differences in volume between the 3D printed versions and the conventional method. The reason for this is that the 3D printed walls are combined with inner gaps in their design by default, which is a beneficial characteristic of the 3D printing technology that enables a reduction in the amount of construction material needed and an increase in the thermal performance of the walls (Veliz et al., 2018; Gomaa et al., 2019).

2.3. Electricity consumption calculation

2.3.1. Calculating the electricity consumption for 3D printed cob and concrete

The electricity consumed for the robotic arm operation during the construction process can be estimated either practically or mathematically. The practical measure of power consumption requires the use of electricity/power meters that only read the power source for the digital fabrication tools being used (i.e. in this case a robotic arm) or, if the tools are battery powered, a calculation of the number of full charges needed to finish the construction process. The mathematical method to estimate the electricity consumption depends on knowing the power ratings in Kilowatts (kWh) of the fabrication tools and the time required to complete the fabrication process. The total electricity consumption can then be obtained using the following equation:

$$\text{Electricity consumption (kWh)} = \text{power demand (kW)} \times \text{Time (hrs)}$$

The fabrication tool used in the study is a KUKA KR60 HA robotic arm. This robot has a direct supply line of electricity but does not have an electricity meter. Therefore, the study used the mathematical estimation of power consumption. The robot operates 3D printing tasks with a payload of approximately 30 kg, and it has 6 motors on each of its axes; the motors have a collective power rating of 16.8 kW when working on maximum capacity, with 60 kg payload on the robot head. The motors are assumed to work initially at 50% of their full capacity, which is 8.4 kW. A sensitivity

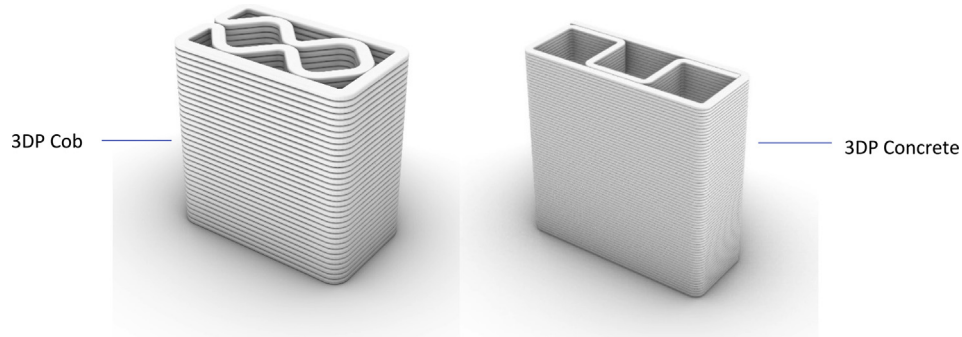


Fig. 1. 3DP cob wall and 3DP concrete wall.

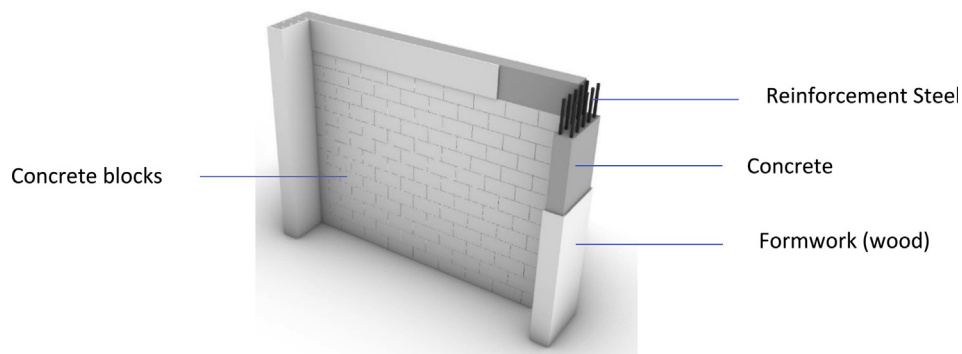


Fig. 2. Conventional concrete construction wall.

Table 1

The specifications for each wall section per method.

Wall name	Method	Area m ²	Thickness	Type	Volume m ³
Conventional Concrete	Conventional	1	NA	solid	0.3 ^a
Conventional Cob	Conventional	1	0.6	solid	0.6
3DP Concrete	3D printed	1	0.4	patterned	0.16
3DP Cob	3D printed	1	0.5	patterned	0.31

^a This volume includes concrete mix, framework, concrete block, reinforcement steel, and mortar.

analysis has been conducted by examining another scenario where the robot runs on its full capacity.

To calculate the required time for the 3D printing process, two factors need to be defined: firstly, the 3D printing speed; and secondly, the perimeter length of the design pattern/path line for the wall, inclusive of all the layers. The operation time can be calculated by dividing the perimeter length over the 3D printing speed. The printing speed differs between 3DP in cob and a 3DP in concrete because of the different properties of the materials. The printing speed for 3DP cob was set at 0.05 m/s. This speed was found to be appropriate for cob printing based on several tests that took place at Cardiff University and the findings of Veliz et al. (2018). The 3DP concrete printing speed was set at 0.25 m/s (Besix, 2019).

The length of the perimeter/path line in 3D printing could be defined as the total length of all the layers that construct the wall unit, which equals the perimeter of a single layer multiplied by the number of layers. This study uses inner patterns for the 3DP walls as adopted in the industry. The selected pattern for the 3DP cob was inspired by 3DP WASP prototypes (3D-WASP), while the chosen pattern for the 3DP concrete was supplied by the CyBe project in Saudi Arabia (CyBe, 2018)(Fig. 3). The length of the total path line for the 3DP cob is 146.3 m and for the 3DP concrete 412 m. This noticeable difference in path line length between cob and concrete

is due to the difference in the 3D printing settings. The printing layer height in the 3DP cob is 30 mm, while in the 3DP concrete it is 10 mm. Hence, more layers are required for the 3DP concrete to achieve the same required 1.0 m height wall. Increased number of layers means a longer total path line. By applying the previous calculations, the electricity consumption was found to be 6.8 kWh for 3DP cob and 3.9 kWh for 3DP concrete.

2.3.2. Electricity consumption for conventional cob and concrete

In conventional constructions, the work is undertaken by manual labour. Nevertheless, in the environmental analysis, the energy requirements and emissions associated with human life are not counted usually (Agustí-juan et al., 2017). A study conducted by Alcott (2012) calculated the human factor, but the results showed that the impact was insignificant. Therefore, human factor is not included in this study, that is, this study does not include the energy consumption to manufacture conventional concrete because all the manufacturing processes were done manually.

2.4. Material characterisation

2.4.1. Cob

Weismann and Bryce (2006) suggested a water to subsoil ratio



Fig. 3. CyBe 3DP concrete pattern (left), 3D WASP 3DP cob pattern (right).

of one part water to every four parts of soil. This converts to 20 kg of water per each 80 kg of subsoil by weight (20: 80%). The recommended amount of straw to be included in the mix is 2% of the weight of the subsoil and water mix. A comprehensive systematic review by Hamard (2016) affirmed the proportions of the cob mixture (78% subsoil, 20% water and 2% fibre i.e. straw). Hamard (2016) also stated that the subsoil formula itself is 15–25% clay to 75–85% aggregate/sand. Similarly, Harrison (1999) recommended a subsoil formula of 20% clay to 80% aggregate/sand.

However, as cob is conventionally mixed in a near dry state due to the low water ratio, the commonly used proportions of water to subsoil do not fit the purpose of the 3D printing technique. The 3D printing technique involves a material extrusion process through tubes and/or hoses; therefore, less viscous material is always preferred to reduce the amount of friction inside the system, which then reduces the loads on the motors. Two comprehensive studies on 3DP cob have recommended a new cob mix that has reduced viscosity. Based on a number of 3D printing tests, the water content in the 3DP cob mixture was increased to 23–25%, while the amount of straw was fixed at 2% (Gomaa et al., 2019) (Table 2).

2.4.2. Concrete

3DP concrete is a mix of cement, fly ash, silica fume, sand, water, superplasticiser, and fibre (Lau et al., 2012; Agustí-juan et al., 2017; Nerella and Mechtcherine, 2016; Anell, 2015). Each of the previously cited studies suggested different ratios of material in the 3D printed concrete mix (Table 3). An extensive review of the literature revealed that Le et al. (2012a) had carried out comprehensive testing of several 3DP concrete mixes to define which had the best workability and usability. Other studies used Le et al. (2012a) as a main starting point to develop their new mixes (such as Labonnote et al., 2016; Ngo et al., 2018; Buswell et al., 2018; Wolfs, 2015; Paul et al., 2018; Malaeb et al., 2015). Hence, this study conducted the LCA on the concrete mix recommended by Le et al. (2012a). However, to further explore the differences in the environmental impacts of the 3DP concrete mixes, two more concrete mixes, taken from Nerella and Mechtcherine (2016) and Anell (2015), will be used in the sensitivity analysis section.

This study used the 35 MPa conventional concrete type and column size $60 \times 20 \text{ cm}^2$ with 8 \emptyset 16 mm steel rods. The beam size

Table 2

The components of 3DP and conventional cob.

	Subsoil		Water		Straw		Total (kg)
	%	Kg	%	Kg	%	Kg	
Cob conventional wall	78.0	748.8	20.0	192	2.0	19.2	960
Cob 3D printed wall	73.0	392.6	25.0	134.4	2.0	10.8	537.8

Table 3

Different 3DP concrete mixes ingredients and their densities based on previous studies.

	Nerella and Mechtcherine, (2016)		Le et al. (2012b)		Anell (2015)		Agustí-juan et al. (2017)	
	Kg/m ³	%	Kg/m ³	%	Kg/m ³	%	Kg/m ³	%
Cement	430	19.5	579	25	659	30	500	20.5
Fly-ash	170	7.7	165	7.1	87	4	0	–
Silicafume	180	8.1	83	3.6	83	4	43.5	1.8
Sand/aggregates	1240	56.1	1241	53.5	1140	52	1713	70.5
Water	180	8.1	232	10	228	10	169	7.
Superplasticiser	10	0.5	16.5	0.7	11.6	0.5	4.32	0.2
Fibre	0	–	1.2	0.05	1.2	0.05	0	–
Total density	2210		2318		2210		2430	

was $40 \times 20 \text{ cm}^2$ with 6 \emptyset 16 mm steel rods, each concrete block was $40 \text{ cm} \times 20 \text{ cm} \times 20 \text{ cm}$, and the formwork was plywood. Plywood sheets have a thickness of 15 mm and are assumed to be used twice (one time per each side). All of the reinforced concrete properties used in the conventional wall were taken from the National Committee for the Saudi Building Code (Table 4).

3. Results and discussion

This section discusses the results of the study in three steps. First, the overall outcome of the study, that is, the comparison of the four types of walls in terms of their environmental impacts. This step will also include a description of the results pertaining to the different properties of each material. The second step explores the breakdown of the impact of each wall type. This aim of this breakdown is to determine which material and/or process has the highest environmental impact within each wall type. Having defined the highest contributors, the third step will be to analyse the sensitivity of each contributor and describe the changes in the environmental impact.

The produced analyses in Simapro were initially in the form of characterised values that show the relative difference in the

Table 4

The construction components of the conventional concrete method.

Concrete Conventional Wall	Percentage	Kg
Concrete blocks (main body)	50%	112.6
Formwork (wood)	16%	6.5
Reinforcement Steel	2%	12.3
Concrete mix	30%	206.1
Mortar	2%	12.5

environmental performance between the four wall types, as can be seen in Fig. 4. In order to obtain a holistic overview of the whole impact of the products, the characterised results must be normalised and weighted using special factors as indicated in the PEFCR guidance (European-Commission, 2017). Normalised and weighted results can then be used as a real representation of the performance in all the impact categories collectively. For example, in Table 5, the characterised values were normalised using the normalisation factor (NF/person), then weighted using the weighting factor (WF/person) to produce the overall improvement in performance per wall type in all the impact categories combined, all as compared to the conventional concrete wall.

3.1. Primary comparison

The results generally align with the results of several other studies (including Agustí-juan et al., 2017; Kafara et al., 2017) which claimed better environmental performance for 3DP technologies when compared to conventional concrete construction. The novel added factor in this study is the introduction of cob as an alternative material in both the conventional and the 3D printing methods. The conventional concrete wall recorded the highest overall environmental impact out of all the other three walls. In addition, the 3DP concrete wall achieved a collective 24% improvement in all the seven relevant impact categories combined when compared to conventional concrete. However, in the global warming category, 3DP concrete performed 27.2% worse than conventional concrete. Unsurprisingly, the 3DP cob showed better environmental performance as compared to the concrete-based walls, with an overall improvement of 85% over the conventional concrete wall and 87.9% improvement in the global warming category only (Fig. 4 and Table 5).

The study initially included the conventional cob wall as a base line as it was anticipated that this will yield the most efficient environmental performance. This was a correct assumption on a collective scale; interestingly, however, both the 3DP cob and the 3DP concrete performed better in comparison with the conventional cob wall in several impact categories, such as marine eutrophication, land use and mineral resources scarcity. These three categories are heavily related to the use of straw and subsoil, which are found in large amounts in conventional cob walls. However, conventional concrete performed better than conventional cob in the mineral resource scarcity category, again due to the huge presence of subsoil in conventional cob (Fig. 4 and Table 5).

When focusing on concrete-based walls, the results revealed that 3DP concrete has an overall improvement in all categories collectively with 24%, except for the global warming category (European Commission, 2017). This is mainly due to the use of concrete and fly ash. Additionally, the reason for the poor performance of conventional concrete in the other impact categories is the presence of reinforcing steel and concrete which contribute highly to CO₂ emissions (Habert et al., 2013). These results could change if the comparisons were done on the basis of a whole building, including all structural elements, because 3D printing technology produces almost zero waste (Xia and Sanjayan, 2016)(Fig. 5 and Table 6).

On the other hand, despite the outperformance of 3DP cob over conventional cob in five of the seven impact categories, conventional cob has shown a much higher overall performance, with 83% improvement over 3DP cob (Fig. 6 and Table 7). This is clearly down to the good performance of conventional cob in two of the most important and highly weighted impact categories: global warming and fine particulate matter formation (European Commission, 2017). It is also due to the high use of electricity in 3DP construction, which severely affects both global warming and fine particulate matter formation. The breakdown of both materials will be given in the following section.

Since the focus of this study was 3DP technologies, a focused comparison on 3DP concrete and 3DP cob is provided in Fig. 7 below. As seen in Table 8, the environmental performance of 3DP cob is 80.0% better than 3DP concrete in the seven impact categories. The graph below (Fig. 5) shows that 3DP cob achieved a better performance in global warming, stratospheric ozone depletion, and fine particulate matter formation, while 3DP concrete performed better in marine eutrophication, land use, and mineral resources scarcity.

3.2. The breakdown of impacts

For a deeper understanding of the results, each wall type was analysed separately through a breakdown of ingredients in order to identify the impact in relation to each sub-material. Also, the overall contribution of all categories will be analysed with a focus on global warming as the most important impact category. The results were normalised and weighted to give a better understanding of each impact category.

With regards to conventional concrete, it was found that 49% of the environmental impact was due to the reinforcing steel which scored the highest contribution out of all the categories, except land

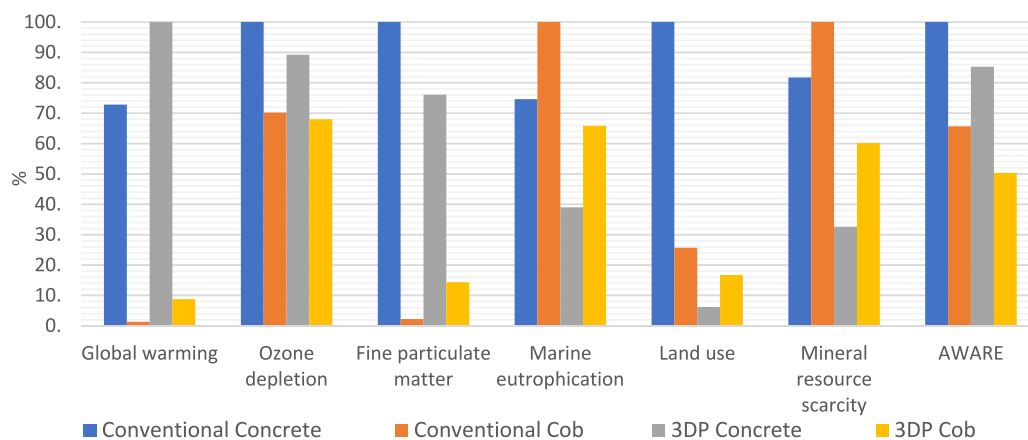


Fig. 4. Chart shows the characterised overall outcome of comparing the four types of walls.

Table 5

Percentage of improvement in environmental performance of the wall types as compared to conventional concrete method. (NF: Normalisation factor; WF: Weighting Factor).

Impact categories	NF/person	WF/person	Conv. Cob	3DP Conc.	3DP Cob
Global warming	8095.53	22.19	98.2%	-27.2%	87.9%
Stratospheric ozone depletion	5.37E-2	6.75	29.8%	10.7%	32.0%
Particulate matter	5.95E-4	9.54	97.8%	23.9%	85.7%
Marine eutrophication	19.545	3.12	-34.0%	47.7%	11.7%
Land use	81.94E+4	8.42	74.3%	93.8%	83.3%
Mineral resource scarcity	6.36E-2	8.08	-18.3%	60.1%	26.4%
AWARE (water depletion)	11468.7	9.03	34.3%	14.7%	49.7%
Overall improvement	-	-	96%	24%	85%

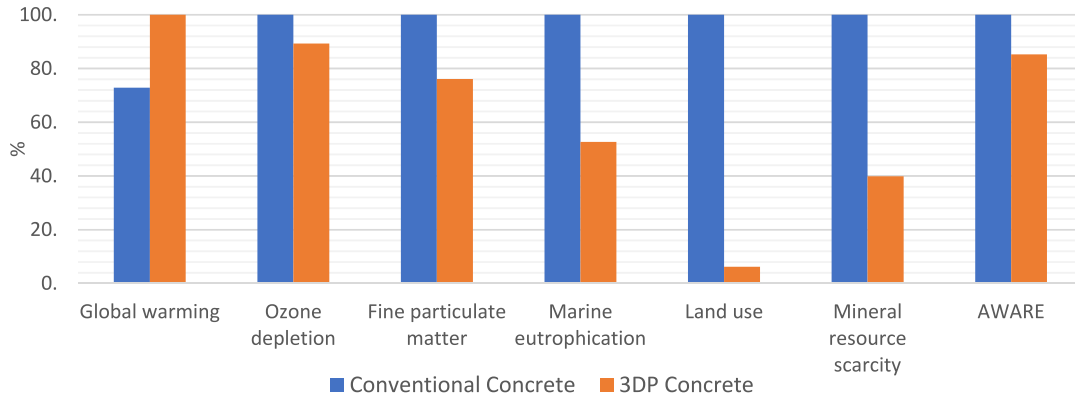


Fig. 5. Comparison between 1 m² 3DP Concrete wall with 1 m² Conventional Concrete.

Table 6

Percentage of improvement between 3DP Concrete and Conventional Concrete.

	Conventional Concrete	3DP Concrete
Global Warming	27.2%	-
Stratospheric Ozone Depletion	-	11%
Fine Particulate Matter	-	24%
Marine Eutrophication	-	47%
Land Use	-	94%
Mineral Resource Scarcity	-	60%
Aware	-	15%
Overall Improvement	-	24.0%

Table 7

Percentage of improvement between 3D Cob and conventional Cob.

	Percentage of Improvement	
	3DP Cob	Conventional Cob
Global Warming	-	85%
Stratospheric Ozone Depletion	3%	-
Fine Particulate Matter	-	84%
Marine Eutrophication	34%	-
Land Use	35%	-
Mineral Resource Scarcity	40%	-
Aware	23%	-
Overall improvement	-	83%

use where plywood scored the highest. Furthermore, concrete scores as the second highest contributor with an overall 19% contribution in all categories (Fig. 8). This finding obviously puts 3DP techniques at an advantage as it does not require the use of

formwork and reinforced steel (CyBe, 2018). However, the high presence of cement in the 3DP concrete wall reduced its environmental performance, especially in the global warming impact

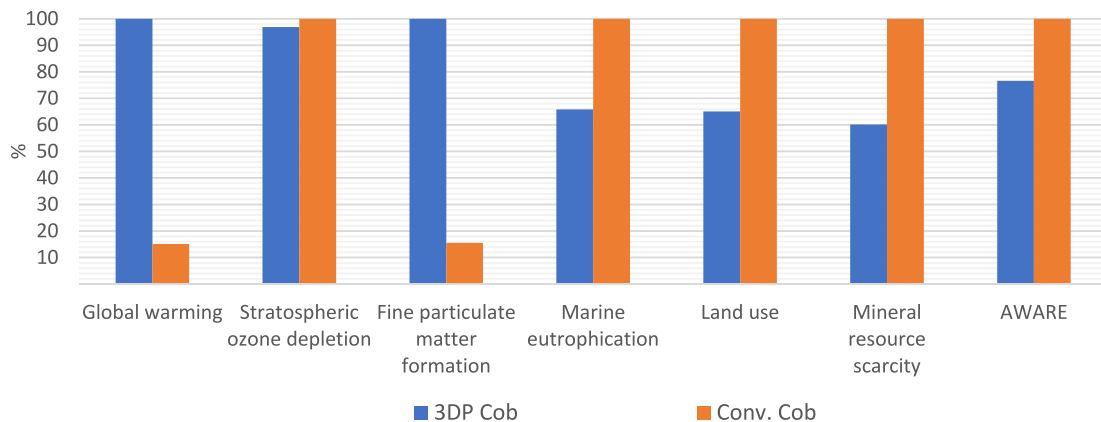


Fig. 6. Comparison between 1 m² 3DP Cob wall with 1 m² conventional Cob.

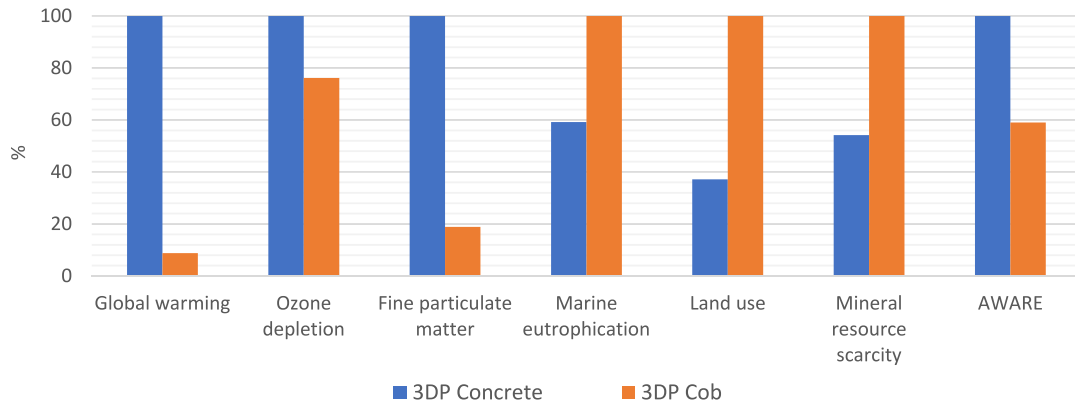


Fig. 7. Comparing 1 m² 3DP concrete with 1 m² 3DP cob.

Table 8
Comparison of the environmental performance between 3DP Cob and 3DP Concrete.

	3DP Concrete	3DP Cob
Global Warming	—	91%
Stratospheric Ozone Depletion	—	24%
Fine Particulate Matter Formation	—	81%
Marine Eutrophication	41%	—
Land Use	63%	—
Mineral Resource Scarcity	46%	—
Aware	—	41%
Overall improvement	—	80.0%

category, where it obtained the worst environmental performance scores out of the three types of wall. The impact breakdown of 3DP concrete shows that cement and fly ash are collectively responsible for 70.8% of the environmental impact and obtained the highest contribution scores out of all the categories. Transportation achieved the next highest score with 12.8% contribution in all the categories (Fig. 9).

In conventional cob construction, straw contributes 68% of the overall impact across all the categories, except mineral resource scarcity, where subsoil contributed the highest score (Fig. 10). On the other hand, the electricity used in 3DP cob, mainly used in the operation of the robotic arm, contributed 83% of the impact across all the categories, followed by straw with an overall score of 7% (Fig. 11). Considering the very low ratio of straw (2%) in the cob

mixture, it can be concluded that straw has a significant effect on overall environmental performance. In addition, 3DP cob was proven to have the best collective environmental performance, even when compared to conventional cob. This is due to the massive reduction in the quantity of material and weights used in 3DP cob in comparison with conventional cob due to the integration of voids in the internal structures and the minimal amount of material used in the wall volume.

3.3. Sensitivity analysis

Based on the previous observations, it is important to test the sensitivity of some materials that were identified to have a large environmental impact and explore how this impact can be improved or reduced. The sensitivity analysis for this study was carried out on the basis of three scenarios: (1) changing the percentage of steel reinforcement in conventional concrete; (2) changing the 3DP concrete mix; and (3) changing the robotic operation payload and geographical location. Conventional cob was excluded from the sensitivity analysis, as it had a significantly better environmental performance than all the other three types. Moreover, there is no demand for conventional cob for construction on the modern construction market.

3.3.1. Conventional concrete

As mentioned earlier, steel contributed the most to the

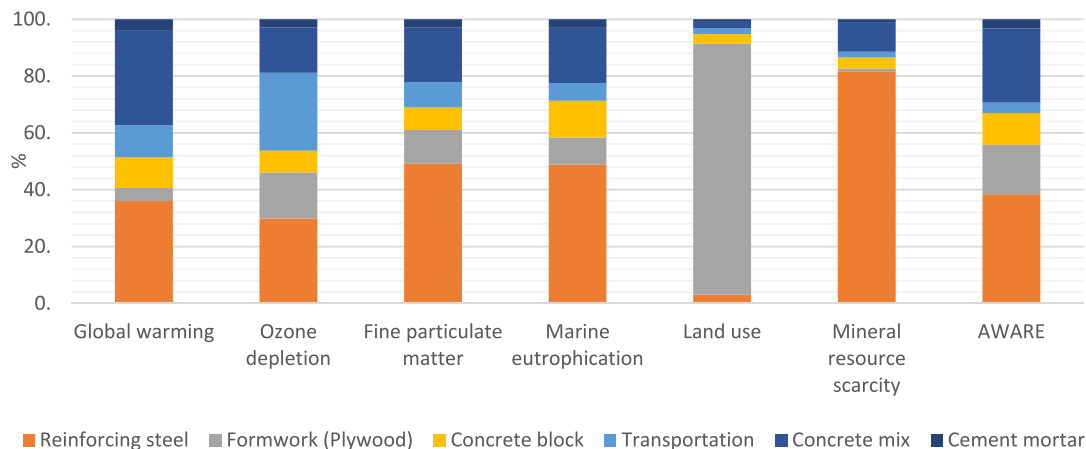


Fig. 8. Breakdown analysis of 1 m² wall of Conventional Concrete type.

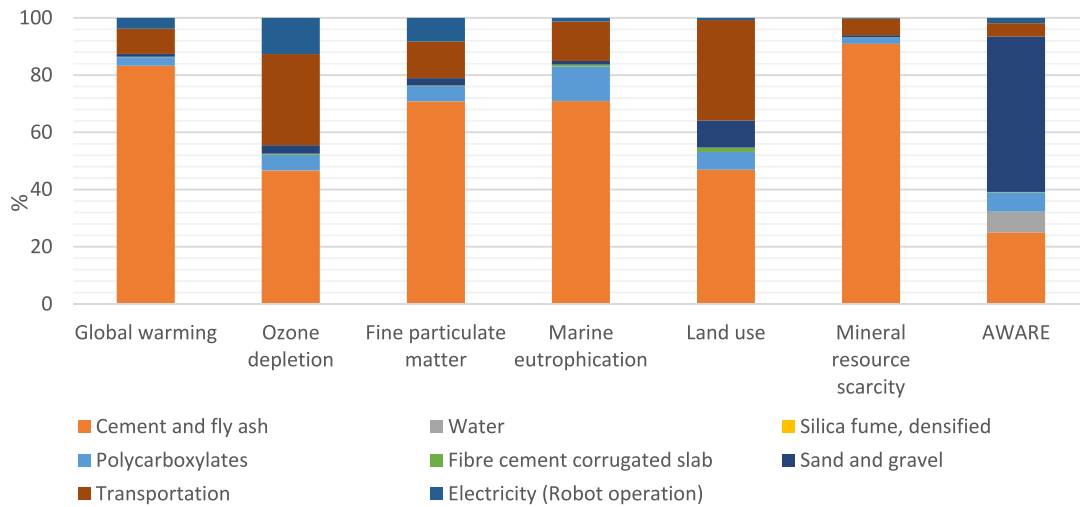


Fig. 9. Breakdown analysis of 1 m² wall of 3DP Concrete.

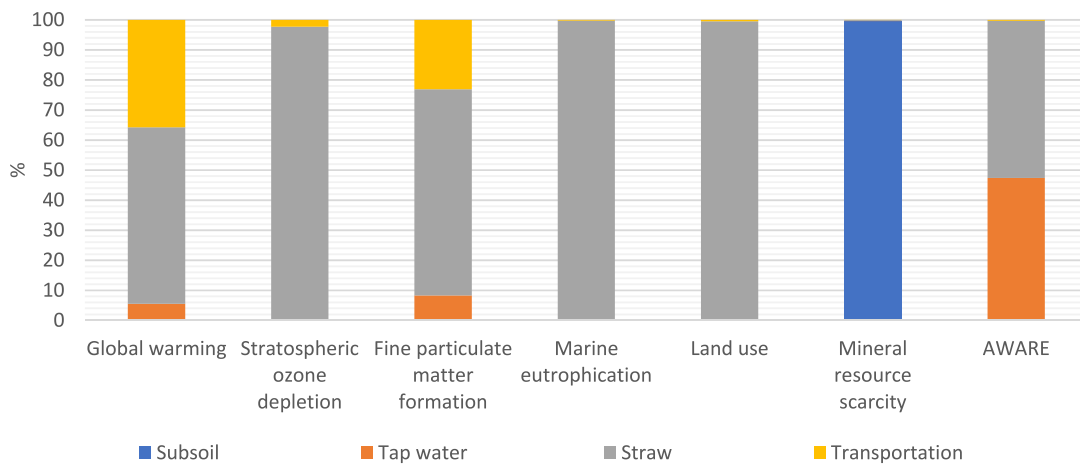


Fig. 10. Breakdown analysis of 1 m² wall of Conventional Cob.

environmental impact of conventional concrete. The quantity of steel used in the wall was originally calculated based on a reinforced 600 × 200 mm² column and 400 × 200 mm² beam which are used in a regular two-storey building. The amount of steel reinforcement and concrete were then reduced by nearly 20% and 22% respectively, to represent a smaller column of 400 × 200 mm² that can be used in a one-storey building, to mimic the walls that were used for the 3DP houses. This reduction in steel and concrete improved the performance of conventional concrete by an overall 17% and 16% in the global warming category when compared to the original concrete wall (Fig. 12).

3.3.2. 3DP concrete

As mentioned earlier, this study explored two more concrete mixes taken from Nerella and Mechtcherine (2016) and Anell (2015) to better understand the variations in the environmental performance associated with changing mix ratios of the cement, fly ash and sand. The results demonstrated that there is no specific component to focus on, as each recipe has a different proportion of components (Table 9). However, as shown, reducing cement and fly ash in the mix does not necessarily guarantee an improvement in the environmental performance of the 3DP concrete (Table 9). It

was observed that the reduction in cement and fly ash ratios in the 3DP concrete mix is usually accompanied by an increase in the sand and aggregate ratios, which then increases the overall quantities of material and consequently increases the environmental impacts of transportation. Therefore, it is concluded that it is important to analyse the main components of the 3DP concrete mix holistically.

It was found that, generally, all the three 3DP concrete mixes performed environmentally better than the conventional concrete wall, by 60.4%, 52.7% and 53.7% for the Nerella and Mechtcherine (2016) mix, the Le et al. mix (2012) and the Anell mix (2015) respectively. However, the Nerella and Mechtcherine (2016) mix had the lowest impact on global warming and all the categories when compared to the other mixes and conventional concrete (Table 10 and Fig. 13). This may be an indicator that recently developed mixes can have the potential of performing better environmentally.

3.3.3. 3DP cob

A few changes were made in the robotic operation concerning electricity consumption and location. Firstly, the robotic operation capacity was changed from 50% to 100%. This means that the payload was changed from 8.4 kW to 16.8 kW. This change led to

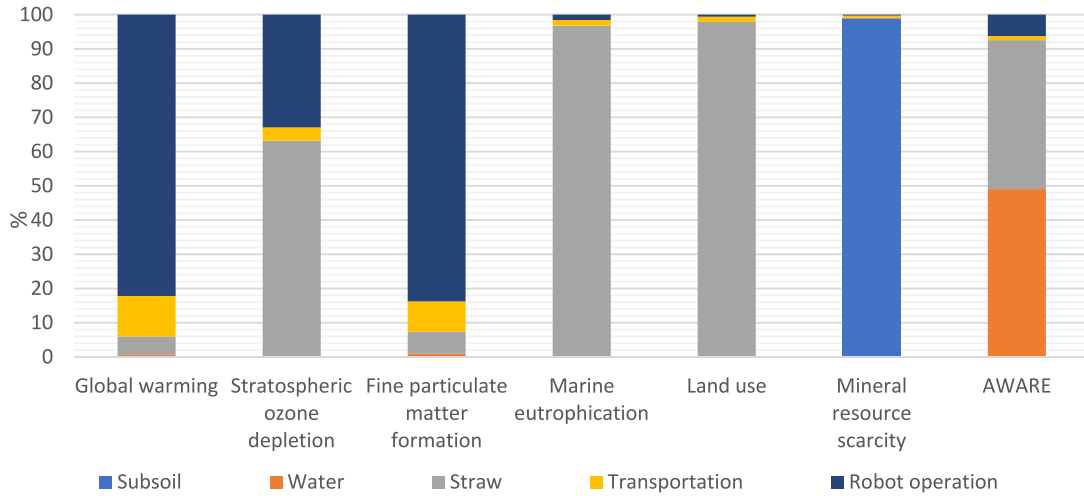


Fig. 11. Breakdown analysis of 1 m² wall of 3DP Cob.

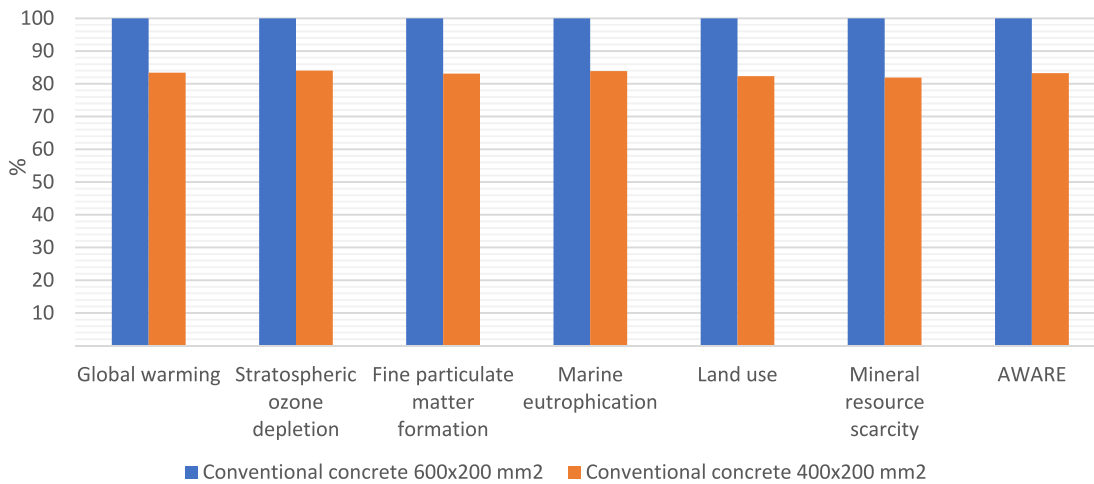


Fig. 12. Comparing main Conventional Concrete wall to the reduced steel and concrete version.

Table 9

The percentage breakdown of contribution towards the environmental impacts for each component in the three 3DP concrete mixes.

	Cement and fly ash	Water	Polycarboxylates	Fibre cement	Sand and gravel	Transportation	Electricity (Robot operation)
Le et al. (2012b)	71%	0.05%	5%	0.3%	2.6%	13%	8.3%
Anell (2015)	72.5%	0.05%	4%	0.3%	2.4%	12.50%	8.5%
Nerella and Mechtcherine, (2016)	68%	0.04%	4%	0.0%	3%	15%	10%

Table 10

The percentage of overall improvement in environmental performance of 3 dP concrete mixes as compared to conventional concrete method.

	3DP Conc (Nerella and Mechtcherine, 2016)	3DP Conc. (Anell, 2015)	3DP Conc (Le et al., 2012b)
Global warming	13%	- 4.6%	- 5.7%
Overall categories	60.4%	53.7%	52.7%

double the amount of electricity consumption that deteriorated the performance of 3DP cob by 55% in both overall and global warming levels (Fig. 14).

The impact of changing the geographical location from Saudi Arabia to Australia was also tested. The electricity in Saudi Arabia is totally produced from non-renewable energy resources (ERCA, 2018), while 19% of electricity generation in Australia comes from

renewable energy sources (Dixit, 2019). This study chose the state of South Australia (SA) as a case study for this sensitivity analysis as more than 50% of its electricity comes from renewable sources (Dixit, 2019). Altering the location from Saudi Arabia to South Australia resulted in an improvement of the environmental performance by 52% overall and 36% in the global warming category (Fig. 15).

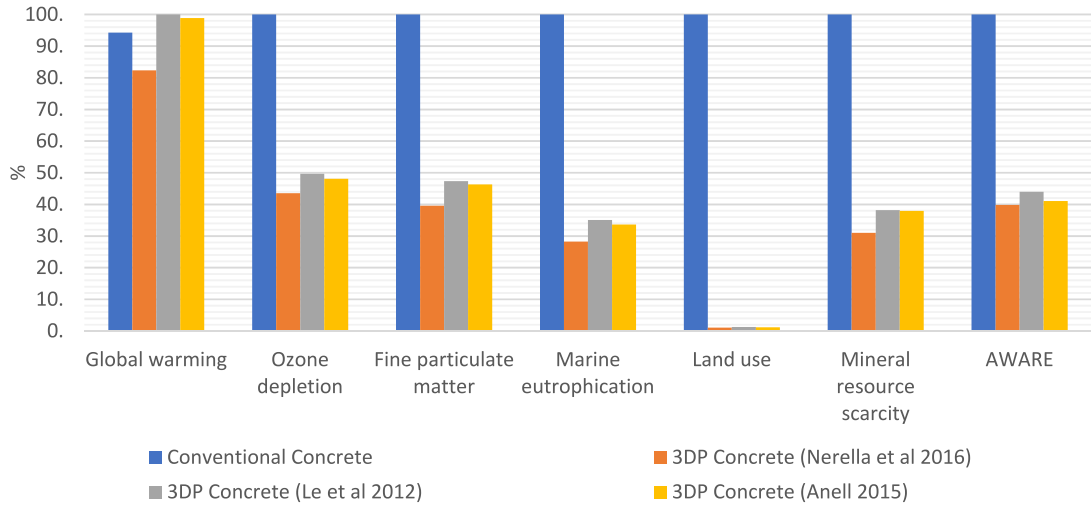


Fig. 13. Comparison of the three 3DP mixes to conventional concrete wall mix.

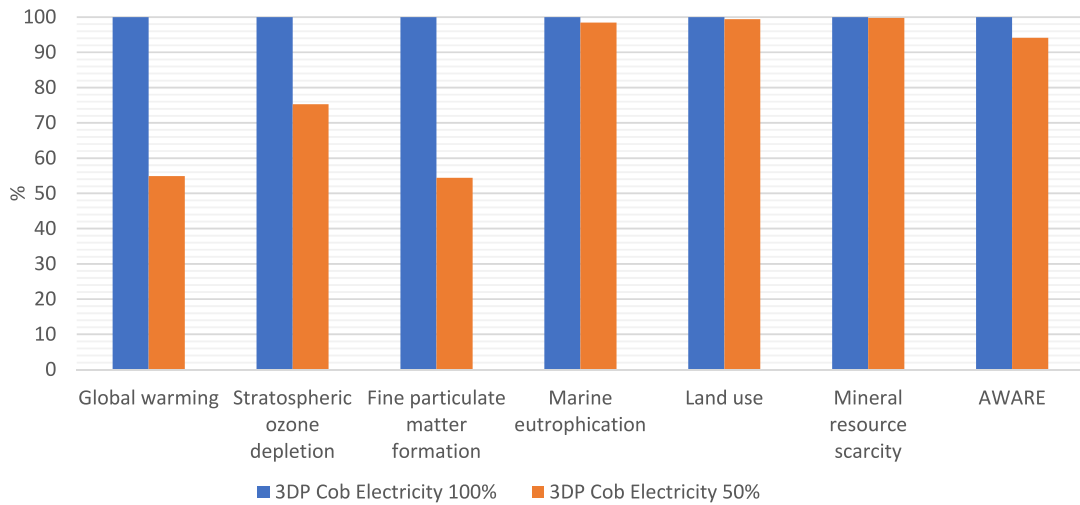


Fig. 14. Comparing 3DP cob 50% electricity with 100% electricity.

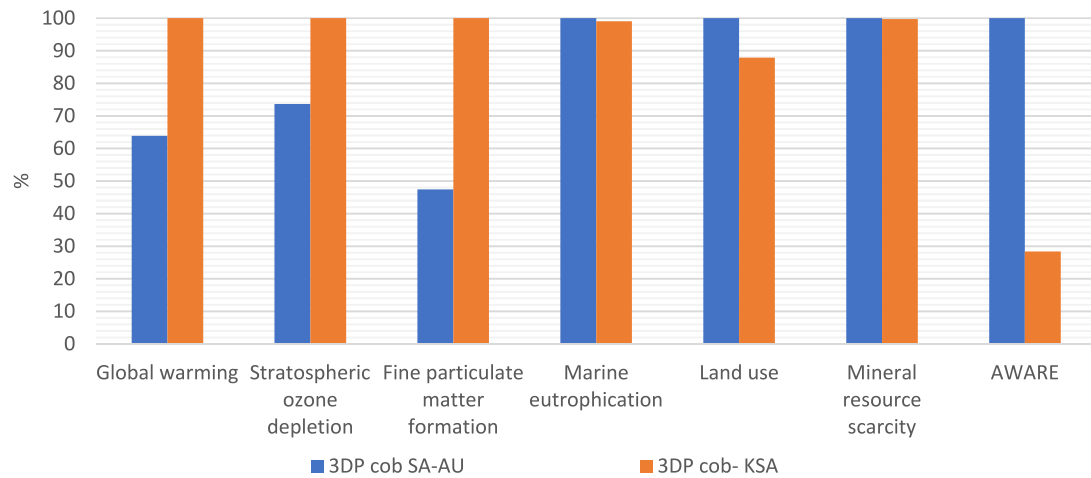


Fig. 15. Comparison of 3DP Cob method in South Australia to 3DP Cob in Saudi Arabia.

4. Conclusion

Digital fabrication technologies have recently been adopted in architectural applications and constructions; however, the environmental impacts of such approaches have not been thoroughly investigated. This study compared the environmental impacts of constructing a wall using 3D printing construction methods with the impact of conventional construction methods. Four different types of materials were tested: conventional concrete, conventional cob, 3D printed (3DP) concrete and 3DP cob.

The study had the following results:

1. Conventional cob has the least overall environmental impact and global warming potential, followed by 3DP cob. As expected, conventional concrete had the highest environmental impact in all categories except global warming.
2. While 3DP concrete had a lesser overall environmental impact (by more than 50%) than conventional concrete, the performance of 3DP cob is still better than 3DP concrete due to its lesser global warming potential, stratospheric ozone depletion and fine particulate matter formation.
3. However, while the overall environmental impact of 3DP concrete is more than that of 3DP cob, it has less impact on marine eutrophication, land use, and mineral resources scarcity.
4. A detailed analysis shows that the high environmental impact of conventional concrete construction is mainly due to the use of reinforcing steel (49% contribution) and concrete (19%).
5. The absence of reinforcing steel bars in 3DP concrete is the main reason for its better environmental performance when compared to the performance of conventional concrete.
6. While conventional cob has a better environmental performance than the other three construction methods, the high content of straw in conventional cob contributes to its overall environmental impact while the use of subsoil contributes to mineral resource scarcity.
7. The consumption of electricity to operate the robotic arm in 3DP cob contributes to 83% of its overall environmental impact, while the very low straw content in the 3DP cob mixture contributes to its low environmental impact.

These results suggest that the environmental impact of conventional concrete is mostly due to its steel reinforcing bars as well as the concrete used. Changing the amount of steel reinforcement and concrete (but keeping it to the standards required for a one-story building) would reduce the environmental impact of conventional concrete. The environmental impact of 3DP concrete is mainly depending on the ratio of the components of the mix, hence in the future modified mixes can reduce further the environmental impact of 3DP concrete.

On the other hand, the environmental performance of 3DP cob is not as affected by the material used as it is by the amount of electricity used to operate the robotic arm. Using renewable energy sources to generate electricity for the robotic operations would significantly reduce the environmental impacts of 3DP cob. The current global trends are moving towards renewable sources of energy (REN21, 2019). Moreover, 3DP cob can generate complex shapes to meet the evolving demands of contemporary construction, which is difficult to achieve manually using conventional cob. In addition, 3DP facilitates modifications, repetitions, and maintenance if needed. However, 3DP cob still suffers some major limitations in terms of structural strength and productivity of the construction process as compared to 3DP concrete and other conventional construction methods. In the context of the limited available information regarding 3DP construction, this study aims to inspire researchers to further investigate 3DP construction and

assess its performance from cradle to grave.

CRediT authorship contribution statement

Hashem Alhumayani: Conceptualization, Methodology, Software, Validation, Formal analysis, Investigation, Resources, Data curation, Writing - original draft, Writing - review & editing, Visualization, Project administration. **Mohamed Gomaa:** Conceptualization, Methodology, Software, Validation, Formal analysis, Investigation, Resources, Data curation, Writing - original draft, Writing - review & editing, Visualization, Project administration. **Veronica Soebarto:** Methodology, Writing - review & editing, Supervision, Project administration. **Wassim Jabi:** Methodology, Writing - review & editing, Supervision, Project administration.

Declaration of competing interest

The authors declare that they have no known competing financial interests or personal relationships that could have appeared to influence the work reported in this paper.

Acknowledgments

The authors would like to acknowledge the help and assistance of Abbas Salhab and Ayman Mogahed for their technical support and guidance. Gratitude is also extended to Dr. Eshrar Latif at Cardiff University for his guidance on life cycle assessment topics.

References

- Agusti-juan, I., et al., 2017. Potential benefits of digital fabrication for complex structures : environmental assessment of a robotically fabricated concrete wall. *J. Clean. Prod.* 154, 330–340. <https://doi.org/10.1016/j.jclepro.2017.04.002>. Available at: (Accessed 15 December 2019).
- Alcott, Blake, 2012. Mill's scissors: structural change and the natural-resource inputs to labour. *J. Clean. Prod.* 21 (1), 83–92. <https://doi.org/10.1016/j.jclepro.2011.08.012>. Available at: (Accessed 20 December 2019).
- Anell, L., 2015. *Concrete 3d Printer*. Lund University, MA Thesis.
- Apis Cor, 2019. *Dubai municipality 3D printed building* [online]. Available at: <https://www.apis-cor.com/dubai-project>. (Accessed 10 December 2019).
- Asif, M., et al., 2017. Life cycle assessment of a three-bedroom house in Saudi Arabia. *Environments* 4 (3), 52. Available at: <http://www.mdpi.com/2076-3298/4/3/52>. (Accessed 12 January 2020).
- ASTM International, 2013. ASTM f2792-12a. Rapid Manufacturing Association, pp. 1–3. Available at: <http://www.ciri.org.nz/nzrma/technologies.html>. (Accessed 10 January 2020).
- Berman, B., 2012. 3-D printing: the new industrial revolution. *Bus. Horiz.* 55 (2), 155–162. <https://doi.org/10.1016/j.bushor.2011.11.003>. Available at:
- Besix, 2019. *BESIX Group* [Online]. Available at: <https://www.besix.com/en/about>. (Accessed 10 August 2019).
- Buswell, R.A., et al., 2018. 3D printing using concrete extrusion: a roadmap for research. *Cement Concr. Res.* 112 (October 2017), 37–49. <https://doi.org/10.1016/j.cemconres.2018.05.006>.
- Buyle, M., Braet, J., Audenaert, A., 2013. Life cycle assessment in the construction sector: a review. *Renew. Sustain. Energy Rev.* 26, 379–388. <https://doi.org/10.1016/j.rser.2013.05.001>.
- Cavalett, O., et al., 2013. Comparative LCA of ethanol versus gasoline in Brazil using different LCIA methods. *Int. J. Life Cycle Assess.* 18 (3), 647–658. <https://doi.org/10.1007/s11367-012-0465-0>.
- Craiveiro, F., et al., 2019. Additive manufacturing as an enabling technology for digital construction: a perspective on Construction 4.0. *Autom. Construct.* 103 (March), 251–267. <https://doi.org/10.1016/j.autcon.2019.03.011>.
- CyBe, 2018. *3D studio 2030* [online]. Available at: <https://cybe.eu/case/3d-studio-2030/>. Accessed: 15 Aug 2019.
- Dixit, M.K., 2019. 3-D printing in building construction: a literature review of opportunities and challenges of reducing life cycle energy and carbon of buildings. *IOP Conf. Ser. Earth Environ. Sci.* 290 (1) <https://doi.org/10.1088/1755-1315/290/1/012012>.
- 3 D-WASP 2020. 3D printers | WASP | leading company in the 3d printing industry. Available at: <https://www.3dwasp.com/en/>. (Accessed 10 January 2020).
- ERCA, 2018. Annual statistical booklet for electricity & seawater desalination industries [Online]. Available at: https://www.ecra.gov.sa/en_us/MediaCenter/doclib2/Pages/SubCategoryList.aspx?categoryID=5. (Accessed 11 December 2019).
- European Commission, 2017. *Product Environmental Footprint Category Rules*

- Guidance. *PEFCR Guidance Document - Guidance For the Development of Product Environmental Footprint Category Rules (PEFCRs)*, p. 238. December 2017, version 6.3.
- European Commission, 2019. European Platform on life cycle assessment. Available at: <https://eplca.jrc.ec.europa.eu/LCDN/developerEF.xhtml>. (Accessed 15 January 2020).
- Faludi, J., et al., 2015. Comparing environmental impacts of additive manufacturing vs traditional machining via life-cycle assessment. *Rapid Prototyp. J.* 21 (1), 14–33. <https://doi.org/10.1108/RPJ-07-2013-0067>.
- Geneidy, O., Ismael, W.S.E., 2018b. Investigating the Application of the Three Dimensional Wall Building Technology in Egypt. *Green Heritage Conference. 6-8 March 2018. The British University in Egypt, Cairo*, pp. 681–696.
- Goedkoop, M., et al., 2009. ReCiPe_main_report_final_27-02-2009_web.pdf doi: 10.029/2003JD004283.
- Gomaa, M., et al., 2019. Thermal performance exploration of 3D printed cob. *Architect. Sci. Rev.* 8628 <https://doi.org/10.1080/00038628.2019.1606776>.
- Habert, G., et al., 2013. Lowering the global warming impact of bridge rehabilitation by using ultra high performance fibre reinforced concretes. *Cement Concr. Compos.* 38, 1–11. <https://doi.org/10.1016/j.cemconcomp.2012.11.008>. Available at:
- Häfliger, I.F., et al., 2017. Buildings environmental impacts' sensitivity related to LCA modelling choices of construction materials. *J. Clean. Prod.* 156, 805–816. <https://doi.org/10.1016/j.jclepro.2017.04.052>.
- Hamard, et al., 2016. Cob, a vernacular earth construction process in the context of modern sustainable building. *Build. Environ.* 106, 103–119. <https://doi.org/10.1016/j.buildenv.2016.06.009>.
- Harrison, R., 1999. *Earth: the Conservation and Repair of Bowhill, Exeter : Working with Cob*. James & James, London.
- Housing program, 2019. Saudi Vision 2030. Available at: <https://vision2030.gov.sa/en/programs/Housing>. (Accessed 14 November 2019).
- Huijbregts, et al., 2017. ReCiPe2016: a harmonised life cycle impact assessment method at Midpoint and endpoint level. *Int. J. Life Cycle Assess.* 22 (2), 138–147. <https://doi.org/10.1007/s11367-016-1246-y>.
- IEA and UNEP, 2018. International energy agency and the united Nations environment Programme - global status report 2018: towards a zero-emission, efficient and resilient buildings and construction sector, 325. Available at: <http://www.ren21.net/status-of-renewables/global-status-report/>. Accessed: 19 January 2020.
- International Energy Agency, 2018. Global energy & CO2 status report. Available at: <https://www.iea.org/publications/freepublications/publication/GECO2017.pdf>. (Accessed 9 December 2019).
- ISO, 2006. Environmental management - life cycle assessment - principles and framework. *Int. Organ. Stand.* 3 <https://doi.org/10.1016/j.ecolind.2011.01.007>.
- Kafara, M., et al., 2017. Comparative life cycle assessment of conventional and additive manufacturing in mold core making for CFRP production. *Procedia Manufacturing* 8 (October 2016), 223–230. <https://doi.org/10.1016/j.promfg.2017.02.028>. Available at:
- Khoshnevis, B., et al., 2006. Mega-scale fabrication by contour crafting. *Int. J. Ind. Syst. Eng.* 1 (3), 301–320. <https://doi.org/10.1504/IJISE.2006.009791>.
- Kreiger, M., Pearce, J.M., 2013. Environmental life cycle analysis of distributed three-dimensional printing and conventional manufacturing of polymer products. *ACS Sustain. Chem. Eng.* 1 (12), 1511–1519. <https://doi.org/10.1021/sc400093k>.
- Labonnote, N., et al., 2016. Additive construction: state-of-the-art, challenges and opportunities. *Autom. Construct.* 72, 347–366. <https://doi.org/10.1016/j.autcon.2016.08.026>. Available at:
- Lau, M., et al., 2012. Digital fabrication. *Computer* 45 (12), 76–79. <https://doi.org/10.1109/MC.2012.407>.
- Le, T.T., et al., 2012a. Hardened properties of high-performance printing concrete. *Cement Concr. Res.* 42 (3), 558–566. <https://doi.org/10.1016/j.cemconres.2011.12.003>.
- Le, T.T., et al., 2012b. Mix design and fresh properties for high-performance printing concrete. *Materials and Structures/Materiaux et Constructions* 45 (8), 1221–1232. <https://doi.org/10.1617/s11527-012-9828-z>.
- Malaeb, Z., et al., 2015. 3D concrete printing: machine and mix design. *Int. J. Civ. Eng. Technol.* 6 (April), 14–22.
- Nerella, Venkatesh Naidu, Mechtcherine, Viktor, 2016. *Studying The Printability Of Fresh Concrete for Formwork-free Concrete Onsite 3D Printing Technology (CON-Print3D)*. 3D Concrete Printing Technology. Elsevier Inc. <https://doi.org/10.1016/b978-0-12-815481-6.00016-6>. Available at:
- Ngo, T.D., et al., 2018. Additive manufacturing (3D printing): a review of materials, methods, applications and challenges. *Compos. B Eng.* 143 (December 2017), 172–196. <https://doi.org/10.1016/j.compositesb.2018.02.012>. Available at:
- NICDP, 2019. Natural resources [online]. Available at: <https://www.ic.gov.sa/en/invest-in-saudi-arabia/natural-resources/>. (Accessed 28 January 2020).
- Paul, S.C., et al., 2018. A review of 3D concrete printing systems and materials properties: current status and future research prospects. *Rapid Prototyp. J.* 24 (4), 784–798. <https://doi.org/10.1108/RPJ-09-2016-0154>.
- Perrot, A., et al., 2018. 3D printing of earth-based materials: processing aspects. *Construct. Build. Mater.* 172, 670–676. Available at: <http://linkinghub.elsevier.com/retrieve/pii/S0950061818308079>.
- PRé Sustainability, SimaPro, 2019. Software to Measure and Improve the Impact of Your Product Life Cycle. Available at: <https://www.pre-sustainability.com/sustainability-consulting/sustainable-practices/custom-sustainability-software>. (Accessed 13 December 2019).
- Quagliarini, E., et al., 2010. Cob construction in Italy: some lessons from the past. *Sustainability* 2 (10), 3291–3308. <https://doi.org/10.3390/su2103291>.
- REN21, 2019. Renewables 2019 Global Status Report. Paris. Available at: <http://www.ren21.net/gsr-2019/>.
- Sala, S., et al., 2018. Development of a weighting approach for the environmental footprint. Available at: <https://eplca.jrc.ec.europa.eu/LCDN/developerEF.xhtml>. (Accessed 28 December 2019).
- Saudi Vision 2030, 2018. Saudi Vision 2030 [online]. Available at: <http://vision2030.gov.sa/en>. (Accessed 29 November 2019).
- Shrubsole, C., et al., 2019. Bridging the gap: the need for a systems thinking approach in understanding and addressing energy and environmental performance in buildings. *Indoor Built Environ.* 28 (1), 100–117. <https://doi.org/10.1177/1420326X17753513>.
- Singh, A., et al., 2011. Review of life-cycle assessment applications in building construction. *J. Architect. Eng.* 17 (March), 15–23. [https://doi.org/10.1061/\(ASCE\)AE.1943-5568.0000026](https://doi.org/10.1061/(ASCE)AE.1943-5568.0000026).
- Soliman, Y., et al., 2015. 3D printing and its urologic applications. *Rev. Urol.* 17 (1), 20–24. Available at: <http://www.pubmedcentral.nih.gov/articlerender.fcgi?artid=4444770&tool=pmcentrez&rendertype=abstract>.
- Soto, B.G. De, et al., 2018. The potential of digital fabrication to improve productivity in construction : cost and time analysis of a robotically fabricated concrete wall. *Autom. Construct.* 92 (2018), 297–311. <https://doi.org/10.1016/j.autcon.2018.04.004>. Available at:
- Tulevech, S.M., Hage, D. J. Spence, Jorgensen, K., Guensler, C.L., Himmler, R., Gheewala, S.H., 2018. Life cycle assessment: a multi-scenario case study of a low-energy industrial building in Thailand. *Energy Build.* 168, 191–200. <https://doi.org/10.1016/j.enbuild.2018.03.011>.
- UNEP/SETAC, 2016. *Global Guidance For Life Cycle Impact Assessment Indicators Volume 1*. Available at: <https://www.lifecycleinitiative.org/training-resources/global-guidance-lcia-indicators-v-1/>. (Accessed 17 December 2019).
- Veliz, R., et al., 2018. Computing Craft: Early Development of a Robotically-Supported Cob 3D Printing System, pp. 1–3.
- Veliz Reyes, A., et al., 2019. Negotiated matter: a robotic exploration of craft-driven innovation, 0(0). *Architect. Sci. Rev.* 1–11. Available at: <https://www.tandfonline.com/doi/full/10.1080/00038628.2019.1651688>.
- Wang, Q., et al., 2014. Investigation of condensation reaction during phenol liquefaction of waste woody materials. *Int. J. Sustain. Develop. Plan.* <https://doi.org/10.2495/SDP-V9-N5-658-668>.
- Weismann, A., Bryce, K., 2006. *Building with Cob*. Green Books Ltd, Devon.
- Wolfs, R.J.M., 2015. *3D Printing of Concrete Structural*. MA Dissertation. Eindhoven Univaersity of Technology.
- Wu, P., et al., 2016. A Critical Review of the Use of 3-D Printing in the Construction Industry, vol. 68, pp. 21–31. *Automation in construction*. Available at: https://ac.els-cdn.com/S0926580516300681/1-s2.0-S0926580516300681-main.pdf?_tid=250f7c63-ec3d-4c30-88f0-b2763d3f5e6b&acdnat=1528375914_f48a2d599618a1e3277a7c39b42f2f90.
- Xia, M., Sanjayan, J., 2016. Method of formulating geopolymers for 3D printing for construction applications. *Mater. Des.* 110, 382–390. <https://doi.org/10.1016/j.matdes.2016.07.136>. Available at:
- Yao, Y., et al., 2019. Life cycle assessment of 3D printing geo-polymer concrete: an ex-ante study. *J. Ind. Ecol.* 116–127. <https://doi.org/10.1111/jiec.12930>.

